DEPARTMENT OF THE ARMY — CORPS OF ENGINEERS

BEACH EROSION BOARD
OFFICE OF THE CHIEF OF ENGINEERS

WAVE VARIABILITY AND WAVE SPECTRA FOR WIND-GENERATED GRAVITY WAVES

TECHNICAL MEMORANDUM NO. 118

WAVE VARIABILITY AND WAVE SPECTRA FOR WIND-GENERATED GRAVITY WAVES

TECHNICAL MEMORANDUM NO.118
BEACH EROSION BOARD
CORPS OF ENGINEERS

AUGUST 1959

FOREWORD

The determination of wave characteristics and the interrelation of these characteristics is an important part of many coastal engineering problems. The average height of a particular irregular wave train in nature may be determined and estimated either from observation or from prediction, but frequently of equal importance is the variability, or degree of variability, of preceding and succeeding waves about this average value. How much higher is the maximum wave, how many times per hundred waves is it apt to occur, with what particular period is it most apt to be associated, what is the relation between wave heights exceeded a certain percent of the time and the probable wave periods associated with these heights, etc., are all questions which are important to the design of coastal structures.

A number of wave records from a wide variety of locations have been subjected to a statistical analysis, and distribution functions of wave heights and periods derived. If the wave length is regarded as equivalent to the wave period squared (as is assumed in this report) length distribution functions may also be derived. The joint distribution relationships between length or period and the wave heights have also been obtained. Following these distribution functions, an analytical expression for the families of wave spectra has also been derived. These spectra have been compared with those proposed by others and are found to be in good agreement with available data.

This report was prepared by Charles L. Bretschneider, a Hydraulic Engineer in the Research Division of the Beach Erosion Board, which is under the general supervision of Joseph M. Caldwell, Chief of the Division. Although the major portion of the research described in this report was carried out as a regular part of the approved research program of the Beach Erosion Board, the work was originally initiated at the Agricultural and Mechanical College of Texas as a doctoral dissertation by the author. The work was carried on by the author at the Board, and submitted as a dissertation at Texas A. & M. in January 1959. As such, it went through the usual college channels, and received normal editing by the English Department there. Subsequent to award of the Ph.D. degree, only minor modifications have been made in the report. At the time of publication of this report Major General W. K. Wilson, Jr. was President of the Board, and R. O. Eaton was Chief Technical Advisor. The report was edited for publication by A. C. Rayner, Chief of the Project Development Division.

Views and conclusions expressed in this report are not necessarily those of the Beach Erosion Board.

This report is published under authority of Public Law 166, 79th Congress, approved July 31, 1945.

CONTENTS

Page

CHAPTER VII - A THEORY OF WAVE SPECTRA FROM JOINT DISTRIBUTION

CHAPTER VIII - GENERATION OF WIND WAVES IN DEEP WATER AND THE WAVE SPECTRA

CHAPTER IX - COMPARISON OF VARIOUS PROPOSED WAVE SPECTRA

TABLES

FIGURES

WAVE VARIABILITY AND WAVE SPECTRA FOR WIND-GENERATED GRAVITY WAVES

By

Charles L. Bretschneider
Hydraulic Engineer, Research Division
Beach Erosion Board

ABSTRACT

Wave records from a wide variety of locations have been utilized in a statistical analysis of the probability distributions of wave heights and wave periods; and a family of wave spectra which allows for an arbitrary linear correlation between wave height and wave period squared is suggested. It is found that the marginal probability distribution of wave heights follows Rayleigh's distribution closely. This conclusion is based upon 90 records of about 100 waves each plus several extra long records taken in deep and shallow water. About half of these records represent time sequences of water level at particular locations and the other half are time sequences of pressure at subsurface depths (from which the wave heights were estimated using the linear wave theory).

The Rayleigh distribution for wave height variability has been suggested previously by Longuet-Higgins and Watters. An apparently new result of the present work is that the marginal distribution of the square of the wave period also follows Rayleigh's distribution remarkably well. From the Rayleigh distribution for wave length variability it is possible to derive the marginal distribution of wave period variability, also verified with the available data.

An analytical expression which allows for non-zero linear correlation between wave height and period squared is suggested for the joint distribution of wave heights and periods. This joint distribution is employed in the determination of the mean wave period for the highest waves. Also an analytical expression for the family of wave spectra is derived from the suggested joint probability distribution of heights and periods. The basic assumption underlying the suggested spectra is the condition of linear correlation between wave height and period squared. These

spectra are compared with those proposed by Darbyshire and Neumann and with the numerically evaluated spectrum obtained recently from Project SWOP and are found to be in good agreement with the latter. The spectrum for a fully developed sea, a special case of the proposed family of spectra, is also consistent with the measurements of Burling and the theoretical work of Phillips which indicate that for high frequencies the spectral energy is inversely proportional to the fifth power of the frequency. It is also found that the present family of spectra predicts a mean square slope of the sea surface which is in closer accord with the data of Cox and Munk than that inferred from the spectra of Darbyshire or Neumann.

It is proposed that in the early stage of wave generation the correlation coefficient between wave height and period squared is nearly unity because of the maximum possible steepness of the waves. As the generation proceeds it is proposed that the correlation decreases, ultimately approaching zero for a fully developed sea. Corresponding to the suggested behavior of the correlation coefficient between wave heights and periods, the initial spectrum is narrow and becomes wider as the generation continues. It is found that the so-called "significant" wave period is closely related to the optimum or modal value of the period spectra and hence the energy of the waves as a group should have a propagational speed approximately equal to the group velocity of the significant waves.

A revision of the wave forecasting relationships proposed in an earlier work by Bretschneider are revised to take into account the variation in spectral width.

CHAPTER I: INTRODUCTION

1. General

Statistical characteristics of the ocean surface are of interest in problems relating to the erosion of beaches, design of coastal and offshore structures, and the design and operation of floating structures. Accumulated wave data, supplementing wave forecasting techniques, have provided means of predicting the effects of wind-generated waves at a coastline. The statistical characteristics of the ocean surface are related to the wave spectra, which in turn may be used to describe the process of wave generation and wave decay.

The first great advance in recent years in the art of wave forecasting was made by Sverdrup and Munk (1947)*, who combined the classical equations of hydrodynamics with empirical data to provide relationships for forecasting waves for amphibious operations during World War II. Their relationships were revised by Arthur (1947) and again by Bretschneider (1951) when more wind and wave data became available. This revised method has been referred to as the Sverdrup-Munk-Bretschneider method, or simply the SMB method. Actually, the B deserves little credit since the important fundamental work was performed by Sverdrup and Munk (1947), after which the revisions became relatively simple once the data were available.

These relationships became even more valuable because of the work by Putz (1952), who obtained empirical distribution functions for wave height variability about the mean height and wave period variability about the mean period. This information was utilized in a paper by Bretschneider and Putz (1951).

Very shortly thereafter, Longuet-Higgins (1952) presented a theoretical distribution function for wave height variability based on the assumption of random phase and a narrow spectrum, the distribution function of which is known as the Rayleigh** distribution. It is of interest to note that the Putz distribution and the Rayleigh distribution are in very close agreement. This agreement is also verified in the present study.

According to Watters (1953) from her correspondence with Dr. H. F. Barber, the Rayleigh distribution for wave height variability can be derived with no knowledge of the wave spectrum, assuming only that elevations of the sea surface with respect to time possess a Gaussian distribution. Data by Watters (1953) and more by Darlington (1954) confirm the Rayleigh distribution. Thus, the narrow spectrum,

*Bibliography beginning on page 182.

**So called because it was derived by Lord Rayleigh in connection with the theory of sound. See Rayleigh (1880).

CHAPTER I: INTRODUCTION

1. General

Statistical characteristics of the ocean surface are of interest in problems relating to the erosion of beaches, design of coastal and offshore structures, and the design and operation of floating structures. Accumulated wave data, supplementing wave forecasting techniques, have provided means of predicting the effects of wind-generated waves at a coastline. The statistical characteristics of the ocean surface are related to the wave spectra, which in turn may be used to describe the process of wave generation and wave decay.

The first great advance in recent years in the art of wave forecasting was made by Sverdrup and Munk (1947)*, who combined the classical equations of hydrodynamics with empirical data to provide relationships for forecasting waves for amphibious operations during World War II. Their relationships were revised by Arthur (1947) and again by Bretschneider (1951) when more wind and wave data became available. This revised method has been referred to as the Sverdrup-Munk-Bretschneider method, or simply the SMB method. Actually, the B deserves little credit since the important fundamental work was performed by Sverdrup and Munk (1947), after which the revisions became relatively simple once the data were available.

These relationships became even more valuable because of the work by Putz (1952), who obtained empirical distribution functions for wave height variability about the mean height and wave period variability about the mean period. This information was utilized in a paper by Bretschneider and Putz (1951).

Very shortly thereafter, Longuet-Higgins (1952) presented a theoretical distribution function for wave height variability based on the assumption of random phase and a narrow spectrum, the distribution function of which is known as the Rayleigh** distribution. It is of interest to note that the Putz distribution and the Rayleigh distribution are in very close agreement. This agreement is also verified in the present study.

According to Watters (1953) from her correspondence with Dr. H. F. Barber, the Rayleigh distribution for wave height variability can be derived with no knowledge of the wave spectrum, assuming only that elevations of the sea surface with respect to time possess a Gaussian distribution. Data by Watters (1953) and more by Darlington (1954) confirm the Rayleigh distribution. Thus, the narrow spectrum,

*Bibliography beginning on page 182.

**So called because it was derived by Lord Rayleigh in connection with the theory of sound. See Rayleigh (1880).

the Gaussian distribution of surface elevations, and the Rayleigh distribution of heights, are all one in the description of the ocean sea surface.

Cartwright and Longuet-Higgins (1956) show that deviations from the Rayleigh distribution may be explained by variation in spectral width.

The Gaussian sea surface has been discussed by Pierson (1954) and again in greater detail with wider applications by Longuet-Higgins (1957).

Making use of the work by Longuet-Higgins (1952), Neumann (1953) proposed a wave spectrum for a fully developed sea based on a multitude of visual wave observations. This wave spectrum is the basis on which is founded a method for forecasting waves described by Pierson, Neumann, and James (1955), sometimes referred to as the PNJ method.

Two other methods for forecasting deep water waves might also be mentioned. The method of Darbyshire (1955) is based on wave data and a wave spectrum somewhat different from that utilized by Neumann (1953). The method of Suthons (1945) is quite similar to that of Sverdrup and Munk (1947).

A very objective verification study of the above four methods was made by Roll (1957) and the general conclusion was that each method gave the best results for the locations from which the bulk of corresponding wave data were obtained. This conclusion is as should be expected.

At present some controversies exist as to which method is the most practical and the most accurate. Although these controversies are discussed in the last chapter of the present study, it is not proposed to make detailed comparisons of various methods of wave forecasting. Such a comparative study is indeed a separate topic, and perhaps one should utilize the graphical techniques proposed by Wilson (1955), the principles of which can be adapted to any method of wave forecasting.

2. Scope of Present Investigation

Essentially, the present study consists of four broad phases: (1) marginal distributions of wave heights, lengths*, and periods; (2) joint distribution of heights and lengths (and heights and periods); (3) a development of wave spectra from the joint distribution function; and (4) revisions in wave forecasting relationships. This study is presented in nine chapters. At the end of the present chapter some of

*For the purpose of this paper the "length" is computed from the wave period and is utilized as $L = T^2$, arbitrary units.

the wave theory is briefly reviewed. Brief summaries of other chapters follow below.

Chapter II describes the nature and source of wave data. Types of wave recording instruments are briefly discussed. Methods used in analyzing the wave records vary from one source of data to another, the reasons for which together with advantages and disadvantages are discussed.

Chapter III discusses theory of wave variability for marginal distributions of heights, lengths, and periods. Chapter IV is the presentation of wave data for comparison with the theory given in Chapter III. It is confirmed that the Rayleigh distribution is applicable to wave height variability. In addition, it is shown that the Rayleigh distribution is equally applicable for wave length (period squared) variability. From the Rayleigh distribution of wave length variability, a distribution function for wave period variability is derived. A comparison is made between theory and data and also with the distributions proposed by Putz (1952). The agreement is very good.

Chapter V outlines the joint distribution between wave height and wave length. It is shown that if the Rayleigh distribution applies to both wave height and wave length variability, it is impossible to derive a joint distribution function which is applicable throughout the entire range of the correlation coefficient from +1 to -1. To partially overcome this difficulty a summation function is introduced. With certain justifiable assumptions, and within certain limits of application, this summation function can be used to determine the mean wave length or the mean wave period of wave heights greater than a given height. A comparison between data and theory is presented in Chapter VI and is fairly good.

Chapter VII presents a development of the wave spectra based on the joint distribution of wave heights and lengths. This development is made without any foreknowledge of the joint distribution function, except that linear regression between H and T^2 is assumed.* Furthermore, the same marginal distribution function must describe both wave height and wave length variability. In the final step, the Rayleigh distribution function for length is introduced to obtain the length spectra of height squared, which is subsequently transformed into the period spectra, and the frequency spectra. The spectra proposed depend on the correlation coefficient between wave height and wave length.

Chapter VIII utilizes the wave spectra developed in Chapter VII, together with additional wave data and other considerations, to obtain a revision in the wave forecasting relationships. The wave spectra equation is transformed to include wind speed by use of the fetch

*Symbols beginning on page 188.

parameter. These parameters include those for significant wave height, mean wave height, significant wave period, mean wave period, correlation coefficient between height and length, minimum duration of wind, mean square sea surface slope, and the spectral width parameter. The above are all functions of the fetch parameter. It is pointed out that these revisions are by no means final, but only an additional step forward in the betterment of wave forecasting, since more suitable wave data should be forthcoming.

Chapter IX contains a summary of the preceding chapters, but the main emphasis is devoted to comparisons of the various proposed wave spectra. It is shown that the family of wave spectra presented in this study is in better agreement with available data than are the other proposed wave spectra.

In addition, suggestions are presented for possible approaches which might be utilized in future studies of wave variability and wave spectra, taking into account the change of correlation coefficient during the generation of waves and also the decay of waves.

3. Basic Considerations in Regard to Theory of Surface Waves

In order to understand the complex nature of ocean waves, and the importance of statistical representations of the sea surface and the wave spectra, it becomes necessary first to review some basic concepts of wave theory. Equations required for subsequent developments will be summarized here. Derivations and discussions of these equations are not repeated since they are readily available from Lamb (1945). In water of constant depth the wave celerity for waves of small amplitude can be represented by the equation of classical hydrodynamics

$$C^2 = (g/k) \tanh kd \qquad (1.1)^*$$

where d is the mean water depth, $k = \frac{2\pi}{L}$ the wave number, and g is the acceleration of gravity. A simple wave is depicted in Figure 1.1,** where H, the wave height (equal to twice the wave amplitude), is the vertical distance between two successive crests; and the period, T, is the time interval between the passage of two consecutive waves. The wave speed is related to wave length and period by

$$L = CT \qquad (1.2)$$

*Equations are numbered according to (1.1), (1.2), (2.1), (2.2), etc; the first number referring to FIRST ORDER HEADING (or chapter) and the second to equation number for that chapter.

**figures are at end of each chapter.

which is in the form of distance equals velocity multiplied by time.

For deep water, defined as $d \geq L/2$, tanh kd tends toward unity, whence from (1.1) and (1.2)

$$C_o^2 = \frac{g L_o}{2\pi} = \left(\frac{gT}{2\pi}\right)^2 \tag{1.3}$$

where the subscript o refers to deep water.

Shallow water waves are defined as those in a depth such that $d \leq L/25$ and (1.1) becomes with sufficient accuracy:

$$C_s^2 = gd \tag{1.4}$$

This study considers only deep water wave characteristics (H_o, T, L_o). As a train of waves propagates from deep to shallow water, only H and L change, but T remains unchanged. For shallow water the wave characteristics H_s and L_s may be obtained from H_o and L_o by use of tables by Wiegel (1954).

The surface profile of a simple sinusoidal wave, such as illustrated by Figure 1.1, is given by

$$\xi = A \cos \theta \tag{1.5}$$

where

ξ = surface elevation
$A = H/2$, wave amplitude
$\theta = kx - \omega t$, phase position
$\omega = \frac{2\pi}{T}$, angular frequency

Wave energy for a progressive sinusoidal wave consists of half potential associated with surface elevation and half kinetic associated with particle velocity. The potential energy, average per unit of surface area is given by

$$E_p = \frac{1}{L}\int_0^L \frac{1}{2}\rho g \xi^2 \, dx = \frac{1}{16}\rho g H^2 \tag{1.6}$$

where ρ is the mass density (slugs per cubic foot) and g is the acceleration of gravity.

The kinetic energy, average per unit area, is given by

$$E_k = \int_{-d}^{\xi} \frac{1}{2}\rho(u^2 + v^2)\, dz = \frac{1}{16}\rho g H^2 \tag{1.7}$$

The total energy, average per unit area, is given by

two methods, there are more waves corresponding to $\bar{T}$ than there are corresponding to T for the same time interval. This results in $\bar{T} > T$ and $T_{1/3} > \bar{T}_{1/3}$, but in general $(T_{1/3})/\bar{T}$ will be approximately equal to $(\bar{T}_{1/3})/\bar{T}$.

The complex nature of ocean waves lead to a family of wave spectra, varying with stage of generation or stage of decay as the case may be. Both the period spectra and the frequency spectra are used throughout the paper. It is important to distinguish between spectra and spectrum. The spectrum is a particular case of the family of spectra. For the family of spectra derived in this study the energy for high frequency is distributed according to ω^n where n varies from -9 to -5. The special case of ω^{-5} is the spectrum for a fully developed sea, and in unit or normal form is represented by a single exponential curve for all wind speeds. Although in standard form a separate curve is obtained for each wind speed the term spectrum is still retained. From the above the term spectrum will apply individually to those proposed by Neumann (1955), Darbyshire (1952), and Darbyshire (1955), each of which when reduced to normal form can be represented by a single curve.

Source (f) consists of wave data from hurricane "Audrey" 1957. Three sections of wave records were made available through the courtesy of the California Oil Company, New Orleans, Louisiana (1957). The records were obtained from the offshore platform in the Gulf of Mexico, location Bay Marchand, in 30 feet of water a few miles from the coast. These data were recorded, using the self-calibrating step-resistance wave gage developed by the California Research Corporation, La Habra, California. The data consist of a mixture of swell propagated across the Continental Shelf and locally generated wind waves in shallow water. The mean wave period and the mean wave height changed somewhat during the period of record, this being the only disadvantage of the records. Records were analyzed by the zero-up cross method. Table 2.6 gives a description of the data used from hurricane "Audrey".

TABLE 2.6

DESCRIPTIVE DATA FOR HURRICANE "AUDREY"

Date	Record Identification	No. of Waves
June 27, 1957	Calco 1	142
June 27, 1957	Calco 2	125
June 27, 1957	Calco 3	70

Source (g) consists of wind wave data from a Berkeley wave tank, University of California. Five short records were obtained from a report by Sibul and Tichner (1956). The parallel resistance wire recorder, developed by the University of California ... described by Morrison (1949), was used for recording these data. These records, analyzed at the Beach Erosion Board, were not investigated as completely as those from the other sources.

TABLE 2.7

DESCRIPTIVE DATA FOR WIND WAVES
BERKELEY WAVE TANK

Record Identification	No. of Waves
Run #24	43
Run #25	42
Run #35	36
Run #31	33
Run #15	34

TABLE 2.3

DESCRIPTIVE DATA FOR TWENTY WIND WAVE RECORDS
FROM LAKE TEXOMA, TEXAS

Station Location	Date	Time (CST) h m	h m	Wind Velocity in Miles per Hour and Direction	Record Identification	No. of Waves
C	March 23, 1951	11 01	- 11 41	29 NNE	E-D	134
C	March 23, 1951	12 41	- 13 11	26 NNE	F-D	121
C	March 29, 1951	09 47	- 10 26	32 NNW	G-D	108
C	March 29, 1951	10 56	- 11 36	30 NNW	H-D	116
A	Dec. 8, 1951	15 25	- 15 29	25 N	L-D	115
A	Dec. 8, 1951	15 31	- 15 35	25 N	M-D	116
A	Dec. 8, 1951	15 40	- 15 45	25 N	N-D	108
A	Dec. 8, 1951	15 59	- 16 04	25 N	O-D	108
C	Jan. 9, 1952	13 17	- 13 57	34 N	P-D	127
C	Jan. 9, 1952	15 07	- 15 47	35 N	Q-D	125
C	Jan. 29, 1952	10 51	- 11 31	39 N	R-D	110
C	Feb. 29, 1952	11 51	- 12 31	38 N	S-D	114
C	Apr. 1, 1952	10 31	- 11 11	29 NNE	T-D	147
C	Apr. 1, 1952	11 21	- 12 01	30 NNE	U-D	148
C	Apr. 9, 1952	12 07	- 12 47	29 NNW	V-D	127
C	Apr. 9, 1952	15 37	- 16 17	28 NNW	W-D	134
C	May 10, 1952	09 45	- 10 15	33 NNE	X-D	109
C	May 10, 1952	11 45	- 12 15	32 NNE	Y-D	107
A	Dec. 8, 1951	15 25	- 17 17	25 N	Long	3,808
A	Dec. 8, 1951	15 25	- 16 04	25 N	Long	908

TABLE 2.4

DESCRIPTIVE DATA FOR HURRICANE WIND
WAVE DATA, LAKE OKEECHOBEE, FLORIDA

Station Location	Date	Time (EST) h m	h m	Record Identification	No. of Waves
12	Aug. 26, 1949	23 43	- 00 24	L.O.-1	131
	Aug. 27, 1949	00 28	- 01 30	L.O.-2	154
	Aug. 27, 1949	01 34	- 02 35	L.O.-3	141
	Aug. 27, 1949	02 39	- 03 25	L.O.-4	115

(1952) sub-surface pressure recorder was used. The instrument was located off a Magnolia Oil Company platform, in 38 to 40 feet of water, some 20 miles from the nearest land area off the Louisiana Coast. The pressure head was installed 30 feet above the sea bottom, or about 8 to 10 feet below the mean water surface in order to obtain a minimum of attenuation of low period waves. A refined in-place calibration was made, using visual observations on a vertical staff, supplemented with a limited amount of data obtained with a movie camera. The record, consisting of 1,500 consecutive waves, was obtained with no definite purpose in mind, except that the wave instrumentation was used in conjunction with other Texas A. & M. research projects. The wave gage was permitted to operate during the period of installation of other instruments, primarily to keep it out of the way of the installation crews. The long wave record covered a period after the passage of a severe cold front; the wind speed during this time remained relatively constant between 30 and 35 knots from the north to north-northeast. That is, the wind was offshore, limiting the fetch to about 15 to 25 miles. These waves are of short enough period to be almost deep water waves, but will be called waves in intermediate water. This long record was analyzed as 15 groups of 100 consecutive waves each, 7 groups of 200 consecutive waves each, 3 groups of 500 consecutive waves each, and 2 groups of 1,000 consecutive waves each. In addition, the record was analyzed by considering the waves of each first minute of each five minute section of the record, thereby building up a group of 107 waves in a manner similar to that utilized for the data from Lake Texoma, Fort Peck Reservoir, and Lake Okeechobee.

The shorter record, 379 consecutive waves, is for wind waves from the southwest, wind between 20 and 25 knots. Because the fetch was quite long, these waves are not deep water but truly waves of intermediate water depth.

The above records were collected and partly analyzed at Texas A. & M. on contract with the Beach Erosion Board. The completion of the work was made at the Beach Erosion Board.

The method of record analysis used for the Gulf of Mexico data is known as the zero-up crossing method originally proposed by Pierson (1954), sometimes referred to as the Pierson method. This method is depicted on Figure 2.6. It might also be mentioned that Pierson and Marks (1952) also proposed a power spectrum analysis of ocean sub-surface pressure records. For the Gulf of Mexico data used in this paper, perhaps the power spectrum analysis was not necessary, since the pressure head was located only 8 to 10 feet below the sea surface rather than on the bottom and also a field calibration was performed. In spite of this care, it is still believed that some wave heights of the very low periods might have been attenuated undesirably. Table 2.5 gives a description of the data used from the Gulf of Mexico.

Results of additional wave data obtained in the Gulf of Mexico are summarized in a report by Bretschneider (1954), the method of analysis being the significant wave method described by Sverdrup (1951). The significant wave method is quite different from that

used for analysis of the Gulf of Mexico data herein. In case of sub-surface pressure recorders, one pressure response factor based on the significant period is used to convert the significant pressure height to the significant surface height. As stated by Snodgrass (1951) and shown by Pierson and Marks (1952), a significant wave method can introduce considerable error. In the analysis used in the present study, each wave period has a separate calibrated response factor. Hence, these data are quite accurate, except perhaps for the very low periods which might have been filtered out completely in the pressure trace, in which case these waves will not appear in the computed surface trace.

TABLE 2.5

DESCRIPTIVE DATA FOR WIND WAVES
OF THE GULF OF MEXICO
(MAGNOLIA PLATFORM 119F)

Date	Time (CST) h m — h m	Wind Velocity in Miles per Hour and Direction	Record Identification	No. of Waves
Dec. 9, 1953	10 34.7 - 10 43.3	30 NE	G-1	100
Dec. 9, 1953	10 43.3 - 10 51.8	30 NE	G-2	100
Dec. 9, 1953	10 51.8 - 11 00.8	31 NE	G-3	100
Dec. 9, 1953	11 00.8 - 11 09.3	33 NE	G-4	100
Dec. 9, 1953	11 09.3 - 11 17.7	35 NE	G-5	100
Dec. 9, 1953	11 17.7 - 11 25.6	35 NE	G-6	100
Dec. 9, 1953	11 25.6 - 11 33.1	35 NE	G-7	100
Dec. 9, 1953	11 33.1 - 11 41.2	36 NE	G-8	100
Dec. 9, 1953	11 41.2 - 11 49.1	38 ENE	G-9	100
Dec. 9, 1953	11 49.1 - 11 56.8	40 ENE	G-10	100
Dec. 9, 1953	11 56.8 - 12 04.8	40 ENE	G-11	100
Dec. 9, 1953	12 04.0 - 12 12.9	40 ENE	G-12	100
Dec. 9, 1953	12 12.9 - 12 21.0	39 ENE	G-13	100
Dec. 9, 1953	12 21.0 - 12 28.9	37 NE	G-14	100
Dec. 9, 1953	12 28.9 - 12 37.1	35 NE	G-15	100
Feb. 26, 1954	10 10.0 -	26 SW	G-16	378
			G-1-5	500
			G-6-10	500
			G-7-15	500
			G-1-10	1000
			G-6-15	1000
			G-X	107

Source (f) consists of wave data from hurricane "Audrey" 1957. Three sections of wave records were made available through the courtesy of the California Oil Company, New Orleans, Louisiana (1957). The records were obtained from the offshore platform in the Gulf of Mexico, location Bay Marchand, in 30 feet of water a few miles from the coast. These data were recorded, using the self-calibrating step-resistance wave gage developed by the California Research Corporation, La Habra, California. The data consist of a mixture of swell propagated across the Continental Shelf and locally generated wind waves in shallow water. The mean wave period and the mean wave height changed somewhat during the period of record, this being the only disadvantage of the records. Records were analyzed by the zero-up cross method. Table 2.6 gives a description of the data used from hurricane "Audrey".

TABLE 2.6

DESCRIPTIVE DATA FOR HURRICANE "AUDREY"

Date	Record Identification	No. of Waves
June 27, 1957	Calco 1	142
June 27, 1957	Calco 2	125
June 27, 1957	Calco 3	70

Source (g) consists of wind wave data from a Berkeley wave tank, University of California. Five short records were obtained from a report by Sibul and Tichner (1956). The parallel resistance wire recorder, developed by the University of California and described by Morrison (1949), was used for recording these data. These records, analyzed at the Beach Erosion Board, were not investigated as completely as those from the other sources.

TABLE 2.7

DESCRIPTIVE DATA FOR WIND WAVES
BERKELEY WAVE TANK

Record Identification	No. of Waves
Run #24	43
Run #25	42
Run #35	36
Run #31	33
Run #15	34

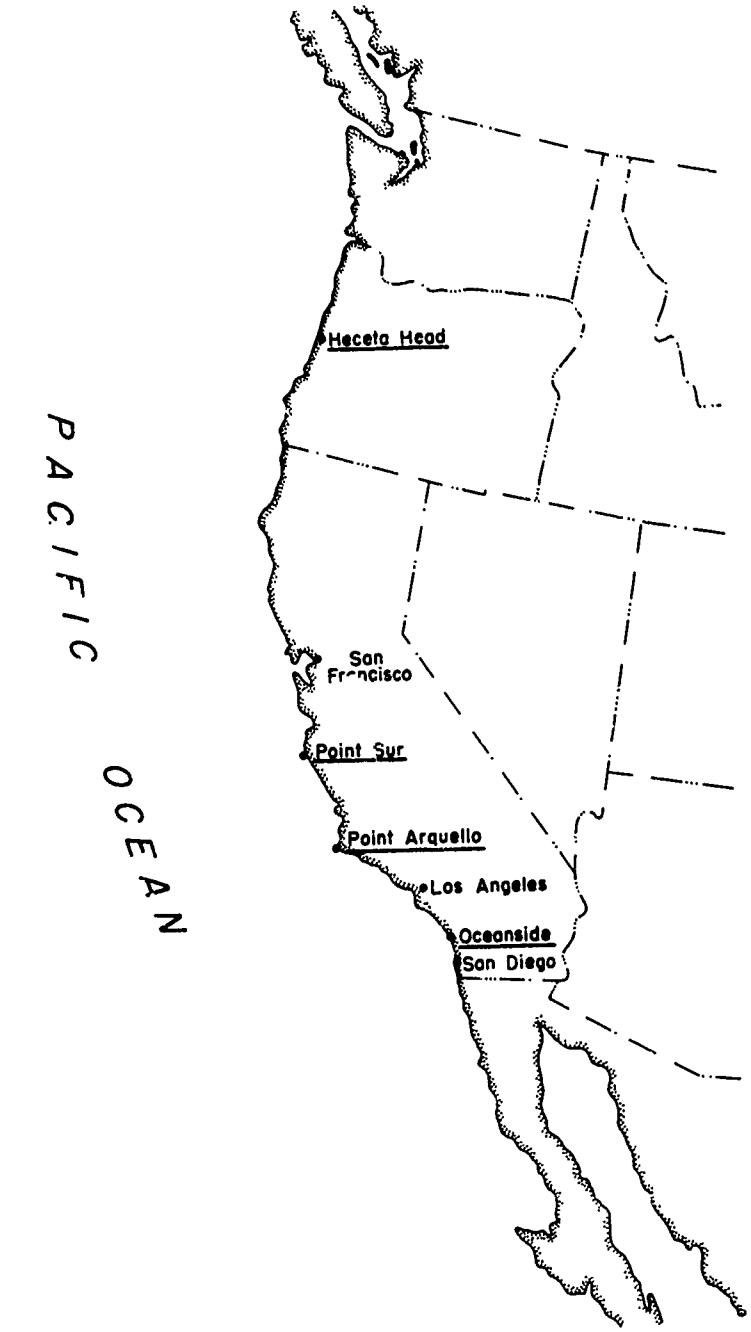

FIGURE 2.1 LOCATION MAP — PACIFIC OCEAN

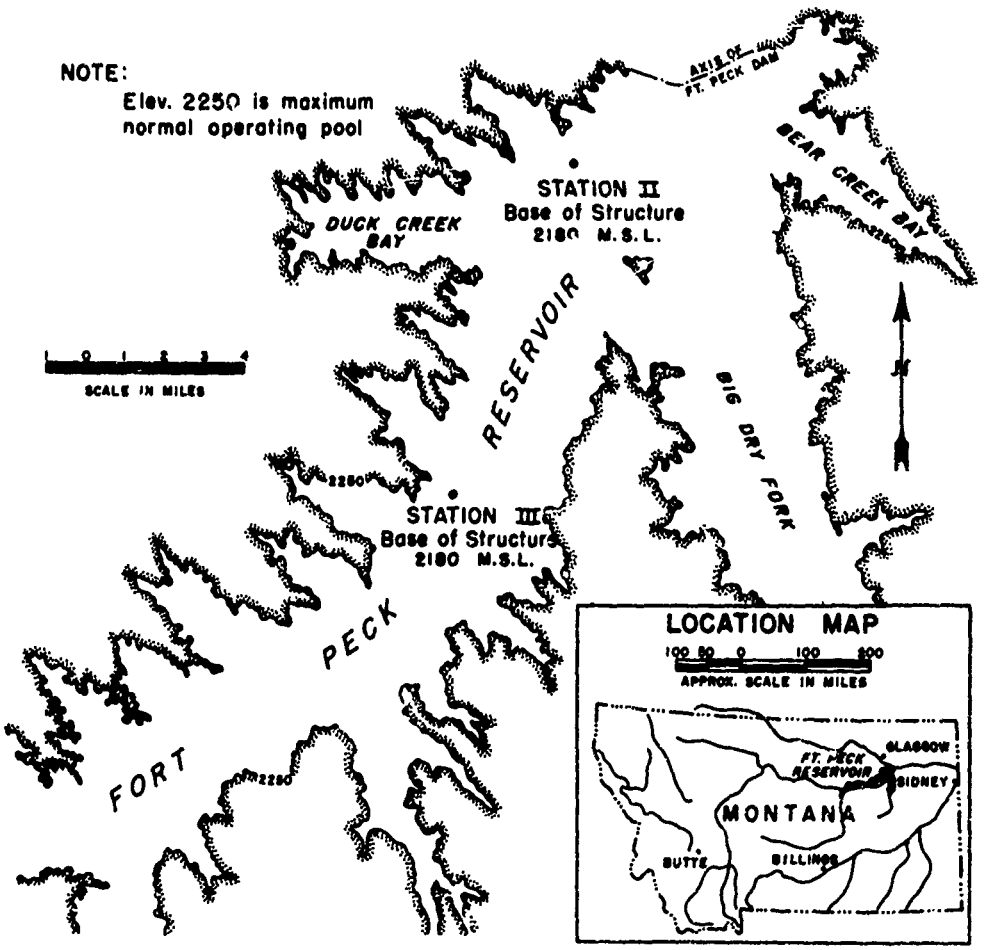

FIGURE 2.2 LOCATION MAP — FORT PECK RESERVOIR

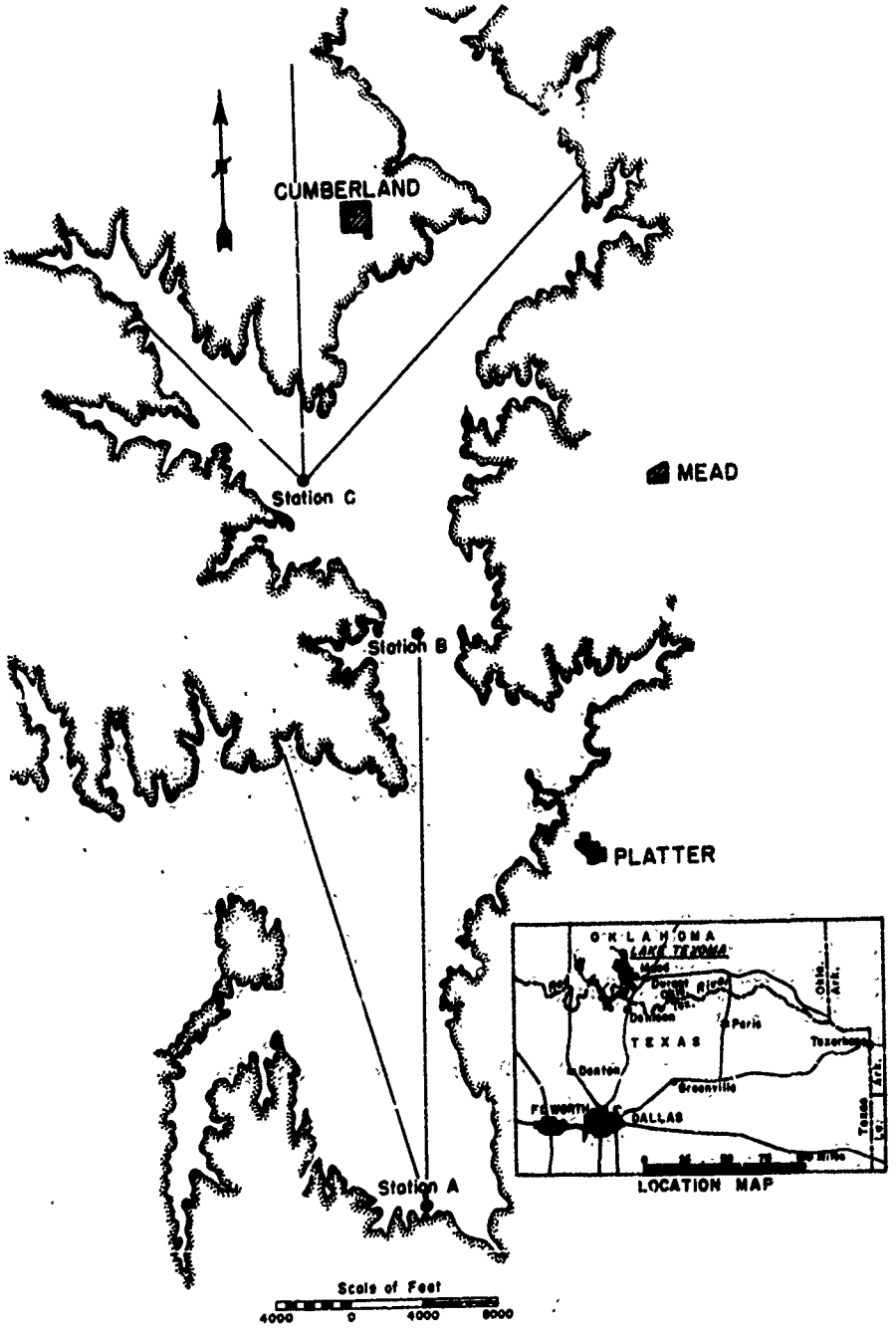

FIGURE 2.3 LOCATION MAP — LAKE TEXOMA

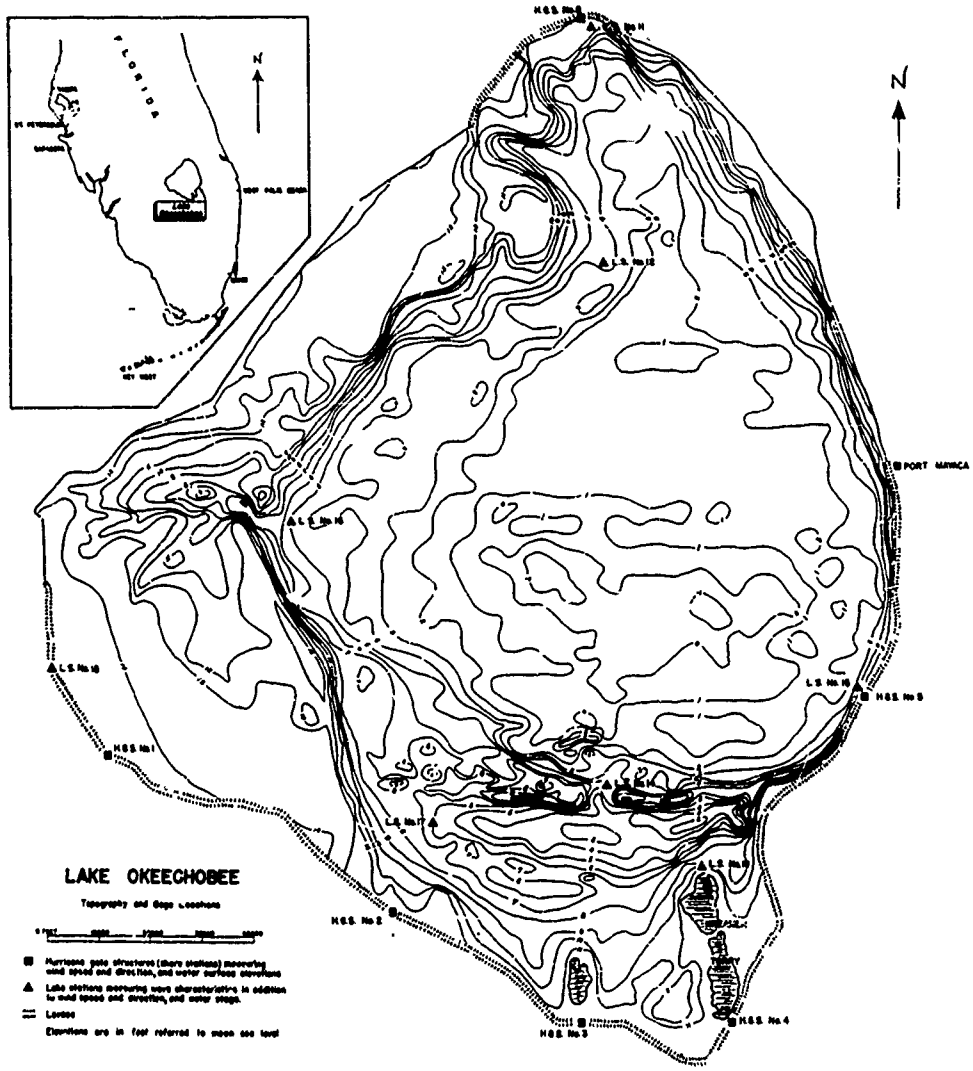

FIGURE 2.4 LOCATION MAP—LAKE OKEECHOBEE

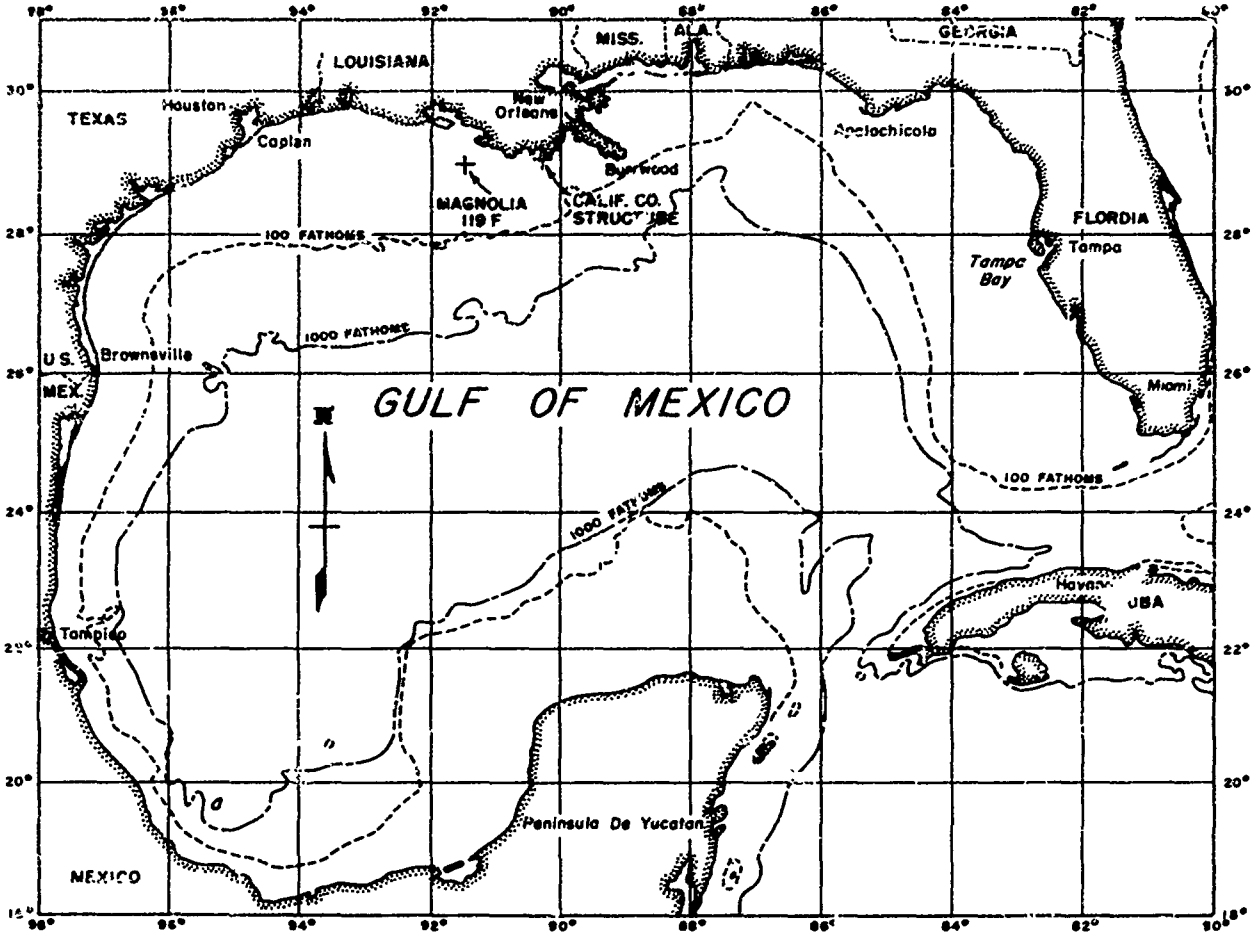

FIGURE 2.5 LOCATION MAP — GULF OF MEXICO

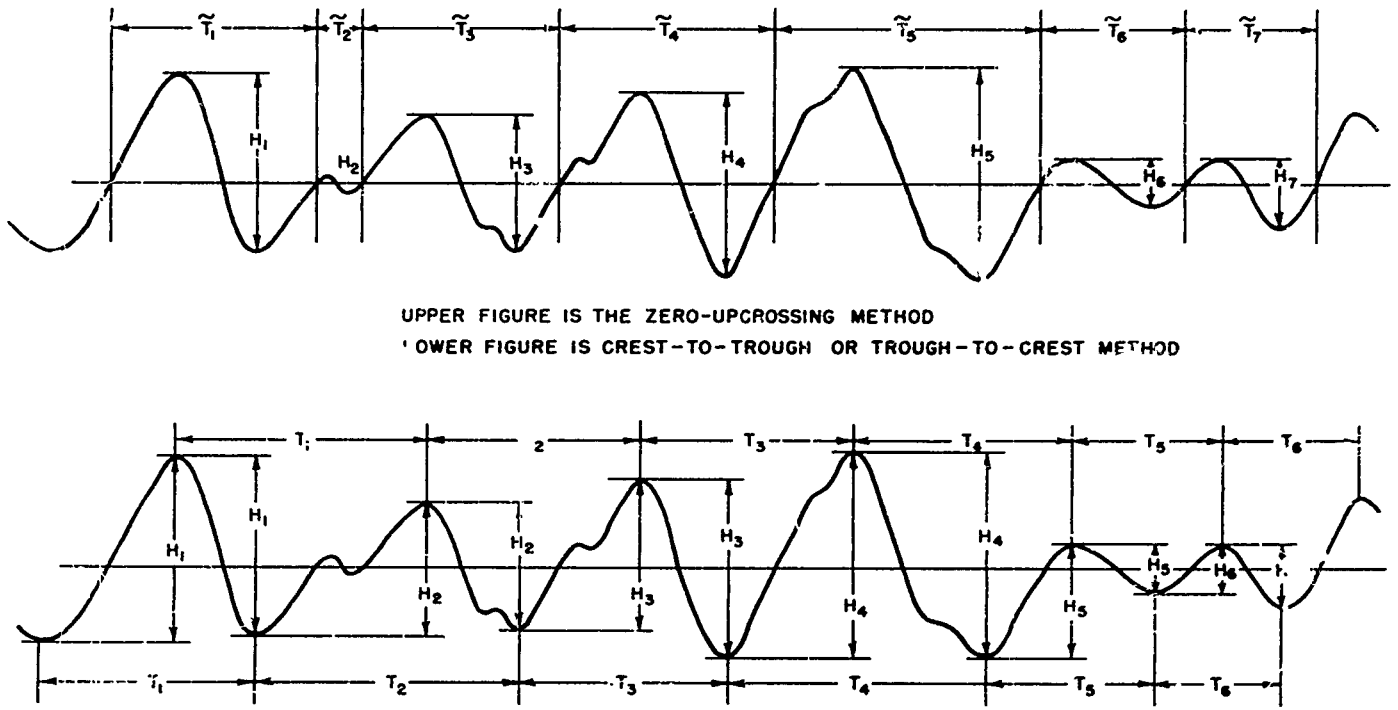

UPPER FIGURE IS THE ZERO-UPCROSSING METHOD

LOWER FIGURE IS CREST-TO-TROUGH OR TROUGH-TO-CREST METHOD

FIGURE 2.6 METHODS OF WAVE RECORD ANALYSES

CHAPTER III: WAVE VARIABILITY AND MARGINAL DISTRIBUTIONS

1. General

Wave variability implies that both the wave amplitudes and periods are constantly changing with respect to time and space as discussed in the preceding section. When H and T are considered together in variance, one speaks of joint distribution. When H and T are considered independently of each other, one speaks of marginal distributions. This chapter is devoted to the marginal distribution functions for wave height, length, and period variability. In order to study each independent variate, it is assumed that the Ergodic theorem applies, which in effect states that a long run average with respect to time is identical to that in space. Previous work on wave height variability and wave period variability are cited in the references.

2. Standard Form and Normal Form

In wave variability, the standard forms of wave characteristics are given in terms of H, T, and L, respectively wave height, wave period, and wave length. Average or arithmetic means are $\overline{H}$, $\overline{T}$, and $\overline{L}$. The normal form is obtained by dividing the standard form by the corresponding means, and by definition

$$\eta = H/\overline{H}$$
$$\tau = T/\overline{T} \qquad (3.1)$$
$$\lambda = L/\overline{L} = T^2/\overline{T^2}$$

These relationships and notations are used extensively throughout the text; a number of operations may be performed on the above equations. For example, it can be verified easily that:

$$\overline{\eta} = \overline{\tau} = \overline{\lambda} = 1.0$$
$$\overline{\eta^2} = \overline{H^2}/(\overline{H})^2 \geq 1.0$$
$$\overline{\tau^2} = \overline{T^2}/(\overline{T})^2 \geq 1.0$$
$$\overline{\lambda^2} = \overline{L^2}/(\overline{L})^2 = \overline{T^4}/(\overline{T^2})^2 \geq 1.0 \qquad (3.2)$$
$$d\eta = \frac{1}{\overline{H}}\, dH$$
$$d\tau = \frac{1}{\overline{T}}\, dT \qquad \text{differentials}$$
$$d\lambda = \frac{1}{\overline{L}}\, dL$$

$$S_H = \bar{H} S_\eta$$

$$S_T = \bar{T} S_\tau \qquad \text{standard deviations}$$

$$S_L = \bar{L} S_\lambda$$

$$\alpha_{3_H} = \alpha_{3_\eta}$$

$$\alpha_{3_T} = \alpha_{3_\tau} \qquad \text{skewness coefficients}$$

$$\alpha_{3_L} = \alpha_{3_\lambda}$$

Other simple operations can be made, but the above are sufficient for the present.

3. Marginal Distribution for Wave Height

Putz Distribution: Based on the analysis of 25 wave records of ocean swell Putz (1952) obtained for wave height variability the gamma type distribution function:

$$F(H) = \frac{1}{\Gamma(p)} \int_0^u x^{p-1} e^{-x}\, dx$$

$$u = p\left[1 + (H - \bar{H})/S_H\right] \qquad (3.3)$$

$$P = \frac{4}{(\alpha_{3_H})^2}$$

where $F(H)$ is the cumulative distribution of H

S_H is the standard deviation of H from the mean

α_{3_H} is the skewness coefficient for H

$\Gamma(p)$ is the gamma function evaluated for the argument x

Putz (19[illegible] presents empirical relationships for the standard deviation and the s[illegible] coefficient as follows:

$$S_H = 0.494\, H + 0.120$$

$$\alpha_{3_H} = 0.80 \qquad (3.4)$$

Eq. (3.3) when evaluated by use of tables for the incomplete gamma functions yields the cumulative distribution. Given the mean height $\bar{H}$, the distribution function predicts the percent of waves equal or less than a given value of H.

Rayleigh Distribution: For wave height variability [Longuet-Higgins (1952) and Watters (1953)] the Rayleigh distribution may [illegible]

written as:

$$p(\eta) = K\eta e^{-B\eta^2} \qquad \text{(See note)}^* \qquad (3.5)$$

Eq. (3.5) will be investigated and compared with that of Putz (1952) and the results of Darlington (1954).

The n^{th} moment about the origin is given by:

$$M_n = \int_0^\infty \eta^n p(\eta)\, d\eta \qquad (3.6)$$

Using the transformation $z = B\eta^2$, $dz = 2\eta B d\eta$, and (3.5) one obtains

$$M_n = \frac{K}{2B} \left(\frac{1}{B}\right)^{\frac{n}{2}} \int_0^\infty z^{\frac{n}{2}} e^{-z}\, dz \qquad (3.7)$$

The integral is that of the gamma function, whence

$$M_n = \frac{K}{2B} \left(\frac{1}{B}\right)^{\frac{n}{2}} \Gamma\left(\frac{n+2}{2}\right) \qquad (3.8)$$

For n = 0 to n = 4 one obtains

$$\begin{aligned} M_0 &= \frac{K}{2B} = 1 \\ M_1 &= \overline{\eta} = 1 \\ M_2 &= \overline{\eta^2} = \frac{4}{\pi} \\ M_3 &= \overline{\eta^3} = \frac{6}{\pi} \\ M_4 &= \overline{\eta^4} = 2\left(\frac{4}{\pi}\right)^2 \end{aligned} \qquad (3.9)$$

*η used by Longuet-Higgins (1952) is from $\eta^2 = \frac{\pi H^2}{2\,\overline{H^2}}$ whereas in this paper $\eta = H/\overline{H}$

From the above the standard deviation skewness coefficient, and kurtosis, respectively, follow

$$\sigma_\eta = \sqrt{\overline{\eta^2} - 1} = 0.5227$$

$$\alpha_{3_\eta} = \frac{\overline{\eta^3} - 3\overline{\eta^2} + 2}{(\sigma_\eta)^3} = 0.6311 \tag{3.10}$$

$$\alpha_{4_\eta} = \frac{\overline{\eta^4} - 4\overline{\eta^3} + 6\overline{\eta^2} - 3}{(\sigma_\eta)^4} = 3.245$$

The Rayleigh distribution (3.5) becomes

$$p(\eta) = \frac{\pi\eta}{2} e^{-\frac{\pi\eta^2}{4}} \tag{3.11}$$

From (3.2) the standard form becomes

$$p(H) = \frac{\pi}{2} \frac{H}{(\overline{H})^2} e^{-\frac{\pi H^2}{4(\overline{H})^2}} \tag{3.12}$$

The cumulative distribution is obtained from

$$P(\eta) = \int_0^\eta p(\eta)\, d\eta = 1 - e^{-\frac{\pi\eta^2}{4}} \tag{3.13}$$

or

in standard form

$$P(H) = 1 - e^{-\frac{\pi H^2}{4(\overline{H})^2}} \tag{3.14}$$

Figure 3.1 is a comparison between (3.3) and (3.14).

Average Wave Height for Heights Greater than a Given Height: It is of interest to know heights of higher waves or the maximum probable height, once the significant waves are forecast. The average of wave heights η_p above a given height η is obtained from:

$$\eta_p = \frac{\int_x^\infty \eta_p(\eta)\, d\eta}{\int_x^\infty p(\eta)\, d\eta} \tag{3.15}$$

Using the Rayleigh type distribution (3.11)

$$\eta_p = \frac{-\int_x^\infty \eta \, d\left(e^{-\frac{\pi\eta^2}{4}}\right)}{-\int_x^\infty d\left(e^{-\frac{\pi\eta^2}{4}}\right)} \tag{3.16}$$

The denominator of (3.16) evaluates at $e^{-\frac{\pi\eta^2}{4}}$, and the numerator may be integrated by parts

$$\int u\,dv = uv - \int v\,du \tag{3.17}$$

Let

$u = \eta \qquad dv = d\left(e^{-\frac{\pi\eta^2}{4}}\right)$

$du = d\eta \qquad v = e^{-\frac{\pi\eta^2}{4}}$, whence

$$\int_x^\infty \eta d\left(e^{-\frac{\pi\eta^2}{4}}\right) = e^{-\frac{\pi\eta^2}{4}} + \int_x^\infty e^{-\frac{\pi\eta^2}{4}}\, d\eta \tag{3.18}$$

or changing the limits

$$\int_x^\infty \eta d\left(e^{-\frac{\pi\eta^2}{4}}\right) = e^{-\frac{\pi\eta^2}{4}} + 1 - \int_0^x e^{-\frac{\pi\eta^2}{4}}\, d\eta \tag{3.19}$$

The remaining integral is the probability integral and can be evaluated by use of tables [Pierce and Foster (1956)] where

$u = \sqrt{\pi/4}\ \eta$ Thus (3.16) becomes

$$\eta_p = \frac{e^{-\frac{\pi\eta^2}{4}} + 1 - \Phi_p}{e^{-\frac{\pi\eta^2}{4}}} \tag{3.20}$$

where

$$\Phi_p = \frac{2}{\sqrt{\pi}} \int_0^x e^{-u^2}\, du \tag{3.21}$$

Representative values of η_p are given in Table 3.1.

TABLE 3.2

MOST PROBABLE MAXIMUM HEIGHTS

N	$\frac{H_{max}}{H_{33}}$	$\eta_{max} = \frac{H_{max}}{\bar{H}}$
10	1.11	1.78
20	1.25	2.00
50	1.42	2.27
100	1.53	2.45
200	1.64	2.62
500	1.77	2.83
1000	1.86	2.98

4. Marginal Distribution for Wave Length

At present no theoretical distribution function has been derived for wave length variability. However, based on empirical data a gamma type distribution function may be developed for wave length variability, which is very similar to the Putz distribution function for wave height variability. In the next chapter on statistical analysis of wave data, it is shown that the distribution function for wave lengths can also be represented by the Rayleigh distribution with the same degree of accuracy as that for wave height variability. Thus

$$p(\lambda) = \frac{\pi}{2}\lambda e^{-\frac{\pi\lambda^2}{4}} \tag{3.22}$$

$$p(L) = \frac{\pi}{2}\frac{L}{(\bar{L})^2} e^{-\frac{\pi L^2}{4(\bar{L})^2}} \tag{3.33}$$

Statistical parameters for λ are the same as those for η .

There may be a physical reason why the Rayleigh type distribution applies for wave length variability as well as for wave height variability, and perhaps a theory may be proposed for such an envolvement. It is not the purpose of this study to develop any such theory, since the data provide sufficient proof that the Rayleigh type distribution is applicable to wave length variability.

5. Marginal Distribution for Wave Period

Putz Distribution: Based on the analysis of 25 ocean wave records of swell, Putz (1952) obtained for wave period variability the gamma type distribution function

$$F(T) = \frac{1}{\Gamma(p)} \int_0^u x^{p-1} e^{-x} dx$$

$$u = p\left[1 + \frac{T - \bar{T}}{S_T}\right] \qquad (3.24)$$

$$p = \frac{4}{(a_{3_T})^2}$$

Where $F(T)$ is the cumulative distribution of T

S_T is the standard deviation in seconds

a_{3_T} is the skewness coefficient

$\Gamma(p)$ is the gamma function evaluated for the argument x.

Putz (1952) relationships for standard deviation and skewness coefficient are given by:

$$S_T = 0.313\,\bar{T} - 0.759$$
$$a_{3_T} = 0.249\,\bar{T} + 2.795 \qquad (3.25)$$

The above relationships are intended for ocean swell. Obviously they fail when $\bar{T}$ is less than about 2.5 seconds. Much of the wind wave data analyzed for the present paper have periods of less than 2.5 seconds.

Period Distribution from the Rayleigh Distribution of Lengths: The marginal distribution function for wave length variability (3.22), can be used to derive a theoretical distribution function for wave period variability by noting

$$p(\tau)\, d\tau = p(\lambda)\, d\lambda \qquad (3.26)$$

A relationship between λ and τ can be defined by

$$\lambda = a\tau^2 \quad , \text{ where} \qquad (3.27)$$

a is a constant to be determined. Using (3.22), (3.26), and (3.27) one obtains

$$p(\tau) = \pi a^2 \tau^3 e^{-\frac{\pi a^2 \tau^4}{4}} \qquad (3.28)$$

Having obtained the form of the distribution function for wave period variability, it becomes necessary to evaluate the factor a and the moments.

The n^{th} moment M_n about the origin becomes

$$M_n = \int_0^\infty \tau^n p(\tau)\, d\tau \tag{3.29}$$

Using the transformation $z = \frac{\pi a^2 \tau^4}{4}$, $dz = \pi a^2 \tau^3 d\tau$, and (3.28) one obtains

$$M_n = \left(\frac{4}{\pi a^2}\right)^{\frac{n}{4}} \int_0^\infty z^{\frac{n}{4}} e^{-z} dz \tag{3.30}$$

The integral of (3.30) is of the gamma form, whence

$$M_n = \left(\frac{4}{\pi a^2}\right)^{\frac{n}{4}} \Gamma\, \frac{n+4}{4} \tag{3.31}$$

Thus

$$\begin{aligned} M_0 &= 1 \\ M_1 &= 1 \\ M_2 &= \overline{\tau^2} = \frac{1}{a} = 1.078715 \\ M_3 &= \overline{\tau^3} = 1.234196 \\ M_4 &= \overline{\tau^4} = 1.481564 \end{aligned} \tag{3.32}$$

From the above the standard deviation, skewness coefficient, and kurtosis, respectively follow:

$$\begin{aligned} \sigma_\tau &= \sqrt{\overline{\tau^2} - 1} = 0.28056 \\ \alpha_{3_\tau} &= \frac{\overline{\tau^3} - 3\overline{\tau^2} + 2}{(\sigma_\tau)^3} = -0.088 \\ \alpha_{4_\tau} &= \frac{\overline{\tau^4} - 4\overline{\tau^3} + 6\overline{\tau^2} - 3}{(\sigma_\tau)^4} = 2.755 \end{aligned} \tag{3.33}$$

For normal distribution $\alpha_3 = 0$ and $\alpha_4 = 3.0$. The distribution function for wave period variability, Eq. (3.28) becomes

$$p(\tau) = 2.7\, \tau^3\, e^{-0.675\, \tau^4} \tag{3.34}$$

or in standard form

$$p(T) = 2.7 \frac{T^3}{(\bar{T})^4} e^{-0.675 \left(\frac{T}{\bar{T}}\right)^4} \tag{3.35}$$

The corresponding cumulative distributions become

$$P(\tau) = 1 - e^{-0.675\, \tau^4} \tag{3.36}$$

$$P(T) = 1 - e^{-0.675 \left(\frac{T}{\bar{T}}\right)^4} \tag{3.37}$$

Figure 3.2 is a comparison between (3.24) and (3.37) for $\bar{T}$ = 10 and 12 seconds. The cumulatives for η based on (3.13) and for τ based on (3.36) are shown in Figure 3.3.

6. Summary of Statistical Parameters

Statistical parameters given above are summarized in Table 3.3, together with the empirical relationships presented by Putz (1952) and Darlington (1954).

TABLE 3.3

SUMMARY OF STATISTICAL PARAMETERS

Reference	Putz (1952)	Darlington (1954)	Longuet-Higgins (1952)	Present Paper (1958)
Standard Deviation				
S_H	$0.49\bar{H} + 0.120$	$0.54\bar{H} - 0.05$ $(0.536\bar{H})^*$	$0.523\bar{H}$	$0.523\bar{H}$
S_T	$0.313\bar{T} - 0.759$	$0.408\bar{T} - 0.676$ $(0.331\bar{T})^*$	-	$0.280\bar{T}$
S_L	-	-	-	$0.523\bar{L}$
Skewness Coefficient				
α_{3_H}	0.80		0.631	0.631
α_{3_T}	$-0.249\bar{T} + 2.795$		-	-0.088
α_{3_L}	-		-	0.631
η_{50}	-		1.418	1.418
η_{33}	1.57	1.603	1.595	1.595
η_{10}	2.03		2.032	2.032
λ_{50}	-		-	1.418
λ_{33}	-		-	1.595
λ_{10}	-		-	2.032

*Least square through the origin.

It is seen from Table 3.3 that the statistical parameters based on theory are in close agreement with those based on data by Putz (1952) and Darlington (1954). Additional verification of these theoretical relationships is presented in the next chapter.

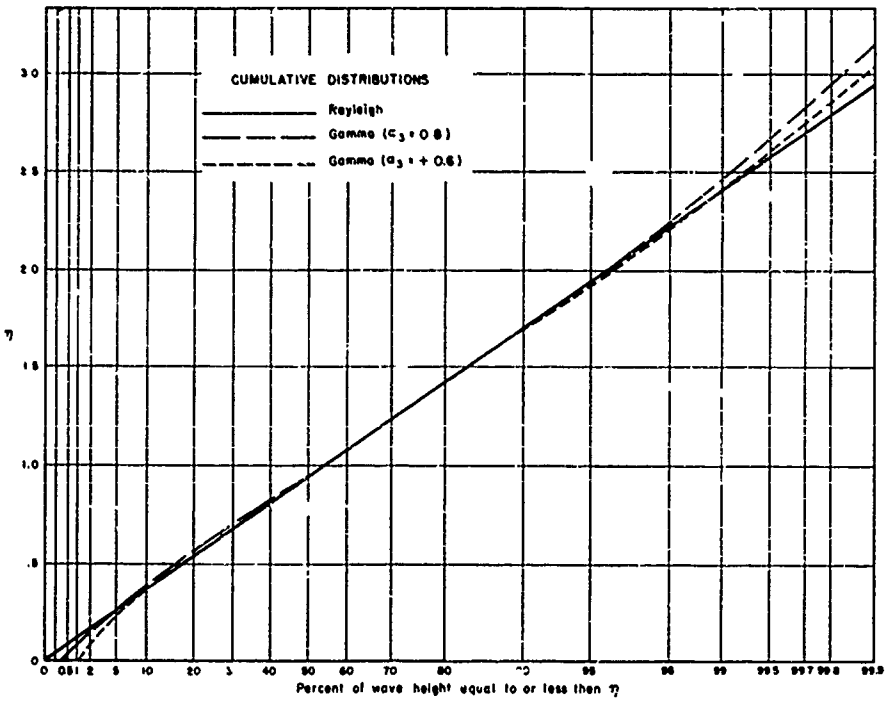

FIGURE 3.1 COMPARISON OF RAYLEIGH DISTRIBUTION WITH GAMMA-TYPE DISTRIBUTION

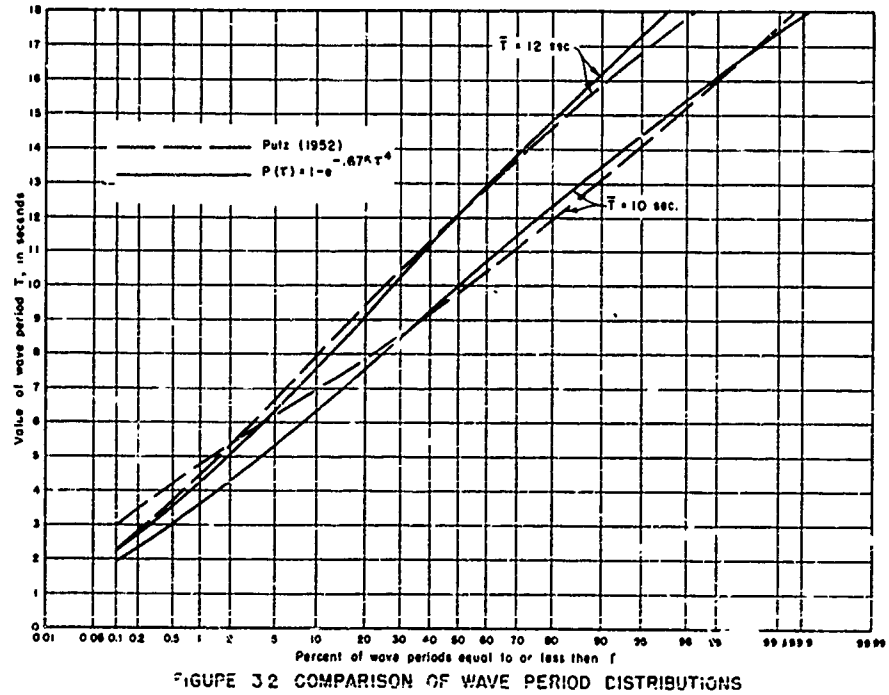

FIGURE 3.2 COMPARISON OF WAVE PERIOD DISTRIBUTIONS

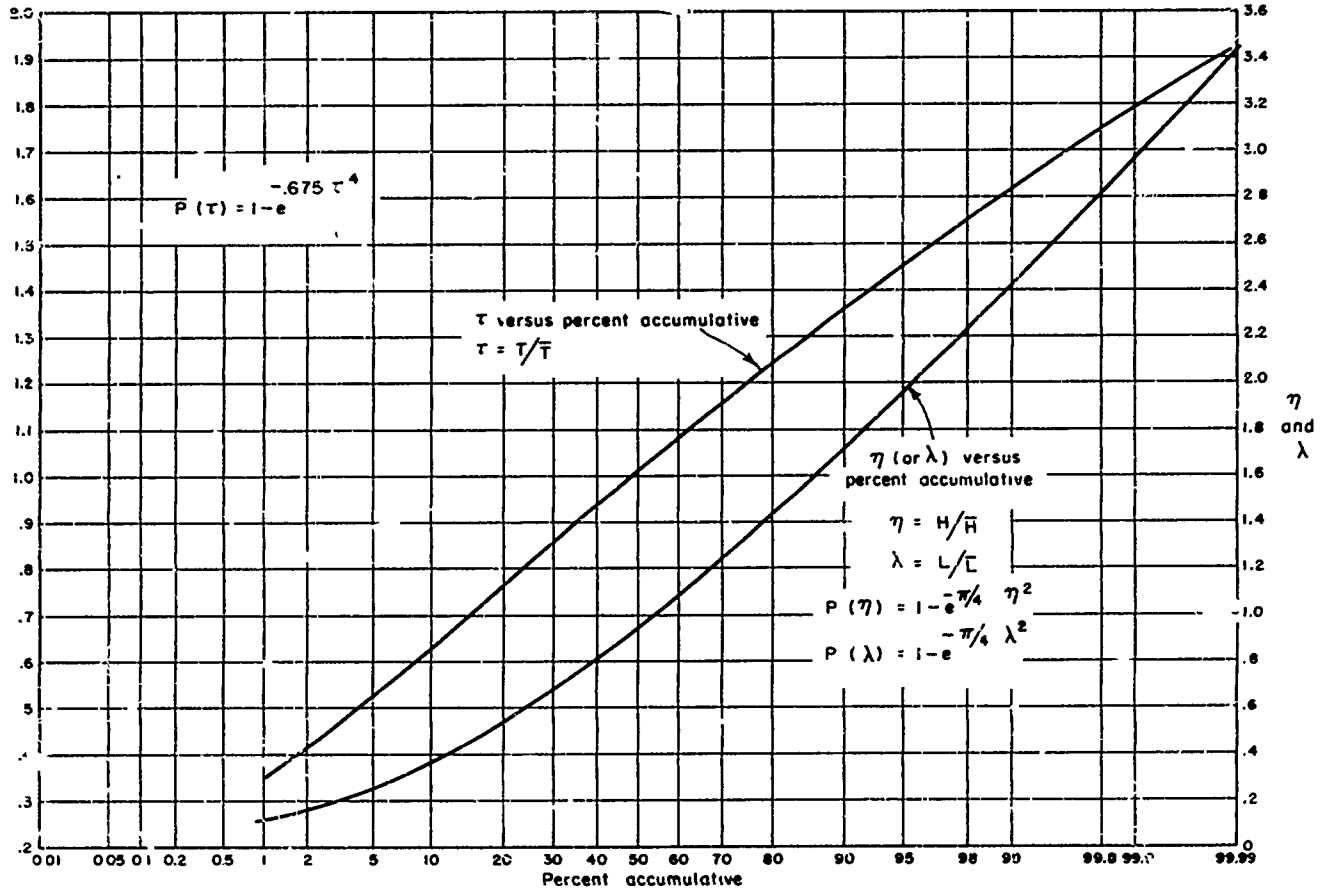

FIGURE 3.3 DISTRIBUTION FUNCTIONS FOR PERIOD VARIABILITY AND HEIGHT VARIABILITY

CHAPTER IV: STATISTICAL ANALYSIS OF WAVE DATA FOR MARGINAL DISTRIBUTIONS

1. General

An abundance of wave records from various sources has been collected and analyzed to determine certain statistical wave parameters which might be compared with the theoretical relationships given in the previous chapter. The source and nature of these data have been discussed in Chapter II.

2. Wave Height Variability

To describe wave height variability, certain statistical parameters are evaluated. These include the mean wave height, mean square wave height, standard deviation from the mean, skewness coefficient, average wave heights for heights greater than a given height, etc. Table 4.1 is a summary of data for wave height variability.

Mean Wave Height: The arithmetic mean wave height is obtained from the analysis of each wave record according to

$$\overline{H} = \frac{1}{N} \sum_{i=1}^{N} H_i \tag{4.1}$$

where $\overline{H}$ is the mean height, H_i the individual wave height, and N the number of waves in the record.

Mean Square Wave Height: The mean square wave height is obtained from

$$\overline{H^2} = \frac{1}{N} \sum_{i=1}^{N} H_i^2 \tag{4.2}$$

and in unit form

$$\overline{\eta^2} = \frac{\overline{H^2}}{(\overline{H})^2} \tag{4.3}$$

Eq. (4.3) is related to the mean wave energy, and $\overline{\eta^2}$ can truly be defined "the energy coefficient."

Standard Deviation from the Mean: The standard (root-mean-square) deviation from the mean wave height is given by

$$S_H = \left[\frac{1}{N} \sum_{i=1}^{N} (H_i - \overline{H})^2 \right]^{\frac{1}{2}} \tag{4.4}$$

The standard deviation from mean height has the dimensions of feet. The unit form of standard deviation is non-dimensional and is given by

$$S_\eta = \sqrt{\overline{\eta^2} - 1} \qquad (4.5)$$

Figure 4.1 shows the relationship of S_H versus $\overline{H}$ for the wave data, together with the theoretical relationship based on the Rayleigh distribution. The relationship based on the Putz (1952) distribution is also shown.

Skewness Coefficient: The skewness coefficient is given by

$$a_{3_H} = \frac{1}{N} \sum_{i=1}^{N} \left(\frac{H_i - \overline{H}}{S_H} \right)^3 \qquad (4.6)$$

The skewness coefficient is a non-dimensional parameter and may be interpreted as a measure of the degree of asymmetry in the distributions, positive and negative values corresponding, respectively, to frequency curves skewed to the right and left. The skewness coefficient has the same numerical value whether in standard or normal form. Figure 4.2 shows a scatter diagram of a_{3H}. The theoretical value of $a_{3H} = 0.631$ is shown by the horizontal line passing approximately through the mean of all data. Based on these data, it is seen that no relationship exists between a_{3H} and $\overline{H}$. The overall mean value of a_{3H} is in close agreement with the Rayleigh distribution.

Average Wave Height for Heights Greater than a Given Height: The average wave height for the highest 50 percent, 33.3 percent, and 10 percent waves have been determined and are summarized in Table 4.1. Figure 4.3 is a plot of data of H_{50} versus $\overline{H}$ together with the theoretical relationship. Similarly, Figure 4.4 is for H_{33} versus $\overline{H}$, and Figure 4.5 is for H_{10} versus $\overline{H}$. The agreement between data and theory is surprisingly good. The scatter of data is greatest for H_{10} versus $\overline{H}$, but this should be expected, since only 8 to 12 waves are used to obtain H_{10}, whereas 30 to 35 are used to obtain H_{33}. Figure 4.6 is the relationship for H_{max} versus $\overline{H}$, where the solid line is based on the most probable $H_{max} = 2.45\overline{H}$ for N = 100 waves.

From the above analysis of wave height variability it can be concluded that the Rayleigh distribution describes wave height variability quite satisfactorily.

TABLE 4.1

SUMMARY OF WAVE HEIGHT DATA

Source and Record	$\overline{H}$ feet	S_H feet	$\overline{\eta^2}$	c_{3_H}	H_{50} feet	H_{33} feet	H_{10} feet	H_{max} feet
a-A	1.50	0.73	1.237	0.77	2.06	2.30	2.78	3.2
a-B	0.65	0.36	1.306	0.69	0.85	1.10	1.46	1.9
a-C	0.95	0.48	1.255	0.48	1.35	1.52	1.90	2.3
a-D	0.87	0.44	1.256	0.80	1.20	1.36	1.80	2.1
a-E	1.92	1.12	1.340	0.60	2.78	3.16	4.14	4.8
a-F	1.82	0.98	1.289	0.31	2.61	2.90	3.71	4.6
a-G	2.22	1.25	1.317	0.78	3.18	3.65	4.69	5.8
a-H	2.07	1.31	1.401	0.62	3.10	3.54	4.36	5.5
a-I	2.73	1.53	1.314	0.46	3.97	4.49	5.72	7.0
a-J	1.13	0.66	1.341	0.70	1.66	1.90	2.50	3.0
a-K	4.29	2.02	1.222	0.66	5.91	6.58	8.37	9.9
a-L	3.19	1.69	1.281	0.44	4.54	5.15	6.41	8.1
a-M	2.87	1.41	1.241	0.41	4.03	4.42	5.34	7.9
a-N	2.62	1.83	1.487	2.23	3.91	4.60	6.85	11.5
a-O	4.63	2.40	1.268	0.48	6.50	7.32	9.22	11.3
a-P	4.62	2.06	1.199	0.47	6.24	6.86	8.78	10.4
a-Q	2.65	1.24	1.219	0.46	3.64	4.07	5.00	6.3
a-R	2.29	1.28	1.312	1.19	3.00	3.73	5.22	8.0
a-S	2.52	1.19	1.223	0.48	3.50	3.91	4.84	5.8
a-T	1.06	0.45	1.181	0.53	1.40	1.55	1.91	2.9
a-U	0.48	0.33	1.473	2.29	0.68	0.60	1.24	2.5
a-V	5.16	2.57	1.248	0.85	7.10	8.11	10.93	12.5
a-W	4.27	1.90	1.198	0.72	5.72	6.38	8.56	10.8
a-X	3.06	1.19	1.151	0.45	4.02	4.40	5.30	6.0
a-Y	0.99	0.45	1.203	2.08	1.34	1.48	1.85	2.4
b- 1	0.78	0.50	1.409	1.11	1.13	1.32	1.92	2.2
b- 2	0.70	0.70	1.306	0.83	1.00	1.14	1.51	1.9
b- 3	1.39	1.00	1.523	0.66	2.21	2.62	3.35	4.0
b- 4	1.54	1.10	1.493	1.93	2.40	2.82	3.69	4.8
b- 5	1.75	1.10	1.418	0.56	2.63	3.02	4.00	5.2
b- 6	1.45	0.93	1.419	2.16	2.20	2.51	3.28	4.6
b- 7	1.58	1.00	1.420	2.03	2.39	2.72	3.52	5.2
b- 8	1.30	0.75	1.337	0.46	1.92	2.18	2.71	3.2
b- 9	1.06	0.63	1.357	0.52	1.57	1.79	2.24	3.0
b-10	0.96	0.70	1.532	1.55	1.46	1.75	2.55	3.6
b-11	1.12	0.63	1.320	0.55	1.64	1.85	2.36	3.0
b-12	1.78	1.00	1.312	0.29	2.58	2.91	3.65	4.4
b-13	1.87	1.10	1.334	0.16	2.78	3.11	3.66	4.2
b-14	1.48	1.00	1.456	0.78	2.25	2.61	3.48	4.7
b-15	1.41	0.85	1.366	0.36	2.12	2.40	2.96	3.8
b-16	1.52	0.88	1.600	-1.48	2.26	2.56	3.17	4.1
b-17	1.61	1.00	1.428	0.68	2.46	2.84	3.74	4.3
b-18	1.54	0.91	1.350	0.10	2.27	2.54	3.14	3.6

TABLE 4.1
(Continued)

SUMMARY OF WAVE HEIGHT DATA

Source and Record	$\bar{H}$ feet	S_H feet	$\overline{\eta^2}$	a_{3_H}	H_{50} feet	H_{33} feet	H_{10} feet	H_{max} feet
b-19	1.76	1.10	1.393	0.57	2.66	3.05	3.85	5.2
b-20	2.03	1.19	1.342	0.05	3.03	3.43	3.98	4.5
C-E-D	0.73	0.51	1.489	0.97	1.13	1.33	1.80	2.4
C-F-D	0.60	0.45	1.563	1.44	0.91	1.13	1.67	2.0
C-G-D	0.90	0.53	1.347	1.08	1.30	1.54	1.93	3.2
C-H-D	0.85	0.47	1.306	-0.43	1.21	1.37	1.92	2.6
C-L-D	1.02	0.57	1.312	0.27	1.49	1.67	1.97	2.6
C-M-D	1.04	0.56	1.289	-0.04	1.49	1.67	1.95	2.4
C-N-D	1.10	0.53	1.232	-0.04	1.51	1.67	2.04	2.4
C-O-D	1.06	0.52	1.231	0.42	1.35	1.59	2.07	2.6
C-P-D	0.82	0.45	1.301	0.59	1.17	1.34	1.72	2.0
C-Q-D	0.81	0.46	1.323	0.54	1.20	1.34	1.65	2.0
C-R-D	1.20	0.82	1.466	1.00	1.83	2.15	2.96	3.8
C-S-D	1.04	0.73	1.493	4.78	1.61	1.87	2.60	3.6
C-T-D	0.64	0.36	1.317	0.87	0.93	1.06	1.35	1.8
C-U-D	0.73	0.45	1.379	0.65	1.09	1.27	1.61	2.0
C-V-D	0.80	0.49	1.376	1.11	1.17	1.37	1.83	2.6
C-W-D	0.77	0.36	1.219	6.72	1.15	1.33	1.77	2.2
C-X-D	0.99	0.57	1.332	-0.14	1.45	1.66	2.09	2.4
C-Y-D	0.91	0.53	1.339	0.98	1.29	1.50	2.02	3.0
d- 1	3.27	1.57	1.23	-0.18	4.52	4.98	6.32	7.5
d- 2	3.48	1.82	1.27	-0.07	4.99	5.59	6.71	8.5
d- 3	2.57	1.24	1.24	0.65	3.54	3.92	5.10	6.6
d- 4	2.36	1.34	1.33	1.14	3.30	3.75	5.12	7.5
e- 1	2.65	1.16	1.193	0.31	3.56	3.94	4.88	5.63
e- 2	3.14	1.35	1.185	0.40	4.25	4.69	5.56	7.13
e- 3	2.94	1.05	1.127	0.95	3.81	4.19	5.06	6.00
e- 4	2.85	1.33	1.216	0.53	3.88	4.31	5.44	8.88
e- 5	3.11	1.39	1.199	-1.14	4.25	4.69	5.75	6.00
e- 6	3.75	1.68	1.200	0.46	5.13	5.69	6.94	8.62
e- 7	3.65	1.46	1.161	0.88	4.88	5.31	6.44	8.63
e- 8	4.34	1.90	1.192	0.83	5.81	6.50	8.19	10.0
e- 9	4.38	1.83	1.174	0.70	5.81	6.44	8.00	10.4
e-10	4.60	2.03	1.194	0.75	6.13	6.81	8.81	11.8
e-11	5.44	2.45	1.203	0.57	7.44	8.31	10.25	11.8
e-12	4.90	2.26	1.213	0.64	6.75	7.56	9.31	11.0
e-13	4.78	2.04	1.182	0.48	6.44	7.13	8.69	10.1
e-14	4.40	2.13	1.233	0.73	5.66	6.81	8.81	10.3
e-15	4.85	2.19	1.203	0.38	6.56	7.38	9.13	10.4

TABLE 4.1
(Continued)

SUMMARY OF WAVE HEIGHT DATA

Source and Record	$\bar{H}$ feet	S_H feet	$\overline{\eta^2}$	a_{3_H}	H_{50} feet	H_{33} feet	H_{10} feet	H_{max} feet
e-1 to 5	2.94	1.28	1.18	0.25	3.94	4.38	5.31	8.88
e-6 to 10	4.14	1.84	1.18	0.75	5.56	6.19	7.69	11.8
e-11 to 15	4.88	2.24	1.21	0.55	6.63	7.44	9.25	11.8
e-1 to 10	3.54	1.65	1.18	-	4.75	5.25	6.50	11.8
e-6 to 15	4.51	2.03	1.20	-	6.13	6.81	8.44	11.8
e-16	4.08	1.86	1.21	1.56				
e-17	5.42	2.29	1.18	0.71	7.22	8.00	9.86	14.6
f- 1	10.7	5.20	1.23	-4.72	15.1	16.7	20.1	24.8
f- 2	11.7	5.70	1.24	1.00	16.2	17.6	21.0	28.1
f- 3	11.3	4.80	1.18	0.64	15.0	16.6	20.8	25.5
g-24	0.038	0.011	1.12	-	0.046	0.052	0.062	0.063
g-15	0.103	0.053	1.27	-	0.145	0.157	0.170	0.176
g-31	0.098	0.038	1.15	-	0.126	0.139	0.167	0.171
g-25	0.055	0.022	1.16	-	0.071	0.078	0.091	0.097
g-35	0.077	0.030	1.15	-	0.100	0.119	0.128	0.136

3. Wave Length Variability

To describe wave length variability for comparison with the Rayleigh distribution, certain statistical parameters are evaluated. These include the mean wave length, mean square wave length, standard deviation from the mean, skewness coefficient, average wave length for lengths greater than a given length, etc. The wave length is not a measured quantity, but computed from theory. In the present analysis the deep water wave length, whether in deep or shallow water, is given according to the Airy theory (Lamb).

$$L_0 = \frac{g T^2}{2\pi} \tag{4.7}$$

It was found that the Rayleigh distribution applied in shallow water only when the deep water wave length and not the shallow water wave length was used. For the convenience of analysis the factor $g/2\pi$ was omitted and the subscript o for deep water was also omitted. Thus for this paper the deep water wave length is defined by

$$L = T^2 (\text{sec}^2) \tag{4.8}$$

To obtain the actual deep water wave length in feet (4.8) must be multiplied by $g/2\pi$. Table 4.2 is a summary of data for wave length variability, using $L = T^2$.

Mean Wave Length: The arithmetic mean wave length is obtained from the analysis of each wave record according to:

$$\bar{L} = \frac{1}{N} \sum_{i=1}^{N} L_i = \frac{1}{N} \sum_{i=1}^{N} T_i^2 \qquad (4.9)$$

Mean Square Wave Length: The mean square wave length is obtained from

$$\bar{L}^2 = \frac{1}{N} \sum_{i=1}^{N} L_i^2 = \frac{1}{N} \sum_{i=1}^{N} \left(T_i^2\right)^2 \qquad (4.10)$$

and in unit form

$$\overline{\lambda^2} = \frac{\overline{L^2}}{(\bar{L})^2} = \frac{\overline{T^4}}{(\overline{T^2})^2} \qquad (4.11)$$

Standard Deviation from the Mean: The standard (root-mean-square) deviation from the mean is given by

$$S_L = \frac{1}{N} \left[\sum_{i=1}^{N} (L_i - \bar{L})^2 \right]^{\frac{1}{2}}, \text{ sec.}^2 \qquad (4.12)$$

The standard deviation from mean length in general has the dimensions of feet, but since period squared is used for length, the dimensions are seconds squared. The unit form of standard deviation is non-dimensional and given by

$$S_\lambda = \sqrt{\bar{\lambda}^2 - 1} \tag{4.13}$$

Figure 4.7 shows the relationship of S_L versus $\bar{L}$ for the wave data, together with the theoretical relationship based on the Rayleigh distribution. The agreement here is quite satisfactory.

Skewness Coefficient: The skewness coefficient is given by

$$\alpha_{3_L} = \frac{1}{N} \sum_{i=1}^{N} \left(\frac{L_i - \bar{L}}{S_L} \right)^3 \tag{4.14}$$

Figure 4.8 shows a scatter diagram of α_{3L} versus mean wave length $\bar{L}$ (seconds squared). The theoretical value of $\alpha_{3L} = 0.631$ is shown by the horizontal line passing approximately through the mean of all data.

Average Wave Length for Lengths Longer than a Given Length: The average wave length for the longest 50 percent lengths, 33.3 percent lengths, and 10 percent lengths have been determined and are summarized in Table 4.2. Figure 4.9 is a plot of data for L_{50} versus $\bar{L}$, together with the theoretical relationship based on the Rayleigh distribution. Similarly Figures 4.10 and 4.11, respectively are for L_{33} versus $\bar{L}$ and L_{10} versus $\bar{L}$. The agreement between data and theory is surprisingly good, and is comparable to that for wave height variability. Figure 4.12 is the relationship for $L_{max} = 2.45\bar{L}$ for N = 100 waves.

From the above analysis of wave length variability it can be concluded that the Rayleigh distribution describes wave length variability quite satisfactorily.

TABLE 4.2

SUMMARY OF DEEP WATER WAVE LENGTH DATA
(Note: $L = T^2$ for convenience)

Source and Record	$\bar{L}$ sec^2	S_L sec^2	$\overline{\lambda^2}$	a_{3_L}	L_{50} sec^2	L_{33} sec^2	L_{10} sec^2	L_{max} sec^2
a-A	201	116	1.333	0.30	293	319	408	576
a-B	149	114	1.587	0.64	248	287	357	484
a-C	207	105	1.257	-0.17	288	306	354	441
a-D	218	79	1.132	-0.50	280	293	337	400
a-E	193	85	1.194	0.56	258	287	354	441
a-F	166	70	1.178	0.38	221	239	300	324
a-G	181	89	1.243	0.78	248	276	371	484
a-H	111	48	1.187	1.26	146	169	212	324
a-I	112	43	1.135	0.32	150	161	202	256
a-J	98	58	1.350	1.53	141	162	232	289
a-K	141	61	1.187	0.90	185	205	280	324
a-L	133	65	1.238	0.66	185	207	260	324
a-M	137	63	1.212	0.76	185	205	273	324
a-N	128	72	1.315	0.57	187	215	268	324
a-O	194	102	1.278	0.24	278	310	381	441
a-P	193	90	1.216	0.19	265	296	347	400
a-Q	88	38	1.185	1.26	117	126	165	256
a-R	98	47	1.229	0.82	133	148	194	361
a-S	106	44	1.172	0.44	141	160	194	196
a-T	98	45	1.212	1.52	130	145	198	289
a-U	122	55	1.205	1.26	162	180	241	361
a-V	145	57	1.154	0.18	189	209	248	289
a-W	134	76	1.324	0.52	197	221	274	400
a-X	132	52	1.154	0.26	172	186	228	256
a-Y	213	105	1.242	0.37	294	325	403	576
b- 1	4.80	2.44	1.259	1.62	6.54	7.4	10.8	13.0
b- 2	4.57	2.48	1.295	0.56	6.56	7.2	9.6	11.6
b- 3	5.98	3.26	1.296	0.43	8.50	9.7	12.3	14.4
b- 4	7.38	4.21	1.325	0.11	10.81	12.2	14.5	18.5
b- 5	7.61	5.39	1.500	0.90	11.85	14.1	18.4	23.0
b- 6	6.49	4.89	1.566	1.34	9.99	12.1	17.5	23.0
b- 7	6.83	4.47	1.429	0.64	10.41	12.1	15.2	23.0
b- 8	5.68	3.69	1.422	0.33	8.38	9.7	13.4	16.8
b- 9	4.82	3.74	1.602	2.46	7.3	8.6	12.9	23.0
b-10	4.83	2.93	1.369	1.17	7.1	8.0	11.5	13.0
b-11	6.40	4.25	1.442	-0.54	9.0	10.4	14.5	19.4
b-12	9.01	5.73	1.404	1.09	13.3	15.5	22.0	24.0
b-13	7.34	4.07	1.307	0.88	10.5	11.8	15.5	24.0
b-14	6.21	3.93	1.400	0.87	9.2	10.7	14.6	19.4
b-15	7.50	4.84	1.417	1.34	10.8	13.1	18.5	24.0
b-16	6.46	4.10	1.403	1.33	9.5	11.1	15.2	19.4
b-17	7.90	5.51	1.487	1.18	12.1	14.2	19.5	24.0
b-18	6.94	4.47	1.414	1.39	10.1	12.0	16.4	24.0

TABLE 4.2
(Continued)

SUMMARY OF DEEP WATER WAVE LENGTH DATA

Source and Record	$\bar{L}$ sec^2	S_L sec^2	$\bar{\lambda}^2$	α_{3_L}	L_{50} sec^2	L_{33} sec^2	L_{10} sec^2	L_{max} sec^2
b-19	7.10	5.74	1.654	2.50	11.0	13.2	19.3	41.0
b-20	7.86	4.76	1.367	2.16	11.8	13.7	19.0	24.0
C-E-D	4.49	2.55	1.323	1.74	6.4	7.2	10.0	13.0
C-F-D	3.68	2.12	1.318	0.29	5.3	6.0	7.5	9.6
C-G-D	6.66	2.82	1.179	0.08	9.0	9.[illegible]	11.7	12.3
C-H-D	5.98	2.59	1.187	0.50	8.0	8.9	11.1	12.3
C-L-D	7.20	4.09	1.323	1.82	10.4	12.1	16.0	23.0
C-M-D	7.06	3.90	1.305	0.58	10.1	11.6	14.3	18.5
C-N-D	6.49	3.42	1.278	0.30	9.3	10.5	12.5	16.0
C-O-D	7.06	4.48	1.403	0.79	10.6	12.4	15.9	21.2
C-P-D	5.65	2.58	1.205	1.20	7.5	8.4	11.3	13.7
C-Q-D	5.85	3.08	1.277	0.83	8.2	9.3	12.2	16.0
C-R-D	7.66	3.32	1.187	8.27	11.3	12.9	16.8	23.0
C-S-D	6.69	4.03	1.361	-0.33	10.0	11.4	14.7	21.2
C-T-D	3.99	1.73	1.188	0.09	5.6	6.3	7.1	9.0
C-U-D	3.78	1.55	1.168	0.53	5.0	5.5	6.6	9.6
C-V-D	5.61	3.34	1.354	1.14	7.7	8.7	12.7	18.5
C-W-D	5.10	2.93	1.331	0.93	7.3	8.3	11.7	14.4
C-X-D	4.35	1.98	1.207	0.45	5.9	6.6	8.0	9.6
C-Y-D	4.89	1.91	1.153	4.11	6.2	7.0	9.0	14.4
d- 1	13.2	10.4	1.63	0.97	20.7	24.9	34.3	41.0
d- 2	18.7	13.5	1.52	1.75	28.8	33.6	44.7	81.0
d- 3	21.3	14.3	1.45	1.03	32.3	37.9	51.1	70.6
d- 4	24.6	13.8	1.27	1.80	36.0	40.8	51.5	64.0
e- 1	27.6	10.2	1.137	-0.54	35.7	45.5	38.4	51.8
e- 2	26.8	13.8	1.265	1.75	33.6	36.5	43.4	59.3
e- 3	30.0	10.0	1.116	3.87	37.8	40.5	46.9	53.3
e- 4	27.5	14.1	1.263	0.79	38.5	43.1	55.2	82.8
e- 5	29.1	15.1	1.270	0.13	41.3	46.5	59.0	74.0
e- 6	24.1	11.9	1.244	1.07	33.4	38.4	48.3	59.3
e- 7	22.4	9.9	1.194	5.19	30.8	34.8	46.0	67.2
e- 8	24.6	[illegible].9	1.162	2.42	31.7	34.8	45.9	60.8
e- 9	23.3	8.9	1.146	-0.11	29.9	32.8	39.6	44.9
e-10	22.2	9.6	1.187	0.91	29.4	32.8	43.6	50.4
e-11	23.8	8.7	1.134	-0.16	30.1	32.8	41.3	53.3
e-12	24.6	8.5	1.119	1.19	31.5	34.6	42.5	50.4
e-13	24.9	10.2	1.168	0.58	32.5	35.9	45.4	56.3
e-14	24.3	11.8	1.235	-0.77	33.5	38.3	48.7	56.3
e-15	24.9	8.8	1.125	1.14	30.5	33.3	39.8	49.0

TABLE 4.2
(Continued

SUMMARY OF DEEP WATER WAVE LENGTH DATA

Source and Record	$\bar{L}$ sec^2	S_L sec^2	$\overline{\lambda^2}$	a_{3_H}	L_{50} sec^2	L_{33} sec^2	L_{10} sec^2	L_{max} sec^2
e- 1 to 5	28.2	12.8	1.210	1.20	37.4	42.4	48.6	61.2
e- 6 to 10	23.3	10.1	1.186	1.90	31.0	34.7	44.7	56.5
e-11 to 15	24.5	9.7	1.156	0.40	34.9	34.9	43.5	53.1
e- 1 to 10	25.8	11.5	1.198	1.55	34.2	38.6	46.7	60.4
e- 6 to 15	23.9	9.9	1.171	1.15	33.0	34.8	44.1	51.9
e-16	22.0	11.2	1.26	0.83				
e-17	39.3	17.5	1.20	1.00	51.9	57.9	74.2	123.2
f- 1	62.2	42.0	1.59	0.97	99	121	163	207
f- 2	66.0	56.7	1.74	1.86	106	128	187	342
f- 3	75.1	52.7	1.50	0.34	115	134	190	289
g-24			1.11					
g-15			1.17					
g-31			1.31					
g-25			1.16					
g-35			1.15					

4. Wave Period Variability

A distribution function for wave period variability was derived in Chapter III from the Rayleigh distribution for wave length variability. For verification of this distribution function and comparison with that given by Putz (1952), certain statistical parameters are evaluated. These include the mean period, mean square wave period, standard deviation from the mean and the skewness coefficient. Table 4.3 is a summary of data for wave period variability.

Mean Wave Period: The arithmetic mean wave period is obtained from the analysis of each wave record according to

$$\bar{T} = \frac{1}{N} \sum_{i=1}^{N} T_i \qquad (4.15)$$

where $\overline{T}$ is the mean period, T_i the individual period, and N the number of waves in the record. Evidently the length of record in seconds is $t = N\overline{T}$.

Mean Square Wave Period: The mean square wave period is obtained from

$$\overline{T^2} = \frac{1}{N}\sum_{i=1}^{N} T_i^2 \tag{4.16}$$

and in unit form

$$\overline{\tau^2} = \frac{\overline{T^2}}{(\overline{T})^2} \tag{4.17}$$

Standard Deviation from the Mean: The standard (root-mean-square) deviation from the mean is given by

$$S_T = \frac{1}{N}\left[\sum_{i=1}^{N} (T_i - \overline{T})^2\right]^{\frac{1}{2}} \tag{4.18}$$

The standard deviation from mean period has the dimensions of seconds. The unit form of standard deviation is non-dimensional and is given by

$$S_\tau = \sqrt{\overline{\tau^2} - 1} \tag{4.19}$$

Figure 4.13 shows the relationship of S_T versus $\overline{T}$ for the wave data, together with the theoretical relationship based on the distribution function for wave period variability derived from the Rayleigh distribution of lengths. The agreement here is quite satisfactory. The relationship presented by Putz (1952) is also shown, but is not in agreement for the wind wave data.

Skewness Coefficient: The skewness coefficient is given by

$$\alpha_{3_H} = \frac{1}{N}\sum_{i=1}^{N}\left[\frac{T_i - \overline{T}}{S_T}\right]^3 \tag{4.20}$$

Figure 4.14 shows a scatter diagram of α_{3T} versus mean wave period $\overline{T}$. The theoretical value of $\alpha_{3T} = -0.088$ is shown by the horizontal line passing approximately through the mean of all data. The relationship given by Putz (1952) is also given. Figure 4.14 shows no relationship between α_{3T} and $\overline{T}$. The scatter of data appears great, but it must be remembered that 100 waves are too few in number to expect a minimum of scatter in the skewness coefficient, and that the overall average is more significant.

TABLE 4.3

SUMMARY OF WAVE PERIOD DATA

Source and Record	$\bar{T}$ sec	S_T sec	$\overline{\tau^2}$	α_3	$T(H_{50})$ se	$T(H_{33})$ sec	$T(H_{10})$ sec	$T(H_{max})$ sec
a-A	13.4	4.62	1.119	-0.53	17.4	15.7	15.4	15
a-B	11.2	4.84	1.187	0.25	14.0	15.2	15.5	16
a-C	13.7	4.38	1.109	-0.91	15.9	16.2	16.3	16
a-D	14.4	3.21	1.050	-1.18	15.6	15.9	15.8	18
a-E	13.5	3.21	1.057	-0.26	14.7	14.4	14.2	14
a-F	12.6	2.65	1.044	-0.32	14.1	14.3	13.7	12
a-G	13.0	3.41	1.069	-0.41	14.0	14.0	14.8	14
a-H	10.3	2.26	1.048	0.38	10.6	10.7	10.9	11
a-I	10.6	2.07	1.038	-0.13	10.8	10.9	11.0	11
a-J	9.5	2.77	1.085	0.54	9.7	9.5	9.2	10
a-K	11.6	2.57	1.049	0.21	11.7	11.7	11.7	12
a-L	11.2	2.77	1.061	0.24	11.8	11.7	11.4	11
a-M	11.4	2.63	1.053	-0.20	11.8	11.8	12.0	12
a-N	10.9	3.08	1.080	0.37	10.8	9.8	8.1	10
a-O	13.4	3.74	1.078	-0.15	14.8	13.9	13.1	10
a-P	13.5	3.33	1.061	-0.15	13.9	14.3	12.9	12
a-Q	9.2	1.95	1.045	0.16	9.3	9.3	9.7	10
a-R	9.7	2.02	1.043	0.61	9.7	9.6	9.4	10
a-S	10.1	1.97	1.038	-0.05	9.9	10.1	9.3	11
a-T	9.7	1.92	1.039	0.72	9.4	9.4	9.4	9
a-U	10.4	3.65	1.123	0.63	10.5	10.3	9.8	2
a-V	11.8	2.41	1.042	-1.21	12.3	12.2	12.3	12
a-W	11.0	3.54	1.104	-0.33	11.8	12.3	12.8	12
a-X	11.3	2.12	1.035	-0.44	11.3	11.2	11.2	12
a-Y	14.1	3.82	1.073	-0.67	14.5	14.7	13.6	14
b- 1	2.13	0.51	1.057	0.71	2.29	2.25	1.97	1.9
b- 2	2.07	0.54	1.067	2.35	2.30	2.31	2.31	3.1
b- 3	2.34	0.71	1.091	0.03	2.61	2.67	2.81	2.2
b- 4	2.59	0.82	1.099	0.32	2.99	3.30	2.93	2.9
b- 5	2.56	1.03	1.161	0.15	3.04	3.18	2.93	2.6
b- 6	2.38	0.91	1.146	0.54	2.88	2.83	2.95	2.9
b- 7	2.46	0.88	1.128	0.22	2.95	3.06	3.08	2.9
b- 8	2.30	0.62	1.073	4.00	2.52	2.50	2.37	2.2
b- 9	2.07	0.73	1.126	1.11	2.31	2.17	2.21	1.2
b-10	2.09	0.68	1.105	0.03	2.38	2.35	2.24	2.2
b-11	2.44	0.67	1.075	0.48	2.62	2.62	2.25	2.7
b-12	2.85	0.94	1.109	0.25	3.20	3.08	3.16	4.4
b-13	2.60	0.76	1.085	0.02	2.93	2.89	2.83	3.2
b-14	2.36	0.80	1.114	0.26	2.75	2.79	2.85	2.7
b-15	2.61	0.83	1.101	0.63	2.98	3.14	3.21	2.5
b-16	2.42	0.77	1.102	0.03	2.84	2.78	2.66	3.0
b-17	2.65	0.94	1.125	0.45	3.11	3.26	3.23	3.7
b-18	2.50	0.83	1.110	0.27	2.89	2.86	2 94	2.5

TABLE 4.3
(Continued)

SUMMARY OF WAVE PERIOD DATA

Source and Record	$\bar{T}$ sec	S_T sec	$\overline{T^2}$	a_3	$T(H_{50})$ sec	$T(H_{33})$ sec	$T(H_{10})$ sec	$T(H_{max})$ sec
b-19	2.49	0.95	1.145	0.91	2.83	2.78	2.81	2.5
b-20	2.64	0.94	1.127	0.22	3.09	3.09	3.23	2.7
C-E-D	2.02	0.64	1.100	-0.29	2.26	2.30	2.24	2.0
C-F-D	1.85	0.51	1.076	2.67	2.10	2.16	2.15	2.1
C-G-D	2.52	0.57	1.051	-0.44	2.60	2.60	2.62	2.4
C-H-D	2.38	0.57	1.057	-0.79	2.47	2.53	2.40	2.0
C-L-D	2.57	0.77	1.090	2.06	2.79	2.75	2.73	2.6
C-M-D	2.54	0.78	1.094	-0.23	2.77	2.72	3.05	4.2
C-N-D	2.43	0.77	1.100	-0.93	2.80	2.68	2.85	3.5
C-O-D	2.51	0.87	1.120	0.36	2.95	2.91	2.76	2.8
C-P-D	2.31	0.56	1.059	-0.44	2.42	2.34	2.42	2.3
C-Q-D	2.34	0.61	1.068	0.68	2.61	2.60	2.63	2.4
C-R-D	2.63	0.86	1.107	-0.03	3.08	3.09	3.21	2.7
C-S-D	2.47	0.77	1.097	0.34	2.95	3.11	2.97	2.7
C-T-D	1.94	0.48	1.061	-0.70	2.08	2.09	2.17	2.3
C-U-D	1.90	0.44	1.054	-1.87	2.06	2.06	2.15	2.1
C-V-D	2.27	0.68	1.090	0.43	2.48	2.39	2.35	2.8
C-W-D	2.16	0.66	1.094	-0.17	2.38	2.43	2.46	2.7
C-X-D	2.02	0.52	1.066	-0.08	2.18	2.24	2.32	2.3
C-Y-D	2.14	0.56	1.069	-1.97	2.33	2.33	2.45	2.3
d- 1	3.38	1.33	1.15	0.18	3.98	4.11	4.74	5.0
d- 2	4.02	1.46	1.13	0.31	4.86	5.21	4.85	4.0
d- 3	4.35	1.54	1.13	1.96	5.01	5.12	5.61	7.0
d- 4	4.72	1.53	1.11	0.29	5.15	5.30	5.98	6.0
e- 1	5.15	1.03	1.040	1.11	5.14	5.11	4.97	5.1
e- 2	5.07	1.04	1.042	-1.57	5.26	5.20	5.32	5.3
e- 3	5.38	1.01	1.035	2.04	5.13	5.01	4.89	3.5
e- 4	5.08	1.32	1.068	0.55	4.76	4.84	4.51	4.7
e- 5	5.03	1.94	1.149	-0.87	4.53	4.68	4.25	3.3
e- 6	4.76	1.20	1.064	1.11	4.54	4.41	4.62	4.3
e- 7	4.51	1.45	1.104	-2.85	4.37	4.19	4.23	4.4
e- 8	4.86	0.97	1.040	0.47	4.57	4.50	4.38	4.6
e- 9	4.74	0.90	1.036	1.08	4.78	4.76	4.78	4.5
e-10	4.60	1.03	1.050	0.43	4.52	4.51	4.75	4.6
e-11	4.79	0.91	1.036	-0.36	4.79	4.76	4.84	4.7
e-12	4.83	1.14	1.056	-3.40	4.69	4.69	4.89	5.1
e-13	4.87	1.07	1.048	-0.47	4.92	4.90	5.04	5.0
e-14	4.77	1.26	1.070	-0.61	4.62	4.59	4.55	4.3
e-15	4.90	0.94	1.037	-0.51	4.78	4.79	4.87	4.8

TABLE 4.3
(Continued)

SUMMARY OF WAVE PERIOD DATA

Source and Record	$\bar{T}$ sec	S_T sec	$\overline{\tau^2}$	a_3	$T(\bar{\eta})$ sec	$T(H_{33})$ sec	$T(H_{10})$ sec	$T(H_{max})$ sec
e- 1 to 5	5.14	1.33	1.066	-0.35	4.96	4.97	4.79	5.3
e- 6 to 10	4.69	1.15	1.060	-0.87	4.56	4.47	4.55	4.6
e-11 to 15	4.83	1.08	1.050	-1.91	4.76	4.75	4.84	5.1
e- 1 to 10	4.92	1.24	1.063	-0.44	4.76	4.72	4.67	5.3
e- 6 to 15	4.76	1.12	1.055	-1.31	4.66	4.61	4.70	5.1
e-16	4.57	1.01	1.053	0.76				
e-17	6.11	1.39	1.052	0.01				
f- 1	7.29	3.00	1.17	0.027	9.10	9.60	10.1	9.4
f- 2	7.45	3.25	1.19	0.615	9.00	9.10	8.0	6.8
f- 3	8.16	2.93	1.13	0.456	9.51	9.70	8.2	10.0
g-24	0.40	0.08	1.039		0.39	0.41	0.40	0.34
g-15	0.54	0.22	1.17		0.67	0.68	0.70	0.78
g-31	0.63	0.15	1.055		0.59	0.61	0.70	0.76
g-25	0.47	0.10	1.049		0.48	0.47	0.40	0.31
g-35	0.53	0.10	1.052		0.55	0.58	0.58	0.64

5. Least Squares Relationships

If it is definitely known that the origin is a point on the curve, the straight line to be fitted has the form of $y = mx$, where m is the slope of the line. It can be shown by least squares condition that $m = \Sigma xy / \Sigma x^2$. Applying these conditions to the relationships presented earlier, one obtains

$$S_\eta = \frac{\Sigma S_{\eta} H}{\Sigma H^2} \qquad \eta_p = \frac{\Sigma H_p H}{\Sigma H^2}$$

$$S_\lambda = \frac{\Sigma S_L L}{\Sigma L^2} \qquad \lambda_p = \frac{\Sigma L_p L}{\Sigma L^2} \qquad (4.21)$$

$$S_\tau = \frac{\Sigma S_T T}{\Sigma T^2}$$

Table 4.4 presents the least squares relationships through the origin for the above parameters, based on data for each source taken separately and also for all sources of data taken together. In addition, the weighted mean values, weighted in accordance with the number of records, are given. For example

$$\overline{S_\eta} = \frac{1}{N} \Sigma f_i S_\eta$$

$$\overline{\eta_p} = \frac{1}{N} \Sigma f_i \eta_p \qquad (4.22)$$

Where $\overline{S_\eta}$ is the weighted mean of standard deviations, N = 85 records, f_i is the number of records for individual sources corresponding to S_η given in Table 4.4.

There is fairly good agreement between theory and the data shown in Table 4.4.

TABLE 4.4

LEAST SQUARES RELATIONSHIPS THROUGH ORIGIN

Source	a	b	c	d	e	f	a-f	Weighted** Mean	Theory
No. Records	25	20	18	4	15	3	85		
S_η	0.499	0.624	0.585	0.512	0.441	0.466	0.477	0.536	0.522
S_λ	0.481	0.547	0.542	0.785	0.425	0.744	0.486	0.546	0.522
η_{50}	1.386	1.502	1.451	1.411	1.345	1.373	1.377	1.421	1.420
λ_{50}	1.377	1.481	1.414	1.822	1.316	1.572	1.381	1.426	1.420
η_{33}	1.561	1.716	1.635	1.570	1.504	1.510	1.534	1.602	1.598
λ_{33}	1.520	1.718	1.604	2.102	1.475	1.878	1.528	1.616	1.598
η_{10}	2.016	2.159	2.170	1.928	1.867	1.846	1.911	2.046	2.03
λ_{10}	1.895	2.362	2.060	2.720	1.793	2.651	1.911	2.087	2.03
η_{max}	2.520	2.746	2.839	2.473	2.280	2.327	2.388	2.589	2.45*
λ_{max}	2.425	3.203	2.715	3.832	2.281	4.122	2.460	2.770	2.45*
S_τ	0.241	0.296	0.263	0.314	0.221	0.306	0.246	0.261	0.281

*Most probable maximum based on N = 100.
**Weighted in accordance with number of records for each source.

6. Relationships Between Wave Period Variability and Wave Length Variability

A relationship between the standard deviation of period and that of length can be obtained by squaring (4.18), dividing by (4.12), and collecting terms, whence

$$\frac{(S_T)^2}{S_L} = \frac{(\overline{T})^2 \, S_\tau^2}{\overline{T^2} \, S_\lambda} \tag{4.23}$$

since $\overline{L} = \overline{T^2}$, and $\overline{\tau^2} = \frac{\overline{T^2}}{(\overline{T})^2}$

Based on the Rayleigh distribution for λ one obtains

$$(S_T)^2 = 0.138 \; S_L \tag{4.24}$$

Figure 4.15 shows a plot of data for $(S_T)^2$ versus S_L, together with the theoretical relationship given by (4.24), and the agreement between data and theory is satisfactory.

Figure 4.16 shows a scatter diagram of skewness coefficients, α_{3T} versus α_{3L}, together with the theoretical point $\alpha_{3T} = -0.088$, $\alpha_{3L} = 0.631$. No relationship is expected between α_{3T} and α_{3L} except the theoretical point, around which the wave data scatter.

If the wave records were more ideal, such being the case for very long records under a state of no change, the scatter would be nil, whence one might infer that the present wave records are not completely satisfactory for the present type of analysis. However, it must be remembered that third moment computations can lead to much scatter when records of 100 waves or less are used. Second moment computations, used for standard deviations are not so sensitive to the short records. Figure 4.16 might have been omitted, but was included primarily to emphasize the importance attached to, and the desirability of, obtaining long wave records. It is not always possible to obtain long records and therefore one must make the best of the scatter peculiar to short wave records. However, the overall averages of the statistical parameters are quite significant, particularly when a few extra long records are available in the general program of analysis. Extra long records available for this presentation are discussed later in the text.

7. Cumulative Distributions

This section presents typical cumulative distributions from each source of data. More or less standard record lengths (approximately

100 waves each) are used for the first seven figures (4.17 through 4.23), one from each source of information. The cumulative plots are in terms of $\eta = H/\overline{H}$ and $\lambda = L/\overline{L} = T^2/\overline{T}^2$. Plotting of points is based on the method of Beard (1952), whence

$$P = \frac{100\left(n-\frac{1}{2}\right)}{N} \qquad (4.25)$$

P is percent cumulative
N is the total number of waves in the record
n is the order of tabulation beginning with the smallest value of η (or λ) at n = 1 to the maximum value of η (or λ) at n = N

In general, Figures 4.17 through 4.23 show that $P(\eta)$ and $P(\lambda)$ have approximately the same distributions for each record, although not necessarily the same from record to record. The above is typical of nearly all the wave records, except a few which had very peculiar distributions. Whether or not the Rayleigh distribution applies, it can be concluded that $P(\eta)$ and $P(\lambda)$, to say the least, have very nearly the same gamma type distributions. However, averages of all the records in terms of η and λ, show both $P(\eta)$ and $P(\lambda)$ to be typical Rayleigh distributions, except for the record from hurricane "Audrey." In this case $P(\lambda)$ includes swell from the main section of the hurricane and locally generated wind waves, the combination of which gives a large spread in wave period, with a correspondingly greater standard deviation.

Figures 4.24 and 4.25 summarize the cumulative distributions $P(\eta)$ and $P(\lambda)$, respectively, for Figures 4.17 - 4.23. The corresponding cumulative distributions $P(\tau)$ are given in Figure 4.26.

For comparison with non-continuous records, the long record from the Gulf of Mexico was utilized. Waves were tabulated for each first minute of every 5-minute section until 107 waves were obtaind. Figure 4.27 shows the cumulative distribution. It is seen that such a method of non-continuous recording, although not completely satisfactory, is not entirely objectionable. However, care must be taken that wind speed and direction and stage of generation remain more or less unchanged during the period of record.

8. Extra Long Wave Record from Gulf of Mexico

The wave record obtained in the Gulf of Mexico consists of 1,500 consecutive waves during a period for which the wind speed and direction remained relatively constant. Figure 4.28 shows cumulative plots of η and λ for 400 consecutive waves, and it is seen to be an improvement over Figure 4.21 based on 100 consecutive waves. The improvement is as should be expected. When 1,000 consecutive waves are used, Figure 4.29, the agreement between $P(\eta)$ and $P(\lambda)$ is

exceptionally good. Figure 4.30 is based on averaging five cumulative distributions of η and λ, each group consisting of 200 waves each, or a total of 1,000 waves. Again there is exceptionally good agreement between $P(\eta)$ and $P(\lambda)$.

9. Extra Long Wave Record From Lake Texoma, Texas

Three thousand eight hundred and eight consecutive wave heights of a continuous record have been tabulated by the U. S. Army Engineer Division, Southwestern. These waves were obtained from Lake Texoma using a step-resistance type wave recorder. During the period of record the wind speed and direction remained unchanged at 30 mph from the north. The fetch being limited, the stage of generation remained unchanged during the period of the record. These data are summarized in Table 4.5.

TABLE 4.5

SUMMARY OF WAVE HEIGHTS FOR CONTINUOUS RECORD

H (feet)	No. of Cases	Cumulative	P	η	η^2
0.2	382	382	10.02	0.197	0.039
0.4	364	746	19.58	0.393	0.154
0.6	371	1117	29.32	0.590	0.348
0.8	552	1669	43.82	0.786	0.618
1.0	527	2196	57.65	0.983	0.966
1.2	540	2736	71.84	1.180	1.392
1.4	350	3086	81.03	1.376	1.893
1.6	321	3407	89.46	1.573	2.474
1.8	150	3557	93.40	1.769	3.129
2.0	144	3701	97.18	1.966	3.865
2.2	49	3750	98.46	2.163	4.679
2.4	42	3792	99.57	2.359	5.565
2.6	11	3803	99.856	2.556	6.533
2.8	5	3808	99.987	2.752	7.574

Statistical analysis of the above record gives the following results:

	Record	Theory
$\bar{H}$	= 1.0173 feet	-
$\overline{\eta^2}$	= 1.2757	1.2732
S_η	= 0.525	0.523
a_{3H}	= 0.400	0.631
η_5	= 2.18	2.24
η_{10}	= 2.03	2.03
η_{33}	= 1.61	1.60
η_{50}	= 1.45	1.42

From the foregoing summary it is seen that this long record is in exceptionally good agreement with the Rayleigh distribution. The cumulative distribution from Table 4.5 is shown in Figure 4.31.

Nine hundred and eight consecutive wave periods of a continuous record (for the same storm above) have been tabulated by the U. S. Army Engineer Division, Southwestern. This information is summarized in Table 4.6.

The cumulative distributions for the data of Table 4.6 are presented in Figure 4.31, wave length variability, and Figure 4.32, wave period variability. This record is in fairly good agreement with theory, based on the Rayleigh distribution for lengths.

Based on the above investigation it is concluded that the Rayleigh distribution is sufficiently accurate to apply for most cases for wave height variability and wave length variability; and the corresponding theoretical distribution function of wave period variability is satisfactory. This statement is made without the application of the Chi square test, which in view of the above and the work of Watters (1953) would appear to be repetitious.

TABLE 4.6

SUMMARY OF WAVE PERIODS FOR CONTINUOUS RECORD

T sec	$L=T_2^2$ sec	No. of Cases	Cumulative	P	τ	λ
0.5	0.25	1	1	0.0551	0.203	0.037
0.6	0.36	3	4	0.385	0.243	0.054
0.7	0.49	10	14	1.49	0.284	0.073
0.8	0.64	9	23	2.48	0.324	0.096
0.9	0.81	5	28	3.03	0.365	0.121
1.0	1.00	9	37	4.02	0.405	0.149
1.1	1.21	7	44	4.79	0.446	0.181
1.2	1.44	17	61	6.66	0.487	0.215
1.3	1.69	16	77	8.43	0.527	0.252
1.4	1.96	19	96	10.52	0.568	0.293
1.5	2.25	16	112	12.28	0.608	0.336
1.6	2.56	31	143	15.69	0.649	0.382
1.7	2.89	23	166	18.23	0.689	0.432
1.8	3.24	33	199	21.86	0.730	0.499
1.9	3.61	10	209	22.96	0.770	0.539
2.0	4.00	41	250	27.48	0.811	0.598
2.1	4.41	20	270	29.68	0.852	0.659
2.2	4.84	60	330	36.29	0.892	0.723
2.3	5.29	47	377	41.46	0.933	0.790
2.4	5.76	80	457	50.28	0.973	0.861
2.5	6.25	52	509	56.00	1.014	0.934
2.6	6.76	68	577	63.49	1.054	1.010
2.7	7.29	33	610	67.13	1.095	1.089
2.8	7.84	35	645	70.98	1.135	1.171
2.9	8.41	13	658	72.41	1.176	1.256
3.0	9.00	44	702	77.26	1.216	1.345
3.1	9.61	21	723	79.57	1.257	1.436
3.2	10.24	31	754	82.98	1.298	1.530
3.3	10.89	23	777	85.52	1.338	1.627
3.4	11.56	36	813	89.48	1.379	1.727
3.5	12.25	27	840	92.46	1.419	1.830
3.6	12.96	23	863	94.99	1.460	1.936
3.7	13.69	12	875	96.31	1.500	2.045
3.8	14.44	4	879	96.75	1.540	2.157
3.9	15.21	4	883	97.19	1.581	2.272
4.0	16.00	7	890	97.96	1.622	2.390
4.1	16.81	2	892	98.18	1.662	2.511
4.2	17.64	5	897	98.73	1.703	2.635
4.3	18.49	2	899	98.95	1.744	2.762
4.4	19.36	4	903	99.39	1.784	2.892
4.5	20.25	1	904	99.50	1.820	3.025
4.6	21.16	2	906	99.72	1.865	3.161
4.8	23.09	1	907	99.83	1.916	3.442
6.0	36.00	1	908	99.94	2.[illegible]	5.38

Statistical analysis of the above record gives:

	Record	Theory
$\bar{\tau}$	= 2.4662	-
$\overline{\tau^2}$	= 1.1007	1.0787
S_τ	= 0.317	0.285
α_{3_τ}	= -0.0558	-0.088
$\overline{T^2}$	= 6.6945	-
$\overline{\lambda^2}$	= 1.325	1.2732
S_λ	= 0.5701	0.523
α_{3_λ}	= 0.8705	0.631
λ_5	= 2.49	2.24
λ_{10}	= 2.19	2.03
λ_{33}	= 1.67	1.60
λ_{50}	= 1.44	1.42

10. Wave Data from Step-resistance Wave Gage Versus Pressure Gage

It appears from the data analyzed in this chapter that there is little difference in the statistical parameters obtained from the step-resistance wave gage and from the pressure gage, and this difference is statistically insignificant. It is difficult to explain the results of Wiegel and Kukk (1957), who reported a significant difference in results obtained by the two methods of recording. Evidently the Rayleigh distribution for wave height variability is not verified for the step-resistance wave gage data reported by Wiegel and Kukk (1957), and these findings are not in agreement with the data analyzed in the present paper. In particular the extra long record from Lake Texoma verifies almost exactly the Rayleigh distribution.

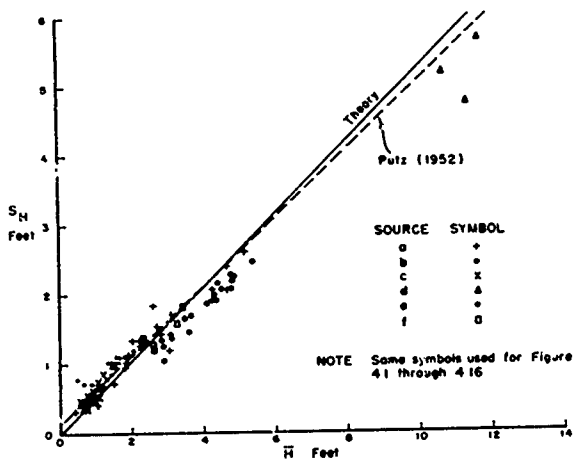

FIGURE 4.1 S_H VERSUS $\bar{H}$

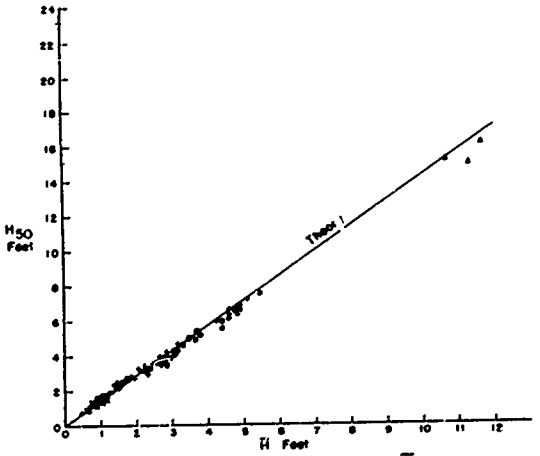

FIGURE 4.3 H_{50} VERSUS $\bar{H}$

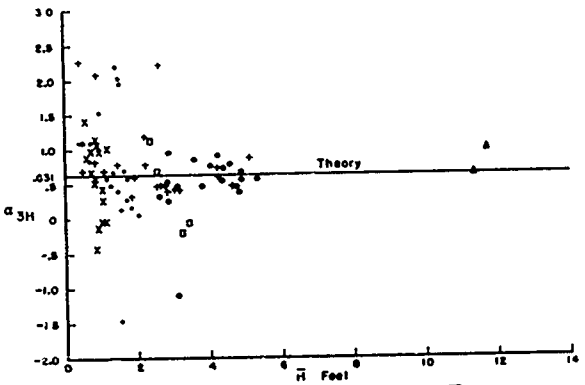

FIGURE 4.2 α_{3H} VERSUS $\bar{H}$

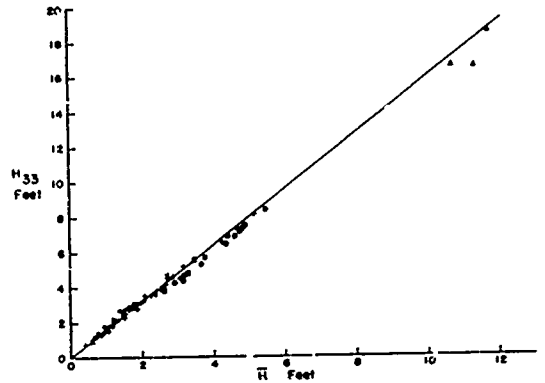

FIGURE 4.4 H_{33} VERSUS $\bar{H}$

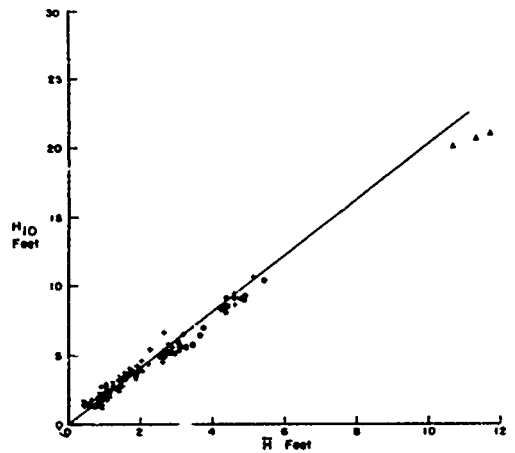

FIGURE 4.5 H_{10} VERSUS $\bar{H}$

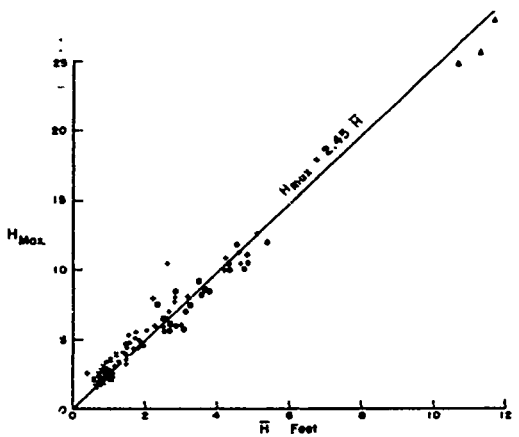

FIGURE 4.6 $H_{Max.}$ VERSUS $\bar{H}$

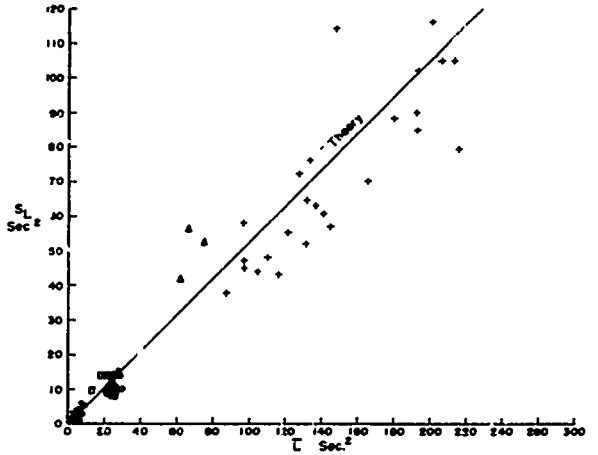

FIGURE 4.7 S_L VERSUS $\bar{L}$

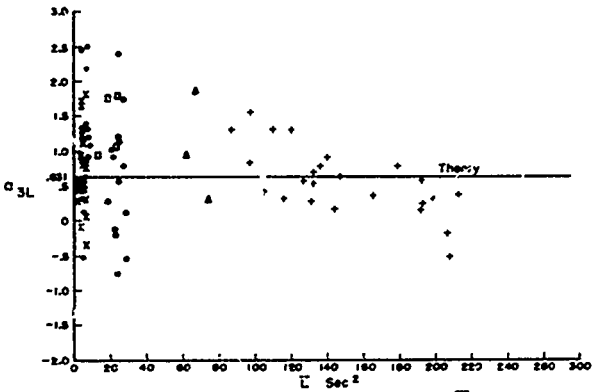

FIGURE 4.8 α_{3L} VERSUS $\bar{L}$

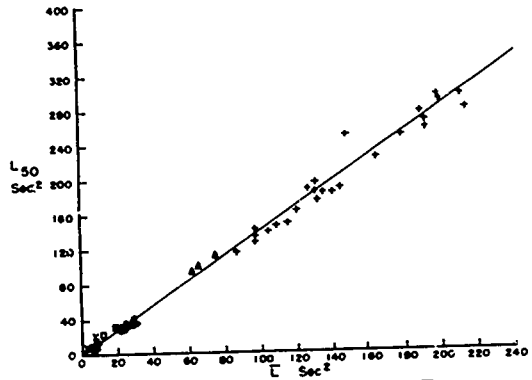

FIGURE 4.9 L_{50} VERSUS τ

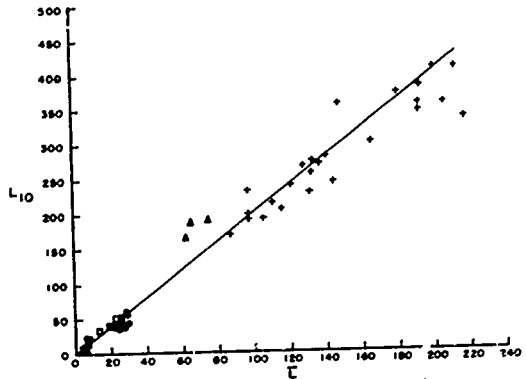

FIGURE 4.11 L_{10} VERSUS τ

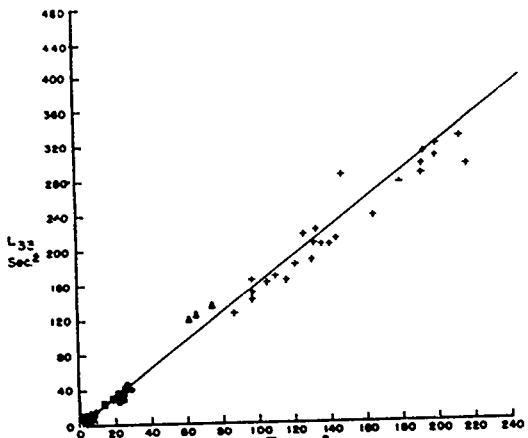

FIGURE 4.10 L_{33} VERSUS τ

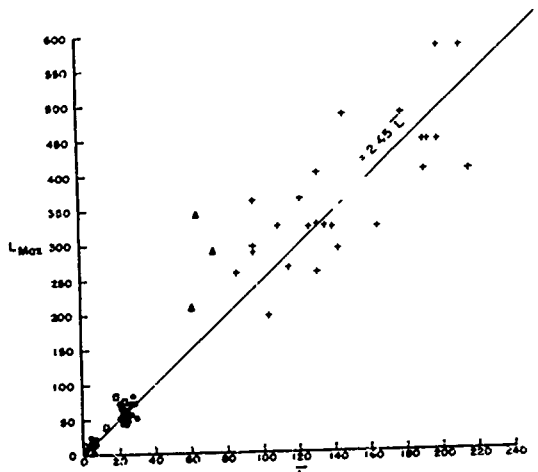

FIGURE 4.12 L_{Max} VERSUS τ

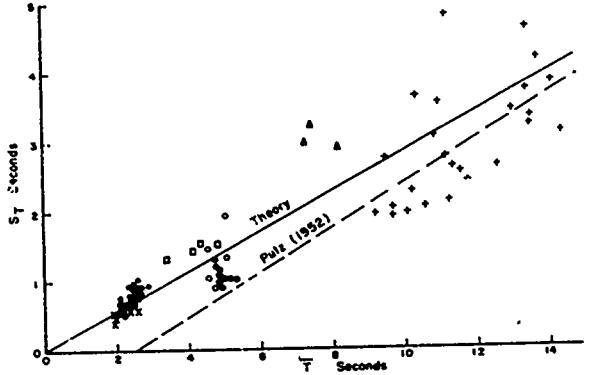

FIGURE 4.13 S_T VERSUS $\overline{T}$

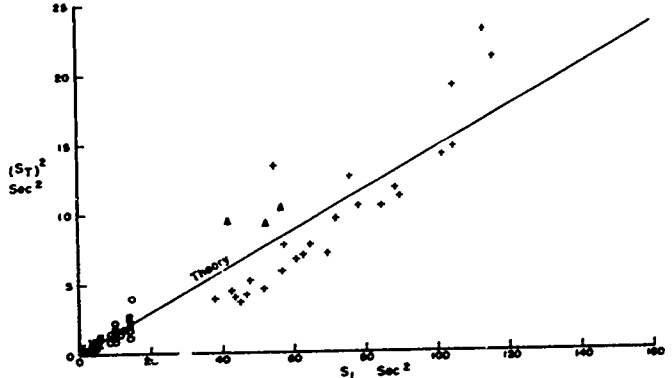

FIGURE 4.15 WAVE PERIOD STANDARD DEVIATION VERSUS WAVE LENGTH STANDARD DEVIATION

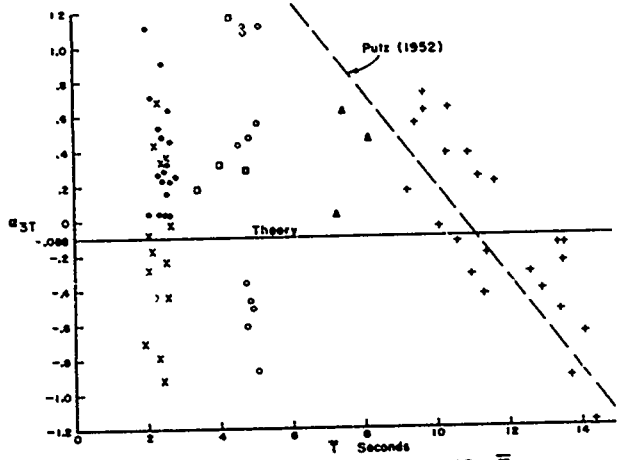

FIGURE 4.14 α_{3T} VERSUS $\overline{T}$

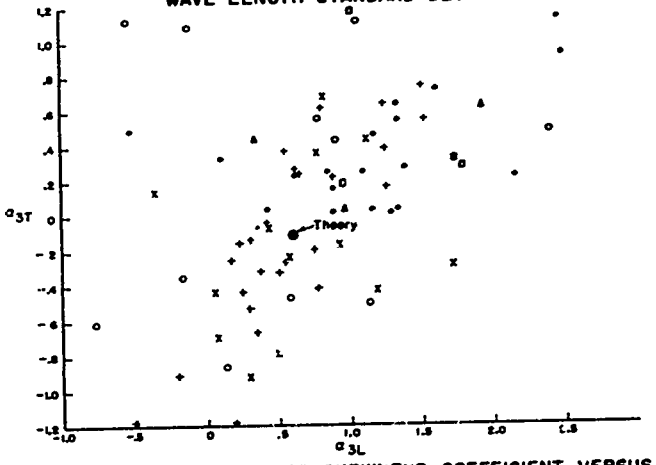

FIGURE 4.16 WAVE PERIOD SKEWNESS COEFFICIENT VERSUS WAVE LENGTH SKEWNESS COEFFICIENT

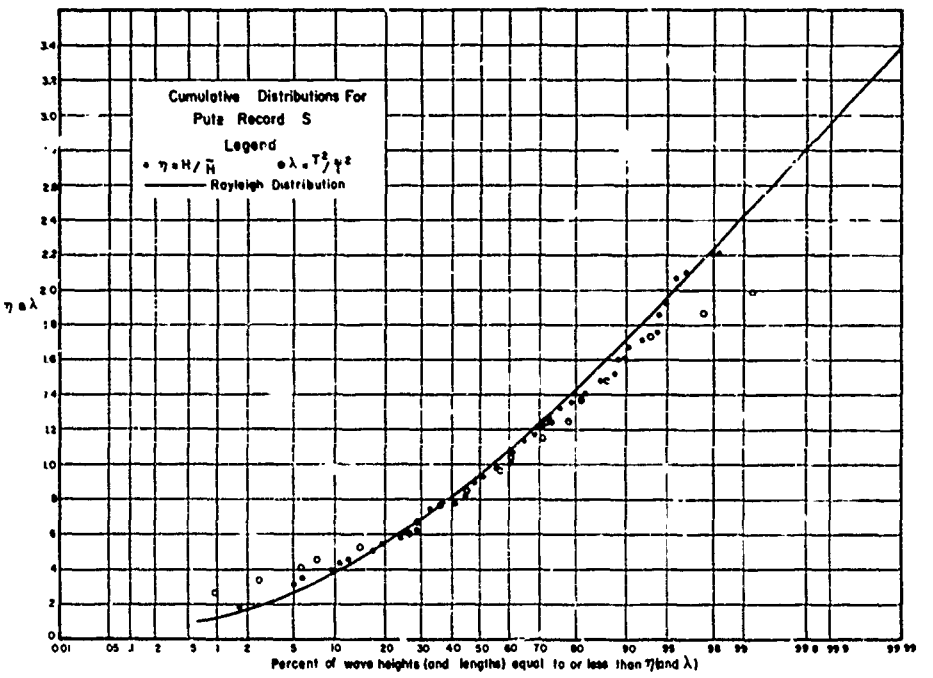

FIGURE 417 CUMULATIVE DISTRIBUTIONS FOR η AND λ

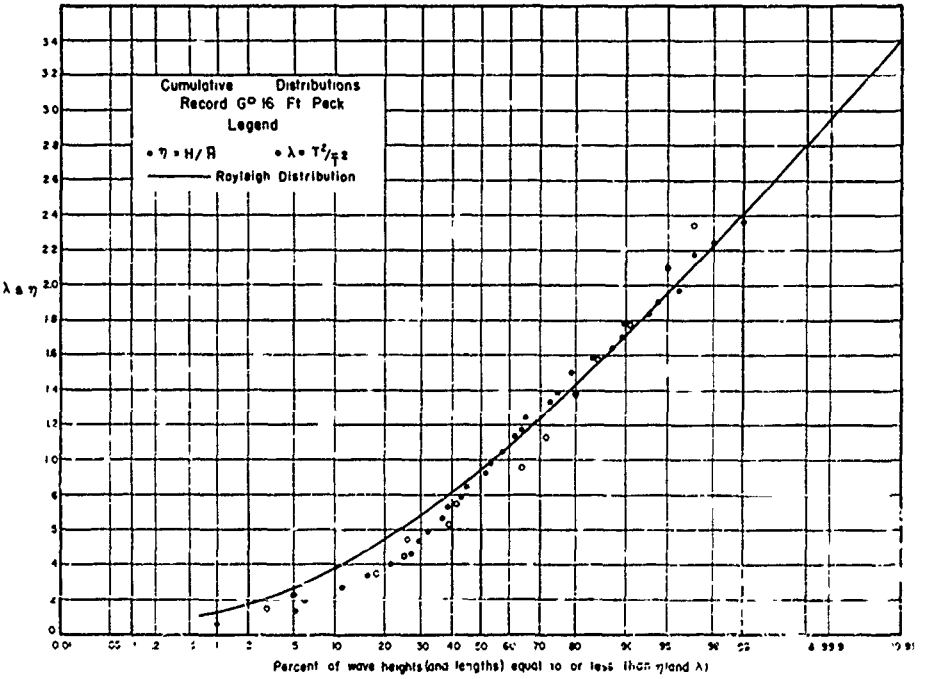

FIGURE 418 CUMULATIVE DISTRIBUTIONS FOR η AND λ

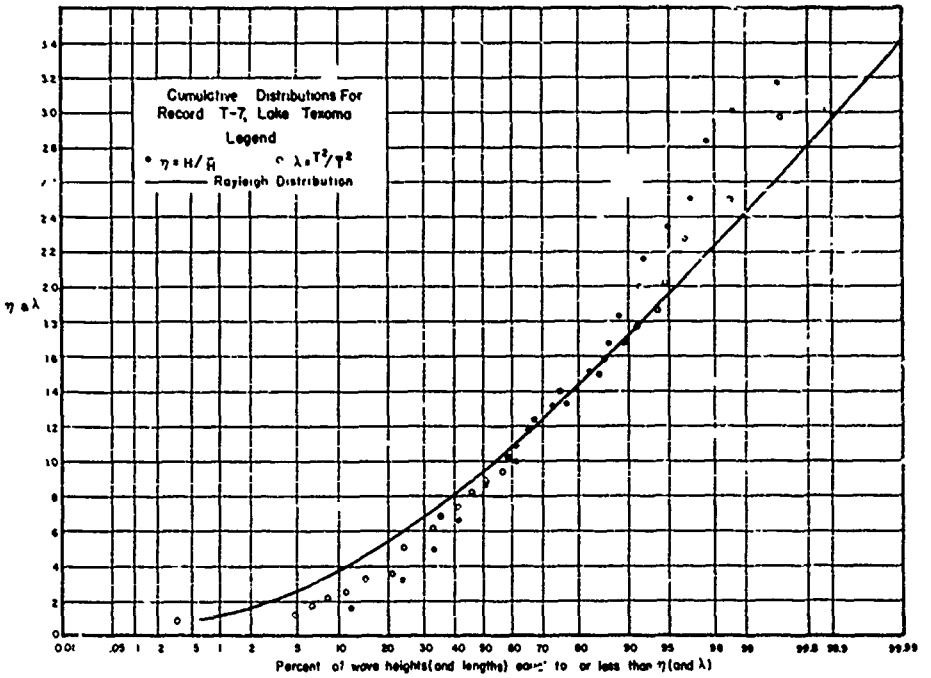

FIGURE 4 19 CUMULATIVE DISTRIBUTIONS FOR η AND λ

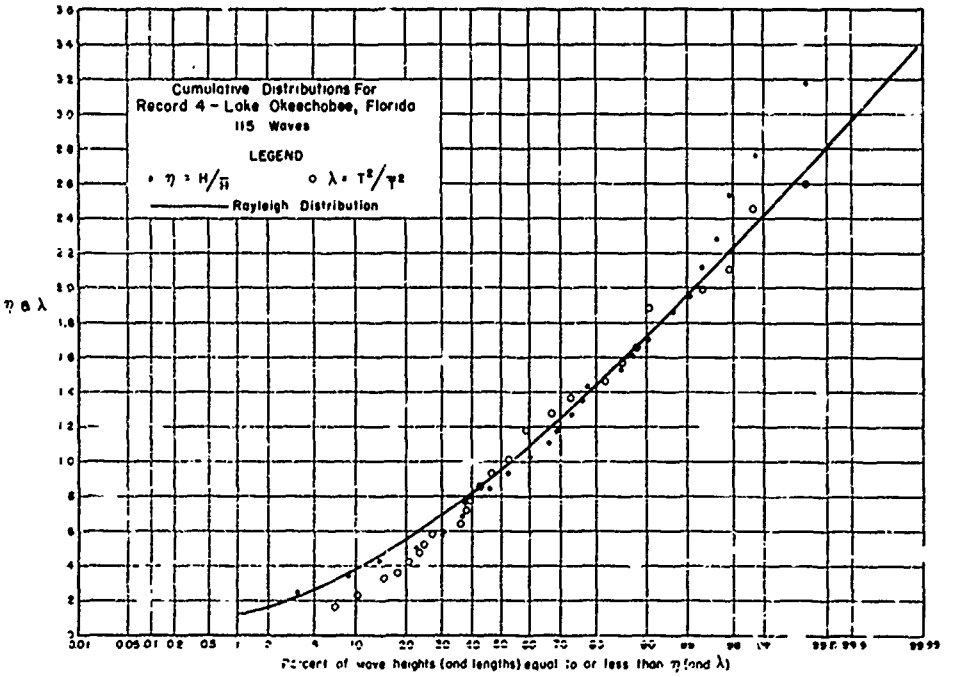

FIGURE 4 20 CUMULATIVE DISTRIBUTIONS FOR η AND λ

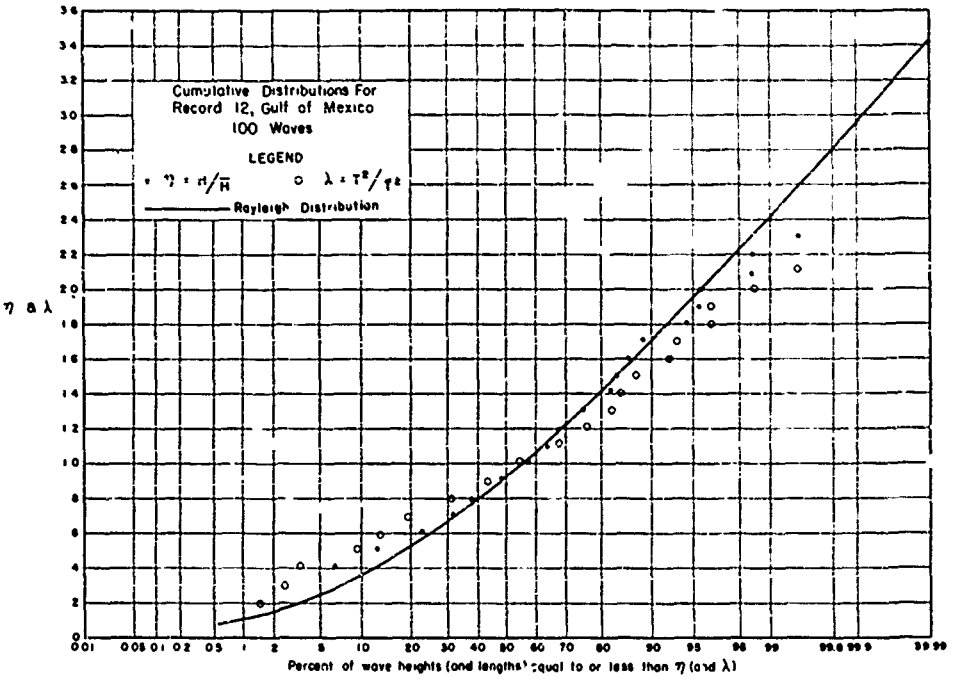

FIGURE 4 21 CUMULATIVE DISTRIBUTIONS FOR η AND λ

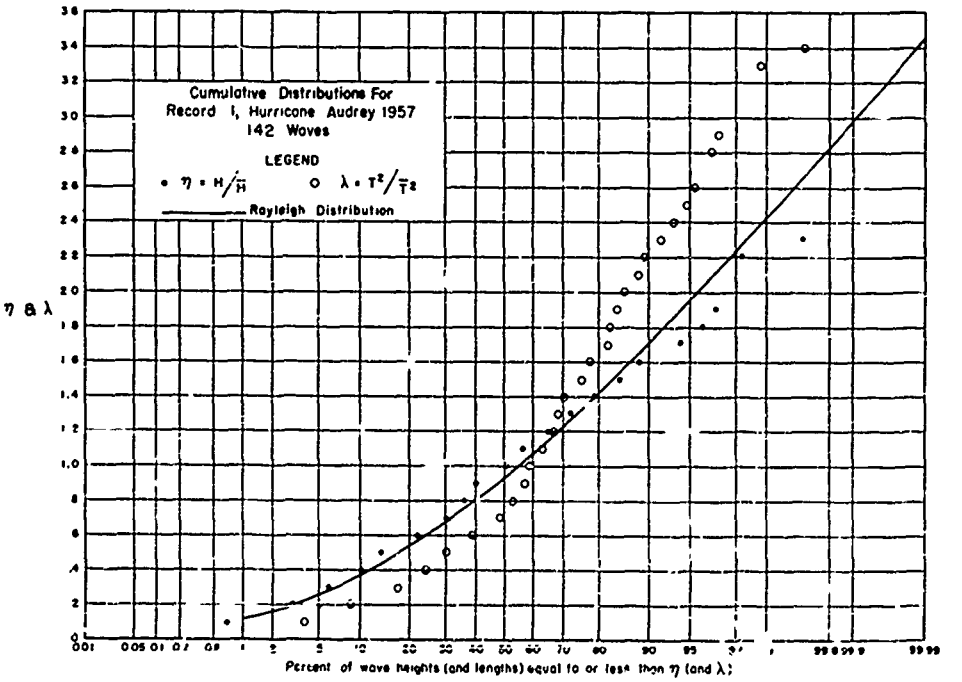

FIGURE 4 22 CUMULATIVE DISTRIBUTIONS FOR η AND λ

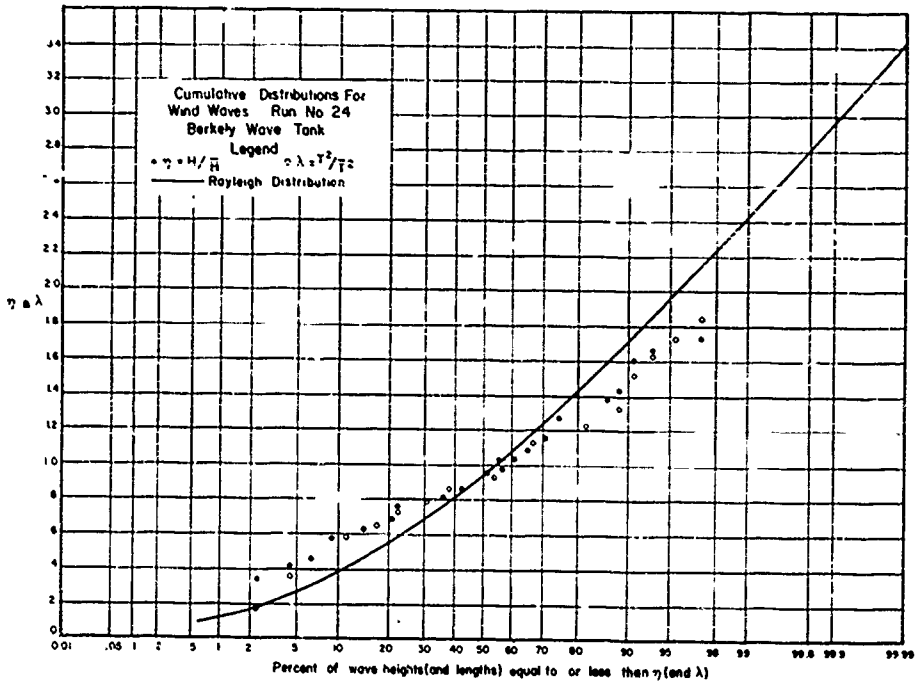

FIGURE 4 23 CUMULATIVE DISTRIBUTIONS FOR η AND λ

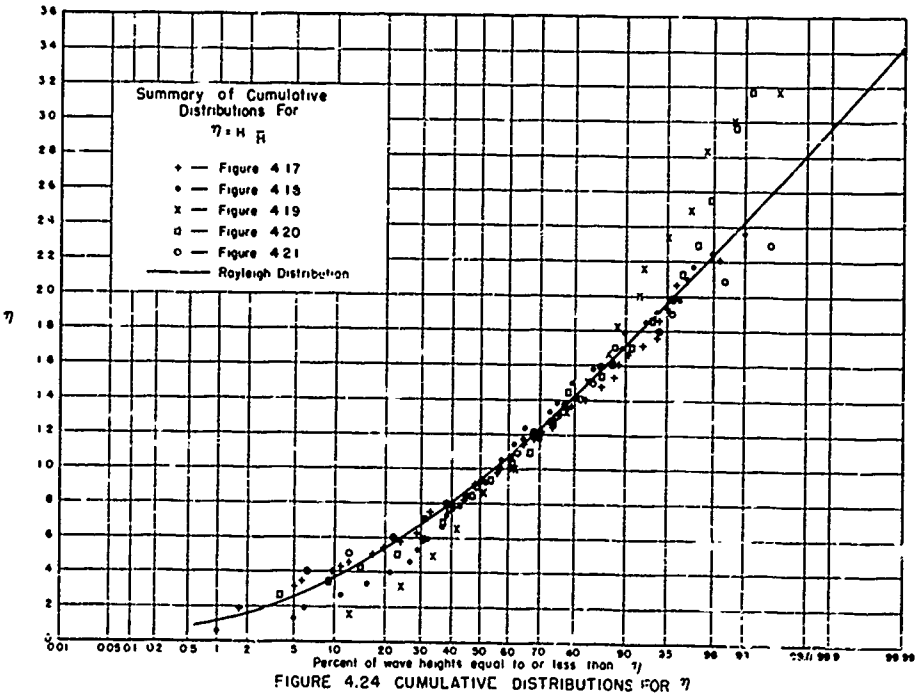

FIGURE 4.24 CUMULATIVE DISTRIBUTIONS FOR η

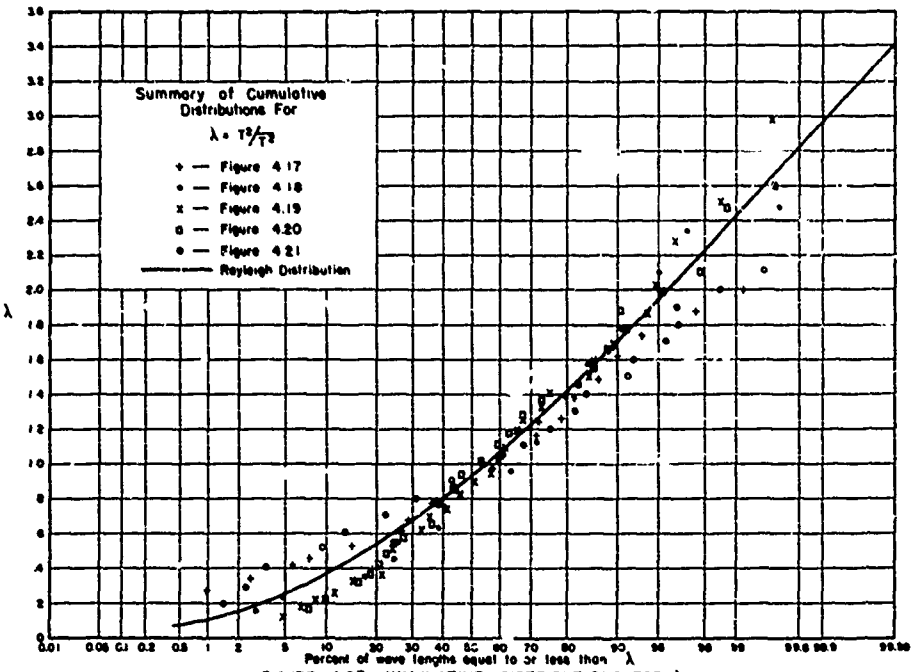

FIGURE 4.25 CUMULATIVE DISTRIBUTIONS FOR λ

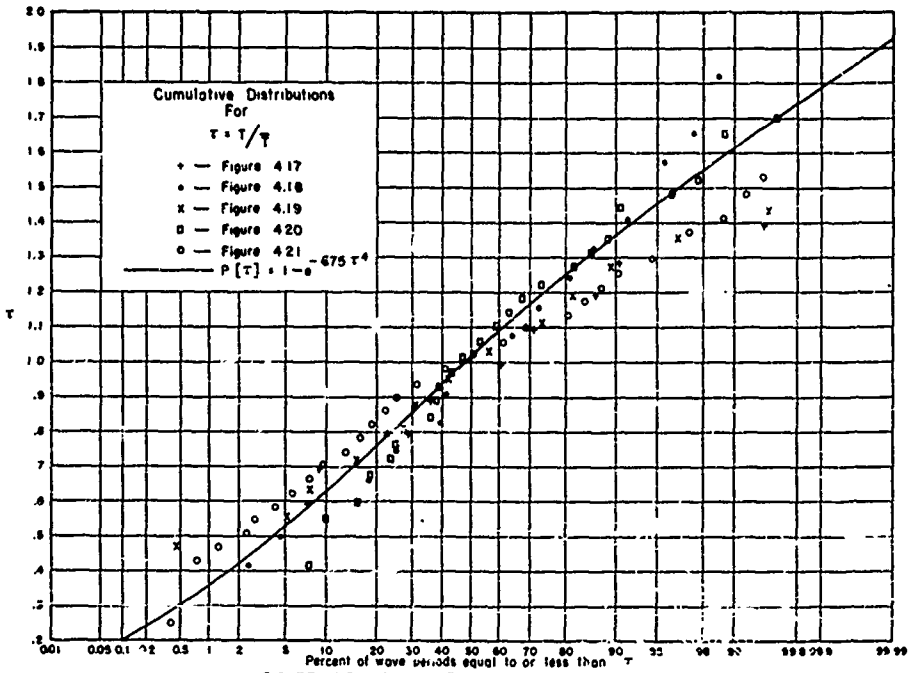

FIGURE 4.26 CUMULATIVE DISTRIBUTIONS FOR τ

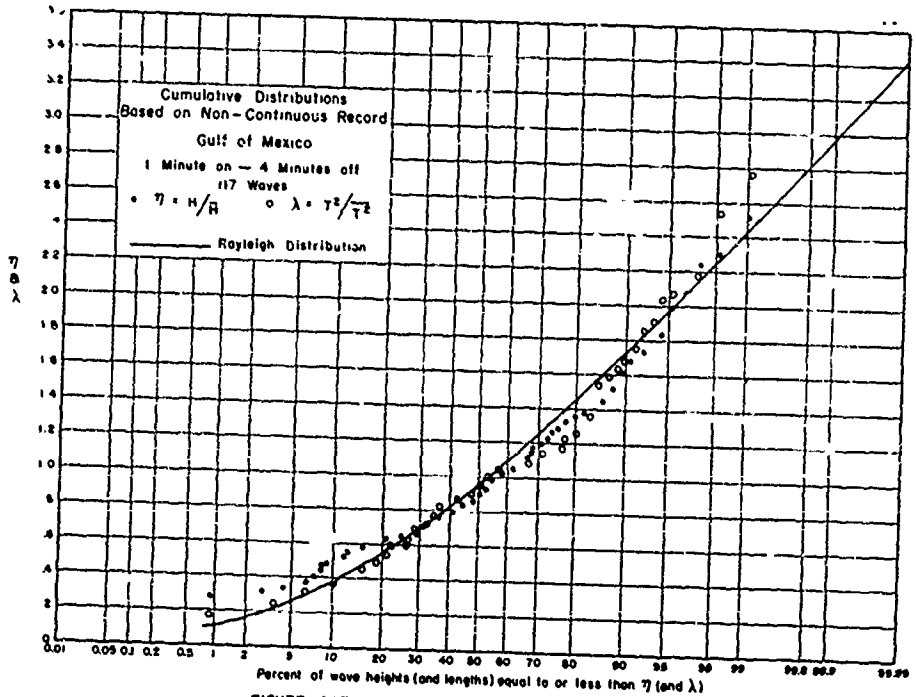

FIGURE 4.27 CUMULATIVE DISTRIBUTIONS FOR η AND λ

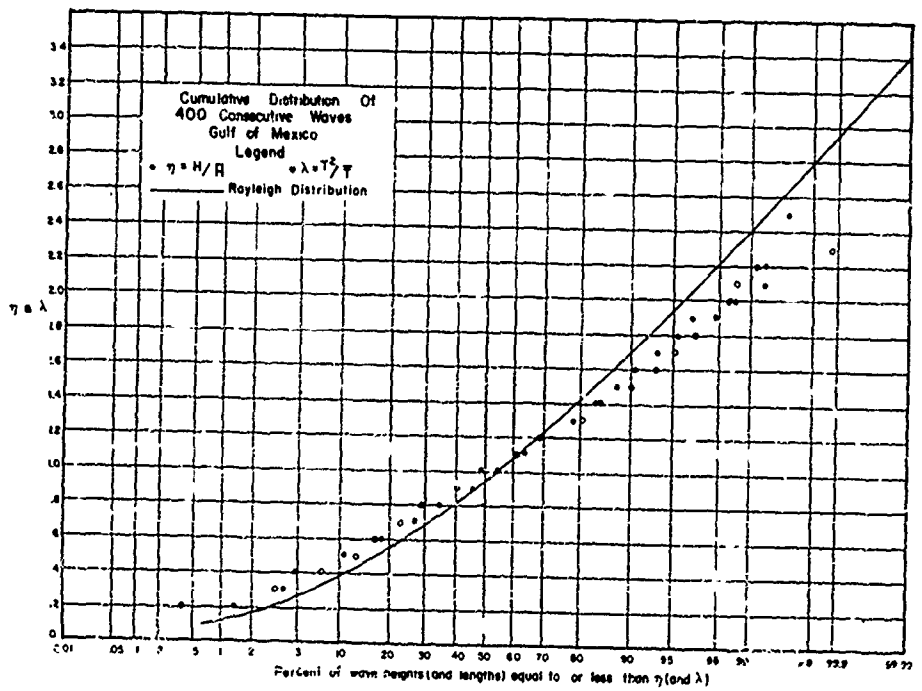

FIGURE 4.28 CUMULATIVE DISTRIBUTIONS FOR η AND λ.

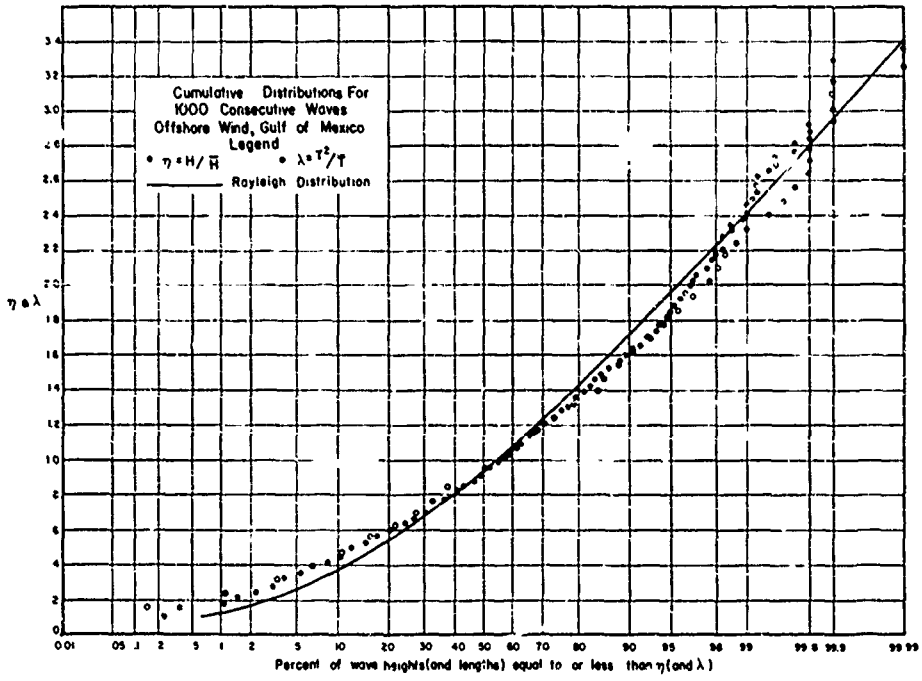

FIGURE 4 29 CUMULATIVE DISTRIBUTIONS FOR η AND λ.

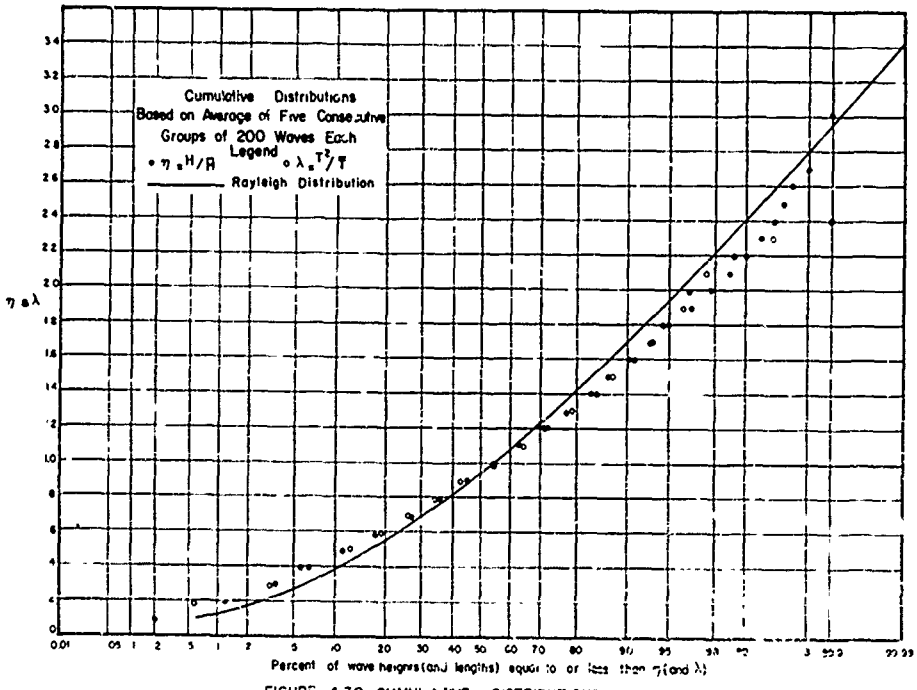

FIGURE 4 30 CUMULATIVE DISTRIBUTIONS FOR η AND λ

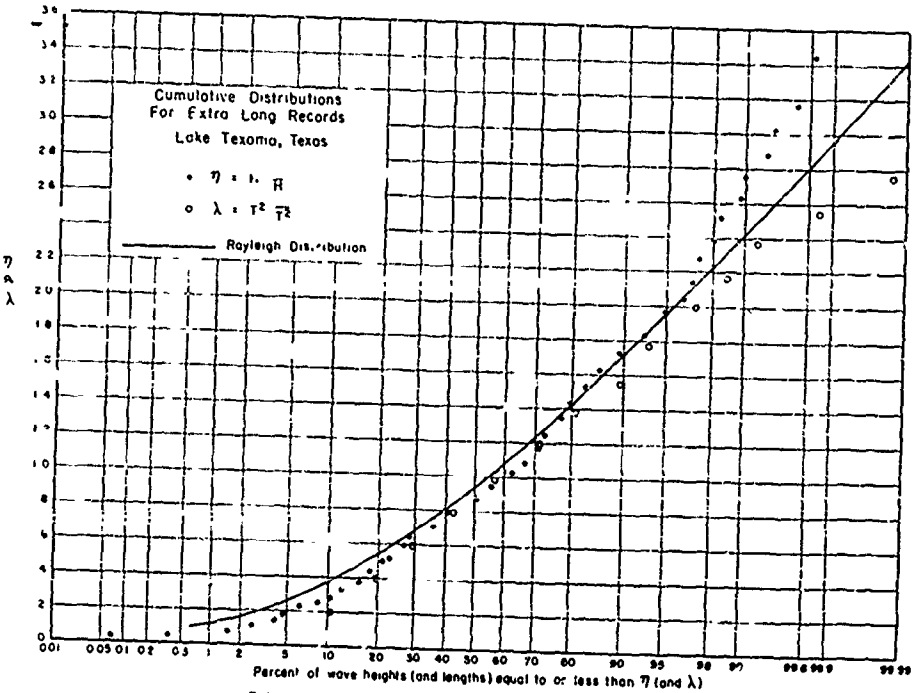

FIGURE 4.31 CUMULATIVE DISTRIBUTIONS FOR η AND λ

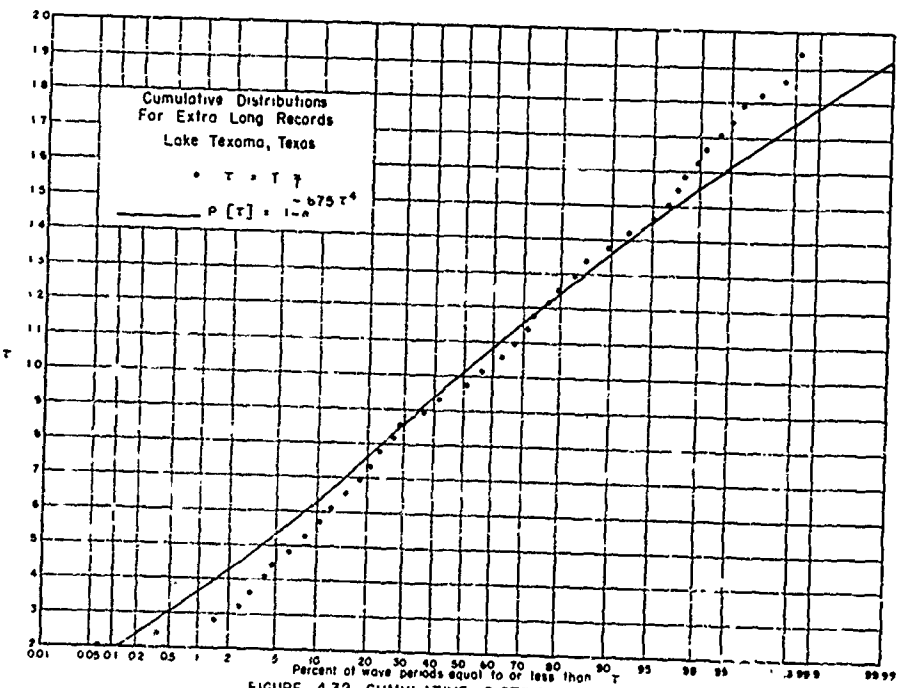

FIGURE 4.32 CUMULATIVE DISTRIBUTIONS FOR τ

CHAPTER V: WAVE VARIABILITY AND JOINT DISTRIBUTION

1. General

The joint distribution of wave heights and lengths (or wave heights and periods) in general is difficult to describe completely for all conditions of correlation. Three special cases, however, can be investigated in detail. Case I, non-correlation, is perhaps the most likely to be encountered by engineers and oceanographers. Cases II and III are the trivial cases for correlation coefficients of $r = +1$ and $r = -1$, respectively. $r = -1$ perhaps never occurs in nature. $r = +1$ might occur in the very early stages of wave generation for high wind speeds and short fetch lengths. $r = +1$ might also tend to occur for very long decayed swell. An important factor, although $r = \pm 1$ are trivial cases, is that these cases represent the boundary limits between which all other cases occur, thereby permitting use of necessary approximations supplemented with wave data to describe the conditions where correlation exists. Figure 5.1, for example, is a scatter diagram of η and λ for a very low degree of correlation. The fact that both marginal distributions $p(\eta)$ and $p(\lambda)$ are of the same type is of some help. The bivariate asymptotic problem of joint distribution for the Rayleigh (or a modified Rayleigh type) distribution has yet to be solved.* If waves possessed the Gaussian distribution, and they sometimes do quite closely, there would be no difficulty since the joint distribution between two normally distributed dependent variates has been covered quite satisfactorily, for example, Uspensky (1937) among others. Wooding (1955) presents an approximate joint distribution for wave amplitude and frequency in random noise.

The correlation coefficient measures the strength of the relationship between two variables, but only when that relationship is linear. It is necessary to assume a linear relationship between η and λ, and this assumption appears justified from the data analysis.

A summation function is introduced for the purpose of estimating the mean period of wave heights above a given height.

2. Some Basic Concepts on Joint Distribution

The general form of the joint distribution function for two dependent variates can be written as the product of two functions

$$p(\eta, \lambda) = p(\eta) \cdot p_{\eta}(\lambda) \qquad (5.1)$$

*Through recent correspondence with Dr. E. J. Gumbel of the Department of Industrial Engineering, Columbia University, New York City, it has been learned that he solved this problem applicable for the correlation coefficient between $r = \pm 0.31396$.

which states that the probability of both a particular value of η and λ occurring simultaneously is equal to the probability that η will occur times the probability that λ will occur, assuming that η occurred. $p(\eta)$ is the marginal distribution function for η, and $p_\eta(\lambda)$ is the conditional probability function of λ, the condition being that η occurred. Eq. (5.1) might also have been written

$$p(\lambda,\eta) = p(\lambda) \cdot p_\lambda(\eta) \tag{5.2}$$

in which case $p(\lambda)$ is the marginal distribution function of λ and $p_\lambda(\eta)$ the conditional probability function of η. The marginal distribution functions are given by:

$$p(\eta) = \int_0^\infty p(\eta,\lambda)\, d\lambda = p(\eta)\int_0^\infty p_\eta(\lambda)\, d\lambda \tag{5.3}$$

$$p(\lambda) = \int_0^\infty p(\lambda,\eta)\, d\eta = p(\lambda)\int_0^\infty p_\lambda(\eta)\, d\eta \tag{5.4}$$

Since the marginal distribution functions are Rayleigh distributions, only the conditional probability functions are required for the complete solution, which will not be attempted in the present study.

The correlation coefficient is given by

$$r(\eta,\lambda) = \frac{\overline{\eta\lambda} - 1}{\left[\left(\overline{\eta^2}-1\right)\left(\overline{\lambda^2}-1\right)\right]^{1/2}} \tag{5.5}$$

where the expectations $E(\eta,\lambda) = \overline{\eta\lambda}$, $E(\eta^2) = \overline{\eta^2}$, and $E(\lambda^2) = \overline{\lambda^2}$ are given by

$$\overline{\eta\lambda} = \int_0^\infty\int_0^\infty \eta\lambda\, p(\eta,\lambda)\, d\eta\, d\lambda \tag{5.6}$$

$$\overline{\eta^2} = \int_0^\infty \eta^2 p(\eta)\, d\eta \tag{5.7}$$

$$\overline{\lambda^2} = \int_0^\infty \lambda^2 p(\lambda)\, d\lambda \tag{5.8}$$

3. Special Cases of Joint Distribution

Case I. Non-correlation of $r = 0$: In Chapter II the marginal type Rayleigh distribution functions were given in normal or unit form:

$$p(\eta) = \frac{\pi}{2}\,\eta\, e^{-\frac{\pi}{4}\eta^2}\;;\quad \eta = \frac{H}{\overline{H}} \tag{5.9}$$

$$p(\lambda) = \frac{\pi}{2}\,\lambda\, e^{-\frac{\pi}{4}\lambda^2}\;;\quad \lambda = \frac{L}{\overline{L}} \tag{5.10}$$

When zero correlation exists the joint probability is the product of the marginal distribution functions, whence (5.1 and (5.2) become

$$p(\eta,\lambda) = p(\eta) \cdot p(\lambda) \tag{5.11}$$

or using (5.9) and (5.10)

$$p(\eta,\lambda) = \frac{\pi^2}{4}\eta\, e^{-\frac{\pi}{4}\eta^2} \cdot \lambda e^{-\frac{\pi}{4}\lambda^2} \tag{5.12}$$

In terms of η and τ (5.12) becomes

$$p(\eta,\tau) = 1.35\,\pi\, e^{-\frac{\pi}{4}\eta^2} \cdot \tau^3 e^{-0.675\tau^4} \tag{5.13}$$

Eq. (5.13) is more useful than (5.12) since the variables actually measured are H and T, L being a computed quantity. Table 5.1 gives the number of waves per 1,000 that would occur on the long run average for 0.2 increments of η and τ.

The integrated equation or the cumulative joint distribution for zero correlation is obtained from

$$P(\eta,\lambda) = \int_0^{\eta}\int_0^{\lambda} p(\eta,\lambda)\, d\eta\, d\lambda \tag{5.14}$$

and using (5.12), the order of integration being indifferent, one obtains

$$P(\eta,\lambda)=\left[1-e^{-\frac{\pi\eta^2}{4}}\right]\left[1-e^{-\frac{\pi\eta^2}{4}}\right] \tag{5.15}$$

Eq. (5.15) gives the percent of waves $P[\eta,\lambda]$ having η equal to or less than some specified value and at the same time having λ equal to or less than some specified value. The only limitation on (5.15) is that no wave can be steeper than the critical value of H/L = 1/7, according to the Michell (1893) theory. In terms of η and τ (5.15) becomes

$$P(\eta,\tau)=\left[1-e^{-\frac{\pi\eta^2}{4}}\right]\left[1-e^{-0.675\,\tau^4}\right] \tag{5.16}$$

Consider the scatter diagram of Figure 5.1, for example, where four quadrants are given: I, $P[1,1]$; II, $P[\infty,1] - P[1,1]$; III, $P[\infty,\infty] - P[\infty,1] - P[1,\infty] + P[1,1]$; and IV, $P[1,\infty] - P[1,1]$. If zero correlation $r(\eta,\lambda) = 0$, exists then

$$\begin{aligned} P_I &= 29.6 \text{ percent} \\ P_{II} &= 24.8 \text{ percent} \\ P_{III} &= 20.8 \text{ percent} \\ P_{IV} &= 24.8 \text{ percent} \end{aligned} \tag{5.17}$$

When zero correlation exists the equations of regression lines are given by

$$\begin{aligned} \eta &= 1 \\ \lambda &= 1 \end{aligned} \tag{5.18}$$

TABLE 5.1

JOINT DISTRIBUTION OF H AND T FOR ZERO CORRELATION
Number of Waves Per 1,000 Consecutive Waves for Various Ranges in Height and Period

Range in Relative Height $H/\bar{H}$	RANGE IN RELATIVE PERIOD $T/\bar{T}$											
	0-0.2	0.2-0.4	0.4-0.6	0.6-0.8	0.8-1.0	1.0-1.2	1.2-1.4	1.4-1.6	1.6-1.8	1.8-2.0	0-2.0	Cumulative
0-0.2	0.03	0.50	2.05	4.86	7.68	8.09	5.31	1.92	0.34	0.03	30.81	30.81
0.2-0.4	0.10	1.41	5.81	13.78	21.76	23.92	15.05	5.44	0.98	0.07	88.32	119.13
0.4-0.6	0.14	2.06	8.54	20.23	31.95	33.65	22.10	7.99	1.44	0.11	128.21	247.34
0.6-0.8	0.16	2.40	9.91	23.48	37.08	39.06	25.65	9.27	1.67	0.12	148.80	396.14
0.8-1.0	0.16	2.40	9.92	23.51	37.13	39.11	25.69	9.28	1.67	0.12	148.99	545.13
1.0-1.2	0.15	2.14	8.87	21.02	33.19	34.97	22.96	8.30	1.49	0.11	133.20	678.33
1.2-1.4	0.12	1.74	7.21	17.07	26.96	28.40	18.65	6.74	1.21	0.09	108.19	786.52
1.4-1.6	0.09	1.30	5.37	12.72	20.09	21.16	13.90	5.02	0.90	0.07	80.62	867.14
1.6-1.8	0.06	0.90	3.72	8.82	13.93	14.67	9.64	3.48	0.63	0.05	55.90	923.04
1.8-2.0	0.03	0.48	1.99	4.72	7.45	7.85	5.15	1.86	0.33	0.03	29.80	952.93
2.0-2.2	0.03	0.42	1.72	4.09	6.45	6.80	4.47	1.61	0.29	0.02	25.	978.83
2.2-2.4	0.01	0.18	0.76	1.80	2.84	2.99	1.97	0.71	0.13	0.01	11.40	990.23
2.4-2.6	0.01	0.09	0.39	0.93	1.47	1.55	1.02	0.37	0.07		5.90	996.13
2.6-2.8		0.04	0.18	0.43	0.67	0.71	0.47	0.17	0.03		2.70	998.83
0-3.0	1.09	16.06	66.44	157.46	248.65	262.93	172.03	62.16	11.18	0.83		
Cumulative	1.09	17.15	83.59	241.05	489.70	752.63	924.66	986.82	998.00	998.83		

Case II. Correlation Coefficient r = +1.0: If the correlation coefficient between η and λ is $r(\eta, \lambda) = +1.0$, then all data will fall on a straight line in the form $y = mx + b$, a regression line. In this case if both η and λ possess independently the Rayleigh marginal distributions, then the slope $m = +1.0$ and the line, passing through $\overline{\eta} = \lambda = 1.0$, will pass through the origin $\eta = \lambda = 0$. Thus the equation of the regression line is

$$\eta = \lambda \quad \overline{\eta_\lambda} = \lambda$$
$$\lambda = \eta \quad \text{or} \quad \overline{\lambda\eta} = \eta \tag{5.19}$$

It can be seen that the joint distribution will be obtained by use of either marginal distribution and the equation of the regression line. Assuming the Rayleigh distribution still applies, and it is possible that it does, one obtains for the joint distribution

$$p(\eta, \lambda) = \frac{\pi\eta}{2} e^{-\frac{\pi\eta^2}{4}} = \frac{\pi\lambda}{2} e^{-\frac{\pi\lambda^2}{4}}$$

$$\eta_\lambda = \lambda \tag{5.20}$$

$$\lambda_\eta = \eta$$

Similar to (5.17), the percent of waves in each quadrant for $r(\eta, \lambda) = +1.0$ is given

$$\begin{aligned} P_I &= 54.4 \text{ percent} \\ P_{II} &= 0 \\ P_{III} &= 45.6 \text{ percent} \\ P_{IV} &= 0 \end{aligned} \tag{5.21}$$

To prove that (5.20) is the relationship for $r = 1.0$, multiply both sides of (5.19) by η and take the mean; and again by λ and take the mean, whence

$$\overline{\eta^2} = \overline{\eta\lambda}$$
$$\overline{\lambda^2} = \overline{\eta\lambda} \tag{5.22}$$

The correlation coefficient r is obtained from (5.5), whence

$$r(\eta,\lambda) = \frac{\overline{\eta\lambda} - 1}{\left[\left(\overline{\eta^2} - 1\right)\left(\overline{\lambda^2} - 1\right)\right]^{\frac{1}{2}}} = \frac{\overline{\eta\lambda} - 1}{\overline{\eta\lambda} - 1} = +1.0 \qquad (5.23)$$

The limitation of (5.21) is that $H/L \leq 1/7$. It can be seen that if $\overline{H/L} = 1/7$ all waves have $H/L = 1/7$ and all are breaking waves. In general H/L = constant for $r = +1.0$, and can apply to long swell having constant steepness, if such a case actually exists.

Case III. Correlation Coefficient, $r = -1.0$: If the correlation coefficient $r(\eta,\lambda) = -1.0$ then all data will fall on a straight line of the form $y = mx + b$. In this case the slope $m = -1.0$ and the line will pass through the point $\overline{\eta} = \overline{\lambda} = 1.0$, but will not pass through the origin. The equations for the regression lines are given by

$$\eta = 2 - \lambda, \text{ or } \overline{\eta}_{\lambda} = 2 - \lambda$$
$$\lambda = 2 - \eta \qquad \overline{\lambda}_{\eta} = 2 - \eta \qquad (5.24)$$

It cannot be assumed that $p(\eta)$ and $p(\lambda)$ are Rayleigh distributions for $r(\eta,\lambda) = -1.0$, since this assumption would lead to an ambiguity. If $r(\eta,\lambda) = -1.0$, then $P_I = P_{III} = 0$, since the regression line passes through $\overline{\eta} = \overline{\lambda} = 1.0$. If $p(\eta)$ and $p(\lambda)$ have the same distribution functions, the number of waves for $\eta \leq 1.0$ is the same as the number of waves for $\lambda \leq 1.0$, then $P_{II} = P_{IV} = 50.0$ percent. If one attempts to apply the Rayleigh distribution $P_{II} = 54.4$ and $P_{IV} = 54.4$ percent, the sum of which is 108.8 percent, an impossibility. Perhaps, the Rayleigh distribution fails at some lower negative value of $r(\eta,\lambda)$. This failure is of no immediate concern, since the distribution function will tend to change for large negative $r(\eta,\lambda)$ due to physical factors. If such a correlation could exist in nature, this would mean that the highest wave has the shortest length and the lowest wave the longest length. This is certainly the trivial case and one must remember that the case of $r(\eta,\lambda) = -1.0$ is considered only as a boundary condition. For two other variates not having the limitations, of breaking ocean waves, it is conceivable $r = -1$, whence

$$\begin{aligned} P_I &= 0 \\ P_{II} &= 50 \text{ percent} \\ P_{III} &= 0 \\ P_{IV} &= 50 \text{ percent} \end{aligned} \qquad (5.25)$$

To prove that (5.24) is the equation for regression line when $r(\eta, \lambda) = -1.0$ multiply both sides first by η and take the mean, and again by λ and take the mean, whence

$$\overline{\eta^2} = \overline{2\eta} - \overline{\eta\lambda}$$

$$\overline{\lambda^2} = \overline{2\lambda} - \overline{\eta\lambda} \tag{5.26}$$

and since $\overline{\eta} = \overline{\lambda} = 1.0$ and using (5.5), one obtains

$$r(\eta, \lambda) = \frac{\overline{\eta\lambda} - 1}{1 - \overline{\eta\lambda}} = -1.0 \tag{5.27}$$

4. Summation Function

An unsuccessful attempt by Bretschneider (1957)[8] was made to find the proper joint distribution function which would satisfy the rules of probability and which would also lead to Rayleigh marginal distribution functions. From the above, it is seen that unless the marginal distributions deviated from the Rayleigh type between $r = 0$ and $r = -1.0$, no continuous joint distribution function could exist over the complete range of $r = +1.0$ through $r = 0$ to $r = -1.0$. To overcome this difficulty somewhat, and at least obtain some important information on joint distribution of waves a new function is introduced, the summation function defined below. Consider the scatter diagram of η versus λ, Figure 5.1, for example, and sum all values of λ with respect to η between $-\Delta\eta/2$ and $+\Delta\eta/2$ as $\Delta\eta$ goes to zero. Denoting this sum as $S_\lambda(\eta)$, the mathematical definition of the summation function is

$$S_\lambda(\eta) = \int_0^\infty \lambda\, p(\eta, \lambda)\, d\lambda \tag{5.28}$$

or using (5.1)

$$S_\lambda(\eta) = p(\eta) \int_0^\infty \lambda\, p_\eta(\lambda) d\lambda \tag{5.29}$$

The integral of (5.29) is nothing more than the equation of the regression line of λ on η, whence

$$\overline{\lambda\eta} = \frac{S_\lambda(\eta)}{p(\eta)} = \int_0^\infty \lambda\, p_\eta(\lambda)\, d\lambda \tag{5.30}$$

thus

$$S_\lambda(\eta) = \overline{\lambda\eta}\; p(\eta) \tag{5.31}$$

A similar equation can be obtained by interchanging λ and η to η and λ. Thus

$$S_\eta(\lambda) = \overline{\eta_\lambda}\; p(\lambda) \tag{5.32}$$

Eqs. (5.31) and (5.32) are the summation equations, which become quite useful once the equations of the regression lines are obtained. It can be shown by the familiar method of least squares when $\overline{\eta^2} = \lambda^2$ that the regression equations for linear regressiors are

$$\overline{\lambda\eta} = 1 + r(\eta - 1) \tag{5.33}$$

and

$$\overline{\eta_\lambda} = 1 + r(\lambda - 1) \tag{5.34}$$

Thus the summation functions (5.31) and (5.32) become

$$S_\lambda(\eta) = \left[1 + r(\eta - 1)\right] p(\eta) \tag{5.35}$$

$$S_\eta(\lambda) = \left[1 + r(\lambda - 1)\right] p(\lambda) \tag{5.36}$$

Assuming linear regression applies at least approximately, and applying the Rayleigh type distribution for $p(\eta)$ and $p(\lambda)$ one obtains the approximate relationships

$$S_{\lambda}(\eta) = \frac{\pi}{2}\left[1 + r(\eta - 1)\right] \eta\, e^{-\frac{\pi \eta^2}{4}} \tag{5.37}$$

$$S_{\eta}(\lambda) = \frac{\pi}{2}\left[1 + r(\lambda - 1)\right] \lambda e^{-\frac{\pi \lambda^2}{4}} \tag{5.38}$$

The approximation is intended where actual distributions tend to deviate from the Rayleigh distribution, or when deviation from linear regression becomes significant.

Eq. (5.38), giving the sum of η, for values of λ, may also be called the λ-spectra of η. This is analogous to the λ-spectra of η^2 derived in a similar manner in Chapter VII.

The λ-spectra of η can be transformed into the τ-spectra of η by noting

$$S_{\eta}(\lambda)\, d\lambda = S_{\eta}(\tau)\, d\tau$$

$$p(\lambda) d\lambda = p(\tau) d\tau \tag{5.39}$$

$$\lambda = a\tau^2 = 0.927\, \tau^2$$

Thus

$$S_{\eta}(\tau) = 2.7\left[(1-r) + 0.927\, r\tau^2\right] \tau^3 e^{-0.675\, \tau^4} \tag{5.40}$$

$S_{\eta}(\lambda)$ and $S_{\eta}(\tau)$ are given respectively in Figures 7.1 and 7.3 of Chapter VII, for comparison with $S_{\eta^2}(\lambda)$ and $S_{\eta^2}(\tau)$.

5. Mean Wave Steepness

The mean wave steepness is given by:

$$\overline{\left[\frac{\eta}{\lambda}\right]} = \int_0^{\infty} \frac{1}{\lambda} S_{\eta}(\lambda)\, d\lambda \tag{5.41}$$

and using (5.38) one obtains

$$\overline{\left[\frac{\eta}{\lambda}\right]} = \frac{\pi}{2}\left[1-r\left(1-\frac{2}{\pi}\right)\right] \tag{5.42}$$

6. Mean Period of Wave Heights Greater than a Given Height

In Chapter III was determined the mean or average height of waves higher than a given height, which requires only the knowledge of the marginal distribution function. To obtain the mean period of wave heights greater than a given height, some knowledge is required of the joint distribution function, the summation function derived above being sufficient in this case. The mean value of λ for any differential element of $\Delta\eta$ is obtained by dividing (5.37) by $p(\eta)$. The mean value of λ for wave heights above a given height is obtained from

$$\lambda(\eta_p) = \frac{\int_x^\infty S_\lambda(\eta)\,d\eta}{\int_x^\infty p(\eta)\,d\eta} \tag{5.43}$$

$$\lambda(\eta_p) = (1-r) + r\,\frac{\int_x^\infty \eta\, p(\eta)\,d\eta}{\int_x^\infty p(\eta)\,d\eta} \tag{5.44}$$

The above integrals have been solved in Chapter III, whence

$$\lambda(\eta_p) = (1-r) + r\eta_p \tag{5.45}$$

where

$$\eta_p = \frac{\eta\, e^{-\frac{\pi\eta^2}{4}} + 1 - \Phi_p}{e^{-\frac{\pi\eta^2}{4}}} \tag{5.46}$$

$$\Phi_p = \frac{2}{\sqrt{\pi}}\int_0^x e^{-u^2}\,du \qquad \text{and} \qquad u = \sqrt{\frac{\pi}{4}}\,\eta$$

Eq. (5.45) can be transformed in terms of wave period by noting

$$\lambda(\eta_p) = K\left[\tau(\eta_p)\right]^2 \tag{5.47}$$

$$\tau(\eta_p) = K^{-\frac{1}{2}}\left[1 - r + r\,\eta_p\right]^{\frac{1}{2}} \tag{5.48}$$

The value of K may be obtained at $r = 0$, for which $\tau(\eta_p) = \bar{\tau} = 1.0$, whence $K = 1$. Thus

$$\tau(\eta_p) = \left[1 - r + r\,\eta_p\right]^{\frac{1}{2}} \tag{5.49}$$

It must be remembered, however, that r is the correlation coefficient between η and λ, which is not necessarily that between η and τ. Table 5.2 gives typical values of $\tau(\eta_p)$ from (5.49) for various values of the correlation coefficient. It must be pointed out that for large values of the negative correlation coefficient, the above equations tend to fail.

TABLE 5.2

MEAN τ OF HIGHEST P-PERCENT OF WAVES

	Correlation Coefficient $r(\eta, \lambda)$										
P	1.0	0.8	0.6	0.4	0.2	0	-0.2	-0.4	-0.6	-0.8	-1.0
0.01	1.632	1.526	1.414	1.290	1.155	1.0	0.8169	0.579	0.044?		
0.05	1.497	1.412	1.321	1.224	1.117	1.0	0.8669	0.7094	0.5050	0.0775	
0.10	1.425	1.351	1.272	1.189	1.098	1.0	0.8808	0.7663	0.6173	0.4171	
0.20	1.340	1.279	1.216	1.148	1.077	1.0	0.9170	0.8259	0.7225	0.6025	0.4517
0.25	1.309	1.253	1.195	1.134	1.069	1.0	0.9205	0.8455	0.7563	0.6557	0.5357
0.30	1.281	1.230	1.177	1.121	1.062	1.0	0.9336	0.8621	0.7841	0.7137	0.5983
0.333	1.265	1.216	1.166	1.114	1.058	1.0	0.9382	0.8720	0.8004	0.7218	0.6332
0.400	1.233	1.190	1.146	1.099	1.051	1.0	0.9465	0.8897	0.8291	0.7635	0.6921
0.500	1.191	1.155	1.118	1.080	1.041	1.0	0.9573	0.9126	0.8656	0.8161	0.7629
0.600	1.152	1.123	1.094	1.063	1.033	1.0	0.9666	0.9321	0.8962	0.8588	0.8198
0.700	1.153	1.093	1.071	1.048	1.024	1.0	0.9753	0.9499	0.9236	0.8971	0.8695
0.800	1.079	1.063	1.048	1.032	1.016	1.0	0.9784	0.9666	0.9495	0.9321	0.9143
0.900	1.042	1.033	1.025	1.016	1.011	1.0	0.9926	0.9829	0.9742	0.9654	0.9566
1.000	1.000	1.000	1.000	1.000	1.000	1.0	1.0000	1.0000	1.0000	1.0000	1.0000

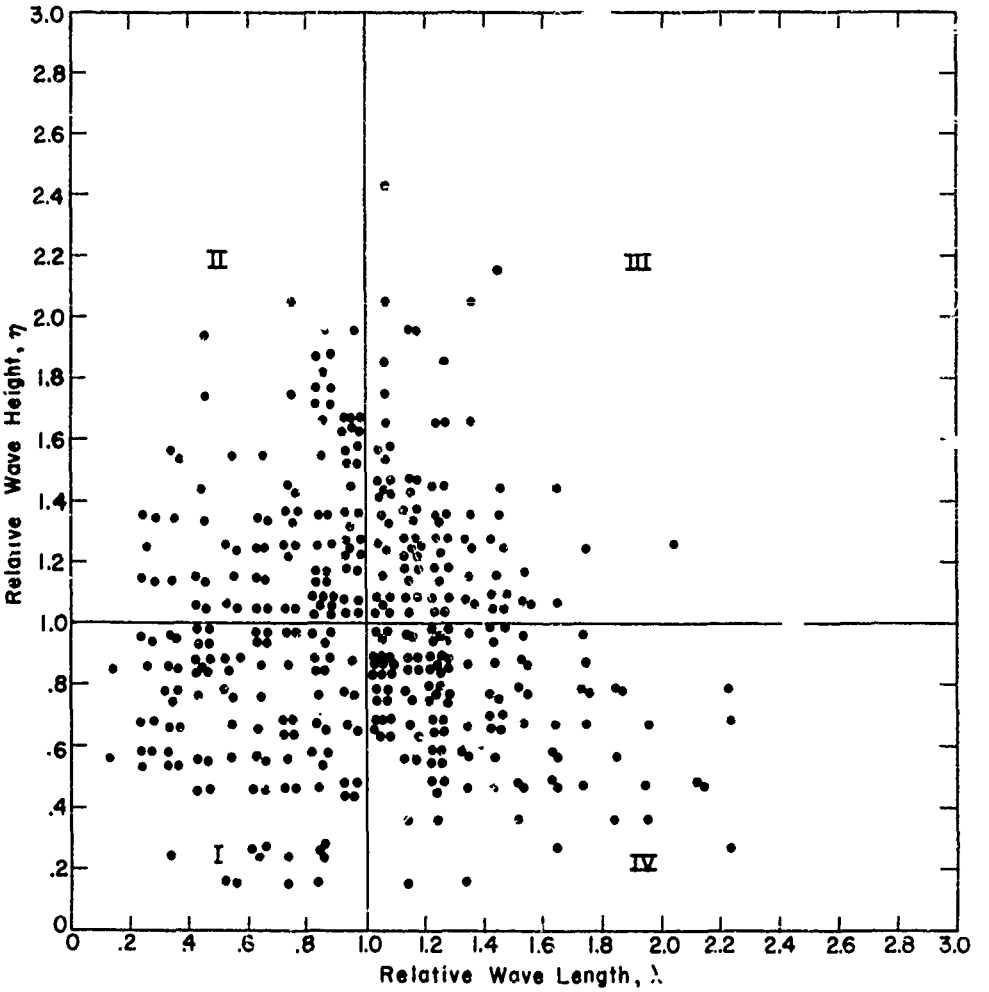

SCATTER DIAGRAM OF η AND λ FOR 400 CONSECUTIVE WAVES FROM GULF OF MEXICO

FIGURE 5.1

CHAPTER VI: STATISTICAL ANALYSIS OF WAVE DATA FOR JOINT DISTRIBUTION

1. General

Wave records discussed in Chapter IV have also been analyzed to determine certain properties of the joint distribution which might be used to compare with the approximate theoretical relationships given in Chapter V.

2. Correlation Coefficient

The correlation coefficient $r(\eta, \lambda)$ between wave height and wave length, determined from each wave record and summarized in Table 6.1, is given by

$$r(\eta, \lambda) = r(H,L) = \frac{\frac{1}{N}\sum_{i=1}^{N}(H_i - \bar{H})(L - \bar{L})}{S_H S_L} = \frac{\overline{\eta\lambda} - 1}{S_\eta S_\lambda} \qquad (6.1)$$

where

$r(H, L)$ is the correlation coefficient between H and L

H_i = individual height, feet

$\bar{H}$ = mean wave height = $\frac{1}{N}\sum_{i=1}^{N} H_i$

L_i = individual length ($L_i = T_i^2$ in sec^2)

$\bar{L}$ = mean length = $\frac{1}{N}\sum_{i=1}^{N} L_i$

S_H = standard deviation of height, feet

S_L = standard deviation of length, sec^2

$\overline{\eta\lambda} = \overline{HL}/\bar{H}\bar{L}$

$S_\eta = S_H/\bar{H}$

$S_\lambda = S_L/\bar{L}$

3. Mean Wave Height of Wave Lengths Greater than a Given Length

In the present discussion the unit forms η, λ, r are used conveniently. The mean wave height η_p of the longest p - percent wave length is a function of the correlation coefficient. For comparison with theory the data in this study were analyzed to include:

(a) $\eta(\lambda_{50})$, mean wave height of the longest 50 percent of wave lengths

(b) $\eta(\lambda_{33})$, mean wave height of the longest 33.3 percent of wave lengths

(c) $\eta(\lambda_{10})$, mean wave height of the longest 10 percent of wave lengths

(d) $\eta(\lambda_1)$, height of longest wave.

$\eta(\lambda_1)$ is assumed approximately equal to $\eta(\lambda_{max})$. This information is summarized in Table 6.1. Figure 6.1 shows these relationships as functions of the correlation coefficient, together with the theoretical relationships and the 95 percent confidence limits. The theoretical relationships for $\eta(\lambda_p)$ are obtained from Chapter V, according to:

$$\eta(\lambda_{50}) = 1 + 0.42\ r$$

$$\eta(\lambda_{33}) = 1 + 0.60\ r \qquad (6.2)$$

$$\eta(\lambda_{10}) = 1 + 1.03\ r$$

$$\eta(\lambda_1) = 1 + 1.66\ r$$

It is seen that agreement between theory and data is fairly good, particularly for $\eta(\lambda_{50})$ and $\eta(\lambda_{33})$. One difficulty with the other two relationships is that the number of waves is too few for the 10 percent and the 1 percent values to expect a minimum scatter. The 95 percent confidence limits for correlation are based on N = 100, average total number of waves per record.

TABLE 6.1

SUMMARY OF η FOR λ_{50}, λ_{33}, λ_{10}, AND λ_{max}

Source and Record	$r(\eta, \lambda)$	$\eta(\lambda_{50})$	$\eta(\lambda_{33})$	$\eta(\lambda_{10})$	$\eta(\lambda_{max})$
a-A	0.43	1.23	1.21	0.93	0.93
a-B	0.63	1.35	1.46	1.26	1.00
a-C	0.51	1.24	1.23	1.12	0.79
a-D	0.45	1.14	1.16	1.22	0.75
a-E	0.33	1.17	1.11	0.92	1.04
a-F	0.56	1.26	1.26	1.33	1.54
a-G	0.31	1.20	1.19	0.85	0.63
a-H	0.28	1.21	1.17	0.79	0.39
a-I	0.14	1.08	0.99	0.68	0.55
a-J	-0.04	1.04	1.22	0.70	0.35
a-K	0.08	1.03	1.00	0.80	0.42
a-L	0.17	1.10	1.02	0.95	1.22
a-M	0.22	1.18	1.09	0.81	0.80
a-N	-0.25	0.85	0.87	0.72	0.50
a-O	0.26	1.10	0.97	0.91	0.89
a-P	0.14	1.00	1.03	0.90	0.74
a-Q	0.08	1.10	1.05	0.80	0.87
a-R	-0.07	1.00	0.96	0.80	0.26
a-S	-0.05	0.98	0.90	0.74	1.03
a-T	-0.15	0.99	0.88	0.64	0.75
a-U	-0.19	0.94	0.92	0.73	0.52
a-V	0.13	1.08	0.89	0.77	0.78
a-W	0.20	1.17	1.08	0.87	0.42
a-X	-0.01	1.00	0.93	0.82	0.98
a-Y	-0.04	0.72	0.96	0.76	0.30
b- 1	0.12	1.10	1.10	1.03	0.89
b- 2	0.38	1.23	1.33	1.26	1.00
b- 3	0.42	1.37	1.24	1.14	2.01
b- 4	0.41	1.32	1.26	1.31	0.78
b- 5	0.48	1.37	1.36	1.34	1.49
b- 6	0.41	1.41	1.45	1.21	1.45
b- 7	0.54	1.37	1.36	1.41	1.35
b- 8	0.29	1.15	1.27	1.02	0.77
b- 9	0.19	1.19	1.24	1.26	1.04
b-10	0.22	1.28	1.35	0.89	1.25
b-11	0.15	1.20	1.19	1.22	0.71
b-12	0.30	1.23	1.22	1.17	1.18
b-13	0.41	1.28	1.33	1.14	0.80
b-14	0.42	1.43	1.36	1.15	0.03
b-15	0.47	1.41	1.35	1.44	1.91
b-16	0.31	1.36	1.34	1.15	1.12
b-17	0.45	1.36	1.45	1.40	1.86

TABLE 6.1
(Continued)

SUMMARY OF η FOR λ_{50}, λ_{33}, λ_{10}, AND λ_{max}

Source and Record	$r(\eta,\lambda)$	$\eta(\lambda_{50})$	$\eta(\lambda_{33})$	$\eta(\lambda_{10})$	$\eta(\lambda_{max})$
b-18	0.42	1.33	1.25	1.40	1.30
b-19	0.27	1.32	1.20	1.15	1.14
b-20	0.48	1.27	1.26	1.20	1.43
c- 5	0.34	1.27	1.26	0.93	1.64
c- 6	0.38	1.35	1.37	1.25	1.67
c- 7	0.16	1.04	1.07	1.06	1.33
c- 8	0.08	1.12	1.08	1.12	1.41
c-12	0.30	1.16	1.17	1.20	0.98
c-13	0.43	1.25	1.23	1.33	1.73
c-14	0.49	1.21	1.28	1.21	0.73
c-15	0.40	1.21	1.25	1.13	1.51
c-16	0.16	1.13	1.10	0.88	0.98
c-17	0.40	1.28	1.23	1.16	1.48
c-18	0.65	1.33	1.33	1.39	0.50
c-19	0.56	1.41	1.51	1.39	1.73
c-20	0.32	1.23	1.23	0.81	0.94
c-21	0.39	1.30	1.34	1.21	1.10
c-22	0.23	1.13	1.11	1.00	1.25
c-23	0.39	1.25	1.17	1.10	0.78
c-24	0.40	1.30	1.33	1.06	1.01
c-25	0.37	1.23	1.27	1.14	1.10
d- 1	0.49	1.24	1.42	1.31	2.17
d- 2	0.41	1.03	0.87	1.27	0.11
d- 3	0.48	1.23	1.32	1.26	0.78
d- 4	0.50	1.18	1.29	1.48	1.31
e- 1	-0.04	1.01	0.89	0.68	0.75
e- 2	0.11	1.02	0.97	0.87	0.40
e- 3	-0.30	0.88	0.84	0.76	0.47
e- 4	-0.17	0.91	0.83	0.61	0.61
e- 5	-0.42	0.82	0.68	0.69	0.72
e- 6	-0.22	0.91	0.79	0.76	0.37
e- 7	-0.42	0.91	0.85	0.64	0.41
e- 8	-0.41	0.89	0.86	0.61	0.49
e- 9	0.02	0.98	0.94	0.71	0.61
e-10	-0.07	1.00	1.00	0.68	0.86
e-11	-0.07	0.96	0.80	0.48	0.44
e-12	-0.17	1.00	0.85	0.62	0.75
e-13	0.06	1.00	0.85	0.71	0.55
e-14	-0.13	0.95	0.80	0.67	0.50
e-15	-0.17	0.91	0.82	0.54	0.45

TABLE 6.1
(Continued)

SUMMARY OF η FOR λ_{50}, λ_{33}, λ_{10}, AND λ_{max}

Source and Record	$r(\eta,\lambda)$	$\eta(\lambda_{50})$	$\eta(\lambda_{33})$	$\eta(\lambda_{10})$	$\eta(\lambda_{max})$
e- 1 to 5	-0.16	0.93	0.84	0.72	0.59
e- 6 to 10	-0.22	0.94	0.89	0.68	0.55
e-11 to 15	-0.10	0.96	0.82	0.60	0.54
e- 1 to 10	-0.19	0.94	0.87	0.70	0.57
e- 6 to 15	-0.16	0.95	0.86	0.64	0.55
e-16	-0.04				
e-17	-0.17				
f- 1	0.61	1.25	1.35	1.39	1.0
f- 2	0.37	1.22	1.26	1.10	1.2
f- 3	0.40	1.26	1.32	1.19	1.2
g-24	-0.09				
g-15	+0.74				
g-31	-0.09				
g-25	0.00				
g-35	+0.35				

4. Mean Wave Length of Wave Heights Greater than a Given Height

The mean wave length λ_p of the highest p - percent wave heights is a function of the correlation coefficient, similar to that for η_p. For comparison with theory the data in this paper were analyzed to include:

(a) $\lambda(\eta_{50})$, mean wave length of highest 50 percent of wave heights

(b) $\lambda(\eta_{33})$, mean wave length of highest 33.3 percent of wave heights

(c) $\lambda(\eta_{10})$, mean wave length of highest 10 percent of wave heights

(d) $\lambda(\eta_1)$, wave length of maximum wave

$\lambda(\eta_1)$ is assumed approximately equal to $\lambda(\eta_{max})$. This information is summarized in Table 6.2. Figure 6.2 shows these relationships as functions of the correlation coefficient, together with the theoretical relationships:

$$\lambda(\eta_{50}) = 1 + 0.42\ r$$

$$\lambda(\eta_{33}) = 1 + 0.60\ r \qquad (6.3)$$

$$\lambda(\eta_{10}) = 1 + 1.03\ r$$

$$\lambda(\eta_1) = 1 + 1.66\ r$$

The agreement between data and theory for $\lambda(\eta_p)$ is quite comparable to that for $\eta(\lambda_p)$, and hence the same general conclusions apply. It is believed that the scatter of data from theory is a peculiarity of the small sample from one record to the next, and is not necessarily of statistical significance. Deviation from linear regression is slight compared to that for $\eta(\lambda_p)$. A test for linearity using the array method and the F distribution shows this deviation from linearity is insignificant, and is discussed later.

TABLE 6.2

SUMMARY OF λ FOR η_{50}, η_{33}, η_{10}, AND η_{max}

Source and Record	$r(\eta, \lambda)$	$\lambda(\eta_{50})$	$\lambda(\eta_{33})$	$\lambda(\eta_{10})$	$\lambda(\eta_{max})$
a-A	0.43	1.24	1.22	1.19	1.12
a-B	0.63	1.44	1.61	1.64	1.72
a-C	0.51	1.23	1.28	1.30	1.24
a-D	0.45	1.14	1.17	1.15	1.49
a-E	0.33	1.14	1.10	1.05	1.02
a-F	0.56	1.23	1.26	1.13	0.87
a-G	0.31	1.13	1.10	1.23	1.08
a-H	0.28	1.03	1.05	1.07	1.09
a-I	0.14	1.02	1.03	1.05	1.03
a-J	-0.04	1.02	0.95	0.86	1.02
a-K	0.08	1.00	0.99	0.99	1.02
a-L	0.17	1.10	1.06	1.01	0.91
a-M	0.22	1.05	1.04	1.05	1.05
a-N	-0.25	0.95	0.83	0.55	0.78
a-O	0.26	1.12	1.03	0.91	0.52
a-P	0.14	1.03	1.09	0.88	0.75
a-Q	0.08	1.02	1.01	1.07	1.14
a-R	-0.07	0.99	0.97	0.93	1.02
a-S	-0.05	0.96	0.97	0.82	1.14
a-T	-0.15	1.01	0.92	0.91	0.83
a-U	-0.19	0.94	0.91	0.86	0.03
a-V	0.13	1.06	1.04	1.05	0.99
a-W	0.20	1.10	1.18	1.24	1.07
a-X	-0.01	1.00	0.98	0.97	1.09
a-Y	-0.04	1.04	1.05	0.93	0.92
b- 1	0.12	1.14	1.09	0.83	0.75
b- 2	0.38	1.21	1.21	1.19	2.10
b- 3	0.42	1.18	1.22	1.36	0.81
b- 4	0.41	1.23	1.21	1.19	1.14
b- 5	0.48	1.28	1.40	1.17	0.89
b- 6	0.41	1.35	1.29	1.36	1.30
b- 7	0.54	1.34	1.43	1.42	1.23
b- 8	0.29	1.17	1.14	1.05	0.85
b- 9	0.19	1.23	1.05	1.10	0.30
b-10	0.22	1.23	1.18	1.05	1.00
b-11	0.15	1.14	1.13	0.82	1.14
b-12	0.30	1.20	1.10	1.14	2.15
b-13	0.41	1.20	1.17	1.11	1.40
b-14	0.42	1.27	1.28	1.32	1.17
b-15	0.47	1.26	1.38	1.46	0.83
b-16	0.31	1.32	1.23	1.32	1.39
b-17	0.45	1.30	1.42	1.41	1.73

TABLE 6.2
(Continued)

SUMMARY OF λ FOR η_{50}, η_{33}, η_{10}, AND η_{max}

Source and Record	$r(\eta, \lambda)$	$\lambda(\eta_{50})$	$\lambda(\eta_{33})$	$\lambda(\eta_{10})$	$\lambda(\eta_{max})$
b-18	0.42	1.28	1.24	1.28	0.90
b-19	0.27	1.25	1.18	1.17	0.88
b-20	0.48	1.26	1.27	1.35	0.93
c- 5	0.34	1.18	1.21	1.12	0.89
c- 6	0.38	1.25	1.31	1.28	1.20
c- 7	0.16	1.05	1.05	1.06	0.86
c- 8	0.08	1.06	1.09	0.99	0.67
c-12	0.30	1.15	1.09	1.07	0.94
c-13	0.43	1.14	1.24	1.36	2.50
c-14	0.49	1.25	1.31	1.28	0.96
c-15	0.40	1.30	1.25	1.10	1.11
c-16	0.16	1.06	0.99	1.05	0.94
c-17	0.40	1.18	1.19	1.20	0.98
c-18	0.65	1.29	1.29	1.38	0.95
c-19	0.56	1.35	1.49	1.33	1.09
c-20	0.32	1.10	1.11	1.19	1.33
c-21	0.39	1.15	1.13	1.23	1.17
c-22	0.23	1.14	1.06	1.00	1.40
c-23	0.39	1.17	1.21	1.23	1.43
c-24	0.40	1.13	1.18	1.24	1.22
c-25	0.37	1.15	1.15	1.25	1.08
d- 1	0.49	1.64	1.96	1.79	1.89
d- 2	0.41	1.25	1.40	1.18	0.85
d- 3	0.48	1.26	1.30	1.51	2.30
d- 4	0.50	1.31	1.23	1.49	1.46
e- 1	-0.04	0.99	0.97	0.91	0.94
e- 2	0.11	1.06	1.02	1.03	1.05
e- 3	-0.30	0.92	0.88	0.81	0.41
e- 4	-0.17	0.86	0.89	0.76	0.80
e- 5	-0.42	0.74	0.79	0.64	0.37
e- 6	-0.22	0.90	0.84	0.89	0.77
e- 7	-0.42	0.88	0.81	0.81	0.86
e- 8	-0.41	0.86	0.84	0.79	0.86
e- 9	0.02	1.00	0.98	0.98	0.87
e-10	-0.07	0.95	0.93	1.02	0.95
e-11	-0.07	0.98	0.96	0.99	0.93
e-12	-0.17	0.91	0.91	0.98	1.06
e-13	0.06	0.99	0.98	1.02	1.00
e-14	-0.13	0.91	0.88	0.85	0.76
e-15	-0.17	0.93	0.93	0.96	0.93

TABLE 6.2
(Continued)

SUMMARY OF λ FOR η_{50}, η_{33}, η_{10}, AND η_{max}

Source and Record	$r(\eta, \lambda)$	$\lambda(\eta_{50})$	$\lambda(\eta_{33})$	(η_{10})	(η_{max})
e- 1 to 5	-0.16	0.91	0.91	0.83	1.00
e- 6 to 10	-0.22	0.92	0.88	0.90	0.91
e-11 to 15	-0.10	0.94	0.93	0.96	1.06
e- 1 to 10	-0.19	0.92	0.90	0.87	1.09
e- 6 to 15	-0.16	0.93	0.91	0.93	1.09
e-16 e-17	-0.04				
f- 1	0.613	1.44	1.57	1.73	1.42
f- 2	0.374	1.34	1.33	1.02	0.70
f- 3	0.398	1.30	1.37	0.95	1.33

5. Mean Wave Period of Wave Heights Greater than a Given Height

The mean wave period τ_p of the highest p - percent wave heights is a function of the correlation coefficient, remembering that the correlation coefficient is that between η and λ. For comparison with theory the data in this study were analyzed to include:

(a) $\tau(\eta_{50})$, mean wave period of highest 50 percent wave heights

(b) $\tau(\eta_{33})$, mean wave period of highest 33.3 percent wave heights

(c) $\tau(\eta_{10})$, mean wave period of highest 10 percent wave heights

(d) $\tau(\eta_1)$, period of maximum wave height

$\tau(\eta_1)$ is assumed approximately equal to $\tau(\eta_{max})$. This information is summarized in Table 6.3. Figure 6.3 shows these relationships as functions of $r(\eta, \lambda)$, together with the theoretical relationships:

$$\tau(\eta_{50}) = \sqrt{1 + 0.42\, r} \qquad \tau(\eta_{10}) = \sqrt{1 + 1.03\, r}$$
$$\tau(\eta_{33}) = \sqrt{1 + 0.60\, r} \qquad \tau(\eta_1) = \sqrt{1 + 1.60\, r} \qquad (6.4)$$

Where r is correlation coefficient between η and λ, the agreement between data and theory is quite comparable to that for λ, η_p).

TABLE 6.3

SUMMARY OF τ FOR η_{50}, η_{33}, η_{10}, AND η_{max}

Source and Record	$r(\eta, \lambda)$	$\tau(\eta_{50})$	$\tau(\eta_{33})$	$\tau(\eta_{10})$	$\tau(\eta_{max})$
a-A	0.43	1.13	1.17	1.15	1.12
a-B	0.63	1.25	1.36	1.38	1.43
a-C	0.51	1.16	1.18	1.19	1.17
a-D	0.45	1.08	1.10	1.10	1.25
a-E	0.33	1.09	1.07	1.05	1.04
a-F	0.56	1.12	1.13	1.09	0.95
a-G	0.31	1.08	1.08	1.14	1.08
a-H	0.28	1.03	1.04	1.06	1.07
a-I	0.14	1.02	1.03	1.04	1.04
a-J	-0.04	1.02	1.00	0.97	1.05
a-K	0.08	1.01	1.01	1.01	1.03
a-L	0.17	1.05	1.04	1.02	0.98
a-M	0.22	1.04	1.04	1.05	1.05
a-N	-0.25	0.99	0.90	0.74	0.92
a-O	0.26	1.10	1.04	0.98	0.75
a-P	0.14	1.03	1.06	0.96	0.89
a-Q	0,08	1.01	1.01	1.05	1.09
a-R	-0.07	1.00	0.99	0.97	1.03
a-S	-0.05	0.98	1.00	0.92	1.09
a-T	-0.15	0.97	0.97	0.93	0.93
a-U	-0.19	0.97	0.99	0.94	0.19
a-V	0.13	1.04	1.03	1.04	1.02
a-W	0.20	1.07	1.12	1.16	1.09
a-X	-0.01	1.00	0.99	0.99	1.06
a-Y	-0.04	1.03	1.04	0.96	0.99
b- 1	0.12	1.08	1.06	0.92	0.89
b- 2	0,38	1.11	1.12	1.45	1.50
b- 3	0.42	1.12	1.14	1.20	0.94
b- 4	0.41	1.15	1.17	1.13	1.12
b- 5	0.48	1.19	1.24	1.14	1.02
b- 6	0.41	1.21	1.19	1.24	1.22
b- 7	0.54	1.20	1.24	1.25	1.18
b- 8	0.29	1.10	1.09	1.03	0.96
b- 9	0.19	1.12	1.05	1.07	0.58
b-10	0.22	1.14	1.12	1.07	1.05
b-11	0.15	1.07	1.07	0.92	1.11
b-12	0.30	1.12	1.08	1.11	1.54
b-13	0.41	1.13	1.11	1.09	1.23
b-14	0.42	1.17	1.18	1.21	1.14
b-15	0.47	1.14	1.20	1.23	0.96
b-16	0.31	1.17	1.15	1.10	1.24
b-17	0.45	1.17	1.23	1.22	1.40

TABLE 6.3
(Continued)

SUMMARY OF τ FOR η_{50}, η_{33}, η_{10}, AND η_{max}

Source and Record	$r(\eta, \lambda)$	$\tau(\eta_{50})$	$\tau(\eta_{33})$	$\tau(\eta_{10})$	$\tau(\eta_{max})$
b-18	0.42	1.16	1.14	1.18	1.00
b-19	0.27	1.14	1.12	1.13	1.00
b-20	0.48	1.17	1.17	1.22	1.02
c- 5	0.34	1.12	1.14	1.11	0.99
c- 6	0.38	1.14	1.17	1.16	1.14
c- 7	0.16	1.03	1.03	1.04	0.95
c- 8	0.08	1.04	1.06	1.01	0.84
c-12	0.30	1.09	1.07	1.06	1.01
c-13	0.43	1.09	1.15	1.20	1.65
c-14	0.49	1.15	1.19	1.17	1.03
c-15	0.40	1.18	1.16	1.10	1.12
c-16	0.16	1.05	1.01	1.05	1.00
c-17	0.40	1.12	1.11	1.12	1.03
c-18	0.65	1.17	1.17	1.22	1.03
c-19	0.56	1.19	1.26	1.20	1.09
c-20	0.32	1.07	1.08	1.12	1.19
c-21	0.39	1.08	1.04	1.13	1.11
c-22	0.23	1.09	1.05	1.04	1.23
c-23	0.39	1.10	1.12	1.13	1.25
c-24	0.40	1.08	1.11	1.15	1.14
c-25	0.37	1.09	1.09	1.14	1.07
d- 1	0.49	1.18	1.22	1.40	1.48
d- 2	0.41	1.15	1.23	1.13	1.00
d- 3	0.48	1.15	1.18	1.29	1.61
d- 4	0.50	1.09	1.12	1.27	1.27
e- 1	-0.04	1.00	0.99	0.97	0.99
e- 2	0.11	1.04	1.03	1.05	1.05
e- 3	-0.30	0.95	0.93	0.91	0.65
e- 4	-0.17	0.94	0.95	0.89	0.93
e- 5	-0.42	0.90	0.93	0.84	0.66
e- 6	-0.22	0.95	0.93	0.97	0.90
e- 7	-0.42	0.97	0.92	0.94	0.98
e- 8	-0.21	0.94	0.93	0.90	0.95
e- 9	0.02	1.01	1.00	1.01	0.95
e-10	-0.07	0.98	0.98	1.03	1.00
e-11	-0.07	1.00	0.99	1.01	0.98
e-12	-0.17	0.97	0.97	1.01	1.06
e-13	0.06	1.01	1.01	1.03	1.03
e-14	-0.13	0.97	0.96	0.95	0.90
e-15	-0.17	0.98	0.98	0.99	0.98

TABLE 6.3
(Continued)

SUMMARY OF τ FOR η_{50}, η_{33}, η_{10}, AND η_{max}

Source and Record	$r(\eta\,\lambda)$	$\tau(\eta_{50})$	$\tau(\eta_{33})$	$\tau(\eta_{10})$	$\tau(\eta_{max})$
e- 1 to 5	-0.16	0.97	0.57	0.93	1.03
e- 6 to 10	-0.22	0.97	0.95	0.97	0.98
e-11 to 15	-0.10	0.99	0.98	1.00	1.06
e- 1 to 10	-0.19	0.97	0.96	0.95	1.08
e- 6 to 15	-0.16	0.98	0.97	0.99	1.07
e-16	-0.04				
e-17					
f- 1	0.613	1.25	1.32	1.39	1.29
f- 2	0.374	1.21	1.22	1.07	0.91
f- 3	0.39	1.17	1.19	1.00	1.23

6. Percent of Waves in Quadrants

The percent of waves in four quadrants for various limits of and have been determined from the wave data, where

$$\begin{aligned} P_I &= P\left[1\,,\,1\right] \\ P_{II} &= P\left[\infty\,,\,1\right] - \left[P\;\;1\,,\,1\right] \\ P_{III} &= P\left[\infty\,,\infty\right] - P\left[\infty\,,\,1\right] - P\left[1\,,\infty\right] + P\left[1\,,\,1\right] \\ P_{IV} &= P\left[1\,,\infty\right] - P\left[1\,,\,1\right] \end{aligned} \tag{6.5}$$

This information is summarized in Table 6.4. Figure 6.4 shows these relationships as functions of the correlation coefficient. No theoretical relationship is shown except for r = 0, r = +1, and r = -1. The solid lines are assumed linear relationships between r = 0 and r = +1.0, which of course represents an approximation not in too bad agreement with data. The dashed lines are 95 percent confidence limits.

TABLE 6.4

SUMMARY OF P_I, P_{II}, P_{III}, AND P_{IV}

Source and Record	$r(\eta, \lambda)$	P_I	P_{II}	P_{III}	P_{IV}
a-A	0.43	40.0	8.3	33.9	17.8
a-B	0.63	50.2	6.0	34.6	9.2
a-C	0.51	38.2	7.9	34.8	19.1
a-D	0.45	32.8	13.1	32.3	21.8
a-E	0.33	36.1	17.8	22.9	23.2
a-F	0.56	38.4	14.2	33.7	13.7
a-G	0.31	34.4	19.4	27.9	18.3
a-H	0.28	34.5	26.7	24.6	14.2
a-I	0.14	32.3	20.1	22.3	25.3
a-J	-0.04	36.2	24.8	15.8	23.2
a-K	0.08	30.1	28.2	18.4	23.3
a-L	0.17	33.2	19.2	21.7	25.9
a-M	0.22	32.6	22.6	27.9	16.9
a-N	-0.25	31.9	23.2	14.7	30.2
a-O	0.26	32.9	20.5	27.5	19.1
a-P	0.14	25.4	27.1	23.9	23.6
a-Q	0.08	32.4	18.4	25.8	23.4
a-R	-0.07	37.0	22.0	15.4	25.6
a-S	-0.05	26.8	26.1	19.7	25.4
a-T	-0.15	31.5	30.0	15.4	23.1
a-U	-0.19	35.6	20.8	11.0	31.8
a-V	0.13	33.4	15.7	25.1	25.8
a-W	0.20	35.0	15.0	30.0	20.0
a-X	-0.01	25.0	20.7	25.6	28.7
a-Y	-0.04	28.9	22.2	26.7	22.2
b- 1	0.12	39.5	18.0	17.0	25.5
b- 2	0.38	31.0	13.0	32.0	24.0
b- 3	0.42	35.0	15.0	27.0	23.0
b- 4	0.41	38.0	17.0	28.0	17.0
b- 5	0.48	41.0	18.0	26.5	14.5
b- 6	0.41	43.0	21.0	27.5	8.5
b- 7	0.54	39.0	18.5	28.0	14.5
b- 8	0.29	38.5	21.0	23.5	17.0
b- 9	0.19	36.0	21.5	24.5	18.0
b-10	0.22	40.5	11.5	24.0	24.0
b-11	0.15	34.5	21.0	26.5	18.0
b-12	0.30	37.3	20.8	26.8	15.3
b-13	0.41	38.5	18.0	29.0	14.5
b-14	0.42	39.8	14.8	29.8	15.8
b-15	0.47	41.0	25.5	22.5	11.0
b-16	0.31	39.0	14.5	32.5	14.0
b-17	0.45	42.5	14.5	31.5	11.5

TABLE 6.4
(Continued)

SUMMARY OF P_I, P_{II}, P_{III}, AND P_{IV}

Source and Record	$r(\eta, \lambda)$	P_I	P_{II}	P_{III}	P_{IV}
b-18	0.42	39.5	20.5	27.0	13.0
b-19	0.27	42.0	22.5	23.0	12.5
b-20	0.48	33.0	29.0	28.0	10.0
c- 5	0.34	36.6	16.8	27.2	19.4
c- 6	0.38	42.8	9.3	27.5	20.4
c- 7	0.16	30.1	22.2	22.2	25.4
c- 8	0.08	35.8	13.8	25.0	25.4
c-12	0.30	34.1	26.3	27.2	12.4
c-13	0.43	36.6	26.3	24.5	11.6
c-14	0.49	32.4	16.7	38.0	12.9
c-15	0.40	38.9	20.3	32.9	7.9
c-16	0.16	33.3	23.4	23.0	20.3
c-17	0.40	38.2	17.8	30.2	13.8
c-18	0.65	40.9	17.3	25.9	15.9
c-19	0.56	45.2	11.4	32.3	10.1
c-20	0.32	30.3	16.6	32.0	21.1
c-21	0.39	42.2	15.6	29.3	13.6
c-22	0.23	36.4	20.7	19.9	23.0
c-23	0.39	40.3	17.5	22.8	19.4
c-24	0.40	39.9	17.0	28.4	14.7
c-25	0.37	38.8	14.0	26.2	21.0
d- 1	0.49	0.397	0.191	0.305	0.107
d- 2	0.41	0.358	0.170	0.321	0.151
d- 3	0.48	0.376	0.177	0.326	0.121
d- 4	0.50	0.330	0.122	0.322	0.226
e- 1	-0.04	29.0	23.0	24.0	24.0
e- 2	0.11	29.0	23.0	24.0	24.0
e- 3	-0.30	23.0	28.0	16.5	32.0
e- 4	-0.17	23.0	28.0	16.5	32.0
e- 5	-0.42	26.0	32.0	12.0	30.0
e- 6	-0.22	26.0	32.0	12.0	30.0
e- 7	-0.42	25.5	29.5	16.5	28.0
e- 8	-0.41	25.5	29.5	16.5	28.0
e- 9	0.02	31.0	26.0	20.5	22.5
e-10	-0.07	31.0	26.0	20.5	22.5
e-11	-0.07	29.0	26.0	18.5	26.5
e-12	-0.17	29.0	26.0	18.5	26.5
e-13	0.06	29.0	27.0	17.0	27.0
e-14	-0.13	29.0	27.0	17.0	27.0
e-15	-0.17				

TABLE 6.4
(Continued)

SUMMARY OF P_I, P_{II}, P_{III}, AND P_{IV}

Source and Record	$r(\eta, \lambda)$	P_I	P_{II}	P_{III}	P_{IV}
e- 1 to 5	-0.16	26.0	26.8	18.6	28.4
e- 6 to 10	-0.22	27.8	28.6	17.2	26.2
e-11 to 15	-0.10	29.0	26.5	17.8	26.8
e- 1 to 10	-0.19	26.9	27.7	17.9	27.3
e- 6 to 15	-0.16	28.4	27.6	17.5	26.5
e-16	-0.04	29.8	25.0	18.8	26.4
e-17					
f- 1	0.613				
f- 2	0.374				
f- 3	0.398				
g-24		25.6	11.6	30.2	32.6
g-15		20.6	11.8	52.9	14.7
g-31		15.2	18.2	33.3	33.3
g-25		33.3	26.2	21.4	19.0
g-35		33.3	16.7	27.8	22.2

7. Confidence Limits For Correlation Coefficients

Because the statistical parameters, including $r(\eta, \lambda)$, will vary from one seemingly similar record to another, even though the sample size remains constant, the correlation coefficient r is merely an estimate subject to sampling error. For any observed value of r one may set limits which will be wide enough to include the true value with any required degree of confidence, say 0.95. These limits are called the 95 percent confidence limits. If r = observed value, then ρ = true value of correlation coefficient. The true value, ρ, although unknown, is not a random variable, so that one should not speak of the probability that ρ lies between the confidence limits. Instead r is the random variable and there is a probability that the confidence interval (between upper and lower confidence limits), which is a function of r, will include the true value, so that in saying of one confidence interval that it does include the true value, there stands only a 5 percent chance of being wrong, and therefore a reasonable chance of being right.

Ninety-five percent confidence limits for correlation coefficients when N = 100, from Fischer (1915), are presented in Table 6.5.

TABLE 6.5

95 PERCENT CONFIDENCE LIMITS FOR CORRELATION COEFFICIENTS N = 100

r	Upper	Lower
0	0.197	-0.197
0.1	0.292	-0.099
0.2	0.383	0.003
0.3	0.470	0.110
0.4	0.554	0.220
0.5	0.635	0.336
0.6	0.713	0.457
0.7	0.796	0.583
0.8	0.862	0.716
0.9	0.932	0.854
1.0	1.000	1.000

For r minus, the 95 percent confidence limits are the negative of the corresponding values for r positive in the above table.

8. Test for Linearity of Regression

Mathematics and the theory for test of linearity of regression will not be repeated here, but is readily available in textbooks on mathematics of statistics, for example, Kenney and Keeping (1956), Part II, Chapter XI.

The continuous records, sources a and e only, were tested. The non-continuous records appear to have appreciable deviation from linear regression, according to Figures 6.1 through 6.4. This may be a peculiarity of these types of non-continuous records.

Data were tabulated in η-rows and λ-columns at 0.5 intervals. The records average about 100 waves each for both sources. Source a averaged 6 rows and 6 columns, whence the number of degrees of freedom $n_1 = 6 - 2 = 4$ and $n_2 = 100 - 6 = 94$, corresponding to values of the F distribution of 2.47 and 3.52 for the 5 percent and 1 percent limits, respectively. Source e averaged 5 rows and 5 columns, corresponding to F values of 2.71 and 4.00 for the 5 percent and 1 percent limits, respectively.

Table 6.6 presents the results of the test for linearity. For both sources it is seen for a number of cases deviation from linear regression is significant for the regression of η on λ. However, in most cases for λ on η the deviation from linear regression is insignificant. Perhaps in some cases an unsatisfactory linear regression of η on λ may be due to such physical factors as breaking waves or limiting η values for small λ. The reverse of λ on η, however, does not appear to have the same restriction. Deviations from the Rayleigh distribution may also have an effect on the linearity of regression.

Based on the above investigation, it is seen that the relationship of $\eta(\lambda_p)$, mean wave height for longest wave lengths is not entirely satisfactory for prediction purposes. It can be concluded, however, that the relationship of $\lambda(\eta_p)$, mean wave length of highest wave heights, is satisfactory; and, therefore, the relationship of $\tau(\eta_p)$, mean wave period of highest wave heights, is also satisfactory for prediction purposes.

TABLE 6.6

TEST FOR LINEARITY OF REGRESSION
(F - Distribution)

Source and Record	$\Sigma(\overline{\eta}_\lambda Y_\lambda)$	$F_{\eta\lambda}$	$\Sigma(\overline{\lambda}_\eta X_\eta)$	$F_{\lambda\eta}$	F 5%	F 1%
a-A	4.6078	7.57	2.0246	1.91	Between	Between
a-B	8.8191	19.72	7.7811	6.43	2.4	3.5
a-C	1.1405	1.51	2.0005	2.90	and	and
a-D	2.2240	2.90	2.8327	9.32	2.5	3.6
a-E	2.8580	2.78	0.6380	0.92		
a-F	1.2390	1.26	1.6890	3.65		
a-G	5.0834	5.12	2.8955	4.57		
a-H	12.7390	11.63	2.0765	3.12		
a-I	9.8605	10.58	1.2777	2.41		
a-J	3.7153	2.86	0.6979	0.05		
a-K	3.5570	4.28	0.5587	0.55		
a-L	2.9492	2.88	1.7755	1.93		
a-M	5.4436	7.33	2.8065	3.82		
a-N	2.6298	1.44	2.8563	2.45		
a-O	3.9536	4.41	3.0744	3.13		
a-P	5.6783	9.52	2.9888	3.77		
a-Q	1.9035	2.24	0.1469	0.19		
a-R	2.5011	2.05	1.1609	1.26		
a-S	9.2409	15.21	0.4710	0.68		
a-T	3.2277	5.14	0.7225	0.88		
a-U	1.0713	0.57	1.7632	2.23		
a-V	3.3342	3.68	1.0425	1.79		
a-W	5.4283	8.12	0.4800	0.35		
a-X	1.4424	1.84	0.0680	0.11		
a-Y	2.0063	2.59	2.8450	3.69		
Ave.		5.49		2.48		
e- 1	1.4047	2.53	1.6553	4.00	2.71	4.0
e- 2	1.3504	2.68	1.8547	2.30		
e- 3	1.8283	5.78	0.8524	2.78		
e- 4	0.8804	1.36	0.6552	0.83		
e- 5	0.5957	1.19	0.3505	0.51		
e- 6	1.6587	3.02	0.0642	0.08		
e- 7	6.7245	33.01	1.4888	3.25		
e- 8	1.7441	3.93	0.8149	2.04		
e- 9	1.4747	3.00	0.2243	0.50		
e-10	3.2596	6.60	0.7310	1.35		
e-11	4.5723	9.44	0.2206	0.53		
e-12	2.8004	5.04	0.7914	2.33		
e-13	2.6396	5.46	0.3534	0.68		
e-14	7.3616	15.30	0.8464	1.20		
e-15	2.2677	4.17	3.1746	11.23	2.71	4.0
Ave.		6.83		2.24		

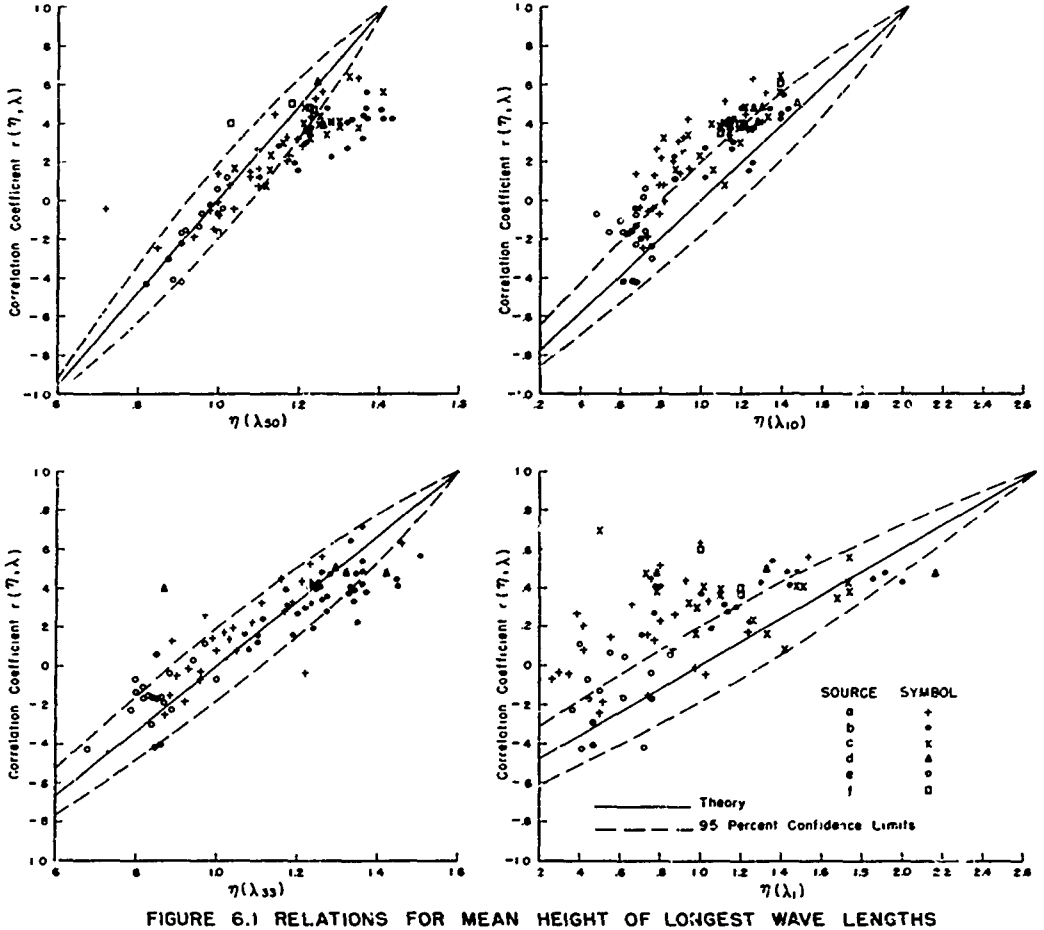

FIGURE 6.1 RELATIONS FOR MEAN HEIGHT OF LONGEST WAVE LENGTHS

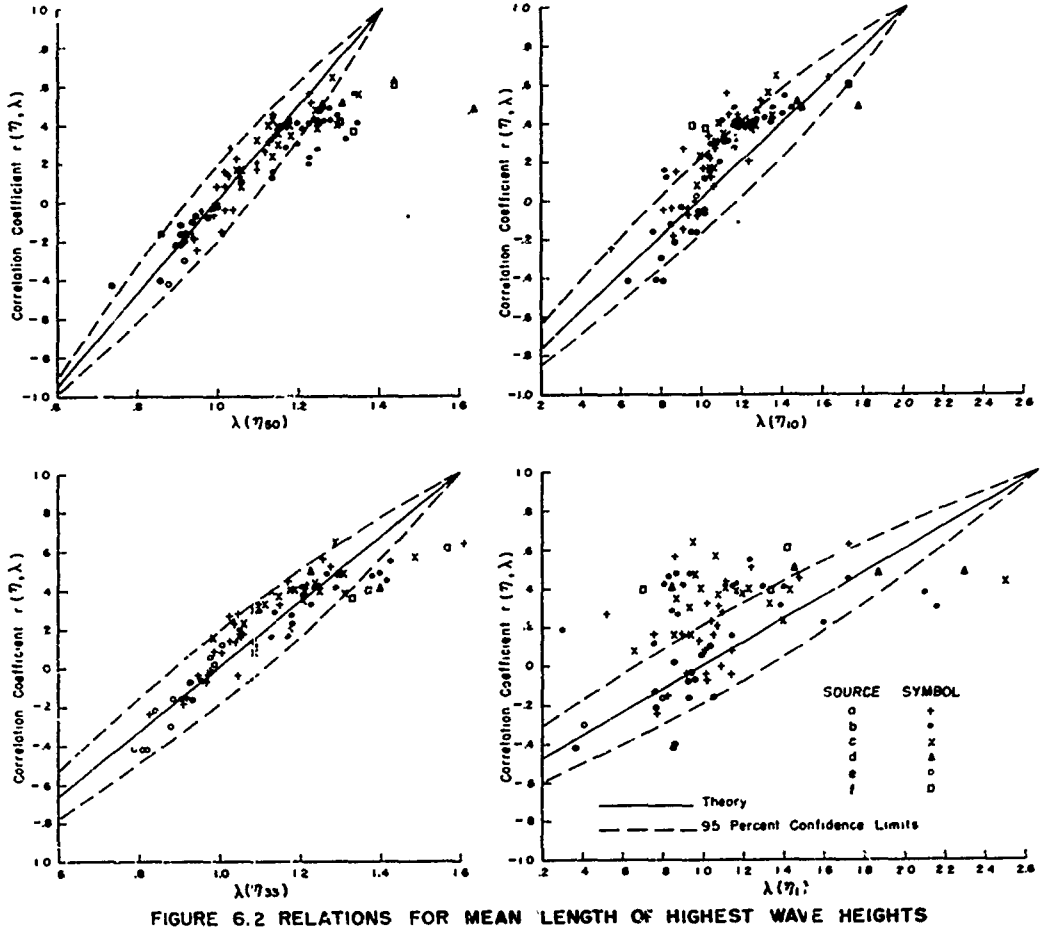

FIGURE 6.2 RELATIONS FOR MEAN LENGTH OF HIGHEST WAVE HEIGHTS

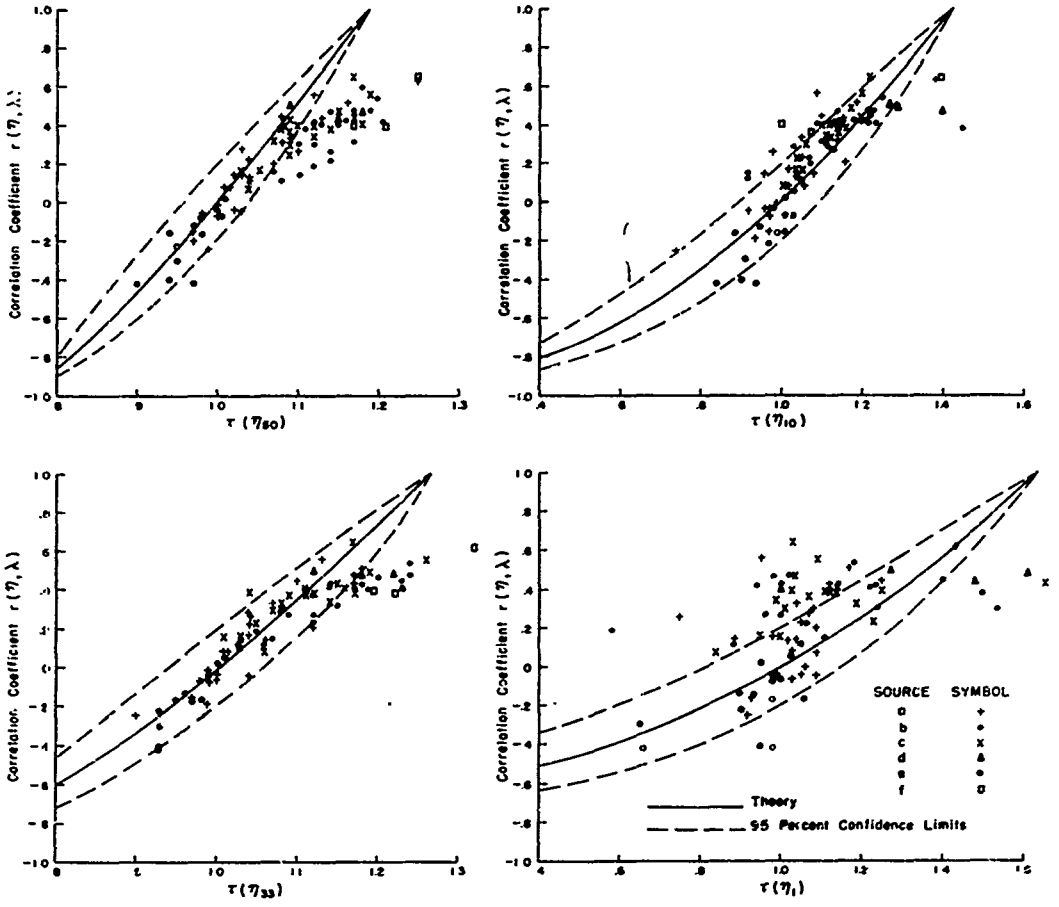

FIGURE 6.3 RELATIONS FOR MEAN PERIOD OF HIGHEST WAVE HEIGHTS

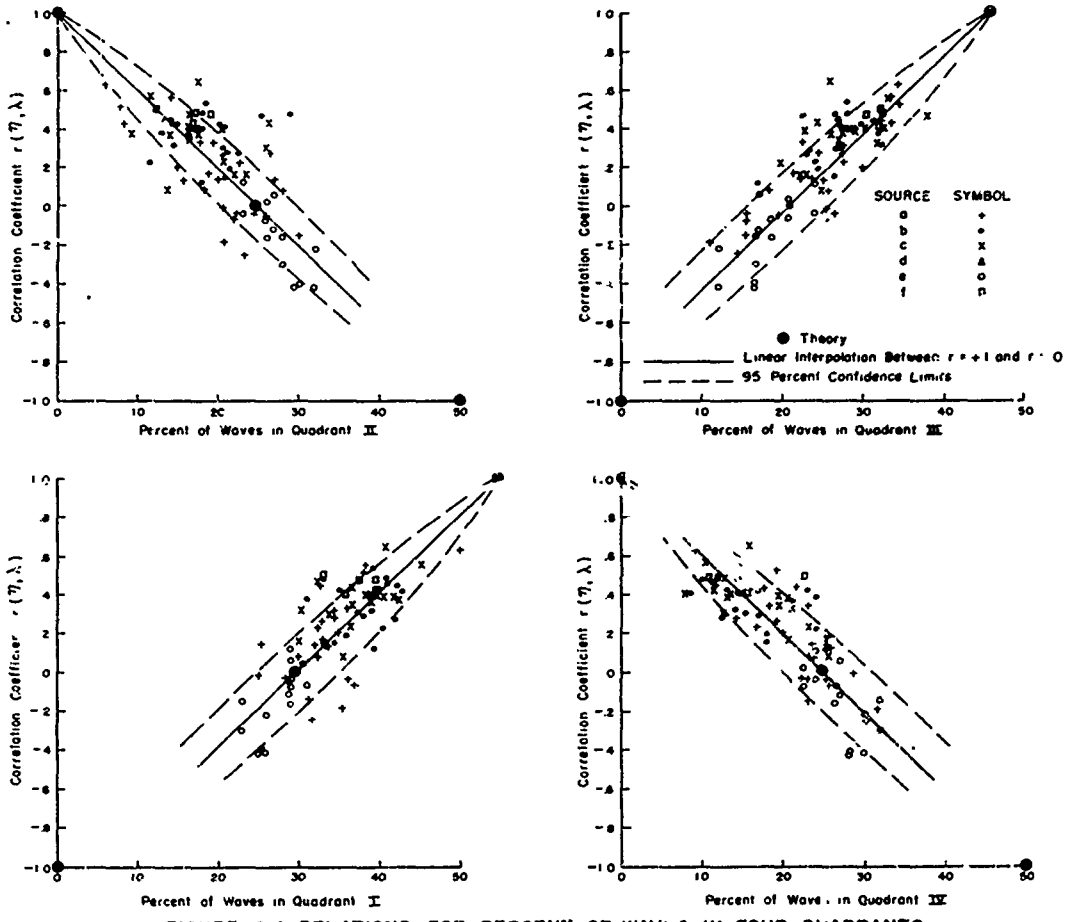

FIGURE 64 RELATIONS FOR PERCENT OF WAVES IN FOUR QUADRANTS

CHAPTER VII: A THEORY OF WAVE SPECTRA FROM JOINT DISTRIBUTION

1. General

A theory of wave spectra for ocean waves is developed from the knowledge of joint distribution of heights and lengths. The unit form of notation is used throughout the development, and the final form in standard units is presented. In the following development certain assumptions are made. These are discussed when need arises in the development. The general derivation can be made without any knowledge of the exact marginal distribution functions, except that $p(\eta)$ and $p(\lambda)$ must be of the same variate, i.e., $\eta^2, a_3\eta^3, a_3\lambda^3$, etc; and it is assumed that linear regression applies for η on λ (or λ on η).

2. Energy Considerations

The definition of wave energy used in simple wave theory refers to the mean wave energy per unit area of surface. To obtain total wave energy per unit width perpendicular to the crest the mean wave energy per unit area of surface is multiplied by the wave length. In unit form the mean wave energy per unit of area surface is defined by

$$q' = \frac{\eta^2}{\overline{\eta^2}} \tag{7.1}$$

and the total energy per unit width is given by

$$Q' = q'\lambda \tag{7.2}$$

where

$$\eta^2 = \frac{\frac{1}{16}g\rho H^2}{\frac{1}{16}g\rho\overline{H^2}}\,\overline{\eta^2} = \overline{\eta^2}\,\frac{H^2}{\overline{H^2}} \tag{7.3}$$

It can be seen from (7.3) that both (7.1) and (7.2) might represent either the potential energy or the kinetic energy, or both.

In the material following η and λ symbols are used, and η^2 will be called energy, although the actual energy must be obtained by use of q' and Q' from above, whence

$$q = \eta^2 \tag{7.4}$$

and

$$Q = \eta^2 \lambda \tag{7.5}$$

In Cartesian coordinate system for two directions let $q = \eta^2$ be parallel to the ordinate and λ parallel to the abscissa, and it will be seen that Q is the area under the line $\eta^2 =$ constant bounded by the interval between 0 and λ. In the same system q will be a point whose coordinates are η^2 and λ.

Consider next a wave record of N waves, in which there are k number of η_i^2 having λ's of class i between $\lambda_i + \frac{\Delta\lambda}{2}$ and $\lambda_i - \frac{\Delta\lambda}{2}$ and the sum of q_i and the sum of Q_i become

$$q_i = \sum_{i=1}^{k} \eta_i^2 = k\overline{\eta_i^2} \tag{7.6}$$

$$Q_i = k\overline{\eta_i^2}\,\lambda_i \tag{7.7}$$

limit as $\Delta\lambda \to 0$

It can now be seen that Q_i is the area under the line $k\overline{\eta_i^2}$ = constant bounded by the interval 0 and λ as $\Delta\lambda \longrightarrow 0$, and that q_i is an element bounded by $k\eta_i^2$ for the increment $\Delta\lambda$, but as $\Delta\lambda \to 0$ q_i becomes a point whose coordinates are $k\eta_i^2$ and λ_i. This point is one of many such points on a curve as the process is repeated for other classes of λ. This curve is called the λ spectra of q or the λ spectra of η^2.

In the above it is not necessary to assume for a complex sea that one may compute q or q_i from the measured wave heights, which appear to be changing with time, and hence it is not necessary to assume individual values of q proportional to η^2 for a complex sea. It is only necessary to assume that the statistical distribution of η_i for each class of λ_i is sufficient such that q_i is proportional to η_i^2. The above appears to be true when all waves are considered as one class, in which case $\eta_i^2 = \eta^2$ the energy coefficient; and for the Rayleigh distribution $\overline{\eta^2} = \frac{4}{\pi}$, which is in agreement with the

data. When classes of λ are considered, it appears also that $\overline{\eta_i^2} = \frac{4}{\pi}$ where

$$\eta_i = \frac{H}{H_i} \tag{7.8}$$

and it appears that the above assumption is satisfactory for derivation of a theoretical family of λ spectra of η^2.

3. Derivation of λ Spectra of η^2

The λ spectra of η^2 is obtained by squaring all η and summing η^2 between $\lambda + \frac{\Delta\lambda}{2}$ and $\lambda - \frac{\Delta\lambda}{2}$ as $\Delta\lambda \longrightarrow 0$ for all λ between 0 and ∞. Mathematically, in terms of the joint distribution function this summation is represented by

$$S_{\eta^2}(\lambda) = \int_0^\infty \eta^2 p(\eta, \lambda) d\eta \tag{7.9}$$

and

$$p(\eta, \lambda) = p(\lambda) \cdot p_\lambda(\eta) \tag{7.10}$$

$S_{\eta^2}(\lambda)$, the summation function of η^2 with respect to λ, is termed the family of λ spectra of η^2. $p(\eta, \lambda)$ is the joint distribution function of η and λ, $p(\lambda)$ the marginal distribution function of λ, and $p_\lambda(\eta)$ the conditional distribution function of η.

From (7.9) and (7.10) one obtains

$$S_{\eta^2}(\lambda) = p(\lambda) \int_0^\infty \eta^2 p_\lambda(\eta)\, d\eta. \tag{7.11}$$

One may suppose that the integral of (7.11) evaluates by definition

$$\overline{\eta_\lambda^2} = \int_0^\infty \eta^2 p_\lambda(\eta) d\eta \tag{7.12}$$

Thus

$$S_{\eta^2}(\lambda) = \overline{\eta_\lambda^2}\, p(\lambda) \tag{7.13}$$

To obtain the complete form of the λ spectra of η^2 one must evaluate $\overline{\eta_\lambda^2}$. This can be done analogous to $\overline{\eta_\lambda^2} = K(\overline{\eta})^2$, assuming only linear regression and $\overline{\eta^2} = \overline{\lambda^2}$, whence

$$\overline{\eta_\lambda^2} = K(\overline{\eta_\lambda})^2 \tag{7.14}$$

where $\overline{\eta_\lambda}$ is the equation of the regression line of η on λ, and from Chapter V

$$\overline{\eta_\lambda} = (1-r) + r\lambda \tag{7.15}$$

and

$$\overline{\eta_\lambda^2} = K_1\left[(1-r) + r\lambda\right]^2 \tag{7.16}$$

The constant K_1 can be solved from the condition that the area under the λ spectra of η^2 is equal to the energy coefficient $\overline{\eta^2}$;

$$\overline{\eta^2} = \int_0^\infty S_{\eta^2}(\lambda)\, d\lambda \tag{7.17}$$

and using (7.13) and (7.16) one obtains

$$\overline{\eta^2} = K_1 \int_0^\infty \left[(1-r) + r\lambda\right]^2 p(\lambda)\, d\lambda \tag{7.18}$$

or expanding and by definition

$$\int_0^\infty p(\lambda)d\lambda = 1.0$$

$$\int_0^\infty \lambda\, p(\lambda)d\lambda = \overline{\lambda} = 1.0 \qquad (7.19)$$

$$\int_0^\infty \lambda^2 p(\lambda)d\lambda = \overline{\lambda^2}$$

Since

$$\overline{\lambda^2} = \overline{\eta^2}$$

$$k_1 = \frac{\overline{\eta^2}}{1 + r^2(\overline{\eta^2} - 1)} \qquad (7.20)$$

Thus

$$S_{\eta^2}(\lambda) = \frac{\overline{\eta^2}\,[1 - r + r\lambda]^2}{1 + r^2(\overline{\eta^2} - 1)}\, p(\lambda) \qquad (7.21)$$

4. τ Spectra of η^2

Eq. (7.21) can be transformed into the τ spectra of η^2 by noting

$$S_{\eta^2}(\lambda)\, d\lambda = S_{\eta^2}(\tau)\, d\tau$$

$$p(\lambda)\, d\lambda = p(\tau)\, d\tau \qquad (7.22)$$

$$\lambda = a\tau^2$$

Thus

$$S_{\eta^2}(\tau) = \frac{\overline{\eta^2}\,[1-r+ar\tau^2]^2}{1+r^2(\overline{\eta^2}\cdot\cdot)}\, p(\tau) \qquad (7.23)$$

In the above r is still the correlation coefficient $r(\eta, \lambda)$.

Assuming the Rayleigh distribution for wave length variability applies over a range of correlation coefficients applicable to wave data, $S_{\eta^2}(\lambda)$ and $S_{\eta^2}(\tau)$ respectively, are given by

$$S_{\eta^2}(\lambda) = \frac{2\,[1-r+r\lambda]^2}{1+0.273\,r^2}\ \lambda e^{-\frac{\pi\lambda^2}{4}} \qquad (7.24)$$

$$S_{\eta^2}(\tau) = \frac{4a^2[1-r+ar\tau^2]^2}{1+0.273\,r^2}\cdot\ \tau^3 e^{-0.675\,\tau^4} \qquad (7.25)$$

In (7.25), a = 0.927 for the Rayleigh distribution, and it must also be remembered that r is $r(\eta, \lambda)$, the correlation coefficient between η and λ. Figures 7.2 and 7.4 respectively, show $S_\eta 2(\lambda)$ and $S_\eta 2(\tau)$ for various values of $r(\eta, \lambda)$ between $r(\eta, \lambda) = -0.4$ and $+0.6$. It is believed that for negative $r(\eta, \lambda)$ greater numerically than shown (-0.4) does not occur in nature; and furthermore, the relationships will tend to fail if applied outside this range. Figures 7.1 and 7.3 show the corresponding spectra, $S_\eta(\lambda)$ and $S_\eta(\tau)$.

5. Period Spectra

The standard form of the period spectra may be obtained from the unit form by noting

$$S_{\eta^2}(\tau)\, d\tau = S_H{}^2(T)\, dT$$

$$\eta = \frac{H}{\bar{H}}$$

$$\tau = \frac{T}{\bar{T}} \qquad (7.26)$$

$$d\eta = \frac{1}{\bar{H}}\, dH$$

$$d\tau = \frac{1}{\bar{T}}\, dT$$

Thus

$$S_H{}^2(T) = \frac{3.434(\bar{H})^2\left[1 - r + 0.927\, r\left(\frac{T}{\bar{T}}\right)^2\right]^2}{1 + 0.273\, r^2} \frac{T^3}{(\bar{T})^4} e^{-0.675\left[\frac{T}{\bar{T}}\right]^4} \qquad (7.27)$$

6. Frequency Spectra

The period spectra may be transformed into the frequency spectra by noting that

$$\int_0 S_H{}^2(T)\, dT = \int_\infty S_H{}^2(\omega)\, d\omega = -\int_0 S_H{}^2(\omega)\, d\omega \qquad (7.28)$$

and

$$\omega = \frac{2\pi}{T} \qquad d\omega = -\frac{2\pi}{T^2}\, dT \tag{7.29}$$

Thus

$$S_H^2(\omega) = \frac{3.434(\bar{H})^2\left[1 - r + 0.927\, r\left(\frac{2\pi}{\omega\bar{T}}\right)^2\right]^2}{1 + 0.273\, r^2}\left(\frac{2\pi}{\bar{T}\omega}\right)^4 \frac{1}{\omega} e^{-0.675\left(\frac{2\pi}{\bar{T}\omega}\right)^4} \tag{7.30}$$

7. Properties of Wave Spectra

From the above proposed wave spectra, one may determine certain properties discussed below.

Peak of τ Spectra of η^2: It is of interest to investigate the peak of the τ spectra of η^2, this representing the band of wave periods around which is concentrated maximum wave energy. This period will be called τ_{op}, the optimum period, and may be obtained from

$$\frac{d\left[S_{\eta^2}(\tau)\right]}{d\tau} = 0 \tag{7.31}$$

whence

$$(1-r)^2\left[3 - 2.7\tau_{op}^4\right] + 2\sigma r(1-r)\tau_{op}^2\left[10 - 5.4\tau_{op}^4\right] + \sigma^2 r^2 \tau_{op}^4\left[7 - 2.7\tau_{op}^4\right] = 0 \tag{7.32}$$

Eq. (7.32) is a quadratic in terms of r, from which it follows

$$Ar^2 + 2Br + C = 0$$

$$r = \frac{-B \pm \sqrt{B^2 - AC}}{A} \tag{7.33}$$

where

$$A = \left[3 - \pi\left(a\tau^2_{op}\right)^2\right] - a\tau^2\left[10 - 2\pi(a\tau^2)^2\right] + (a\tau^2)^2\left[7 - \pi(a\tau^2)^2\right]$$

$$B = \left[-3 + \pi(a\tau^2)^2\right] + a\tau^2\left[5 - \pi(a\tau^2)^2\right]$$

$$C = 3 - \pi(a\tau^2)^2$$

Table 7.1 gives typical values of τ_{op} for various correlation coefficients, $r(\eta, \lambda)$.

TABLE 7.1

τ_{op} AND $\tau(\eta_{33})$ VERSUS CORRELATION COEFFICIENT

$\pi(a\tau^2_{op})^2$	$r(\eta, \lambda)$	τ_{op}	$\tau(\eta_{33})$	$\frac{\tau_{op}}{T(H_{33})}$
3.00	0	1.0267	1.0000	1.0267
3.25	0.0616	1.0475	1.0183	1.0287
3.50	0.1199	1.0671	1.0353	1.0307
3.75	0.1753	1.0856	1.0513	1.0326
4.00	0.2280	1.1032	1.0662	1.0347
4.25	0.2810	1.1200	1.0810	1.0361
4.50	0.3346	1.1363	1.0958	1.0370
4.75	0.3874	1.1517	1.1101	1.0375
5.00	0.4421	1.1665	1.1248	1.0371
5.25	0.4986	1.1808	1.1398	1.0360
5.50	0.5573	1.1946	1.1551	1.0342
5.75	0.6193	1.2080	1.1711	1.0315
6.00	0.6846	1.2210	1.1877	1.0280
6.25	0.7450	1.2335	1.2029	1.0245
6.50	0.8296	1.2457	1.2242	1.0176
6.75	0.9109	1.2574	1.2436	1.0111
7.00	1.0000	1.2689	1.2649	1.0032

Relation of Optimum Period to Significant Period: The significant wave definition has been selected quite arbitrarily. It was found that observers tend to report a mean or representative value of the higher wave groups, which was termed the significant height, and the corresponding average period of the high groups was called the significant period. It was found from wave record analysis

that this significant wave agreed quite satisfactorily with the highest one-third waves in the complete record. Hence, the significant wave became attached to the average height of the highest one-third waves, thereby being a statistical parameter. The significant period being defined as the average period of the highest one-third waves was not a useful statistical parameter since no knowledge existed in regard to correlation. The significant period is only a useful statistical parameter when the correlation between η and λ is known, and it has been discussed in the two preceding chapters. The significant period being related to the higher wave groups should be expected to bear a close relationship to the optimum period. It is shown and verified in Chapter V that the significant period is given by

$$\tau(\eta_{33}) = \tau_{1/3} = \sqrt{1+0.60\,r} \tag{7.34}$$

Table 7.1 shows $\tau_{1/3}$ for the various values of $r(\eta, \lambda)$. The column of $\frac{T_{op}}{T(H_{33})}$ also presented in Figure 7.5 shows that the significant period is very closely related to the optimum period, as should be expected. Thus the significant period has a definite significance in the study of ocean waves.

Mean Square Wave Steepness: The mean square wave steepness is given by

$$\overline{\left[\frac{\eta}{\lambda}\right]^2} = \int_0^\infty \left(\frac{1}{\lambda}\right)^2 S_{\eta^2}(\lambda)\,d\lambda \tag{7.35}$$

or using (7.26)

$$\overline{\left[\frac{\eta}{\lambda}\right]^2} = \frac{2}{1+0.273r^2}\int_0^\infty [(1-r)+r\lambda]^2\; e^{-\frac{\pi\lambda^2}{4}}\;\frac{d\lambda}{\lambda} \tag{7.36}$$

Expanding (7.36) one obtains

$$\overline{\left[\frac{\eta}{\lambda}\right]^2} = \frac{2}{1+0.273r^2}\left[\int_0^\infty \left[\frac{(1-r)^2}{\lambda} + 2r(1-r) + r^2\lambda\right] e^{-\frac{\pi\lambda^2}{4}}\right] \tag{7.37}$$

The last two terms of the above integral lead to finite results, but the first term must be integrated from a lower limit λ_{min}, discussed later. In this respect one obtains

$$\overline{\left[\frac{\eta}{\lambda}\right]^2} = \frac{2}{1+0.273r^2}\left[2r(1-r)+\frac{2}{\pi}r^2+(1-r)^2\int_{\lambda_{min}}^{\infty}\frac{1}{\lambda}e^{-\frac{\pi\lambda^2}{4}}\,d\lambda\right] \qquad (7.38)$$

Consider the exponential integral

$$E_1(x) = 2\int_{\lambda_{min}}^{\infty}\frac{1}{\lambda}e^{-\frac{\pi\lambda^2}{4}}\,d\lambda \qquad (7.39)$$

Let $z = \frac{\pi\lambda^2}{4}$ $\quad dz = \frac{\pi}{2}\lambda\,d\lambda$

whence

$$E_1(x) = \int_{z_{min}}^{\infty}\frac{1}{z}e^{-z}\,dz = \int_{z_{min}}^{1}\frac{1}{z}e^{-z}\,dz + \int_{1}^{\infty}\frac{1}{z}e^{-z}\,dz \qquad (7.40)$$

The last half of the above integral is obtained from Jahnke, et. al. (1945)

$$E_1(1) = \int_{1}^{\infty}\frac{1}{z}e^{-z}\,dz = 0.219383934 \qquad (7.41)$$

Expanding by series the first part of the integral of (7.40), and integrating, one obtains

$$\int_{z_{min}}^{1}\frac{1}{z}e^{-z}\,dz = \left[\ln z - z\left(1-\frac{z}{2.2!}+\frac{z^2}{3.3!}-\frac{z^4}{4.4!}+\cdots\right)\right]_{z_{min}}^{1} \qquad (7.42)$$

It will be noted that $z_{min} << 1$, hence need be considered only for evaluation of the term lnz. Using the first five terms of the above series one obtains

$$\int_{z_{min}}^{1} \frac{1}{z} e^{-z} dz = -\ln z_{min} - 0.8039 \tag{7.43}$$

Whence

$$E_i(x) = -\ln z_{min} - 0.5845 \tag{7.44}$$

and since $z = \frac{\pi \lambda^2}{4}$ and $\lambda = 0.927\, \tau^2$

$$E_i(x) = -2 \ln \lambda_{min} - 0.3464 = 4 \ln \tau_{min} - 0.2684 \tag{7.45}$$

The final form for mean square wave steepness becomes

$$\left[\frac{\overline{\eta}}{\lambda}\right]^2 = \frac{4}{1+0.273\, r^2} \left[r(1-r) + \frac{r^2}{\pi} + (1-r)^2 (-\ln \tau_{min} - 0.0671)\right] \tag{7.46}$$

The selection of τ_{min} is discussed in the next chapter.

Mean Square Sea Surface Slope: Mean square sea surface slope relationships were derived by Cox and Munk (1956) by use of the directional spectrum, the work of which is not repeated here. However, a less rigorous method is used which results in the same expression. A simple sinusoidal gravity wave may be represented by

$$\xi = A \cos kx \tag{7.47}$$

where A is the amplitude H/2 and $k = 2\pi / L$. The wave slope is obtained from

$$\frac{d\xi}{dx} = -k A \sin kx \tag{7.48}$$

The mean square slope of the single wave is obtained from

$$\overline{\left[\frac{d\xi}{dx}\right]^2} = \frac{1}{L}\int_0^L \left[\frac{d\xi}{dx}\right]^2 dx = \frac{1}{8}(2\pi)^2 \left[\frac{H}{L}\right]^2 \tag{7.49}$$

Next a train of waves may be considered for which the crest lengths are sufficiently long, such as one might infer from a wave record obtained by use of any conventional wave recorder, and assume that the statistics are sufficient such that the means are equivalent to those obtained from discrete sets of sinusoidal waves propagated unidirectional; whence the mean square sea surface slope is obtained from

$$\sigma^2 = \frac{1}{N}\sum_{i=1}^{N} \overline{\left[\frac{d\xi}{dx}\right]^2} \tag{7.50}$$

Thus

$$\sigma^2 = \frac{1}{8}(2\pi)^2 \overline{\left[\frac{H}{L}\right]^2} \tag{7.51}$$

Where

$\overline{\left[\frac{H}{L}\right]^2}$ is the mean square wave steepness

Eq. (7.51) is that which one might obtain when only a wave record is available, a very minimum of information. The fact, however, is that the waves may be short crested and directional, and the assumption of sufficient statistics is required. At first it appears that this assumption is not in order, but it can be shown that σ^2 obtained from (7.51) is equivalent to that derived by Cox and Munk (1956) using the directional spectrum. The mean square wave steepness $\overline{[H/L]^2}$ may be obtained by use of the joint distribution function

$$\overline{\left[\frac{H}{L}\right]^2} = \int_0^\infty \int_0^\infty \overline{\left[\frac{H}{L}\right]^2} \, p(H,L)\, dH dL \tag{7.52}$$

or from the period spectrum

$$\overline{\left[\frac{H}{L}\right]^2} = \int_0^\infty \frac{1}{L^2} S_H^2(T)\,dT \tag{7.53}$$

thus

$$\sigma^2 = \frac{1}{8} \int_0^\infty k^2 S_H^2(T)\,dT \tag{7.54}$$

which is identical to that obtained by Cox and Munk (1956), from which the notation is $T_T = 1/8\ S_H^2(T)$.

In terms of frequency ω (7.54) becomes

$$\sigma^2 = \frac{1}{8} \int_0^\infty \frac{\omega^4}{g^2} S_H^2(\omega)\,d\omega \tag{7.55}$$

According to the notation used by Neumann and Pierson (1957)[a]

$$S_H^2(\omega)\,d\omega = 4\left[A(\mu)\right]^2 d\mu \tag{7.56}$$

Where μ is the same as ω and $A = H/2$.

It can be shown that in unit form

$$\overline{\left[\frac{\eta}{\lambda}\right]^2} = \overline{\left[\frac{H}{L}\right]^2}\left[\frac{\bar{H}}{\bar{L}}\right] \tag{7.57}$$

Thus

$$\sigma^2 = \frac{(2\pi)^2}{8}\ \overline{\left[\frac{\eta}{\lambda}\right]^2}\left[\frac{\bar{H}}{\bar{L}}\right]^2 \tag{7.58}$$

where $\overline{\left[\frac{\eta}{\lambda}\right]^2}$ is obtained from (7.46).

Although the family of spectra are not intended for very steep waves, (7.58) for all H/L = 1/7($[\eta/\lambda]^2 = 1.0$) reduces to (7.51), and predicts a maximum value of mean square sea surface slope

$$\sigma^2_{max} = 0.10$$

The maximum value of σ^2 can be obtained also by use of the Michell (1893) theory by considering all waves initially have H/L = 1/7 and following the procedure from (7.49). Using surface elevation ξ as a function of x obtained from Michell (1893) one obtains

$$\sigma^2_{max} = 0.11$$

and perhaps the family of spectra can be extended quite far into earlier generation.

Spectral Width Parameter: It is of interest to investigate the spectral width parameter, since this will cast some light on the change in wave spectra during generation and also during decay. According to Williams and Cartwright (1957) a non-dimensional spectral width parameter is defined by

$$\epsilon = \sqrt{1 - \frac{M_2^2}{M_0 M_4}} \qquad (7.59)$$

where the n^{th} moment M_n of $E(\omega)$ about the origin is

$$M_n = \int_0^\infty \omega^n E(\omega)\, d\omega \qquad (7.60)$$

$E(\omega)$ is the energy spectrum in terms of the frequency $E(\omega) = 1/8\ \rho\ g\ S_{H2}\ (\omega)$. With the proper transformation the λ spectra of η^2 can be used to advantage, whence

$$M_0 = \int_0^\infty S_{\eta^2}(\lambda)\, d\lambda$$

$$M_2 = \int_0^\infty S_{\eta^2}(\lambda) \frac{d\lambda}{\lambda} \qquad (7.61)$$

$$M_4 = \int_0^\infty S_{\eta^2}(\lambda) \frac{d\lambda}{\lambda^2}$$

Thus

$$M_0 = \frac{4}{\pi}$$

$$M_2 = \frac{\frac{4}{\pi}}{1+0.273\, r^2}\left[\left(\frac{\pi}{2}-1\right)(1-r)^2+1\right] \tag{7.62}$$

$$M_4 = \overline{\left[\frac{\eta}{\lambda}\right]^2}$$

The mean square sea surface slope and the spectral width parameter are discussed again in the next chapter.

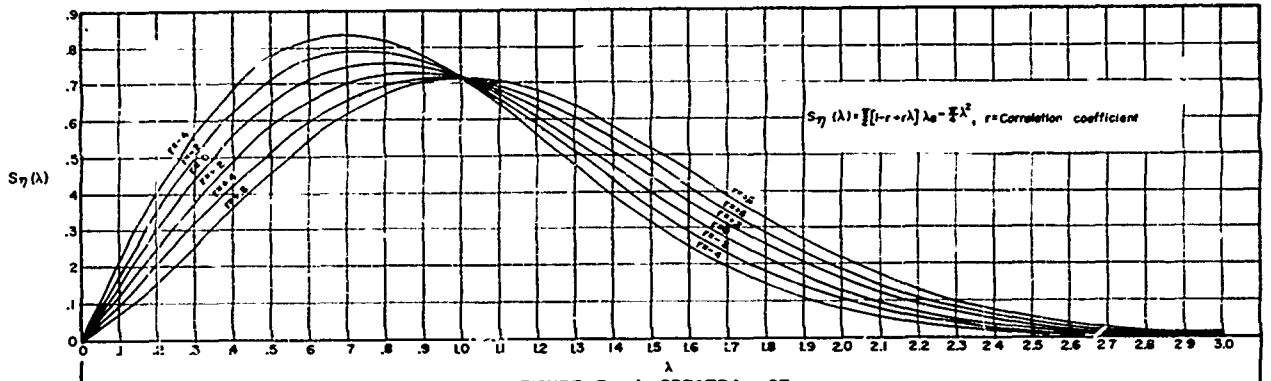

FIGURE 7.1 λ-SPECTRA OF η

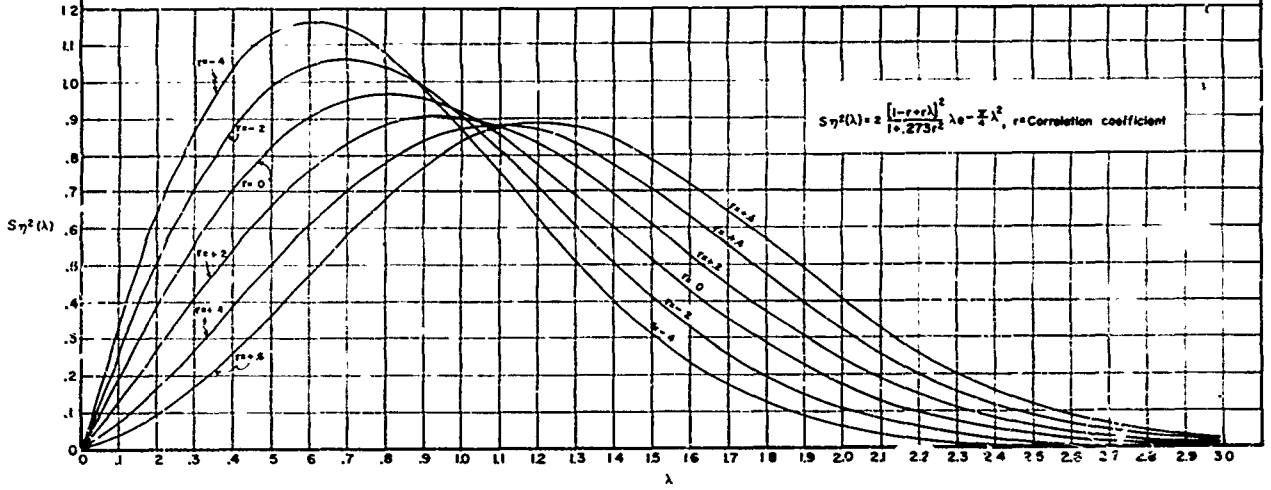

FIGURE 7.2 λ-SPECTRA OF η^2

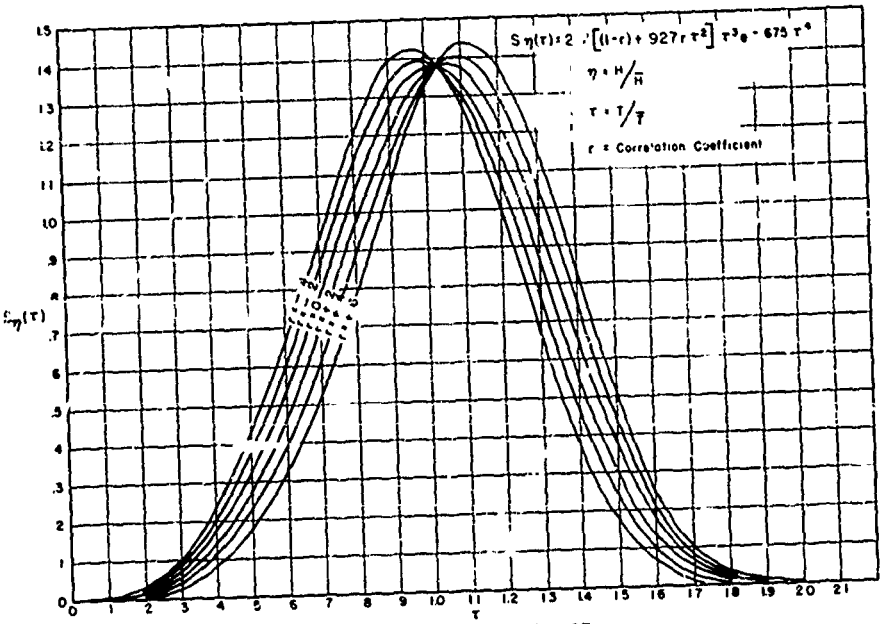

FIGURE 73 τ-SPECTRA OF η

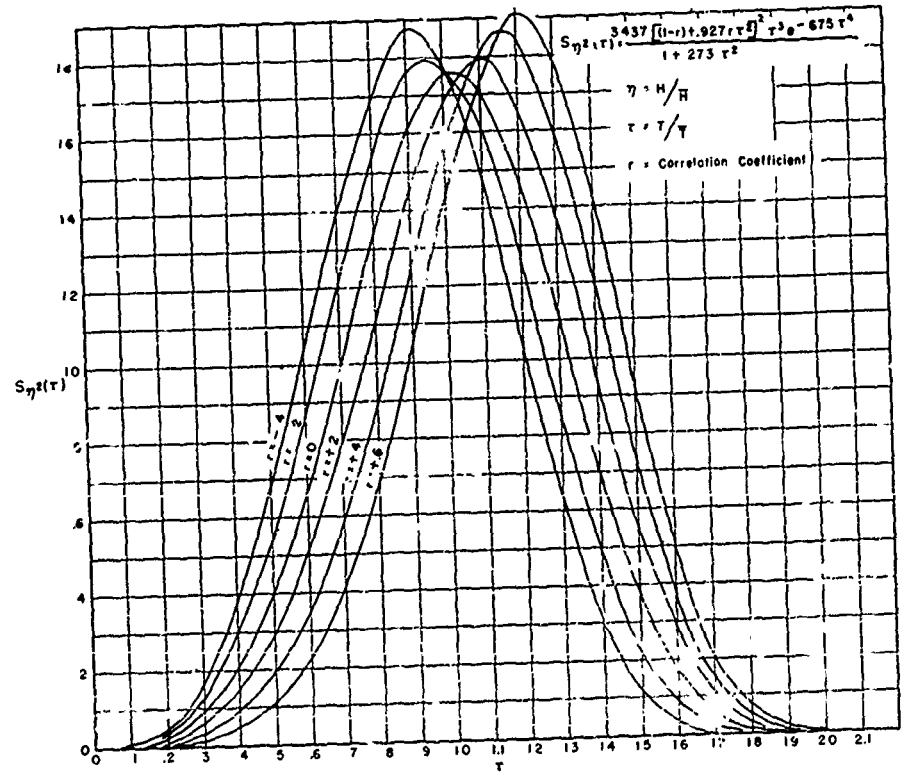

FIGURE 74 τ-SPECTRA OF η^2

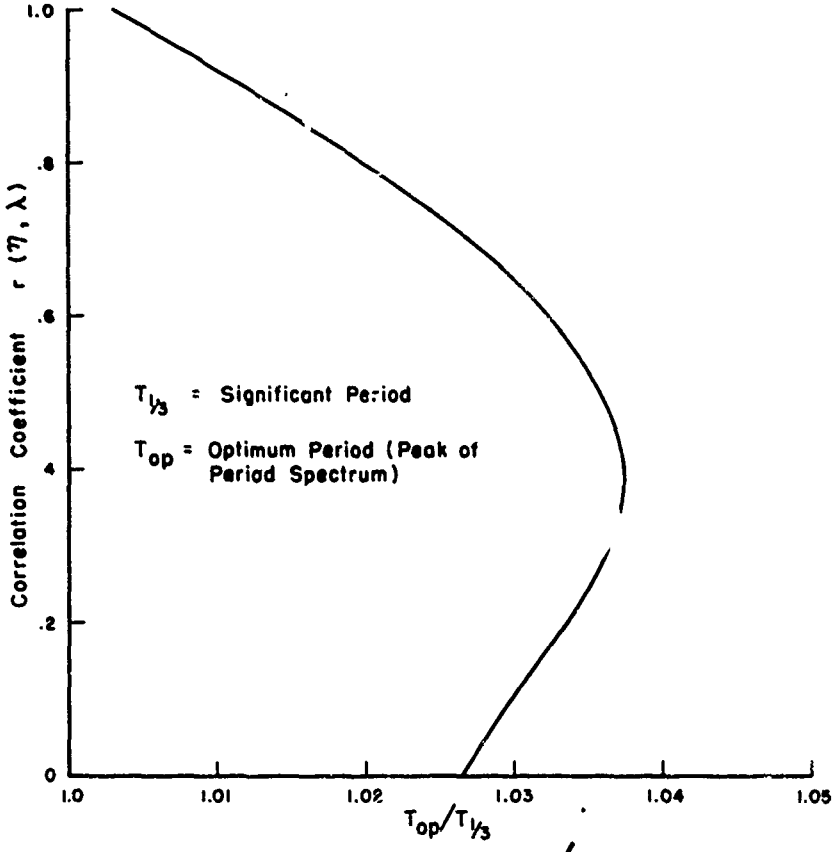

FIGURE 7.5 RATIO OF $T_{OP}/T_{1/3}$ VERSUS CORRELATION CO[illegible]ICIENT

CHAPTER VIII: GENERATION OF WIND WAVES IN DEEP WATER AND THE WAVE SPECTRA

1. General

The preceding section presented the general form of the period spectra and also the frequency spectra. The family of wave spectra in general is very useful in explaining the generation of the so-called complex sea, composed of waves of variable amplitudes and frequencies. In part, spectrum of waves is evolved by the generation of waves from all points within the fetch area.

The wave spectra can be used to advantage in describing the limits of the wave forecasting parameters, originally proposed by Sverdrup and Munk (1947) and revised later by Bretschneider (1952)[a]. The forecasting relationships mentioned above are revised again in this section.

2. Deep Water Wave Generation Parameters

The growth of wind waves in deep water under the action of wind may be represented by the following parameters:

$$\frac{gH}{U^2} = f_1\left(\frac{gF}{U^2}, \frac{gt}{U}\right) \tag{8.1}$$

and

$$\frac{gT}{2\pi U} = f_2\left(\frac{gF}{U^2}, \frac{gt}{U}\right) \tag{8.2}$$

where

H = wave height
T = wave period
g = acceleration of gravity
F = fetch length, distance over which the wind blows
U = wind speed
t = duration of wind

Eqs. (8.1) and (8.2) result from the application of the PI-theorm (Buckingham, 1914) and dimensional analysis. This operation has been performed previously by others, for example, Johnson (1950). The above forms of the parametric equations were arrived at from an entirely different approach through the theoretical work of Sverdrup and Munk (1947). In the following the mean wave height and mean wave period become quite useful, whence, for (8.1) and (8.2), respectively,

$$\frac{g\bar{H}}{U^2} = F_1 \tag{8.3}$$

$$\frac{g\bar{T}}{2\pi U} = F_2 \tag{8.4}$$

where F_1 and F_2 are functions of wind speed, fetch length, and wind duration. The significant wave height according to the Rayleigh distribution is given by

$$H_{33} = 1.6\ \bar{H} \tag{8.5}$$

The significant wave period is related to the mean wave period through the correlation coefficient $r(\eta, \lambda)$

$$T(H_{33}) = \bar{T}\sqrt{1+0.6r} \tag{8.6}$$

The use of Eqs. (8.5) and (8.6) permits the interchange between the mean wave and the significant wave, when such need arises.

3. Wave Spectra In Terms Of Generation Parameters

The period spectra is given by (7.35) of the previous chapter. The corresponding frequency spectra is given by (7.38). Using (8.3) and (8.4), the corresponding spectra, (7.35) and (7.38) respectively, become

$$S_H^2(T) = \frac{\left[1-r+0.927\, r\left(\frac{gT}{2\pi F_2 U}\right)^2\right]^2}{1+0.273\, r^2} \cdot \frac{g^2 T^3}{(2\pi)^4} e^{-0.675\left[\frac{gT}{2\pi U F_2}\right]^4} \tag{8.7}$$

and

$$S_H^2(\omega) = \frac{\left[1-r+0.927\, r\left(\frac{g}{F_2 U\omega}\right)^2\right]^2}{1+0.273\, r^2} \cdot g^2\omega^{-5} e^{-0.675\left[\frac{g}{F_2 U\omega}\right]^4} \tag{8.8}$$

where

$$\alpha = 3.437 \frac{F_1^2}{F_2^4} = 16\pi^2 \left[\frac{H}{L}\right]^2 \tag{8.9}$$

and

$$\frac{F_1^2}{F_2^4} = \left[\frac{g\bar{T}}{U^2}\right]^2 \left[\frac{2\pi U}{g\bar{T}}\right]^4 = 4\pi^2 \left[\frac{2\pi H}{g(\bar{T})^2}\right]^2 \tag{8.10}$$

For large ω (8.8) becomes

$$S_H^2(\omega) = \frac{\left[1 - r + 0.927\, r \left(\frac{g}{F_2 U \omega}\right)^2\right]^2}{1 + 0.273\, r^2} \alpha g^2 \omega^{-5} \tag{8.11}$$

Eq. (8.11) can be compared with that given by Burling (1955).

$$S_H^2(\omega) = \alpha g^2 \omega^{-5} \tag{8.12}$$

Eq. (8.12) is based on the high frequency components under steady state conditions, and has also been proven to be true by Phillips (1957) for an entirely different approach by use of the definition of the energy spectrum and dimensional analysis, a priori reasoning. For this to be true for a fully developed sea, (8.11) must reduce to (8.12), thereby suggesting zero correlation. Thus, a fully developed sea is in a steady state of non-correlation, unrestricted by fetch length and wind duration, and F_1 and F_2 reach upper limits. Based on very accurate measurements Burling (1955) obtained for α an absolute constant:

$$\alpha = 7.4 \times 10^{-3} \tag{8.13}$$

4. Evaluation of Upper Limits for Wave Generation

The fully developed sea is specified by zero correlation and (8.7) and (8.8) respectively, become:

$$S_H^2(T) = \alpha \frac{g^2 T^3}{(2\pi)^4} e^{-0.675 \left[\frac{gT}{2\pi U F_2}\right]^4} \tag{8.14}$$

$$S_H^2(\omega) = \alpha g^2 \omega^{-5} e^{-0.675 \left(\frac{g}{F_2 U \omega}\right)^4} \tag{8.15}$$

Since (8.13) is obtained for a fully developed sea, this represents a minimum value, α_{min}. For α to be a minimum, F_2, of (8.14) must be a maximum. There may be some argument that F_2 ought to be based on (8.15), but this concept is contrary to wave observations. As shown in Chapter VII, there is an optimum period, T_{op}, for which occurs a peak, or maximum concentration of wave energy. Since T_{op} is closely related to T_{33}, F_2 should be based more correctly on (8.14). The optimum period T_{op} is obtained from

$$\frac{d\left[S_H{}^2(T)\right]}{dT} = 0 \tag{8.16}$$

and using (8.14), one obtains:

$$(F_2)_{max} = \sqrt[4]{0.9}\ \frac{g\,T_{op}}{2\pi U} \tag{8.17}$$

When the corresponding group velocity appropriate to T_{op} is equal to the wind speed, maximum wave generation will have been reached, and the energy front will tend to leave the generating area. Since the group velocity will be on the order of one-half the phase velocity appropriate to T_{op}, one obtains

$$\frac{C_g}{U} = 1.0 = \frac{1}{2}\left(\frac{g\,T_{op}}{2\pi U}\right) \tag{8.18}$$

Thus

$$(F_2)_{max} = 2\ \sqrt[4]{0.9} = 1.95 \tag{8.19}$$

According to the work of Sverdrup and Munk (1947) the maximum value of $F_2 = 1.369$ (since $\bar{T} = T_{1/3}$, zero correlation for a fully developed sea). Later revisions by Bretschneider (1952)[6] place the upper limit of $F_2 = 1.45$, a low compromise between results obtained from additional wave data and 1.369. Neumann (1952) utilizes the value of $F_2 = 1.369$. These values of $F_2 = 1.369$ and 1.45 correspond to $gF/U^2 \approx 10^5$. Perhaps the asymptotic value of $F_2 = 1.95$ has not been completely visualized, since it will occur near $gF/U^2 = 6 \times 10^5$, as shown by the data in Figures 8.1 and 8.2. In fact, some data show F_2 in excess of 2.0, but this excess may be due to scatter of data and slight errors in observations.

Assuming $(F_2)_{max} = 1.95$ as determined above and supported by observations, one may proceed to evaluate $(F_1)_{max}$ for a fully developed sea.

Previous investigators have reported maximum values of $\frac{gH_{33}}{U^2}$

$$\left[\frac{gH_{33}}{U^2}\right]_{max} = 0.26 \text{ Sverdrup and Munk (1947)}$$

$$\left[\frac{gH_{33}}{U^2}\right]_{max} = 0.30 \text{ Rossby and Montgomery (1935)}$$

The value of 0.26, based on the theoretical work of Sverdrup and Munk (1947), was also utilized by Bretschneider (1952).

Using (8.3), (8.5), and (8.9), one obtains for minimum value of α:

$\alpha_{min} = 6.28 \times 10^{-3}$ for $\frac{gH_{33}}{U^2} = 0.26$

$\alpha_{min} = 8.36 \times 10^{-3}$ for $\frac{gH_{33}}{U^2} = 0.30$

Thus it is seen that in both cases, α_{min} is close to the value given by Burling (1955). In view of $F_2 = 1.95$, indications are that $\frac{gH_{33}}{U^2} = 0.26$ has not yet attained the upper limit associated with the fully developed sea. Perhaps the value of 0.3 slightly exceeds the limit of the fully developed sea, which might have resulted from the method of observations. In order to obtain a more accurate value of $(F_1)_{max}$ for a fully developed sea, one must consider the source of data, and the accuracy of the methods used in obtaining the data. Field data, winds and waves, used by Sverdrup and Munk (1947), Rossby and Montgomery (1935), Neumann (1952), and also Bretschneider (1952) as a matter of fact, entail a certain amount of subjectiveness. Although these data become quite useful when averages are considered, greater accuracy is required for establishing the theoretical upper limits. The more recent data used by Burling (1955) for obtaining $\alpha = 7.4 \times 10^{-3}$ are very reliable measurements, making use of the capacitance wire recorder developed by Tucker and Charnock (1955). This instrument records very accurately high frequency components of the wave system not normally recorded with any degree of satisfaction by other methods.

In view of the above one must concede, based on very accurate measurements of Burling (1955) that $\alpha_{min} = 7.4 \times 10^{-3}$, and for $(F_2)_{max} = 1.95$, one obtains

$$(F_1)_{max} = 0.178 \tag{8.20}$$

corresponding to

$$\left[\frac{gH_{33}}{U^2}\right]_{max} = \frac{0.178}{0.625} = 0.282 \tag{8.21}$$

5. Evaluation of Lower Limits for Wave Generation

Evaluation of the lower limits for generation of wind waves is a little more difficult than that for the upper limits. The lower limits are governed by $gF/U2$ very small and H/L very steep as supported by numerous wave tank studies, Bretschneider and Rice (1951) and Johnson and Rice (1952). The theoretical maximum wave steepness is given according to Michell (1893)

$$\frac{H}{L} = \frac{1}{7} \tag{8.22}$$

For the sea to have maximum steepness, all individual waves must be at maximum steepness. Hence, a scatter diagram of H versus L will show all data on a straight line with a slope of 1/7. A plot of η versus λ will have a slope of 45 degrees, corresponding to a correlation coefficient of $r(\eta, \lambda) = +1.0$.

For the above condition one finds

$$\frac{\bar{H}}{\bar{L}} = \frac{1}{7} \qquad \frac{H_{33}}{L(H_{33})} = \frac{1}{7}$$

$$r = +1.0 \qquad L(H_{33}) = 1.6\bar{L} \tag{8.23}$$

$$\left[\frac{\bar{H}}{L}\right] = \frac{1}{7} \qquad T(H_{33}) = 1.265\bar{T}$$

and from (8.9) one obtains

$$a_{max} = \frac{16\pi^2}{49} = 3.25 \tag{8.24}$$

Since α_{max} relates the maximum ratio of F_1^2/F_2^4, it is tempting to extend the generation parameters, Figure 8.1, asymptotically at some value of gF/U^2 lower than that reported for wave tank data. This would lead to minimum values of F_1 and F_2 guided by wave data.

Another method of obtaining the minimum values is to consider the lowest possible period that might be generated and the lowest possible wind speed or the critical wind speed required to make the sea surface rough. This approach is somewhat superficial but leads to essentially the same results as the other method. Assuming the capillary limit $T_{min} = 0.074$ seconds and $L_{min} = 1.7$ cm and the critical wind speed of 6 meters per second, and using (8.24), the extreme lower limits are obtained:

$$\frac{gT}{2\pi U} = 0.0193$$

$$\frac{gT(H_{33})}{2\pi U} = \frac{gT_{1/3}}{2\pi U} = 0.0244$$

$$\frac{gH}{U^2} = 0.000357 \qquad (8.25)$$

$$\frac{gH_{33}}{U^2} = 0.000572$$

$$\frac{gF}{U^2} = 0.0046$$

Eq. (8.25) may be considered the extreme lower limits, and in actuality $\frac{gF}{U^2}$ must be greater than 0.0046 in order to develop a spectrum of waves for a wind speed of 6 meters per second. Furthermore, for wind speeds greater than 6 meters per second the fetch F must be greater than that required for 6 meters per second, since wave lengths generated by higher winds will be longer. The spectrum of waves is correspondingly built up from all values of $\frac{gT}{2\pi U}$ and $\frac{gH}{U^2}$ generated by fetches from greater than $\frac{gF}{U^2} = 0.0046$ to the ultimate $\frac{gF}{U^2}$ as limited by wind speed, actual fetch length, and duration of wind. Hence, one should expect the spectra in unit form to be more narrow with a higher peak for a young sea than a fully developed sea.

6. Transition Zone

The transition zone for wave generation includes that between the lower and upper limits discussed above. Much more data are available for significant wave heights and significant wave periods. The mean wave height is statistically related to the significant wave height. The mean wave period is related to the significant period through the correlation coefficient, $r(\eta, \lambda)$. The lower limit of generation begins at $r(\eta, \lambda) = +1.0$ where $T_{1/3} = 1.265\,\bar{T}$ and the upper limit is at $r(\eta, \lambda) = 0$, where $T_{1/3} = \bar{T}$. Evidently the correlation coefficient $r(\eta, \lambda)$ and $(T_{1/3})/\bar{T}$ are functions of $\frac{gF}{U^2}$ and $\frac{gt}{U}$. Since the ratio of $(T_{1/3})/\bar{T}$ changes from 1.265 to 1.0 over a very wide range of generation, it is logical to assume as a first approximation that this transition is gentle and regular. The wave data establish quite accurately the relationship for $(gT_{1/3})/2\pi U$. The exact relationship of $g\bar{T}/2\pi U$ versus $\frac{gF}{U^2}$ in the transition is not completely established due to the lack of sufficient wave data. However, a limited amount of wave data from Fort Peck Reservoir and Lake Texoma are available for this aspect of the problem. These data are summarized in Table 8.1. Fetch lengths for these data are not well established, due to irregular channel effects. The parameter of $\frac{gF}{U^2}$ is eliminated by using $\frac{g\bar{H}}{U^2}$ and $\frac{g\bar{T}}{2\pi U}$ versus $r(\eta, \lambda)$, where $r(\eta, \lambda)$ is related to $(T_{1/3})/\bar{T}$ which in turn is assumed to be a slowly changing function of $\frac{gF}{U^2}$. Figure 3.3 shows the relationships of $g\bar{T}/2\pi U$, $(gT_{1/3})/2\pi U$, and $g\bar{H}33/U^2$ all as functions of $r(\eta, \lambda)$. The scatter of data seems excessive but it should be remembered that 100 waves are too small a number to expect a minimum of scatter in terms of the correlation coefficient. The 95 percent confidence limits for the correlation coefficients are also shown.

Figure 8.1, the Fetch Graph, represents the revised wave forecasting relationships, based on the above considerations, together with additional relationships discussed below. The data shown is that originally used by Bretschneider (1951).

7. Duration Graph

The preceding sections were devoted to wave generation as a function of fetch length, assuming unlimited duration. The Duration Graph, Figure 8.2, may be obtained by use of the Fetch Graph, Figure 8.1, and the considerations following.

TABLE 8.1

SUMMARY OF DEEP WATER WIND WAVE DATA

Source and Record	U mph	H_{33} feet	$\frac{gH_{33}}{U^2}$	$T_{1/3}=T(H_{33})$ seconds	$\frac{gT_{1/3}}{2\pi g}$	r
			(FORT PECK RESERVOIR)			
b- 1	20.7	1.32	0.0460	2.25	0.378	0.12
b- 2	19.7	1.14	0.0437	2.31	0.408	0.38
b- 3	26.0	2.62	0.0380	2.67	0.358	0.42
b- 4	26.7	2.82	0.0580	3.30	0.430	0.41
b- 5	30.8	3.02	0.0480	3.18	0.360	0.48
b- 6	31.6	2.57	0.0375	2.83	0.311	0.41
b- 7	30.2	2.72	0.0445	3.06	0.353	0.54
b- 8	30.4	2.18	0.0350	2.50	0.286	0.29
b- 9	30.6	1.79	0.0281	2.17	0.245	0.19
b-10	29.8	1.75	0.0294	2.35	0.274	0.22
b-11	23.8	1.85	0.0486	2.62	0.383	0.15
b-12	26.6	2.91	0.0610	3.08	0.403	0.30
b-13	26.5	3.11	0.0660	2.89	0.380	0.41
b-14	25.3	2.61	0.0610	2.79	0.384	0.42
b-15	24.2	2.40	0.0670	3.14	0.450	0.47
b-16	22.2	2.56	0.0775	2.78	0.435	0.31
b-17	21.1	2.64	0.0950	3.26	0.535	0.45
b-18	22.6	2.54	0.0740	2.86	0.440	0.42
b-19	23.9	3.05	0.0795	2.78	0.405	0.27
b-20	27.6	3.43	0.0670	3.09	0.389	0.48
			(LAKE TEXOMA, TEXAS)			
c- 5	29	1.33	0.0236	2.30	0.276	0.34
c- 6	26	1.13	0.0250	2.16	0.289	0.38
c- 7	32	1.54	0.0224	2.60	0.283	0.16
c- 8	30	1.37	0.0227	2.53	0.294	0.08
c-12	25	1.67	0.0400	2.75	0.384	0.30
c-13	25	1.67	0.0400	2.92	0.406	0.43
c-14	25	1.67	0.0400	2.88	0.401	0.49
c-15	25	1.59	0.0378	2.91	0.405	0.40
c-16	34	1.34	0.0173	2.34	0.240	0.16
c-17	35	1.34	0.0163	2.60	0.259	0.40
c-18	39	2.15	0.0211	3.09	0.276	0.65
c-19	38	1.87	0.0193	3.11	0.285	0.56
c-20	29	1.06	0.0370	2.09	0.251	0.32
c-21	30	1.27	0.0210	2.06	0.239	0.39
c-22	29	1.37	0.0242	2.39	0.287	0.23
c-23	28	1.33	0.0252	2.43	0.303	0.39
c-24	33	1.66	0.0227	2.24	0.236	0.40
c-25	32	1.50	0.0218	2.33	0.254	0.37

The duration of time required for wave generation depends on the fetch distance traveled and the group velocity appropriate to the most energetic waves. The general form of F = Cgt (fetch distance is equal to group velocity times time) can be applied in differential form $dt = \frac{1}{C_g} dF$, where C_g, the group velocity is a variable and increases with time and distance. In parametric form the expression becomes

$$\frac{gt}{U} = \int_0^X \frac{U}{C_g} d\left(\frac{gF}{U^2}\right) \tag{8.26}$$

where

$$\frac{C_g}{U} = \frac{1}{2}\left[\frac{gT_{op}}{2\pi U}\right] = \frac{1}{2}\left[\frac{\text{"}}{2\pi U}\right]\frac{T_{op}}{T_{1/3}} \tag{8.27}$$

$T_{op}/T_{1/3}$ is a function of $r(\eta, \lambda)$ and hence of $\frac{gF}{U^2}$, from which one obtains tU/F as a function of $\frac{gF}{U^2}$. The curve of tU/F versus gF/U^2 is shown in Figure 8.1. The curves of $\frac{gT_{1/3}}{2\pi U}$ and $\frac{gH_{33}}{U^2}$ as functions of $\frac{gF}{U^2}$ can be expressed as functions of gt/U. This is shown in Figure 8.2, together with the wave data taken from Bretschneider (1951).

8. Wave Generation Parameters

Table 8.2 gives a summary of wave generation parameters. In addition to those discussed above, other parameters are discussed below.

Mean Wave Steepness: The mean wave steepness can be represented as a function of $\frac{gF}{U^2}$, and in standard form

$$\left[\frac{\bar{H}}{L}\right] = \frac{\pi \bar{H}}{2L}\left[1 - r\left(1 - \frac{2}{\pi}\right)\right] \tag{8.28}$$

$\bar{H}/L$ is given as a function of $\frac{gF}{U^2}$ in Figure 8.1 from which can be computed $\left[\frac{H}{L}\right]$ using r from Table 8.2.

TABLE 8.2

SUMMARY OF DEEP WATER WAVE GENERATION PARAMETERS

$\frac{gF}{U^2}$	$\frac{gt}{U}$	$\frac{tU}{F}$	$\frac{gH_{1/3}}{U^2}$	$\frac{\bar{\tau}_{1/3}}{2\pi U}$	$r(\eta,\lambda)$	$\frac{T_{1/3}}{\bar{T}}$
0.01	0.63	63.0	0.000574	0.0247	0.998	1.2645
0.02	1.14	57.0	0.000611	0.0258	0.995	1.2637
0.04	2.06	51.5	0.000738	0.0288	0.992	1.2629
0.06	2.92	48.6	0.000867	0.0316	0.985	1.2613
0.08	3.70	46.3	0.000957	0.0334	0.981	1.2602
0.10	4.50	45.0	0.00105	0.0353	0.979	1.2598
0.20	8.00	40.2	0.00143	0.0425	0.965	1.2566
0.40	14.1	35.5	0.00195	0.0521	0.949	1.2526
0.60	20.3	33.9	0.00235	0.0591	0.936	1.2497
0.80	25.7	32.1	0.00269	0.0646	0.927	1.2474
1.00	31.0	31.0	0.00301	0.0695	0.916	1.2450
2.00	54.0	27.0	0.00430	0.0869	0.878	1.2357
4.00	94.0	23.5	0.00610	0.108	0.827	1.2231
6.00	129	21.5	0.00743	0.124	0.790	1.2141
8.00	160	20.0	0.00855	0.137	0.762	1.2071
10.0	192	19.2	0.00951	0.147	0.740	1.2017
20.0	306	15.3	0.0129	0.179	0.671	1.1845
40.0	488	12.2	0.0175	0.215	0.590	1.1636
60.0	654	10.9	0.0208	0.240	0.546	1.1524
80.0	792	9.90	0.0232	0.261	0.513	1.1437
100	920	9.20	0.0252	0.279	0.486	1.1367
200	1,520	7.60	0.0337	0.337	0.400	1.1355
400	2,440	6.10	0.0441	0.403	0.322	1.0918
600	3,300	5.50	0.0522	0.453	0.275	1.0794
800	4,056	5.07	0.0583	0.486	0.243	1.0705
1,000	4,800	4.80	0.0641	0.519	0.220	1.0640
2,000	8,000	4.00	0.0841	0.618	0.160	1.0469
4,000	13,800	3.45	0.1110	0.735	0.102	1.0301
6,000	18,960	3.16	0.130	0.816	0.079	1.0232
8,000	23,760	2.97	0.145	0.872	0.062	1.0183
10,000	28,100	2.81	0.157	0.924	0.052	1.0154
20,000	48,200	2.41	0.195	1.10	0.027	1.0080
40,000	82,000	2.05	0.234	1.28	0.010	1.0030
60,000	112,800	1.88	0.253	1.39	0.006	1.0018
80,000	140,000	1.75	0.264	1.46	0.002	1.0006
100,000	168,000	1.68	0.270	1.54	0.001	1.0
150,000	228,000	1.52	0.277	1.67	0	1.0
200,000	286,000	1.43	0.279	1.74	0	1.0
300,000	393,000	1.31	0.281	1.84	0	1.0
400,000	496,000	1.24	0.282	1.90	0	1.0
500,000	595,000	1.19	0.282	1.93	0	1.0
600,000	702,000	1.17	0.282	1.95	0	1.0

TABLE 8.2
(Continued)

SUMMARY OF DEEP WATER WAVE GENERATION PARAMETERS

$\frac{gF}{U^2}$	$\frac{H}{L}$	$\left(\frac{H}{L}\right)$	α	σ^2	ϵ	$\frac{H_{1/3}}{(T_{1/3})^2}$
0.01	0.1394	0.1397	3.07	0.0958	0.464	0.767
0.02	0.1355	0.1361	2.90	0.0910	0.465	0.748
0.04	0.1309	0.1316	2.71	0.0856	0.466	0.725
0.06	0.1270	0.1282	2.55	0.0813	0.467	0.708
0.08	0.1257	0.1272	2.50	0.0800	0.468	0.699
0.10	0.1235	0.1251	2.41	0.0775	0.474	0.687
0.20	0.1155	0.1179	2.11	0.0691	0.479	0.645
0.40	0.1040	0.1071	1.71	0.0575	0.487	0.585
0.60	0.0969	0.1005	1.48	0.0510	0.494	0.548
0.80	0.0925	0.0965	1.35	0.0471	0.497	0.525
1.00	0.0885	0.0928	1.24	0.0440	0.510	0.508
2.00	0.0803	0.0860	1.02	0.0389	0.547	0.464
4.00	0.0722	0.0794	0.824	0.0343	0.572	0.426
6.00	0.0659	0.0739	0.686	0.0325	0.596	0.393
8.00	0.0618	0.0703	0.603	0.0311	0.616	0.371
10.0	0.0590	0.0678	0.550	0.0303	0.632	0.359
20.0	0.0522	0.0621	0.431	0.0290	0.677	0.328
40.0	0.0472	0.0583	0.352	0.0285	0.713	0.309
60.0	0.0444	0.0559	0.311	0.0276	0.736	0.294
80.0	0.0412	0.0527	0.268	0.0274	0.750	0.278
100	0.0392	0.0507	0.243	0.0272	0.766	0.267
200	0.0352	0.0469	0.196	0.0265	0.792	0.242
400	0.0300	0.0416	0.142	0.0256	0.819	0.221
600	0.0273	0.0386	0.118	0.0253	0.832	0.208
800	0.0261	0.0374	0.108	0.0249	0.840	0.201
1,000	0.0248	0.0359	0.0972	0.0249	0.846	0.194
2,000	0.0223	0.0330	0.0786	0.0243	0.863	0.179
4,000	0.0201	0.0294	0.0638	0.0233	0.875	0.167
6,000	0.0189	0.0289	0.0564	0.0223	0.882	0.159
8,000	0.0183	0.0281	0.0529	0.0213	0.885	0.155
10,000	0.0175	0.0270	0.0484	0.0204	0.888	0.155
20,000	0.0151	0.0235	0.0360	0.0178	0.896	0.131
40,000	0.0133	0.0208	0.0279	0.0141	0.901	0.116
60,000	0.0121	0.0190	0.0231	0.0120	0.902	0.107
80,000	0.0110	0.0173	0.0191	0.0102	0.903	0.0969
100,000	0.0105	0.0165	0.0174	0.0093	0.904	0.0928
150,000	0.00916	0.0143	0.0133	0.0073	0.905	0.0809
200,000	0.00850	0.0134	0.0114	0.0063	0.906	0.0751
300,000	0.00766	0.0119	0.0093	0.0051	0.907	0.0676
400,000	0.00721	0.0113	0.0082	0.0046	0.908	0.0637
500,000	0.00699	0.0110	0.0077	0.0043	0.909	0.0617
600,000	0.00685	0.0107	0.0074	0.0042	0.910	0.0604

Mean Square Sea Surface Slope: The mean square sea surface slope for wave generation as a function of $\frac{gF}{U^2}$ can be obtained from (7.54) and (7.56), Chapter VII, by noting that one may write $\tau_{min} = T_{min} / \bar{T}$ as

$$\tau_{min} = \frac{\frac{g T_{min}}{2\pi U}}{\frac{g\bar{T}}{2\pi U}} \tag{8.29}$$

whence the mean square wave steepness is given by:

$$\overline{\left[\frac{\eta}{\lambda}\right]^2} = \frac{4}{1+0.273\,r^2}\left\{r(1-r) + \frac{r^2}{\pi} + (1-r)^2\left[\ln\frac{g\bar{T}}{2\pi U} - \ln\frac{g T_{min}}{2\pi U} - 0.0671\right]\right\} \tag{8.30}$$

The mean square sea surface slope is given by

$$\sigma^2 = \frac{a}{32}\overline{\left[\frac{\eta}{\lambda}\right]^2} \tag{8.31}$$

where

$$a = 16\pi^2\left[\frac{H}{L}\right]^2 \tag{8.32}$$

Spectral Width Parameter: The spectral width parameter is given by

$$\epsilon = \sqrt{1 - \frac{a}{8\pi\sigma^2}\left[\frac{\left(\frac{\pi}{2}-1\right)(1-r)^2 + 1}{1+0.273\,r^2}\right]^2} \tag{8.33}$$

Since $\frac{g\bar{T}}{2\pi U}$, $\frac{gT_{min}}{2\pi U}$, and r are functions of $\frac{gF}{U^2}$, it can be seen that (8.30) through (8.33) are also functions of $\frac{gF}{U^2}$, which is as should be expected. The exact values of $\overline{\left[\frac{\eta}{\lambda}\right]^2}$, σ^2, a, and ϵ depend on the proper selection of $\frac{gT_{min}}{2\pi U}$, which must be obtained from measurements.

If it is assumed for the present that $\frac{gT_{min}}{2\pi U} = 0.0193$, as given by (8.25), one obtains

$$\overline{\left[\frac{\eta}{\lambda}\right]^2} = \frac{4}{1+0.273r^2}\left\{r(1-r)+\frac{r^2}{\pi}+(1-r)^2\left[3.88+\ln\frac{g\bar{T}}{2\pi U}\right]\right\} \qquad (8.34)$$

In all probability $\frac{gT_{min}}{2\pi U}$ will be somewhat greater than 0.0193, particularly for large values of $\frac{gF}{U^2}$. Until $\frac{gT_{min}}{2\pi U}$ is determined as a function of $\frac{gF}{U^2}$, the use of (8.34) will result perhaps in values of $\overline{\left[\frac{\eta}{\lambda}\right]^2}_{gT_{min}}$ somewhat higher than the true values. For example, if one selected $\frac{gT_{min}}{2\pi U} = 3(0.0193)$, one factor 3.88 in the above equation will be replaced by $3.88 - \ln 3 = 2.78$.

Using (8.34) in its present form values of α, σ^2, and ϵ have been computed as a function of $\frac{gF}{U^2}$, and are summarized in Table 8.2. α and σ^2 are also shown in Figure 8.1.

9. Instrument Attenuation

All wave-measuring instruments, with the exception of a vertical capacitance (or resistance) wire type, impose an attenuation curve on the high frequency part of the spectrum, thus artificially narrowing the spectrum, which, in effect, reduces the values of ϵ and σ^2 from the theoretical values given above. For this reason it is difficult to determine whether $\frac{gT_{min}}{2\pi U}$ is at some low limit as governed by theory or whether $\frac{gT_{min}}{2\pi U}$ has a finite low limit as imposed by nature.

It is a well-known fact that a pressure gage below the mean surface will attenuate low period waves, otherwise visually observed. Condiser, for example (8.34) for zero correlation in the following form:

$$\overline{\left[\frac{\eta}{\lambda}\right]^2} = 4\left[-0.0671-\ln\tau_{min}\right] \qquad (8.35)$$

where $\tau_{min} = \frac{T_{min}}{\bar{T}}$

For a pressure recorder located 10 feet below the mean water surface, assume all waves of $d/L_o \geq 0.5$ are filtered out. Since $L_o = \frac{gT^2}{2\pi}$, one obtains $T_{min} = 2$ seconds. (If all waves of $d/L_o \geq 1$, $T_{min} = 1.4$ seconds.) For $d/L_o \geq 0.5$ and $d = 10$ feet, (8.35) becomes

$$\overline{\left[\frac{\eta}{\lambda}\right]^2}_{ob} = 4\,[-0.76 + \ln \bar{T}] \tag{8.36}$$

The subscript ob is used for observed value. If, on the other hand, $T_{min} = 0.074$ seconds as governed by the capillary limit, then

$$\overline{\left[\frac{\eta}{\lambda}\right]^2}_{tr} = 4[2.53 + \ln \bar{T}] \tag{8.37}$$

The subscript tr is used for true value.

The ratio R of observed to true $\left[\overline{\frac{\eta^2}{\lambda}}\right]$ becomes

$$R = \frac{-0.76 + \ln \bar{T}}{2.53 + \ln \bar{T}} \tag{8.38}$$

Values for R for various mean period $\bar{T}$ are given below:

$\bar{T}$	4	6	8	10	12	14	16
R	0.16	0.239	0.286	0.320	0.344	0.362	0.379

Since σ^2 is given by (8.31), this will also be reduced correspondingly. The spectral width parameter given by (8.33) is similarly affected. Instrument attenuation also effects the mean wave steepness $\left[\frac{\eta}{\lambda}\right]$ but to a lesser extent.

Equation for σ^2 given in the paper by Bretschneider (1957)[c] is in error by the factor of 1/8, and the corresponding values computed are too large by a factor of 8. The correct form of σ^2 and ϵ are presented in the present paper.

10. Comments on Critical Wind Speed

It seems appropriate to make a few comments on critical wind speed. The extreme lower limit for gravity wave generation presented

earlier is based on the assumption of a critical wind speed and the capillary wave limit, and results in the mean square sea surface slope as a function of the fetch parameter gF/U^2. If, on the other hand, only the capillary wave limit had been selected for the lower limit of generation, the mean square sea surface slope would be a function not only of the fetch parameter but also of the mean wave period, a dimensional quantity. In this case one would obtain a separate curve of σ^2 versus gF/U^2 for each mean wave period. However one might also have obtained σ^2 as a function only of gF/U^2 by selecting arbitrarily some low limit of gF/U^2 without reference to critical wind speed and capillary wave limit, in which case no discussion would be necessary.

Munk (1947) presented a paper on critical wind speed for air - sea boundary processes, but since has voiced opinion that such might not be the case after all. Reference is made to the work of Cox and Munk (1956). Later, Munk (1957) appears to be dubious as to whether a critical wind speed exists, citing the work of Mandelbaum (1956) and Lawford and Veley (1956). Evidently a controversy exists as to whether or not a critical wind speed actually exists. However, such a controversy need not affect the results presented herein, since what is to have kept one from selecting arbitrarily an extreme low limit of gF/U^2 by extrapolating $g\bar{H}/U^2$ and $g\bar{T}/2\pi U$ to maximum steepness $H/L = 1/7$, guided only by the data in the range of low gF/U^2?

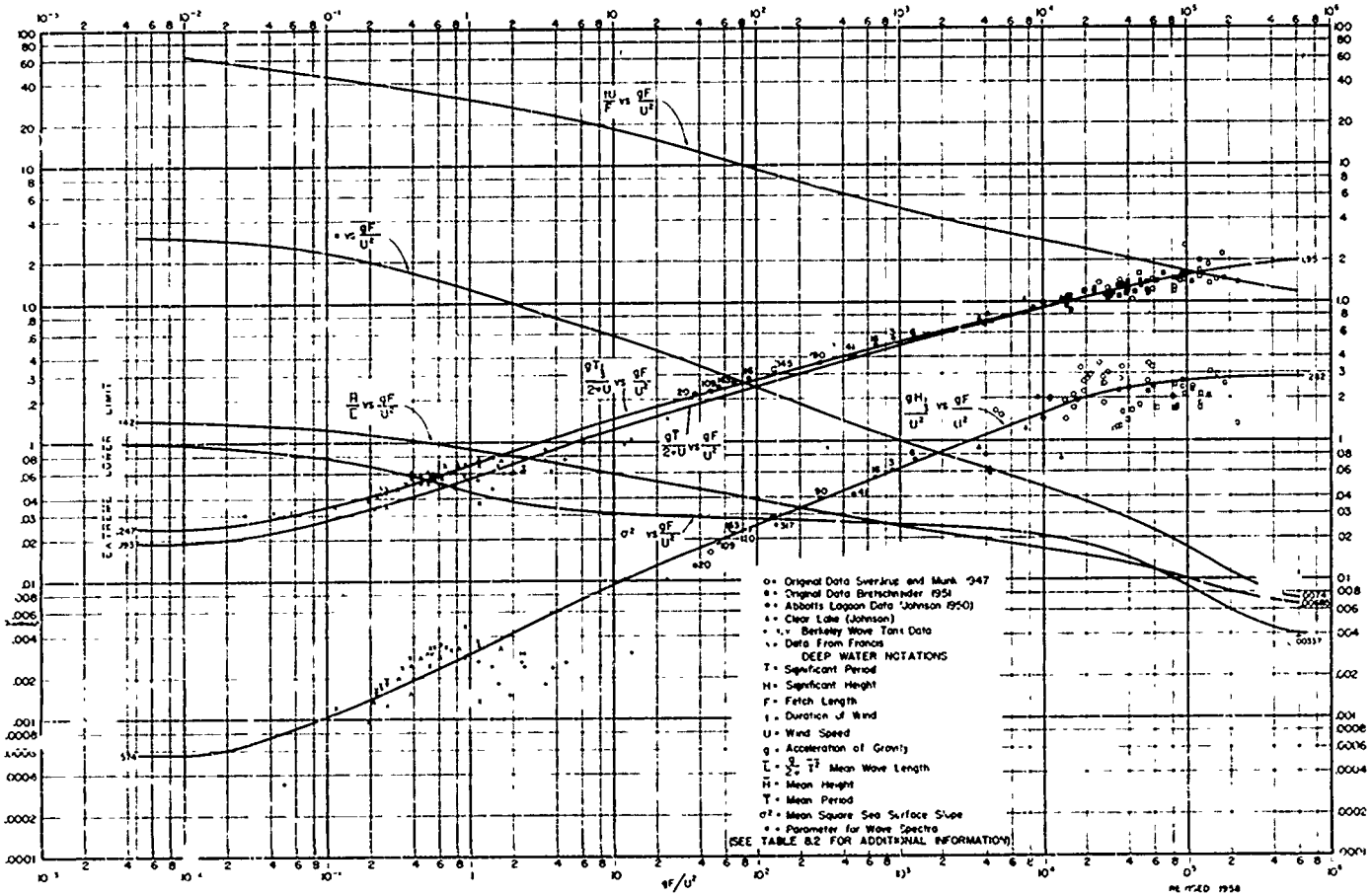

FIGURE 8.1 FETCH GRAPH FOR DEEP WATER

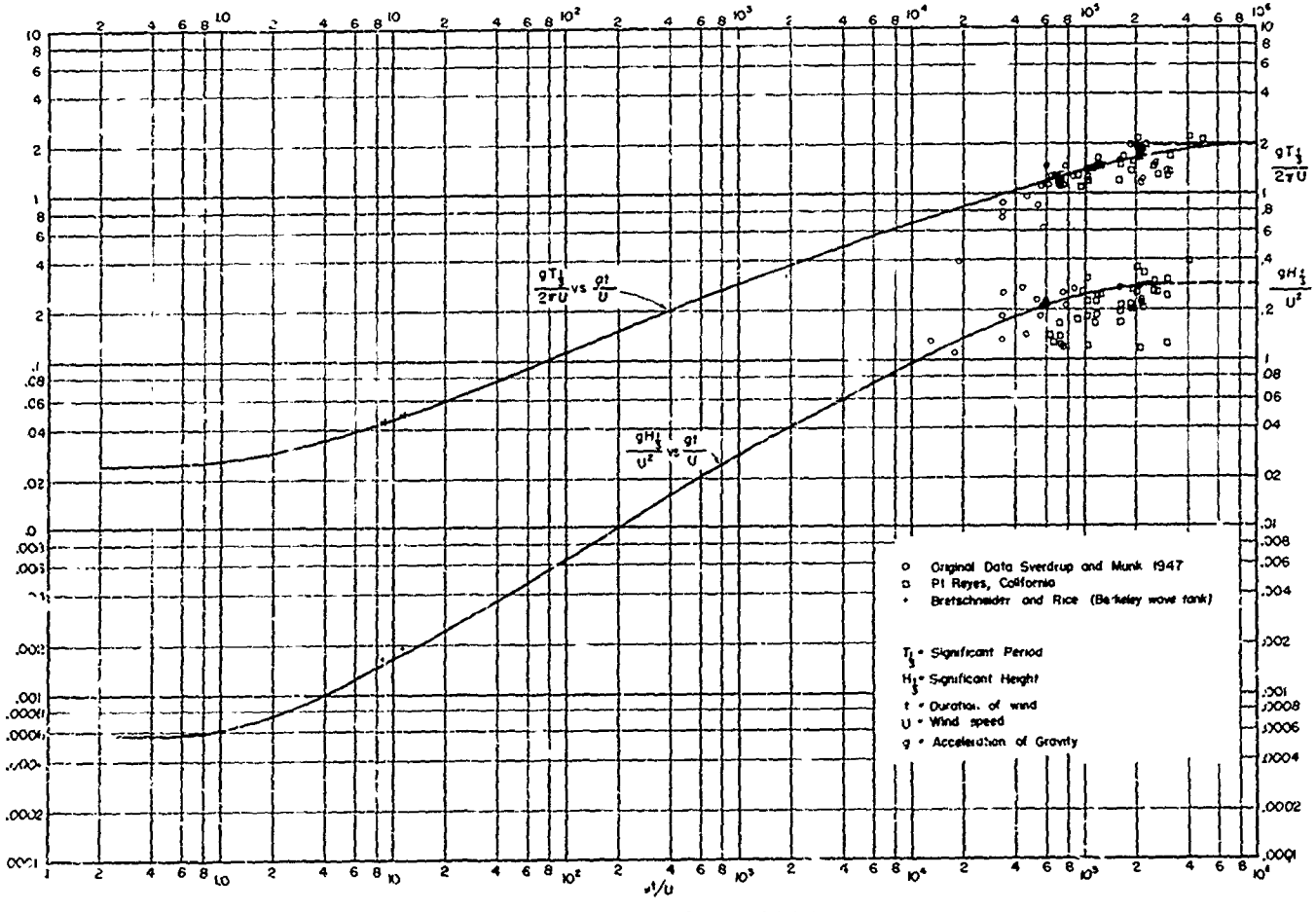

FIGURE 8.2 DURATION GRAPH

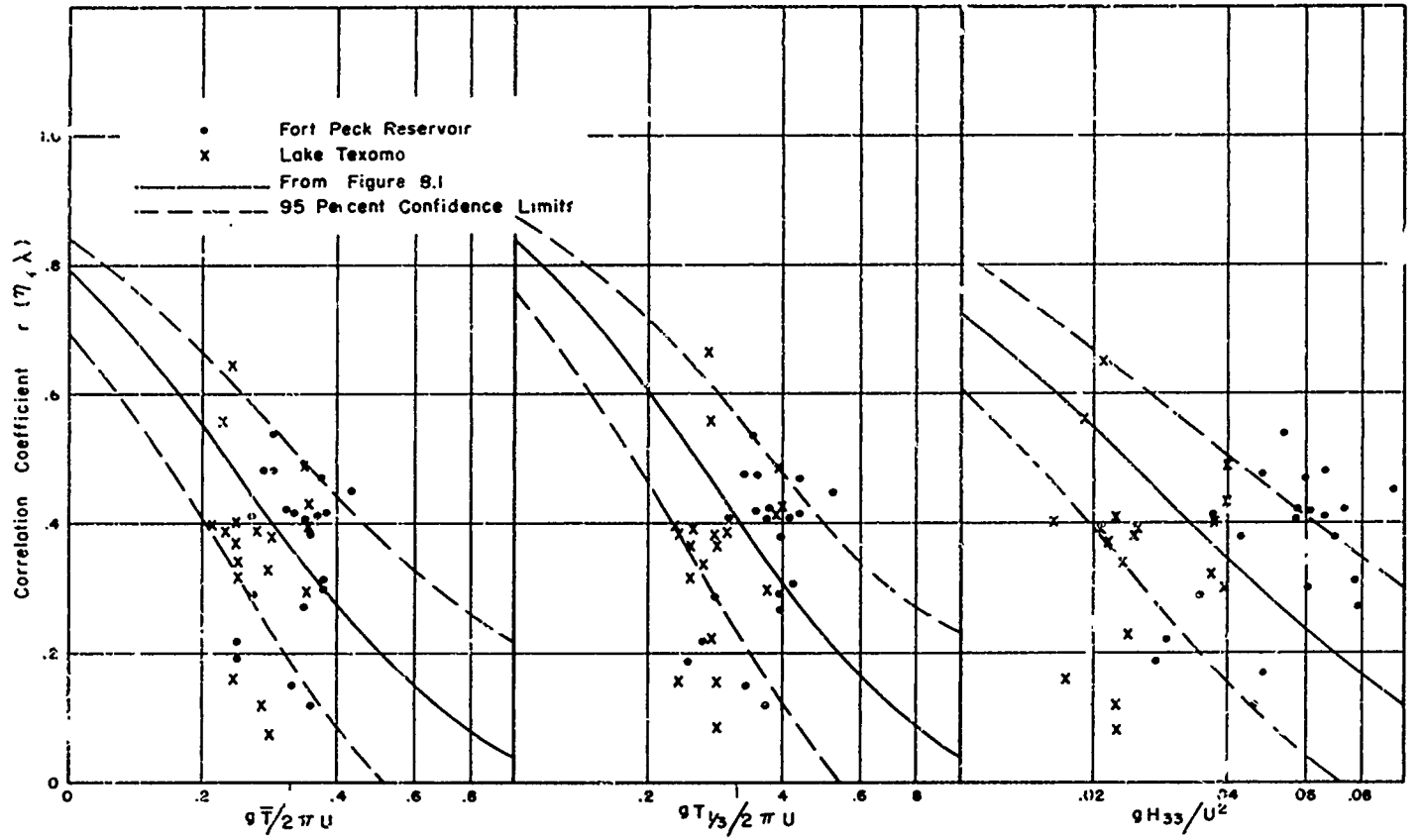

FIGURE 8.3 GENERATION PARAMETERS VERSUS CORRELATION COEFFICIENT

CHAPTER IX: COMPARISON OF VARIOUS PROPOSED WAVE SPECTRA

1. General

It is of interest to make comparisons of the various proposed wave spectra. These are Darbyshire (1952), Darbyshire (1955), Neumann (1955), and that of the present study. Recently Neumann and Pierson (1957) made a detailed comparison of the above various theoretical wave spectra, not including that of the present author, the material of which had not yet been circulated. The work of Neumann and Pierson (1957) will not be repeated here, except that as pertinent to the present discussion. The Roll and Fisher (1956) modification of the Neumann spectrum and the Darbyshire spectrum were compared with the Neumann spectrum. This comparison, made with data by Neumann and Pierson (1957), showed that the Neumann spectrum fitted the data satisfactorily, whereas the other spectra were unsatisfactory. It is shown that the appropriate spectrum from the family of spectra proposed in the present paper fits the above data equally well if not better.

In the discussion following, the four wave spectra are denoted by D_1, D_2, N, and B, corresponding respectively to Darbyshire (1952), Darbyshire (1955), Neumann (1955), and Bretschneider (present paper).

The D_1 and D_2 spectra were presented originally in terms of the gradient wind speed. The surface wind speed, usually considered at normal anemometer level (10 meters above mean sea level in case of the oceans), is equal to about two-thirds of the gradient wind speed, but may be quite different under various conditions of atmospheric stability or sea-air temperature differences. So that all spectra utilize the same wind elevation, the gradient wind speed in the D_1 and D_2 spectra are replaced by 3/2 of the surface wind speed. The symbols $S_H2\ (T)$ and $S_H2\ (\omega)$ are retained respectively for the period spectrum and the frequency spectrum, although H_T2 and $H_\omega 2$ have been used by others. The comparison is limited to the fully arisen or near fully arisen sea, so that the B spectrum for zero correlation need only be discussed.

2. The Various Proposed Spectra

Where the surface wind speed is used and the units of $S_H2\ (T)$ are FT^2/sec the four period spectra are:

$$(D_1)\quad S_H^2(T) = C_1 g^2 T^2 e^{-35.8\left[\frac{gT}{2\pi U} - 1.09\right]^2}$$

$$(D_2)\quad S_H^2(T) \begin{cases} = C_2 g^2 T^5 \left[\sqrt{\frac{2\pi U}{g}} - bT\right]^2 & 0 \le T \le 5\sqrt{\frac{2\pi U}{g}} \\ = 0 & T > 5\sqrt{\frac{2\pi U}{g}} \end{cases} \qquad (9.1)$$

$$(N)\quad S_H^2(T) = C_3 g^2 T^4 e^{-2\left[\frac{gT}{2\pi U}\right]^2}$$

$$(B)\quad S_H^2(T) = \frac{\alpha g^2}{(2\pi)^4} T^3 e^{-0.675\left[\frac{gT}{2\pi U F_2}\right]^4}$$

where the constants are given by

$C_1 = 1.87 \times 10^{-4}$ sec

$C_2 = 5.7 \times 10^{-8}$ sec^{-3}

$b = 0.2$ sec$^{-1/2}$

$C_3 = 2.0 \times 10^{-5}$ sec^{-1}

$\alpha = 3.437\, F_1^2 / F_2^4$ dimensionless

$F_1 = \frac{g\bar{H}}{U^2} = f_1\left(\frac{g\bar{F}}{U^2}, \frac{gt}{U}\right)$ dimensionless

$F_2 = \frac{g\bar{x}}{2\pi U} = f_2\left(\frac{g\bar{F}}{U^2}, \frac{gt}{U}\right)$ dimensionless

With the proper transformation, the corresponding frequency spectra are given by:

$$(D_1) \qquad S_H{}^2(\omega) = \left[C_1 (2\pi)^3 \; g^2 \omega^{-4}\right] e^{-35.8\left(\frac{g}{U\omega} - 1.03\right)^2}$$

$$(D_2) \qquad S_H{}^2(\omega) \begin{cases} = \left[C_2 (2\pi)^6 g^2 \omega^{-7}\right]\left[\sqrt{\frac{2\pi U}{g}} - \frac{2\pi b}{\omega}\right]^2 \\ \omega \geq \frac{1}{5}\left(\frac{2\pi g}{U}\right)^{\frac{1}{2}} \geq 0 \\ = 0 \\ \omega > \frac{1}{5}\left(\frac{2\pi g}{U}\right)^{\frac{1}{2}} \end{cases} \qquad (9.2)$$

$$(N) \qquad S_H{}^2(\omega) = C_3 (2\pi)^5 g^2 \omega^{-6} e^{-2\left[\frac{g}{U\omega}\right]^2}$$

$$(B) \qquad S_H{}^2(\omega) = \alpha g^2 \omega^{-5} e^{-0.675\left[\frac{g}{U\omega F_2}\right]^4}$$

3. Evolvement of Proposed Spectra

D_1 - Darbyshire (1952):- The D_1 spectrum evolved from frequency-analysis of wave records obtained from sub-surface pressure type wave records. This investigation was based on records of waves made on the north coast of Cornwall, in the Irish Sea, and in Lough Neagh. Synoptic meteorological charts were used to obtain fetch lengths, and gradient winds. The wave pressure transducer was on the sea bed at a depth of about 50 feet. The usual hydrodynamic relationships (presented earlier) were used to convert bottom pressure to surface elevation, prior to the frequency analysis. For wave periods less than about 6 seconds the bottom pressure fluctuations, reduced to such a low level that the process was no longer practicable, were ignored by Darbyshire. Hence, the high frequency components are missing. Water depths on the order of the mean wave lengths encompassed much of the fetch length. Because of wave energy loss due to bottom friction and refraction due to currents, the low frequency components are somewhat attenuated.

D_2 - Darbyshire (1955): The D_2 spectrum evolved by frequency-analyzing wave records obtained from a ship-borne wave recorder in the North Atlantic. There is some doubt as to the exact calibration of this instrument, but it is known to behave similar to a sub-surface pressure recorder, and the high frequency components are attenuated. Although frequency analysis of wave records should give the best estimate of the wave spectrum, there is no way of taking into account the energy of those components filtered out or not recorded by a pressure recorder.

N - Neumann (1955): The N spectrum evolved in a different manner than either the D_1 or D_2 spectra. On the basis of visual observations from assumed fully developed seas, Neumann (1955) obtained an empirical envelope curve for the data plotted in terms of H/T^2 versus $(T/U)^2$, which is given by

$$H = (\text{const})\, T^2 e^{-\left(\frac{g}{2\pi U}\right)^2} \tag{9.3}$$

where T was defined as an apparent wave period and is given the symbol $\tilde{T}$. The enveloped curve was not determined statistically, but was constructed visually. There is some question as to whether or not the symbol should be T or $\tilde{T}$, since visual observations with a stop watch are difficult to make.

Since the energy is proportional to wave height squared, Neumann in effect assumed the period spectrum of H^2 to be proportional to the square of (9.3). Such a procedure could only be used if (9.3) was the equation obtained by a least squares technique. The constant in the N spectrum (9.1) or (9.2) was obtained by squaring (9.3) and forcing the area under the resulting curve to be equal to $4/\pi(\overline{H})^2$, the so-called energy coefficient obtained by Longuet-Higgins (1952). Hence the area under the N spectrum must be correct, provided that of Longuet-Higgins (1952) is correct, and this seems to be true. Whether the shape, peak, and width are correct needs to be investigated by use of proper wave data. Although the first operation, squaring (9.3), may not necessarily be based on correct assumptions, the evaluation of the constant in the above manner tends toward compensation because there are a multitude of such exponential equations which might represent approximately the true wave spectrum, provided the area beneath the curve is equal to $4/\pi(\overline{H})^2$.

One difficulty with the method assumed by Neumann (1952) is that the constant evolved takes on the dimension of seconds^{-1}, resulting in wave height proportional to the 5/2 power of the wind speed for a fully developed sea. The above cannot be reconciled,

either with data or by dimensional homogenity, and is sort of a paradox since a constant of seconds^{-1} and $U^{5/2}$ go together just as a dimensionless constant and U^2 go together. A very important factor, however elementary it may be, is that the period spectrum of H^2 cannot be obtained by squaring the enveloped curve of data in terms of H, since this has the same mathematical implication as squaring the equation of a distribution function. The wave period distribution function, itself, is not to be squared, but the individual height components are squared and then summed according to the height distribution function. This fact was brought to light in the development of the family of spectra in the present paper.

B - Bretschneider (present paper): As stated before, the family of B spectra evolved directly from the joint distribution function, and was derived theoretically without any necessary foreknowledge of the distribution functions, except that linear regression between H and T^2 was required. Based on the statistical analysis of wave data, it was found that the Rayleigh distribution applied to wave height variability and also wave length (T^2) variability. Thus the family of B spectra was determined theoretically, by squaring all components of H and summing according to the distribution function. Because the B spectra evolved in this manner, all high frequency components are present in the theoretical spectra.

The fact that high frequency components might have been attenuated or even filtered out by use of pressure records used in the statistical analysis has no effect on the derivation of the family of wave spectra, once the distribution functions were decided upon.

Whereas the area under the N spectrum was forced to be equal to $4/\pi(\bar{H})^2$, the area of $4/\pi(\bar{H})^2$ under the B spectra evolved as a physical property. Only the B spectrum for zero correlation is used in the material following.

4. Physical Properties of Period Spectra

Energy. The area under the spectra is equal to $\overline{H^2}$, the mean square wave height, and when multiplied by $1/8\,\rho g$ gives the total energy in the spectra whence

$$E = \frac{1}{8}\rho g \overline{H^2} \tag{9.4}$$

where

$$\overline{H^2} = \int_0^\infty S_{H^2}(T)\,dT = -\int_0^\infty S_{H^2}(\omega)\,d\omega \tag{9.5}$$

thus

$$
\begin{aligned}
&(D_1) \qquad \overline{H^2} = 0.0098 \frac{U^3}{g} \\
&(D_2) \qquad \overline{H^2} = 0.00825 \frac{U^4}{g^2} \\
&(N) \qquad \overline{H^2} = 0.00594 \frac{U^5}{g^3} \\
&(B) \qquad \overline{H^2} = \frac{4}{\pi} F_1^2 \frac{U^4}{g^2}
\end{aligned}
\tag{9.6}
$$

When U is in ft/sec, g = 32.16 ft/sec^2 and $\overline{H^2}$ is in ft^2; when U is in cm/sec, g = 980 cm/sec^2, and $\overline{H^2}$ is in cm^2. For D_1 and D_2 spectra $\overline{H^2} = 1.44\ (\overline{H})^2$ and for N and B spectra $\overline{H^2} = 4/\pi\ (\overline{H})^2$. For all four spectra $H_{33} \sim 1.6\ \overline{H}$. Thus

$$
\begin{aligned}
&(D_1) \qquad \frac{gH_{33}}{U^2} = 0.131 \left(\frac{U}{g}\right)^{-\frac{1}{2}} \\
&(D_2) \qquad \frac{gH_{33}}{U^2} = 0.121 \\
&(N) \qquad \frac{gH_{33}}{U^2} = 0.216 \left(\frac{U}{g}\right)^{\frac{1}{2}} \\
&(B) \qquad \frac{gH_{33}}{U^2} = 1.6\ F_1
\end{aligned}
\tag{9.7}
$$

For D_1 the constant 0.131 has the dimension of sec$^{\frac{1}{2}}$ and for N the constant 0.216 sec$^{-\frac{1}{2}}$. For a fully developed sea $F_1 = 0.177$. Table 9.1 gives typical values of H_{33} versus U for a fully developed sea based on (9.7).

TABLE 9.1

H_{33} VERSUS U
FOR FULLY DEVELOPED SEA

Spectrum	D_1	D_2	N	B
U (knots)	Significant Height, feet			
10	1.6	1.1	1.4	2.5
15	2.9	2.4	3.9	5.7
20	4.5	4.2	7.9	10.0
25	6.3	6.6	13.8	15.7
30	8.3	9.5	21.8	22.6
35	10.5	12.9	32.0	30.8
40	12.8	16.8	44.7	40.2
45	15.3	21.3	60.0	50.1
50	17.9	26.3	78.1	62.8
55	20.6	31.8	99.2	75.9
60	23.5	37.8	123.3	90.4

Wave heights for D_1 are considerably lower than those for D_2, N, and B, because the D_1 spectrum is based on waves which were influenced considerably by shallow water, possibly bottom friction and currents. Wave heights for D_2 are lower than those for B by a constant ratio of 2.34, which would indicate that D_2 is based on waves not of a fully developed sea. Whereas $F_1 = 0.177$ for the B spectrum the corresponding value for D_2 would be $F_1 = 0.177/2.34 = 0.0755$.

Wave heights for the N spectrum are quite comparable to those for the B spectrum for winds between 25 and 40 knots. At 45 knots and above and 20 knots and below the departures become quite noticeable.

Mean Wave Period: If zero correlation exists between H and T, it can be shown that the period spectrum has properties of the corresponding period distribution function, where the zero moment about the origin is used as the normalizing function. It may be assumed that these wave periods correspond to those based on the crest to trough method of analysis. It was shown earlier that zero correlation quite likely exists between H and T for a fully developed sea. From the above discussion one may obtain the mean wave period.

$$\bar{T} = \frac{\int_0^\infty T S_{H^2(T)}\, dt}{\int_0^\infty S_{H^2(T)}\, dt} \qquad (9.8)$$

If zero correlation exists $\bar{T}$ is also the significant period, but if zero correlation does not exist, say for a young sea, then (9.8) results in $\bar{T}'$ instead of $\bar{T}$, but this will not affect the comparisons following.* Using (9.8) one obtains for the various spectra:

$$
\begin{aligned}
&(D_1) \quad \frac{g\bar{T}}{2\pi U} = 1.194 \\
&(D_2) \quad \frac{g\bar{T}}{2\pi U} = \frac{10}{3}\left(\frac{g}{2\pi U}\right)^{\frac{1}{2}} \\
&(N) \quad \frac{g\bar{T}}{2\pi U} = \sqrt{\frac{32}{9\pi}} = 1.064 \\
&(B) \quad \frac{g\bar{T}}{2\pi U} = F_2
\end{aligned}
\tag{9.9}
$$

Optimum Period and Maximum Energy: The optimum period T_{op} corresponding to maximum energy of the period spectrum is obtained from

$$
\frac{d\left[S_H^2(T)\right]}{dT} = 0 \tag{9.10}
$$

Thus

$$
\begin{aligned}
&(D_1) \quad \frac{gT_{op}}{2\pi U} = 1.125 \\
&(D_2) \quad \frac{gT_{op}}{2\pi U} = 3.57\left[\frac{g}{2\pi U}\right]^{\frac{1}{2}} \\
&(N) \quad \frac{gT_{op}}{2\pi U} = 1.00 \\
&(B) \quad \frac{gT_{op}}{2\pi U} = 1.027 F_2
\end{aligned}
\tag{9.11}
$$

*As shown later the apparent wave period $\bar{\bar{T}}$ is related to the mean crest to trough period $\bar{T}$.

and

$$
\begin{aligned}
&(D_1) \quad \left[S_H^2(T)\right]_{max} = 9.2 \times 10^{-3} U^2 \\
&(D_2) \quad \left[S_H^2(T)\right]_{max} = 5.3 \times 10^{-3} \frac{U^{3.5}}{g^{1.5}} \\
&(N) \quad \left[S_H^2(T)\right]_{max} = 4.34 \times 10^{-3} \frac{U^4}{g^2} \\
&(B) \quad \left[S_H^2(T)\right]_{max} = 0.279 \frac{F_1^2 U^3}{F_2 g}
\end{aligned}
\tag{9.12}
$$

and

$$
\begin{aligned}
&(D_1) \quad \frac{T_{op}}{\bar{T}} = 0.931 \\
&(D_2) \quad \frac{T_{op}}{\bar{T}} = 1.0715 \\
&(N) \quad \frac{T_{op}}{\bar{T}} = 0.94 \\
&(B) \quad \frac{T_{op}}{\bar{T}} = 1.027
\end{aligned}
\tag{9.13}
$$

For a fully developed sea $F_1 = 0.177$ and $F_2 = 1.95$. Typical values of $[S_H^2(T)]_{max}$ are given in Table 9.2; for the B spectrum values are also given for $F_1 = 0.106$ and $F_2 = 1.0$, a moderately generated sea.

TABLE 9.2

TYPICAL VALUES OF $[S_{H^2}(T)]_{max}$, FT^2/sec

U Knots	Spectrum D_1	D_2	N	B $F_1=0.177$ $F_2=1.95$	B $F_1=0.106$ $F_2=1.0$
10	0.91	0.09	0.04	0.14	0.098
15	2.09	0.38	0.21	0.47	0.33
20	3.72	1.03	0.67	1.11	0.775
25	5.81	2.25	1.64	2.17	1.52
30	8.37	4.26	3.40	3.75	2.62
35	11.39	7.30	6.30	5.96	4.16
40	14.88	11.61	10.75	8.90	6.22
45	18.83	17.61	17.22	12.67	8.85
50	23.25	25.45	26.25	17.38	12.10
55	28.13	35.54	38.43	23.13	16.15
60	33.48	48.18	54.43	30.02	21.0

Higher Moments: The n^{th} moment of T about the origin is given by

$$M_n = \frac{1}{H^2}\int_0^\infty T^n S_{H^2}(T)\,dT$$

It can be shown for unit form ($\tau = T/\bar{T}$) that

$$\overline{\tau^2} = \frac{M_2}{(M_1)^2}$$

$$\overline{\tau^3} = \frac{M_3}{(M_1)^3} \qquad (9.14)$$

$$\overline{\tau^4} = \frac{M_4}{(M_1)^4}$$

From (9.14) one obtains the standard deviation, skewness coefficient and kurtosis, respectively.

$$\sigma_\tau = \sqrt{\overline{\tau^2} - 1}$$

$$a_{3_\tau} = \frac{\overline{\tau^3} - 3\overline{\tau^2} + 2}{(\sigma_\tau)^3} \qquad (9.15)$$

$$a_{4_\tau} = \frac{\tau^4 - 4\overline{\tau^3} + 6\tau^2 + 2}{(\sigma_\tau)^4}$$

Table 9.3 summarizes results from the above equations.

TABLE 9.3

SUMMARY OF MOMENTS

Parameter	D_1	D_2	N	B
$\overline{\tau^2}$	1.004252	1.05001	1.10447	1.07815
$\overline{\tau^3}$	1.012113	1.145449	1.32536	1.234196
$\overline{\tau^4}$	1.024739	1.288640	1.70778	1.481564
σ_τ	0.0652	0.224	0.3231	0.281
a_{3_τ}	-2.321	-0.405	+0.3543	-0.088
a_{4_τ}	100	2.740	2.779	2.755

5. Elimination of Wind Speed from Period Spectra

The comparison of wave spectra in terms of wind speed is not too satisfactory a method, since this comparison depends on relations between wave height, wave period and wind speed. In particular, the wind speed comparison is unfair for the D_1 and D_2 spectra which are based on gradient wind speed reduced to surface wind speed by $U_g = 1.5U$. The surface wind speed can be eliminated from the various spectra, thereby bringing comparisons to a common level. This is done by use of (9.6) and (9.9), whence

$$(D_1)\quad S_{H^2}(T) = 8.05\,\overline{H^2}\,\frac{T^2}{(\bar{T})^3}\,e^{-51\left[\frac{T}{\bar{T}}-0.91\right]^2}$$

$$(D_2)\quad S_{H^2}(T) = 14.74\,\overline{H^2}\,\frac{T^5}{(\bar{T})^6}\left[1-\frac{2T}{3\bar{T}}\right] 0 \le T \le 1.5\bar{T} \qquad (9.16)$$

$$(N)\quad S_{H^2}(T) = \left(\frac{64}{9\pi}\right)^3 \frac{\overline{H^2}\,T^4}{(\bar{T})^5}\,e^{-\frac{64}{9\pi}\left(\frac{T}{\bar{T}}\right)^2}$$

$$(B)\quad S_{H^2}(T) = 2.7\,\overline{H^2}\,\frac{T^3}{(\bar{T})^4}\,e^{-0.675\left(\frac{T}{\bar{T}}\right)^4}$$

It is interesting to note that the dimensional constants in the D_1, D_2, and N spectra vanish. All spectra are in terms of two measurable quantities H and T, and the comparisons are on the same level. If zero correlation exists the period distribution function is related to the period spectrum according to

$$p(T) = \frac{1}{(\bar{H})^2} S_{H^2}(T) \qquad (9.17)$$

or in unit form

$$S_{\eta^2}(\tau) = \overline{\eta^2}\,p(\tau);\quad \overline{\eta^2} = \frac{\overline{H^2}}{(\bar{H})^2} \qquad (9.18)$$

Since the area under the curve of $p(\tau)$ is unity, the area under the curve of $S_{\eta^2}(\tau)$ is $\overline{\eta^2}$. For D_1 and D_2 spectra $\overline{\eta^2} = 1.44$ and for N and B spectra $\overline{\eta^2} = 4/\pi$. Thus

$$(D_1)\quad S_{\eta^2}(\tau) = 11.6\,\tau^2\,e^{-51[\tau-0.91]^2}$$

$$(D_2)\quad S_{\eta^2}(\tau) = 21.2\,\tau^5\left[1-\frac{2\tau}{3}\right]^2 \quad 0 \le \tau \le 1.5 \qquad (9.19)$$

$$(N)\quad S_{\eta^2}(\tau) = \frac{4}{\pi}\left(\frac{64}{9\pi}\right)^3 \tau^4 e^{-\left(\frac{64}{9\pi}\right)\tau^2}$$

$$(B)\quad S_{\eta^2}(\tau) = 3.437\,\tau^3\,e^{-0.675\,\tau^4}$$

and

$$
\begin{aligned}
(D_1) \quad & p(\tau) = 8.07\,\tau^2 e^{-51[\tau - 0.92]^2} \\
(D_2) \quad & p(\tau) = 14.74\,\tau^5 \left[1 - \frac{2\tau}{3}\right]^2 \quad 0 \le \tau \le 1.5 \\
(N) \quad & p(\tau) = \left(\frac{64}{9\pi}\right)^3 \tau^4 e^{-\frac{64\tau^2}{9\pi}} \\
(B) \quad & p(\tau) = 2.7\,\tau^3 e^{-0.675\,\tau^4}
\end{aligned}
\tag{9.20}
$$

Table 9.4 gives values of $S_\eta{}^2(\tau)$ versus τ for various spectra. The standard form of the period spectrum is related to normal form by

$$
S_H{}^2(T) = \frac{(\overline{H})^2}{(\overline{T})} S_\eta{}^2(\tau) = \frac{\overline{H^2}}{(\overline{T})} \frac{1}{\overline{\eta^2}} S_\eta{}^2(\tau) \tag{9.21}
$$

Data from Table 9.4 are plotted in Figure 9.1 for the D_2, N, and B spectra; the D_1 spectrum is greatly peaked and out of range of the other three spectra, and is not shown in Figure 9.1. It is of interest to note the degree of closeness between the N and B spectra. Both have the same area, $4/\pi$, but the B spectrum is more peaked and more nearly the shape of normal distribution. These two curves cross in three places, at about $\tau = 0.28$, 0.86, and 1.43. Although from Table 9.3 α_{4_τ}, the kurtosis, is slightly greater for the N spectrum than for the B spectrum, the B spectrum actually has greater peakedness. Hence the word "peakedness" instead of α_{4_τ} could be misleading. The D_2 spectrum has the lowest value of α_{4_τ}, but its peakedness is greater than either the N or B spectra, but some of this is due to greater area under the D_2 spectrum than under N or B.

TABLE 9.4

$S_\eta 2(\tau)$ VERSUS τ

$\tau = T/T$	D_1	D_2	N	B
0.1		0.0002	0.001	0.003
0.2		0.020	0.024	0.050
0.3		0.033	0.098	0.092
0.4		0.167	0.263	0.216
0.5	0.001	0.295	0.525	0.412
0.6	0.027	0.594	0.849	0.680
0.7	0.739	1.016	1.172	1.003
0.8	4.01	1.515	1.424	1.335
0.9	9.349	2.003	1.553	1.609
1.0	7.675	2.366	1.542	1.750
1.1	2.226	2.434	1.406	1.690
1.2	0.229	2.110	1.188	1.465
1.3	0.008	1.417	0.928	1.099
1.4		0.513	0.681	0.707
1.5			0.464	0.383
1.6			0.300	0.169
1.7			0.185	0.061
1.8			0.105	0.017
1.9			0.054	0.004
2.0			0.028	
τ_{op}	0.931	1.0715	0.94	1.027
$\left[S_\eta 2(\tau)\right]_{max}$	9.8	2.44	1.589	1.754

6. Physical Properties of the Frequency Spectra

Optimum Frequency and Maximum Energy: The optimum frequency ω_{op} corresponding to maximum energy of the frequency spectra is obtained from:

$$\frac{d\left[S_H 2\ (\omega)\right]}{d\omega} = 0 \qquad (9.22)$$

Thus

$$(D_1)\quad \frac{g}{U\omega_{op}} = 1.15$$

$$(D_2)\quad \frac{g}{U\omega_{op}} = 3.88\left(\frac{g}{2\pi U}\right)^{\frac{1}{2}}$$

$$(N)\quad \frac{g}{U\omega_{op}} = \sqrt{\frac{3}{2}} = 1.225 \qquad (9.23)$$

$$(B)\quad \frac{g}{U\omega_{op}} = \sqrt[4]{\frac{5}{2.7}}\, F_2 = 1.166\ F_2$$

and

$$(D_1)\quad S_{H^2}(\omega)_{max} = 0.071\,\frac{U^4}{g^2}$$

$$(D_2)\quad S_{H^2}(\omega)_{max} = 0.147\,\frac{U^{4.5}}{g^{2.5}} \qquad (9.24)$$

$$(N)\quad S_{H^2}(\omega)_{max} = 0.033\,\frac{U^6}{g^4}$$

$$(B)\quad S_{H^2}(\omega)_{max} = \frac{2.12\,F_1^2\,F_2\,U^5}{g^3}$$

The units of $\left[S_H2(\omega)\right]_{max}$ are in ft^2 sec. Table 9.5 gives typical values of $\left[S_H2(\omega)\right]_{max}$ for various wind speeds for a fully developed sea. For the B spectrum $F_2 = 1.95$ represents a fully developed sea, and $F_2 = 1.0$ a moderately developed sea.

TABLE 9.5

TYPICAL VALUES $\left[S_{H^2}(\omega)\right]_{max}$ FT^2 sec

U Knots	Spectrum D1	D2	N	B F_1=0.177 F_2=1.95	B F_1=0.106 F_2=1.0
10	5.6	8.35	0.72	5.4	1.0
15	28.5	51.7	8.2	41	7.6
20	89.5	188	46.5	173	32
25	218	518	177	530	98
30	453	1,170	530	1,540	284
35	840	2,340	1,315	2,830	525
40	1,435	4,300	2,880	5,400	1,000
45	2,300	7,200	5,860	9,800	1,815
50	3,500	11,700	11,000	16,750	3,100
55	5,050	18,000	18,000	27,000	5,000
60	7,250	26,700	33,300	41,800	7,750

Expected Number of Zeros: Each time the surface elevation passes through still water level a zero crossing is made. It was shown by Rice (1945) that for a random process, the expected number of zeros is given by

$$EXP(0) = 2\left[\frac{\int_0^\infty \omega^2 S_{H^2}(\omega)d\omega}{\int_0^\infty S_{H^2}(\omega)d\omega}\right]^{\frac{1}{2}} \tag{9.25}$$

From this relationship Pierson (1954), and also Neumann (1955), define an apparent mean wave period $\bar{T}$, which is different than $\bar{T}$ obtained by use of (9.8), according to

$$\bar{T} = \left[\frac{\int_0^\infty \frac{1}{T^2} S_{H^2}(T)dT}{\int_0^\infty S_{H^2}(T)dT}\right]^{-\frac{1}{2}} \tag{9.26}$$

It can be seen that the so-called mean apparent wave period is nothing more than

$$\overline{\tau} = \left[\overline{\left[\frac{1}{T}\right]^2}\right]^{-\frac{1}{2}} \neq \left[\frac{1}{\overline{T}}\right]^{-1} \tag{9.27}$$

Applying (9.26) to the various spectra one obtains

$$\begin{aligned}
&(D_1) \quad \frac{g\overline{\tau}}{2\pi U} = 1.22 \\
&(D_2) \quad \frac{g\overline{\tau}}{2\pi U} = 2.98\left[\frac{2\pi g}{U}\right]^{\frac{1}{2}} \\
&(N) \quad \frac{g\overline{\tau}}{2\pi U} = \frac{1}{2}\sqrt{3} = 0.866 \\
&(B) \quad \frac{g\overline{\tau}}{2\pi U} = 0.83\, F_2
\end{aligned} \tag{9.28}$$

The ratio of the apparent mean period to the mean wave period becomes

$$\begin{aligned}
&(D_1) \quad \frac{\overline{\tau}}{\overline{T}} = 1.02 \\
&(D_2) \quad \frac{\overline{\tau}}{\overline{T}} = 0.894 \\
&(N) \quad \frac{\overline{\tau}}{\overline{T}} = 0.82 \\
&(B) \quad \frac{\overline{\tau}}{\overline{T}} = 0.83
\end{aligned} \tag{9.29}$$

It is seen that there will be more apparent wave periods $\bar{\tau}$ defined by the zero-up crossing method than there are periods $\bar{T}_2$ defined by the crest to trough method. One should expect more $\bar{\tau}$ than T since the crest to trough method neglects the small reversals in surface slope that cross the zero line. If all these bumps were considered in the analysis of waves the distributions of both H and T might conceivably be different. Furthermore, there would be more T than $\bar{\tau}$, since there are also bumps in the troughs and on the crests of the larger waves, which would not cross through zero elevation. (See Figure 2.6, Chapter II.)

The wave period corresponding to ω_{op} is written as T of ω_{op} or $T(\omega_{op})$, where

$$\frac{gT(\omega_{op})}{2\pi U} = \frac{g}{U\omega_{op}} \tag{9.30}$$

The ratios of $T(\omega_{op})$ to $\bar{T}$ and $\bar{\tau}$ are given below

$$\begin{array}{lll} (D_1) & \dfrac{T(\omega_{op})}{\bar{T}} = 0.96 & \dfrac{T(\omega_{op})}{\bar{\tau}} = 0.94 \\ (D_2) & \dfrac{T(\omega_{op})}{\bar{T}} = 1.16 & \dfrac{T(\omega_{op})}{\bar{\tau}} = 1.30 \\ (N) & \dfrac{T(\omega_{op})}{\bar{T}} = 1.15 & \dfrac{T(\omega_{op})}{\bar{\tau}} = 1.4 \\ (B) & \dfrac{T(\omega_{op})}{\bar{T}} = 1.17 & \dfrac{T(\omega_{op})}{\bar{\tau}} = 1.4 \end{array} \tag{9.31}$$

Spectral Width Parameter: The spectral width parameter, ϵ, is given by

$$\epsilon = \sqrt{1 - \frac{M_2^2}{M_0 M_4}} \tag{9.32}$$

where the n^{th} moment M_n of $S_H2(\omega)$ about the origin is obtained from

$$M_n = \int_0^\infty \omega^n S_H^2(\omega)\, d\omega \tag{9.33}$$

Thus

$$\begin{aligned}
&(D_1) \quad \epsilon = 0.334 \\
&(D_2) \quad \epsilon = 0.665 \\
&(N) \quad \epsilon = 0.815 \\
&(B) \quad \epsilon = \sqrt{1 - \frac{\frac{\pi}{4}}{\ln \overline{T}_{T_{min}} - 0.071}}
\end{aligned} \tag{9.34}$$

ϵ for the B spectrum for values of $\overline{T}/T_{min}$ are given below

$\overline{T}/T_{min}$	2.5	3.0	3.5	4.0	4.5	5.0	6.0	10.0	20.0	60.0	100.0
ϵ	0.29	0.49	0.58	0.64	0.67	0.70	0.74	0.81	0.85	0.89	0.91

For $\overline{T}/T_{min} = 10$ the spectral width parameter for N and B spectra are comparable which could be interpreted, for example, the N spectrum does not include wave periods less than 1.0 second for a wave record having a mean period of 10 seconds. Similarly the D_2 spectrum omits $T < 2.3$ seconds and D_1 omits $T < 4.0$ seconds for a record having a mean period of 10 seconds.

High Frequency Relationships: For large ω the various spectra reduce to

$$\begin{aligned}
&(D_1) \quad S_H^2(\omega) = C_1 (2\pi)^3 g^2 \omega^{-4} \\
&(D_2) \quad S_H^2(\omega) = C_2 (2\pi)^6 g^2 \omega^{-7} \frac{2\pi U}{g} \\
&(N) \quad S_H^2(\omega) = C_3 (2\pi)^5 g^2 \omega^{-6} \\
&(B) \quad S_H^2(\omega) = \alpha g^2 \omega^{-5}
\end{aligned} \tag{9.35}$$

According to the work of Burling (1955) and also Phillips (1957)[b] the frequency spectrum for high frequency (large ω) should reduce according to the B spectrum. It was shown earlier for plus one correlation (infant stage of generation) that $S(\omega)$ for high frequency reduced proportional to ω^{-9}. Evidently there is a transition from ω^{-9} to ω^{-5}. The D_2 spectrum can be interpreted as one of young sea. This view is supported by the comparative results in Table 9.1. The N spectrum (ω^{-6}) is perhaps close to that for a fully developed sea. It is difficult to account for ω^{-4} in the D_1 spectrum, except that D_1 is based on waves which were influenced considerably by shallow water and currents.

Mean Frequency: The mean frequency $\bar{\omega}$ may be defined when zero correlation exists, and is obtained from.

$$\bar{\omega} = \frac{\int_{\infty}^{0} \omega S_{H^2}(\omega) d\omega}{\int_{\infty}^{0} S_{H^2}(\omega) d\omega} \tag{9.36}$$

Thus

$$\begin{aligned}
&(D_1) \quad \frac{U\bar{\omega}}{g} = 0.904 \\
&(D_2) \quad \frac{U\bar{\omega}}{g} = \frac{10}{35}\left[\frac{2\pi U}{g}\right]^{\frac{1}{2}} \\
&(N) \quad \frac{U\bar{\omega}}{g} = \sqrt{\frac{32}{9\pi}} = 1.064 \\
&(B) \quad \frac{U\bar{\omega}}{g} = \frac{1.111}{F_2}
\end{aligned} \tag{9.37}$$

and

$$\begin{aligned}
&(D_1) \quad \frac{\bar{\omega}\,\bar{T}}{2\pi} = 1.076 \\
&(D_2) \quad \frac{\bar{\omega}\,\bar{T}}{2\pi} = 0.95 \\
&(D_3) \quad \frac{\bar{\omega}\,\bar{T}}{2\pi} = 1.113 \\
&(D_4) \quad \frac{\bar{\omega}\,\bar{T}}{2\pi} = 1.111
\end{aligned} \tag{9.38}$$

7. Elimination of Wind Speed from Frequency Spectra

Further comparisons can be made by eliminating the wind speed from the various frequency spectra, and might be made by use of (9.6) and (9.9) as before, or perhaps make use of (9.27) or (9.37) instead of (9.9). It matters little which is used since the comparisons are relative to certain parameters; and it appears that use of (9.37) is satisfactory. Using (9.6) and (9.37) one obtains for the various frequency spectra

$$
\begin{aligned}
&(D_1) \quad S_{H^2}(\omega) = 6.38\,\overline{H^2}\,\frac{(\bar{\omega})^3}{\omega^4} e^{-42.6\left[\frac{\bar{\omega}}{\omega} - 0.985\right]^2} \\
&(D_2) \quad S_{H^2}(\omega) = 20.8\,\overline{H^2}\,\frac{(\bar{\omega})^6}{\omega^7}\left[1 - 0.7\,\frac{\bar{\omega}}{\omega}\right]^2 \\
&(N) \quad S_{H^2}(\omega) = 2\left(\frac{9\pi}{16}\right)^2 \overline{H^2}\,\frac{(\bar{\omega})^5}{\omega^6} e^{-\frac{9\pi}{16}\left(\frac{\bar{\omega}}{\omega}\right)^2} \\
&(B) \quad S_{H^2}(\omega) = \sqrt{\pi}\,\overline{H^2}\,\frac{(\bar{\omega})^4}{\omega^5} e^{-\sqrt{\frac{\pi}{16}}\left(\frac{\bar{\omega}}{\omega}\right)^4}
\end{aligned}
\tag{9.39}
$$

If one defines the relative frequency $\nu = \frac{\omega}{\bar{\omega}}$, the unit form of the frequency spectra becomes

$$
\begin{aligned}
&(D_1) \quad S_{\eta^2}(\nu) = 9.2\,\nu^{-4} e^{-42.6\left[\nu^{-1} - 0.985\right]^2} \\
&(D_2) \quad S_{\eta^2}(\nu) = 30.0\,\nu^{-7}\left[1 - 0.7\,\nu^{-1}\right]^2 ; 0 \leq \nu \leq 0.7 \\
&(N) \quad S_{\eta^2}(\nu) = \frac{81\pi}{32}\,\nu^{-6} e^{-\frac{9\pi}{16}\,\nu^{-2}} \\
&(B) \quad S_{\eta^2}(\nu) = \frac{4}{\sqrt{\pi}}\,\nu^{-5} e^{-\sqrt{\frac{\pi}{16}}\,\nu^{-4}}
\end{aligned}
\tag{9.40}
$$

TABLE 9.6

$S_\eta 2(\nu)$ VERSUS ν

ν	D_1	D_2	E	B
0.1				
0.2				
0.3				
0.4			0.030	
0.5			0.428	0.058
0.6			1.244	0.943
0.7	0.0851		1.825	2.120
0.8	1.1230	2.232	1.896	2.334
0.9	7.1300	3.086	1.688	1.945
1.0	9.11[illegible]	2.696	1.358	1.449
1.1	4.9129	2.032	1.042	1.035
1.2	1.6581	1.453	0.781	0.732
1.3	0.4414	1.019	0.579	0.520
1.4	0.1042	0.710	0.429	0.374
1.5	0.0243	0.498	0.318	0.272
1.6	0.0054	0.352	0.238	0.201
1.7	0.0013	0.252	0.179	0.151
1.8	0.0003	0.183	0.136	0.114
1.9	0.0001	0.134	0.104	0.088
2.0		0.099	0.080	0.069
2.1		0.074	0.062	0.054
2.2		0.056	0.049	0.043
2.3		0.043	0.038	0.035
2.4		0.033	0.031	0.028
2.5		0.025	0.025	0.023
2.6				
ν_{op}	0.97	0.857	0.77	0.774
$\left[S_\eta 2(\nu)\right]_{max}$	9.50	3.09	1.93	2.36

If one is interested in the probability distribution function for frequency variability, it follows.

$$(D_1) \qquad p(\nu) = 6.38\,\nu^{-4}\, e^{-42.6\left[\nu^{-1}-0.985\right]^2}$$

$$(D_2) \qquad p(\nu) = 20.8\,\nu^{-7}\left[1-0.7\,\nu^{-1}\right]^2 \tag{9.41}$$

$$(N) \qquad p(\nu) = 2\left(\frac{9\pi}{16}\right)^2 \nu^{-6}\, e^{-\frac{9\pi}{16}\nu^{-2}}$$

$$(B) \qquad p(\nu) = \sqrt{\pi}\,\nu^{-5}\, e^{-\sqrt{\frac{\pi}{16}}\,\nu^{-4}}$$

Table 9.6 gives values of $S_{\eta}2(\nu)$ versus ν for various frequency spectra.

Data from Table 9.6 are plotted in Figure 9.2 for the D_2, N, and B spectra. It is of interest to note the closeness between the D_2, N, and B spectra. When all three spectra are in unit form, and if the same mean wave height and mean wave period were predicted for each, there would be little disagreement between any of the three spectra, except that the area under D_2 is larger than that under either N or B by a factor of $1.44 \doteq 4/\pi$. However, in standard form, using the wind speed as a parameter, there certainly is considerable disagreement between the various spectra as the wind speed changes. Evidently methods of measuring wind speed and wave heights and periods are critical factors.

8. Distribution of Periods

Two definitions of wave periods have been used, T, the wave period by crest-to-trough method, and $\bar{T}$, the wave period by zero-up crossing method. From (9.29) it is seen that the mean of these two periods is related by a constant. From the analysis of the data on wave period variability, Chapter IV, it appears that the same distribution function might apply for either method of analysis, whence

$$p(\bar{\tau})\,d\bar{\tau} = p(\tau)\,d\tau \tag{9.42}$$

where

$$\hat{\tau} = \frac{\hat{T}}{\bar{T}} \quad \text{and} \quad \tau = \frac{T}{\bar{T}}$$

Actually the spectrum proposed by Neumann (1955) is assumed to be based on $\hat{T}$ rather than T, but these are interchangeable by use of (9.29). The statistical parameters given in Table 9.3 for N and B spectra and Figure 9.1 imply that these two distributions are nearly the same, assuming zero correlation applies for either spectra.

9. Mean Square Sea Surface Slope

The mean square sea surface slope is given by

$$\sigma^2 = \frac{1}{8} \int_0^\infty k^2 S_H^2(T) dT, \text{ where}$$

$$k = \frac{2\pi}{L} = \frac{(2\pi)^2}{gT^2} = \frac{1}{\tau^2} \frac{(2\pi)^2}{g(\bar{T})^2} \tag{9.43}$$

Thus

$$(D_1) \qquad \sigma^2 = 1.03 \times 10^{-3} \frac{g}{U}$$

$$(D_2) \qquad \sigma^2 = 9.1 \times 10^{-4} \left(\frac{U}{g}\right)^2 \tag{9.44}$$

$$(N) \qquad \sigma^2 = 1.56 \times 10^{-2} \frac{U}{g}$$

$$(B) \qquad \sigma^2 = (0.43) \frac{F_1^2}{F_2^4} \left[-\ln \tau_{min} - 0.067\right]$$

It is noted that σ^2 varies as U^{-1} for D_1; U^2, for D_2; U, for N; and depends on gF/U^2 for B when zero correlation exists, and becomes independent of gF/U^2 for a fully developed sea.

The solution of (9.43) might also have been made by use of (9.16), in which case one obtains:

$$(D_1) \qquad \sigma^2 = 0.268(2\pi)^4 \frac{\overline{H^2}}{g^2(\overline{T})^4}$$

$$(D_2) \qquad \sigma^2 = 0.345(2\pi)^4 \frac{\overline{H^2}}{g^2(\overline{T})^4} \qquad (9.45)$$

$$(N) \qquad \sigma^2 = 0.85(2\pi)^4 \frac{\overline{H^2}}{g^2(\overline{T})^4}$$

$$(B) \qquad \sigma^2 = (0.34)(2\pi)^4[-\ln \tau_{min} - 0.0671]\frac{\overline{H^2}}{g^2(\overline{T})^4}$$

It is important to note that all four spectra predict σ^2 in terms of the same non-dimensional parameter, related to the square of the wave steepness, and this is as should be expected. According to (9.45), σ^2 given by all four spectra might be interpreted as a function of gF/U^2, since in general wave steepness is a function of gF/U^2. Eq. (9.45) can be transformed into (9.44) by use of (9.6) and (9.9).

Whereas σ^2 predicted from (9.44) results in larger differences for same measured wind speed, σ^2 predicted from (9.45) results in lesser differences for same measured wave heights and periods. The most nearly correct spectrum, and also forecasting relationships as a matter of fact, is that which satisfies best σ^2 from both (9.44) and (9.45), correspondingly.

For $\tau_{min} = 0.1$ (corresponding to $T_{min} = 1.0$-second for a 10-second mean period or $T_{min} = 0.5$ second for a 5-second mean period) both N and B spectra predict almost identical values of σ^2 according to (9.45).

Since $\sigma^2_{max} = 0.1$ all four spectra of (9.44) fail for some high value of $\overline{H^2}/(\overline{T})^4$, prior to critical steepness of $H/L = 1/7$ for all gravity waves. This should be expected, since (9.45) applies to a fully developed, or near fully developed sea, in which case critical steepness does not exist. For a younger sea the general form of the B spectra, including correlation, predicts $\sigma^2_{max} = 0.1$ coincident with critical steepness for all gravity waves $H/L = 1/7$. For the family of B spectra σ^2 as a function of $H_{33}/T^2_{1/3}$ may be obtained from Table 8.2 of Chapter VIII.

The above discussion is limited to gravity waves only, $T_{min} = 0.074$ second. According to the measurements of Cox and Munk (1956) it was found that on the average the mean square sea surface slope measurements were about 3.3 times greater for a clean surface than for an oil slick surface under similar meteorological conditions. It has been inferred by Cox and Munk (1956) and Neumann and Pierson (1957) that the measurements from the slick surface represent only the gravity wave components and that the clear surface includes both capillary and gravity waves.

Although the B spectra is not intended to include capillary waves, it is tempting to assume that capillary waves might be included. For if such an assumption is made, one may investigate the contribution of σ^2 due to capillary waves, since σ^2 is proportional to the negative of ln T_{min}. For example, if $T_{min} = 0.0025$ second (far into the capillary range) instead of 0.074 second, σ^2 will be increased by $\ln \frac{0.074}{0.0025} = 3.4$. However, there is no extremely lower limit to which one might justifiably take T_{min}, since at $T_{min} = 0$, the equation predicts $\sigma^2 = \infty$.

10. Reported Data Suitable For Wave Spectra Comparisons

Reported data can be used to check the various proposed spectra, provided these data are applicable to conditions for which the spectra are intended. Although some data are available and a comparison is made with the various spectra, it must be emphasized that a concrete conclusion in regard to the wave spectra is somewhat difficult.

Mean Square Sea Surface Slope Measurements: Data are reported on mean square sea surface slope by Schooley (1954), Cox and Munk (1956) and Farmer (1956).

Schooley's measurements were made in the Anacostia River. There is some question as to whether contamination of the river surface had any effect on the capillary wave components. The river fetch is very short, and for the wind speeds experienced, cannot be compared with the spectra for fully developed sea.

Measurements by Cox and Munk were made under two conditions, normal clean sea surface and a surface covered with oil slicks. Measurements for the clean surface include components of σ^2 due to capillary waves as well as gravity waves, whereas those for the oil slick surface eliminate capillary wave effects. What other effects the oil slick has on the processes between wind and sea are not known. The measurements were made for fetches on the southern side of the Pacific high, near the Hawaiian Islands, and in general the fetches were on the order of 1,000 nautical miles. Darbyshire (1957), however, pointed out that these measurements were carried out in a sea surrounded by small islands and the actual fetch did not exceed 5 miles. Neumann and Pierson (1957), on the contrary, claim that waves from the open sea could have passed through the gaps in the islands by refraction and diffraction. Along with the measurements of σ^2 Cox and Munk (1956) also report visual observations of significant waves, heights within $\pm \frac{1}{2}$ foot and periods within $\pm \frac{1}{2}$ second. These observations show that the effective fetch is greater than 5 miles. Evidently the waves generated over the long fetches are refracted and diffracted, and in addition, local wind generated waves are superimposed thereon. A careful review of the wave observations seems to point to the fact that this is the case. For some of the records the waves are predominantly swell, since the corresponding winds are much too low to generate the reported waves.

The measurements of Farmer (1956) were taken on the southern side of the Bermuda high, but there is some question as to an error by a factor of four in the calibration. In general, Farmer (1956) states that his measurements are in fairly good agreement with those of Cox and Munk (1956).

From the above it seems appropriate only to consider the data of Cox and Munk (1956). Figure 9.3 shows a comparison of σ^2 versus $\left[H_{33}/T^2_{1/3}\right]^2$ for the data and the various spectra. The D_1, D_2, and N spectra show a linear relationship with respect to the square of the steepness parameter. The general form or family of B spectra is used for the corresponding σ^2, which are given in Table 8.2 of Chapter VIII. The scatter of data is great and a very low degree of correlation is found between observed and predicted σ^2 for any of the four spectra. The overall mean of σ^2 is in closer agreement to that predicted from the B spectra than from either D_1, D_2, or N spectra. It is not difficult to account for much scatter of the data, since σ^2 is proportional to H_{33}^2 and inversely proportional to $T^4_{1/3}$. Mean values of significant waves for these data are about $H_{33} = 4$ feet and $T_{1/3} = 4$ seconds. If these observations are within $\pm \frac{1}{2}$ foot and $\pm \frac{1}{2}$ second, the maximum range in scatter from the computed σ^2 will be a factor on the order of 0.5 to 2.0, therefore, no conclusions can be made in regard to Figure 9.3, except that all spectra seem to predict σ^2 between the data for clean surface and that for slick surface.

Figure 9.4 shows a comparison of σ^2 versus wind speed for the data and the various spectra. Only the data for the slick surface are used, since all spectra are intended to exclude capillary waves. For the data Cox and Munk (1956) present statistical linear relationships for σ^2 versus wind speed for both a clean surface and a slick surface. In case of the clean surface the relationship is very good. For the slick surface there are two few data to place much confidence in the linear relationship. In fact, the data appear to fit a curved relationship equally well if not better. The D_2 spectrum predicts a parabolic relationship of σ^2 versus wind speed, but the curve is reverse to that indicated by the data. The N spectrum predicts a linear relationship of σ^2 versus U in fairly good agreement with the statistical least squares relationship of Cox and Munk (1956) for the data from slick surfaces. The family of B spectra predicts curved relationships of σ^2 versus U for different fetch lengths, and appears to be in fairly good agreement with the data, provided the effective fetch is less than 100 nautical miles. The exact effective fetch lengths for oil slick surfaces applicable to these data are not known. Based on both Figures 9.3 and 9.4, it is believed by the present author that the order in which agreement is best between data and spectra is B, N, D_2, and D_1, recognizing that opinions of others may be N, B, D_2 and D_1, or some other order.

Computed Spectrum From Data on Project SWOP: Project SWOP, Chase, Cote, Marks, Pierson, Bonne, Stephenson, Vetter, and Walden (1957) is the first comprehensive project of its kind for obtaining the energy spectrum of waves under one particular meteorological set of conditions. Neumann and Pierson (1957) have concluded that the measurements from project SWOP verified the Neumann spectrum, at least for one particular wind speed of 18.7 knots. Darbyshire (1957), although appearing to agree with the conclusions of Neumann and Pierson, remarks that the situation may not necessarily be a typical deep water one; the measurements were carried out at a point approximately 300 miles south of Nova Scotia and about 100 miles to the southeast of the nearest point on the 100-fathom line and the waves might have been affected by the Gulf Stream. What actual effects these conditions have on the distortion of the spectrum is difficult to assess, and is a problem for future studies. It is the opinion of this author, however, since the measurements were sufficiently remote from the major part of the Gulf Stream that its effect is perhaps insignificant.

Figure 9.5 shows comparison of the N and B spectra with the data from SWOP, where $k = \frac{26}{27}$ seconds as used by Neumann and Pierson (1957). In order to determine the B spectrum it is necessary that F_1 and F_2 be determined. It is reported in SWOP that the significant wave height was 6.6 feet, which is also in agreement with that predicted by the Neumann equation for an 18.7-knot wind. This

corresponds to $\overline{H} = 0.625\ (6.6) = 4.1$ feet, from which $F_1 = g\overline{H}/U^2 = 0.133$ and $gH_{33}/U^2 = 0.213$; from Figure 8.1 of Chapter VIII this corresponds to $gF/U^2 = 28{,}000$ and $(gT_{1/3})/2\pi U = 1.13$, and the minimum fetch length is 142 nautical miles. It is seen that this corresponds to near zero correlation, whence $F_2 = g\overline{T}/2\pi U = 1.13$. For a correlation coefficient $r(\eta, \lambda) = +0.2$, $F_2 = 1.13/\sqrt{1 + 0.6}\ r = 1.065$ and for $r(\eta, \lambda) = +0.4$, $F_2 = 1.02$. Figure 9.5 for the B spectrum is based on $r(\eta, \lambda) = 0$, $F_1 = 0.133$ and $F_2 = 1.13$. The area under the B spectrum is equal to that under the N spectrum, $(4/\pi)(\overline{H}/2)^2$, and this should be expected since both spectra utilize the same value of $\overline{H}$. The condition of fully developed sea has not yet been reached according to the B spectrum. For much greater fetch lengths and wind duration, Figure 8.1 would predict $H_{33} = 8.7$ feet instead of 6.6 feet, in which case the area under the B spectrum would be 1.74 times that for the N spectrum. However, since $H_{33} = 6.6$ feet was reported, this value should be used instead of 8.7 feet to determine F_1 and F_2.

The area under the computed spectrum from data on project SWOP is about 20 to 25 percent greater than that under either the N or B spectra. The peak of the computed spectrum is almost exactly verified by the B spectrum, but if the computed spectrum is multiplied by 0.8 to make the areas under all curves equal then the peak of the N spectrum is almost exactly verified. The high frequency end of the computed spectrum is almost exactly verified by the N spectrum, but if the computed spectrum is multiplied by 0.8 then the high frequency end of the B spectrum is almost verified. It is reported by project SWOP that a certain amount of white noise was presented and the data had to be corrected accordingly. The greatest amount of white noise is associated with the high frequency components. If the data had been corrected for twice the computed white noise instead of only the computed white noise, the area under the computed spectrum would be very nearly equal to that under either the N or B spectra. In this case the peak of the computed spectrum changes very little but the high frequency components change appreciably with the result that the B spectrum is verified almost exactly for all frequencies. It appears that this would be the logical correction, since the B spectrum for high frequency verifies the work of Burling (1955) and Phillips (1957)[b].

There is a slight chance that correlation $r(\eta, \lambda)$ is not zero, since the relationship of $g\overline{T}/2\pi U$ (Figure 8.1) is extrapolated from lower values of the fetch parameter. Perhaps the maximum value of $r(\eta, \lambda)$ is less than +0.2. If this be the case, the peak of the B spectrum is raised slightly and shifted toward high frequency components. For $r(\eta, \lambda) = +0.4$ the peak becomes more pronounced and shifts further toward high frequencies, such as illustrated in Figure 9.6. Actually, there is little difference between the B spectrum for $r(\eta, \lambda) = 0$ and $r(\eta, \lambda) = +0.4$, since these curves are within the 95 percent confidence limits for $r(\eta, \lambda) = +0.2$. Thus

it is fair to assume the B spectrum for $r(\eta,\lambda) = 0$ is satisfactory for the comparative test between the N spectrum and the computed spectrum. It was not intended to omit the D_2 spectrum from the data test for project SWOP, since this was covered by Neumann and Pierson (1957).

It is only logical that this writer be inclined to stress preference for the B spectrum, recognizing that Neumann and Pierson (1957) prefer the N spectrum, and Darbyshire (1957) the D_2 spectrum. One important fact, however, which is in agreement with all concerned, is that the family of B spectra is one more theoretical expression to be tested for use of future data. For such a test to be made, the correlation coefficient $r(\eta,\lambda)$ as well as H and T (or Δ E and k) must be determined.

11. Comments on Decay of Wind Generated Gravity Waves

When waves decay in deep water the longer period waves travel faster and farther than the shorter period waves. In this process the steepness decreases and the correlation rotates to greater positive values. The general form of B spectra still applies, since now $\bar{H}$ and $\bar{T}$ are functions of the decay parameters instead of the fetch parameters. The unit form of the B spectra again becomes peaked and narrow, since the area under the curve is still $4/\pi\,(\bar{H})^2$. However, since $T_{1/3}$ increase and H_{33} decrease with the increased decay distance the area under the curve as well as the peak decreases for the standard form of the B spectra. At a particular decay distance the peak of the B spectra increases with time, since the mean wave period decreases with time. Theoretically for a fixed decay distance the mean period should decrease to its original value in the fetch area after a time equal to that required for the shortest period waves to be propagated to the fixed decay distance. However, since the small heights contributing to the mean in the fetch area will have been attenuated beyond measurement, the mean period at the fixed decay distance will never decrease to a value as low as that in the fetch area.

When deep water waves are propagated over shallow water, the long period waves feel bottom first and become attenuated, resulting in a shift of energy to lower wave periods, opposite to the shift of energy for decay of deep water waves over deep water. Observations in the Gulf of Mexico indicate a decrease in significant wave period shoreward from deep water for onshore winds. This causes a rotation in correlation coefficient from positive to zero in deep water toward negative in shallow water.

The final distribution of waves and the wave spectra depend on the initial conditions at the end of the fetch and in the fetch, and the method in which decay takes place. Refraction and diffraction as well as possible breaking waves will also contribute to the form and shape of the wave spectrum at the end of a decay distance. This

problem, however, is far from being solved at present. Figure 9.7 is an illustrative scheme which might be worthy of further considerations. This figure depicts a steepness parameter, $H_{33}/T_{1/3}^2$, [$(\overline{H}/(\overline{T})^2$ could also be used)] as a function of rotation of the regression line of H on T^2. The curves for the deep water decay zone result from decaying over deep water elements of the joint distribution function for zero correlation. The decay function from Sverdrup and Munk (1947) was used, although some other calibrated decay function might have been used. A whole family of such curves exist, depending on the stage of generation when decay commences. Curves for the shallow water wave zone result from decaying over shallow water elements of the joint distribution function for zero correlation, taking bottom friction into account. Use was made of the dissipation function originally presented by Putnam and Johnson (1949), and applied by Bretschneider and Reid (1954). Only one condition was investigated, and that was for a bottom of constant depth. Evidently a whole family of such curves exists for a bottom of constant depth, and perhaps relationships are possible for a bottom of constant slope, or for the Continental Shelf area. Computations as well as the data show that rotation of correlation is positive for waves decaying in deep water and negative for shallow water. If the initial correlation is positive, say for a very young sea or for deep water swell, it is also possible to obtain zero or negative correlation when further decay takes place over shallow water. Such conditions are expected over the Continental Shelf area.

A forecasting method is desirable which will predict not only the characteristic heights and periods but also the correlation coefficient. Such a method would permit the determination of the mean wave period of the highest p-percent wave heights. In this respect the joint distribution function is equally as important as the wave spectral function. In fact the joint distribution function may be more desirable, since the wave spectral function evolves from the joint distribution function, whereas the converse might not be possible. Perhaps a filter technique, similar to that utilized by Pierson, Neumann, and James (1955) might be quite useful. However, any of the above methods, whether used individually or collectively, require refinements and calibration, using reliable wave data. It is believed that in future analyses of wave data much might be gained by determining correlation coefficients as well as characteristic waves and energy spectra.

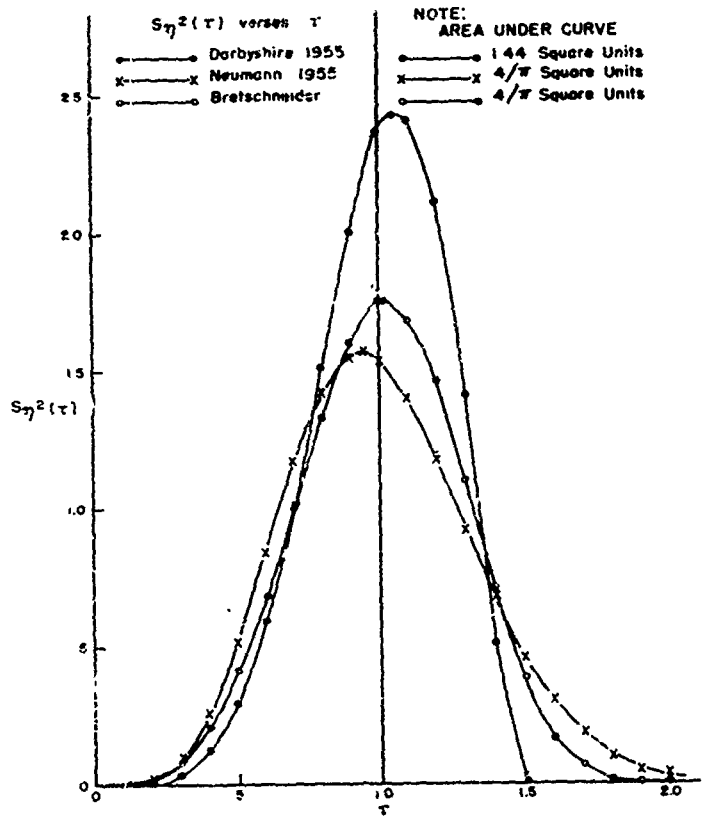

FIGURE 9.1 THEORETICAL PERIOD SPECTRA

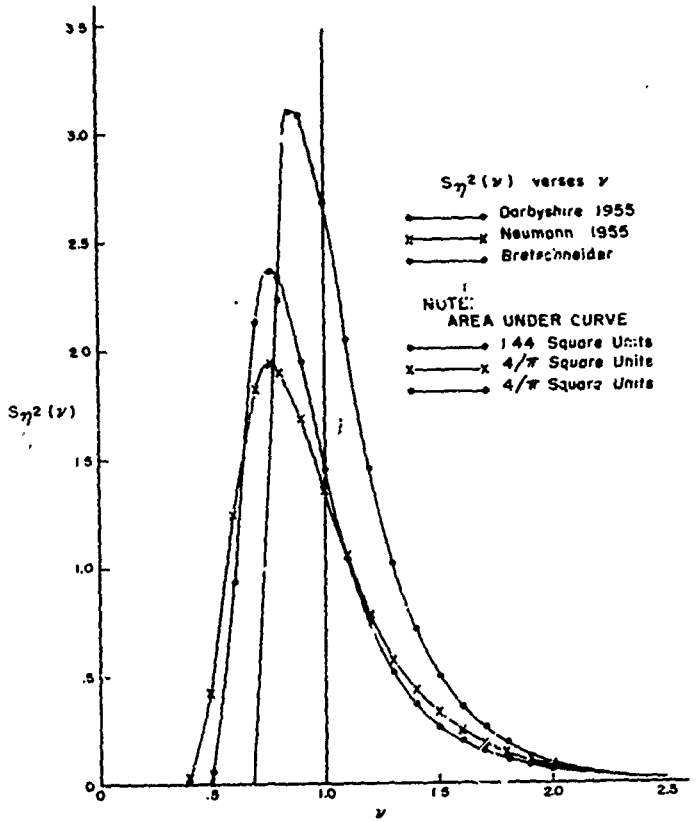

FIGURE 9.2 THEORETICAL FREQUENCY SPECTRA

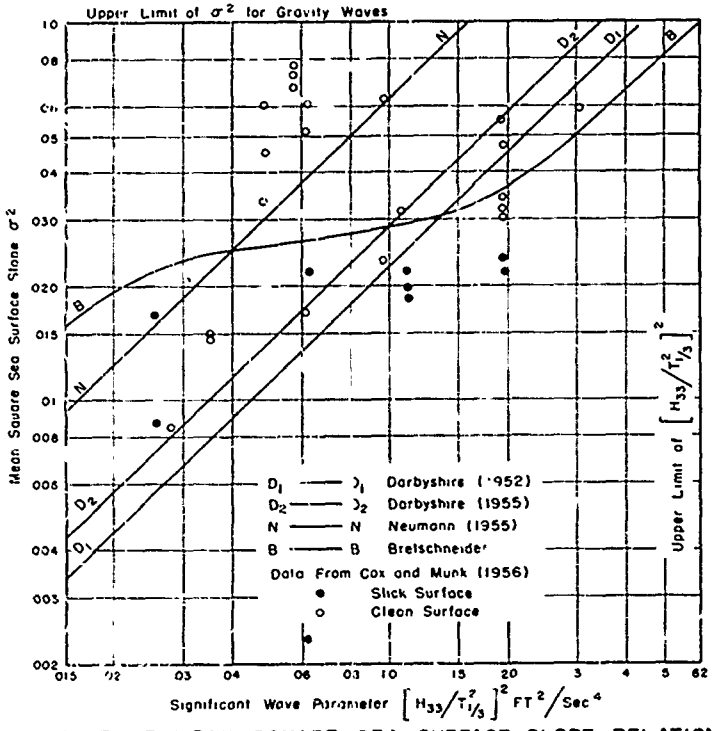

FIGURE 93 MEAN SQUARE SEA SURFACE SLOPE RELATIONS

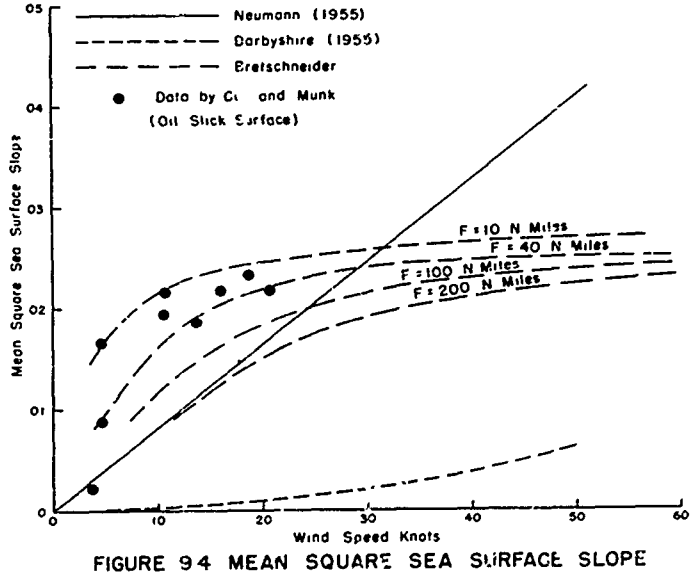

FIGURE 94 MEAN SQUARE SEA SURFACE SLOPE RELATIONSHIPS FOR SLICK SURFACES

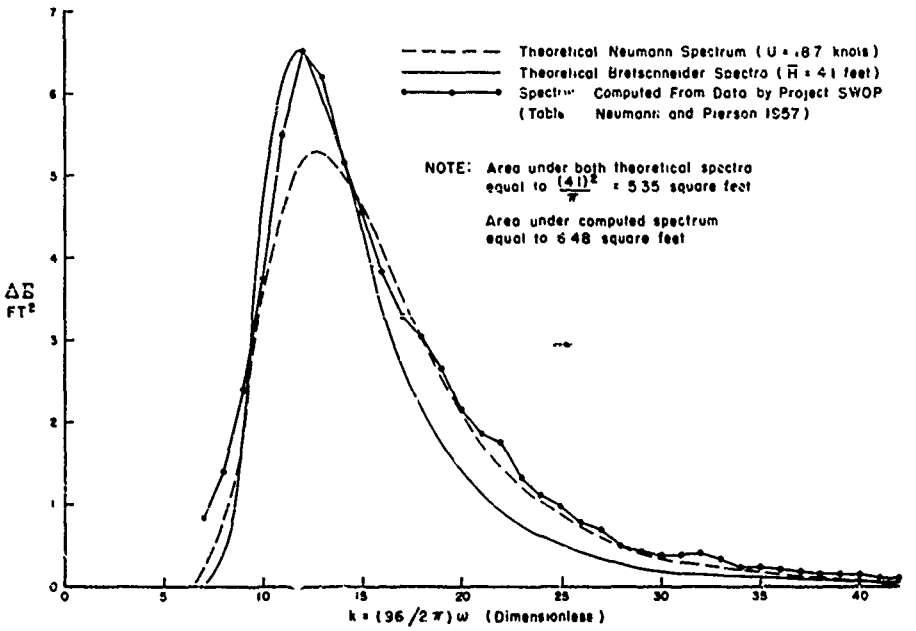

FIGURE 9.5 THEORETICAL SPECTRA COMPARED WITH COMPUTED SPECTRUM FROM DATA

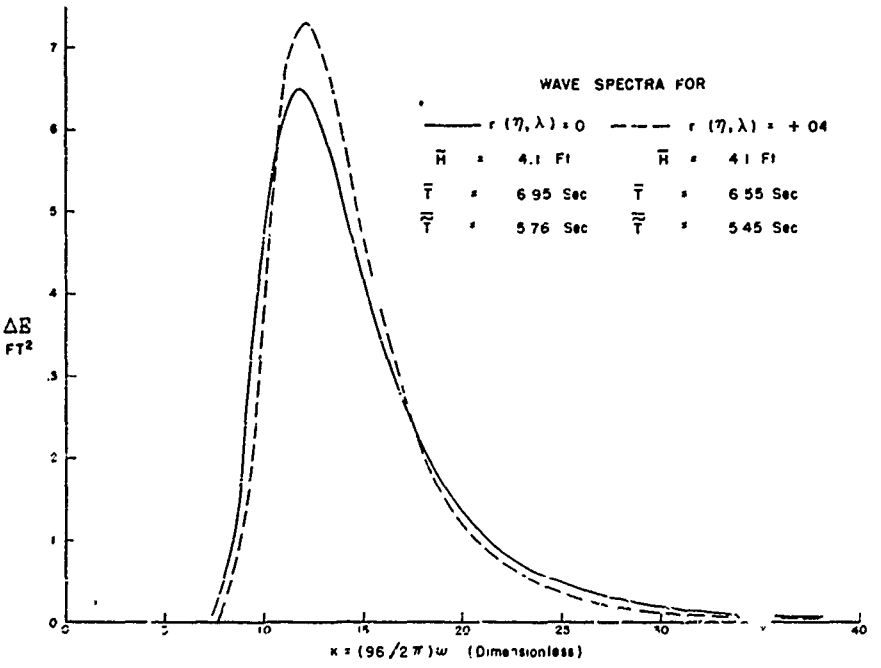

FIGURE 9.6 SPECTRA FOR r (η,λ) = 0 AND r (η,λ) = +.04

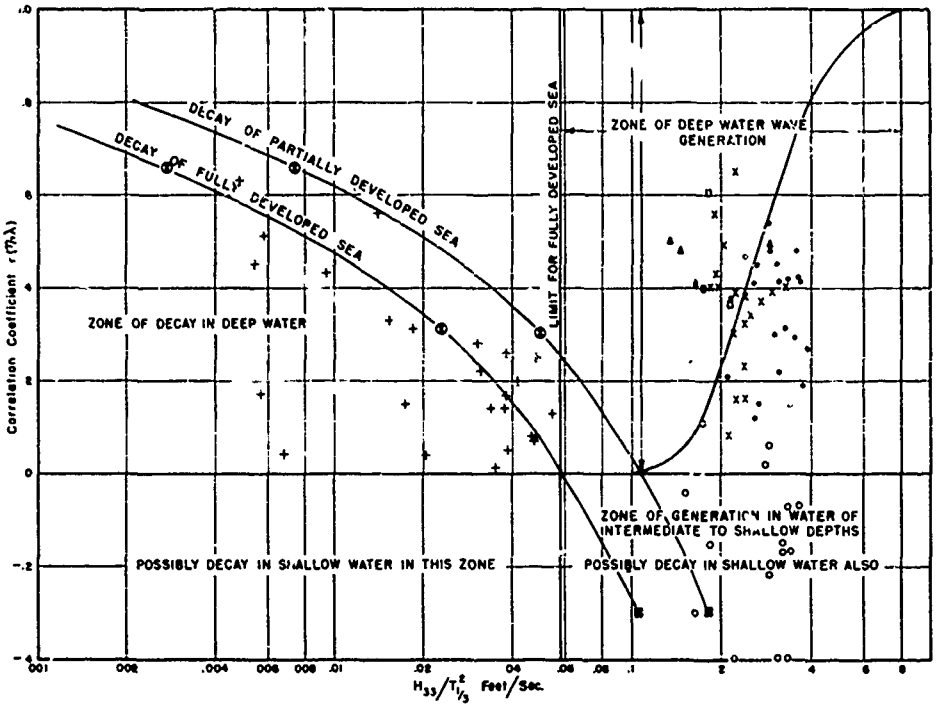

SOURCE	SYMBOL	TYPE OF WAVES
a	+	Deep Water Swell
b	•	Wind Generated Waves in Deep Water
c	X	Wind Generated Waves in Deep Water
d	Δ	Hurricane Wind Waves, Lake Okeechobee
e	o	Wind Generated Waves, Intermediate to Shallow Water
f	□	Combination Swell and Wind Waves, Hurricane Audrey (1957)

FIGURE 9.7 ILLUSTRATIVE SCHEME FOR ROTATION OF CORRELATION

ACKNOWLEDGEMENTS

Much appreciation is extended to various people and organizations for making available a bulk of wave data and wave records used in this research. Information was made available through the courtesy of Professor J. W. Johnson and Mr. R. R. Putz of the University of California, Berkeley; Mr. C. P. Besse of The California Company, New Orleans; the Beach Erosion Board, and other offices of the U. S. Army Corps of Engineers.

Although portions of the research were carried out as a part of the approved research program of the Beach Erosion Board, the work originally was initiated at Texas Agricultural and Mechanical College. Appreciation is extended to the staff of the Beach Erosion Board for time and personnel made available for completion of the work, under its regular research program.

Appreciation is extended to the members of the Committee for the Department of Oceanography, Texas Agricultural and Mechanical College for review and guidance of this research. In particular, this includes Professor Robert O. Reid, who from time to time reviewed the progress made and encouraged additional work leading to the last chapter of this dissertation.

BIBLIOGRAPHY

Arthur, R. S. (1947). Revised Wave Forecasting Graphs and Procedures. Scripps Institution of Oceanography, Wave Report No. 73, 14 pages.

Barber, N. F., and F. Unsell (1948). The Generation and Propagation of Ocean Waves and Swell, Phil. Trans., 240, pp. 527-560.

Beach Erosion Board (1952). Description and Operating Instructions for Wave Gage WH-1. The Bulletin of the Beach Erosion Board, Office of the Chief of Engineers, No. 4, Vol. 6, pp. 1-12.

Beard, L. R. (1952). Statistical Methods in Hydrology. Office, Chief of Engineers, Department of the Army, Washington, D. C., July 1952, 35 pages.

Bretschneider, C. L. (1951). Revised Wave Forecasting Curves and Procedure. Technical Report No. HE-155-47, Institute of Engineering Research, University of California, Berkeley (unpublished), 28 pages.

-- and R. R. Putz (1951). Discussion of Paper "Problems of Wave Action on Earth Slopes", by Martin A. Mason, Trans. ASCE, Vol. 116, Paper No. 2472.

-- and E. K. Rice (1951). The Generation and Decay of Wind Waves in a Sixty-foot Channel. Technical Report HE-116-327, Institute of Engineering Research, University of California, Berkeley (unpublished), 3 pages.

-- (1952)[a]. Revised Wave Forecasting Relationships. Proceedings of Second Conference on Coastal Engineering, Ch. I. pp. 1-5.

-- (1952)[b]. The Generation and Decay of Wind Waves in Deep Water. Trans. A.G.U., Vol. 33.

-- (1954). Field Investigation of Wave Energy Loss in Shallow Water Ocean Waves. Beach Erosion Board Technical Memorandum No. 46, 21 pages and appendices.

-- and R. O. Reid (1954). Changes in Wave Height Due to Bottom Friction, Percolation, and Refraction. Beach Erosion Board Technical Memorandum No. 45, 36 pages.

-- (1957)[a]. Joint Distribution of Wave Heights and Lengths. Presented at the 1957 Annual Meeting of the American Geophysical Union, Washington, D. C. (unpublished).

Bretschneider, C. L. (1957)[b]. Review of "Practical Methods for Observing and Forecasting Ocean Waves by Means of Wave Spectra and Statistics", U.S.H.O. Pub. No. 603, by Willard J. Pierson, Jr., Gerhard Neumann, and Richard W. James. Trans. A.G.U., Vol. 38, No. 2, pp. 264-266.

-- (1957)[c]. Revisions in Wave Forecasting: Deep and Shallow Water. Sixth International Conference on Coastal Engineering, Gainesville, Florida.

-- (1958). Selection of Design Wave for Offshore Structures. Journal of Waterways and Harbors Division, Proc., ASCE, WW2, Paper 1568, pp. 1568-1 to 1568-37.

Buckingham, E. (1914). On Physically Similar Systems. Phys. Rev., 4,345.

Burling, R. W. (1955). Wind Generation of Waves on Water. Ph. D. Dissertation, Imperial College, University of London.

Caldwell, J. M. (1952). The Step-Resistance Wave Gage. Proc. First Conference Coastal Engineering Instruments. Council on Wave Research, Berkeley, California, pp. 44-60.

California Oil Company (1957). Letter from California Oil Company, Enclosure of Wave Records, Hurricane "Audrey" 1957.

Cartwright, D. E., and M. S. Longuet-Higgins (1956). The Statistical Distribution of the Maxima of a Random Function. Proc. R. Soc., A, 237, pp. 212-232.

Chase, J., L. J. Cote, W. Marks, E. Mehr, W. J. Pierson, Jr., F. C. Ronne, G. Stephenson, R. C. Vetter, and R. G. Walden (1957). The Directional Spectrum of a Wind Generated Sea as Determined from Data Obtained from the Stereo Wave Observation Project. New York University, Coll. Eng., Res. Div., Technical Report.

Corps of Engineers, U. S. Army (1950). Waves and Wind Tides in Inland Waters, Lake Okeechobee, Florida, CW-167 Project Bulletin No. 2, Jacksonville District, Jacksonville, Florida.

-- (1951). Waves in Inland Reservoirs, Fort Peck, Montana, CW-164 Project Bulletin No. 1, Fort Peck District, Montana.

-- (1953). First Interim Report on Wind and Wave Investigation, Denison Dam (Lake Texoma) Red River, Texas and Oklahoma, Tulsa District, Tulsa, Oklahoma.

-- (1955)[a]. Waves and Wind Tides in Shallow Lakes and Reservoirs, CW-167 Summary Report, Jacksonville District, Florida.

-- (1955)[b]. Memorandum Office of Chief of Engineers to Beach Erosion Board. Subject: Preparation of Joint Report on "Wave Action on Inland Reservoirs (CW-164 and 165)"; incl. sums of tabulated wave data. On file.

Cox, C., and W. H. Munk (1956). Slopes of the Sea Surface Deduced from Photographs of Sun Glitter: Bulletin of the Scripps Institution of Oceanography of the University of California, La Jolla, California, Vol. 6, No. 9, pp. 401-488.

Chinn, A. J. (1949). Summary Report on Shore Wave Recorder Mark III, Technical Report HE-116-303, Fluid Mechanics Laboratory, University of California, Berkeley (unpublished).

Darbyshire, J. (1952). The Generation of Waves by Wind. Proc. R. Soc., A 215, pp. 299-328.

-- (1955). An Investigation of Storm Waves in the North Atlantic Ocean. Proc. R. Soc., A 230, pp. 299-328.

-- (1957). A Note on the Comparison of Proposed Wave Spectrum Formulae. Deutsche Hydrographische Zeitschrift, Band 10, Heft 5, pp. 184-190.

Darlington, C. R. (1954). The Distribution of Wave Heights and Periods in Ocean Waves, Q.J.R. Met. Soc., 80, pp. 619-626.

Farmer, H. G. (1956). Some Recent Observations of Sea Surface Elevation and Slope. Woods Hole Oceanographic Institution, Tech. Rep., ref. No. 56-37, 29 pages and Appendix A.

Fisher, R. A. (1915). Frequency Distribution of the Values of the Correlation Coefficient in Samples from an Indefinitely Large Population. Biometrika 10, 1915, p. 507.

Gerhardt, J. R., K. H. John, and I. Katz (1955). A Comparison of Step-Pressure, and Continuous-Wire Gage Wave Recordings in the Golden Gate Channel, Trans. A.G.U., Vol. 38, pp. 235-250.

Isaacs, J. D. and R. L. Wiegel (1950). The Thermopile Wave Meter. Trans. A.G.U., Vol. 30, pp. 711-716.

Jahnke, E. and F. Emde (1945). Tables of Functions, 4th Ed., Dover Publ., New York 19, N. Y., 306 pages.

Johnson, J. W. (1950). Relationships between Wind and Waves, Abbots Lagoon, California. Trans. A.G.U., Vol. 31, pp. 390-392.

-- and E. K. Rice (1952). A Laboratory Investigation of Wind-Generated Waves. Trans. A.G.U., Vol. 33, No. 6, pp. 845-854.

Lamb, Horace B. (1945). Hydrodynamics, 6th Ed., Dover Publ., New York, N. Y., 738 pages.

Lawford, A. L. and V. F. C. Veley (1956). Changes in the Relationship between Wind and Water Movement at Higher Wind Speeds. Trans. A.G.U., Vol. 37, pp. 691-693.

Kenney, J. F. and E. S. Keeping (1954). Mathematics of Statistics, 3d Ed., D. Von Nostrand Company, Inc., Princeton, New Jersey, Part I, 348 pages.

Longuet-Higgins, M. S. (1952). On the Statistical Distribution of the Heights of Sea Waves. Jour. Mar. Res., Vol. XI, No. 3, pp. 345-366.

-- (1957). The Statistical Analysis of a Random Moving Surface. Phil. Trans., R. Soc. of London, A 966, pp. 321-387.

Mandelbaum, Hugo (1956). Evidence for a Critical Wind Velocity for Air-Sea Boundary Processes. Trans. A.G.U., Vol. 37, pp. 685-690.

Michell, J. H. (1893). On the Highest Waves in Water. Phil. Mag., Vol. 36, No. 5, pp. 430-435.

Morison, J. R. (1949). Measurement of Wave Heights by Resistants. Bulletin of the Beach Erosion Board, Corps of Engineers, U. S. Army, Vol. 3, No. 3, pp. 16-22.

Munk, Walter H. (1947). A Critical Wind Speed for Air-Sea Boundary Processes. J. Mar. Res., Vol. 6, pp. 203-218.

-- (1949). Solitary Wave Theory. Annals New York Academy of Science, Vol. 51, pp. 376-424.

-- and R. S. Arthur (1951). Forecasting Ocean Waves. Compendium of Meteorology, Amer. Met. Soc., pp. 1082-1089.

-- (1957). Comments on a Review by C. L. Bretschneider of "Practical Methods for Observing and Forecasting Ocean Waves by Means of Wave Spectra and Statistics", H. O. Pub. 603, by W. J. Pierson, Jr., G. Neumann, and R. W. James.

Neumann, G. (1952). On Ocean Wave Spectra and a New Method of Forecasting Wind-Generated Sea. Beach Erosion Board Technical Memorandum No. 43, 42 pages.

-- and W. J. Pierson, Jr., (1957)[a]. Comparison of Various Theoretical Wave Spectra. Proc. Sympos.: The Behavior of Ships in a Seaway, Chapter 7, Wageningen.

-- and W. J. Pierson, Jr., (1957)[b]. A Detailed Comparison of Various Theoretical Wave Spectra and Wave Forecasting Methods. Deutsche Hydrographische Zeitschrift, Z 10, 73, 134.

Phillips, O. M. (1957)[a]. On the Generation of Waves by Turbulent Wind. Journal of Fluid Mechanics, Vol. 2, Part 5, pp. 417-445.

— (1957)[b]. The Equilibrium Range in the Spectrum of Wind-Generated Waves. Report, Mechanical Engineering Department, The Johns Hopkins University, 15 pages.

Pierce, B. O. and R. M. Foster (1956). Short Table of Integrals. Ginn and Company, New York, 4th Ed., 189 pages.

Pierson, W. J., Jr. (1954). An Interpretation of the Observable Properties of "Sea" Waves in Terms of the Energy Spectrum of the Gaussian Record. Trans. A.G.U., Vol. 35, pp. 747-757.

— and W. Marks (1952). The Power Spectrum Analysis of Ocean-Wave Records. Trans. A.G.U., Vol. 33, pp. 834-844.

— and G. Neumann, and R. W. James (1955). Observing and Forecasting Ocean Waves by Means of Wave Spectra and Statistics, Hydrographic Publication No. 603, U. S. Navy Dept., 284 pages.

Putnam, J. A. and J. W. Johnson (1949). The Dissipation of Wave Energy by Bottom Friction. Trans. A.G.U., Vol. 30, No. 1, pp. 67-74.

Putz, R. R. (1952). Statistical Distribution for Ocean Waves. Trans. A.G.U., Vol. 33, No. 5, pp. 685-692.

Rayleigh, Lord (1945). The Theory of Sound, 1st American Edition, Dover Publications, New York.

Reid, R. O. and C. L. Bretschneider (1953). Surface Waves and Offshore Structures: The Design Wave in Deep or Shallow Water, Storm Tide, and Forces on Vertical Piling and Large Submerged Objects. Technical Report, Texas A. & M. Research Foundation, 36 pages.

Rice, S. O. (1945). Mathematical Analysis of Random Noise. The Bell System Tech. Jour., Vol. 23, pp. 282-332; Vol. 24, pp. 46-156.

Roll, H., and G. Fisher (1956). Eine Kritische Bemenkung Zum Neumann-Spektrum der Seegange, Deut. Hydr. Zs., 9, pp. 9-14.

Roll, H. U. (1957). Forecasting Surface Gravity Waves. Conference on Long Waves and Storm Surges, National Institute of Oceanography, Wormley, England, May 27-31.

Rossby, C. G. and R. B. Montgomery (1935). The Layer of Frictional Influence in Wind and Ocean Currents. Papers in Phys. Oceanog. and Meteorol., Vol. 3, No. 3, 101 pages.

Saville, T., Jr. (1954). The Effect of Fetch Width on Wave Generation. Beach Erosion Board Technical Memorandum No. 70, 9 pages.

Schooley, A. H. (1954). A Simple Optical Method for Measuring the Statistical Distribution of Water Surface Slopes. J. Opt. Soc. Am., Vol. 44, pp. 37-40.

Sibul, J. O. and E. G. Tickner (1956). Model Study of Overtopping of Wind-Generated Waves on Levees with Slopes of 1:3 and 1:6. Beach Erosion Board Technical Memorandum No. 80, 27 pages.

Snodgrass, F. E. (1951). Wave Recorders, Proceedings First Conference on Coastal Engineering, Council on Wave Research, The Engineering Foundation, Ch. 7, pp. 69-81.

Suthons, Commander C. T. (1945). The Forecasting of Sea and Swell Waves. Naval Met. Branch, England.

Sverdrup, H. U., and W. H. Munk (1947). Wind, Sea, and Swell: Theory of Relations for Forecasting. H. O. Pub. No. 601, U. S. Navy Department, 44 pages.

Tucker, M. J. and H. Charnock (1955). A Capacitance Wire Recorder for Small Waves. Proc. 5th Conference Coastal Engineering, Sept. 1, 1944, pp. 177-188.

Uspenky, J. V. (1937). Introduction to Mathematical Probability, McGraw-Hill Book Company, Inc., 411 pages.

Watters, Jessie K. A. (1953). Distribution of Height in Ocean Waves, New Zealand Journal of Science and Technology, Sect. B, Vol. 34, pp. 408-422.

Wiegel, R. L. (1954). Gravity Waves Tables of Functions. Council on Wave Research, The Engineering Foundation, 33 pages.

-- and J. Kukk (1957). Wave Measurements along the California Coast. Trans. A.G.U., Vol. 38, No. 5, pp. 667-674.

Williams, A. J. and D. E. Cartwright (1957). A Note on Spectra of Wind Waves. Trans. A.G.U., Vol. 38, No. 6, pp. 864-866.

Wilson, B. W. (1955). Graphical Approach to the Forecasting of Waves in Moving Fetches. Beach Erosion Board Technical Memorandum No. 73, 31 pages.

Wooding, R. A. (1955). An Approximate Joint Probability Distribution for Amplitude and Frequency in Random Noise, New Zealand Journal of Science and Technology, Sec. B, Vol. 36, No. 6, pp. 537-544.

SYMBOLS

A	wave amplitude, also used as a constant
a	constant = 0.927
B	constant
C	wave celerity, also used as a constant
C_o	deep water wave celerity
C_s	wave celerity in shallow water
C_1, C_2, C_3	constants
C_g	group velocity of waves
d	water depth
E	wave energy
Ei(x)	exponential integral
F	fetch length
F_1	gH/U^2
F_2	$gT/2\pi U$
f_1, f_2	functions
f_i	frequency of occurrence of data for class i
g	acceleration of gravity
H	wave height (STANDARD FORM)
H_i	individual wave height
$\overline{H}$	mean wave height
H_{50}	mean of highest 50-percent wave heights
H_{33}	mean of highest 1/3 wave heights or significant wave height (also $H_{1/3}$)
H_{10}	mean of highest 10-percent wave heights
H_1	mean of highest 1-percent wave heights

H_{max}	maximum wave height and also most probable maximum height
$k = 2\pi/L$	wave number, and also
$k = 96/2\pi$	seconds for computed spectrum
K, K_1	constants
L	wave length (STANDARD FORM, used in terms of $L = T^2$, sec^2)
$L_o = gT^2/2\pi$	deep water wave length
L_s	wave length in shallow water
L_i	individual wave length (used in terms of $L_i = T_i^2$, sec^2)
$\bar{L}$	mean wave length (used in terms of $\bar{L} = \overline{T^2}$)
L_{50}	mean of longest 50-percent wave lengths
L_{33}	mean of longest 1/3 wave lengths
L_{10}	mean of longest 10-percent wave lengths
L_1	mean of longest 1-percent wave lengths
L_{max}	maximum wave length, also most probable maximum length
M	moment
M_n	n^{th} moment about origin
m	slope in equation $y = mx + b$
N	total number of waves in a record
n	order of data from $n = 1$ to $n = N$
n_1, n_2	degrees of freedom
P	used to denote cumulative probability
p	used to denote probability density
$p(\eta)$, $p(H)$	probability density of wave height
$p(\lambda)$, $p(L)$	probability density of wave length
$p(\tau)$, $p(T)$	probability density of wave period

$p(\eta,\lambda)$, $p(\eta,\tau)$, $p(H,L)$, $p(H,T)$	joint probability densities
$p_\eta(\lambda)$, $p_\lambda(\eta)$	conditional probability functions
q', q, Q', Q	related to wave energy
S_H, S_η	standard deviation of wave height
S_L, S_λ	standard deviation of wave length
S_T, S_τ	standard deviation of wave period
$S_\eta(\lambda)$, $S_\lambda(\eta)$, $S_\eta(\tau)$	summation functions, also λ-spectra of η, η-spectra of λ, and τ- spectra of η, respectively
$S_\eta^2(\lambda)$	λ-spectra of η^2
$S_\eta^2(\tau)$	τ-spectra of η^2
$S_\eta^2(\nu)$	ν-spectra of η^2
$S_H2(T)$	period spectra (of H^2)
$S_H2(\omega)$	frequency spectra (of H^2)
T	wave period (STANDARD FORM, crest to trough method)
T_i	individual wave period
$\overline{T}$	mean wave period (crest to trough method)
$T_{1/3}$	significant wave period, period of highest 1/3 wave heights
$\widetilde{T}$	apparent wave period (zero-up crossing method)
$\overline{\widetilde{T}}$	mean apparent wave period (zero-up crossing method)
T_{op}	optimum period (for period spectra)
t	time or duration
U	surface wind speed
U_g	gradient wind speed
u	horizontal particle velocity, also used in expressions for gamma and normal distribution functions, and for change of variable

v	vertical particle velocity, also used for change of variable
x	horizontal distance, also used in differential dx
z	used in change of variables
α	constant 7.4×10^{-3}
a_3	skewness coefficient, $a_{3H} = a_{3\eta}, a_{3L} = a_{3\lambda}$, $a_{3T} = a_{3\tau}$ for wave height, length, and period, respectively
Γ	gamma function
$\Delta\lambda$	increment of λ
ΔE	element of energy for computed spectrum
ϵ	spectral width parameter
$\eta = H/\overline{H}$	wave height (NORMAL FORM)
η_p	mean of highest p-percent heights
$\eta_{(\lambda p)}$	mean height of longest p-percent lengths
$\eta(\lambda_{50})$	mean height of longest 50-percent lengths
$\eta(\lambda_{33})$	mean height of longest 1/3 lengths
$\eta(\lambda_{10})$	mean height of longest 10-percent lengths
$\eta(\lambda_1)$	mean height of longest 1-percent lengths
$\eta(\lambda_{max})$	height of longest wave length
$\overline{\eta_\lambda}$	regression line of η on λ
$\theta = kx - \omega t$	phase position
$\lambda = L/\overline{L} = T^2/\overline{T^2}$	wave length (NORMAL FORM)
λ_p	mean of longest p-percent lengths
$\lambda(\eta_p)$	mean length of highest p-percent heights
$\lambda(\eta_{50})$	mean length of highest 50-percent heights
$\lambda(\eta_{33})$	mean length of highest 1/3 heights

$\lambda(\eta 10)$	mean length of highest 10-percent heights
$\lambda(\eta_1)$	mean length of highest 1-percent heights
$\lambda(\eta_{max})$	length of highest wave
$\overline{\lambda\eta}$	regression line of λ on η
$\nu = \frac{\omega}{\omega'}$	wave frequency (NORMAL FORM)
ξ	elevation of wave surface and is a function of phase position
π	3.1416
ρ	mass density of water; true value of correlation coefficient
σ^2	mean square sea surface slope
$\tau = T/\overline{T}$	wave period (NORMAL FORM)
$\tau(\eta_p)$	mean period of highest p-percent heights
$\tau(\eta_{50})$	mean period of highest 50-percent heights
$\tau(\eta_{33})$	mean period of highest 1/3 heights
$\tau(\eta_{10})$	mean period of highest 10-percent heights
$\tau(\eta_1)$	mean period of highest 1-percent heights
$\tau(\eta_{max})$	period of highest wave
τ_{op}	optimum period (τ -spectra of η^2)
Φ_p	probability integral
$\omega = 2\pi/T$	angular frequency (NORMAL FORM)
ω_{op}	optimum frequency (ω -spectra of η^2)